



Universidad de León

**Instituto Universitario de Biomedicina
(IBIOMED)**

Programa de doctorado Biomedicina y Ciencias de la Salud

Tesis doctoral

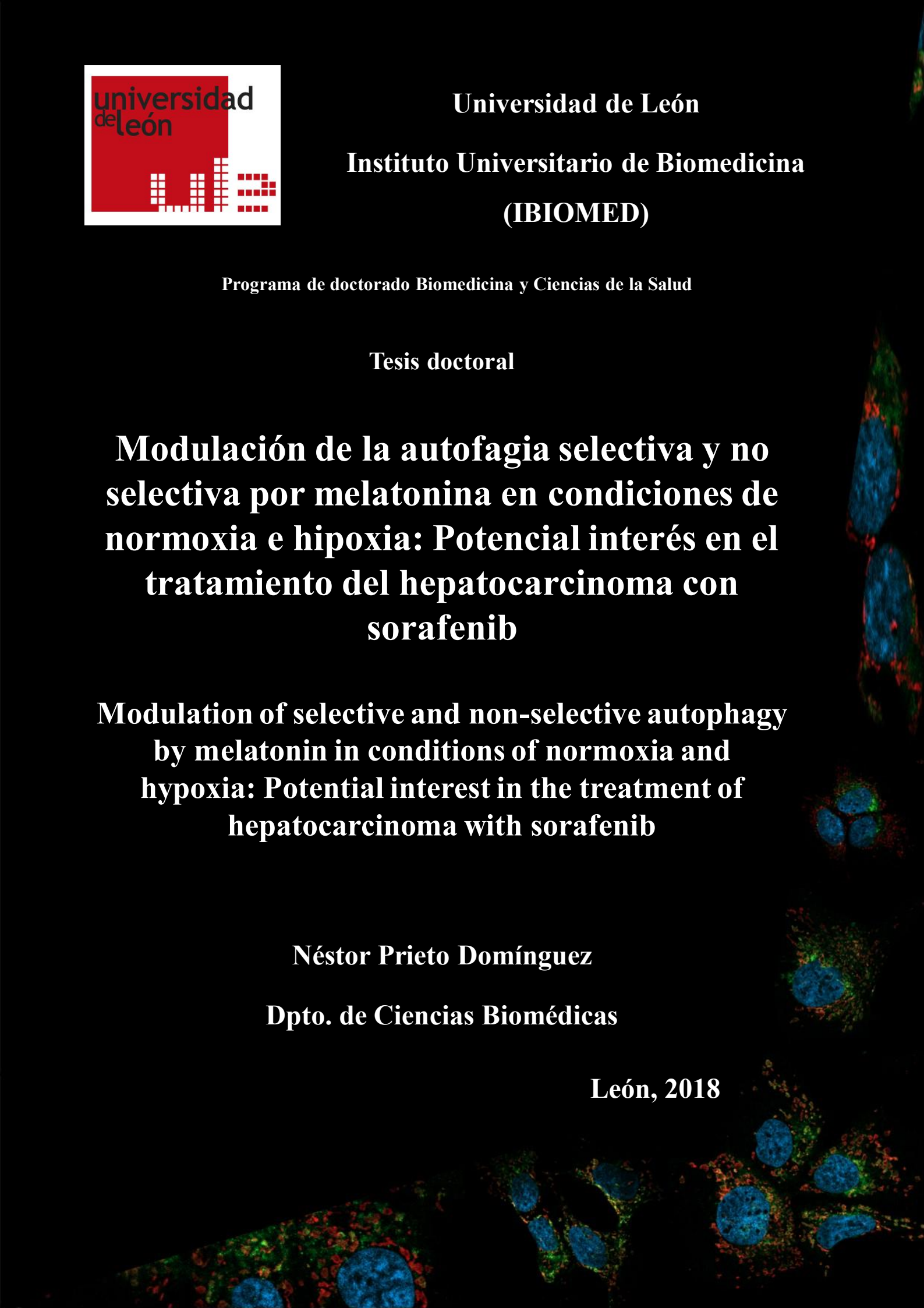
Modulación de la autofagia selectiva y no selectiva por melatonina en condiciones de normoxia e hipoxia: Potencial interés en el tratamiento del hepatocarcinoma con sorafenib

Modulation of selective and non-selective autophagy by melatonin in conditions of normoxia and hypoxia: Potential interest in the treatment of hepatocarcinoma with sorafenib

Néstor Prieto Domínguez

Dpto. de Ciencias Biomédicas

León, 2018





Universidad de León

Instituto Universitario de Biomedicina (IBIOMED)

Modulación de la autofagia selectiva y no selectiva por melatonina en condiciones de normoxia e hipoxia: Potencial interés en el tratamiento del hepatocarcinoma con sorafenib

Modulation of selective and non-selective autophagy by melatonin in conditions of normoxia and hypoxia: Potential interest in the treatment of hepatocarcinoma with sorafenib



Memoria presentada por D. Néstor Prieto Domínguez
para la obtención del título de Doctor por la Universidad de León

León, Septiembre de 2018



INFORME DEL DIRECTOR DE LA TESIS¹

(Art. 13.2 del RD 99/2011)

Los Dres. D. Javier González Gallego y D. Jose Luís Mauriz Gutiérrez como Directores² de la Tesis Doctoral titulada “Modulación de la autofagia selectiva y no selectiva por melatonina en condiciones de normoxia e hipoxia: potencial interés en el tratamiento del HCC con sorafenib” realizada por D. Néstor Prieto Domínguez en el programa de doctorado Biomedicina y Ciencias de la Salud, informa favorablemente el depósito de la misma, dado que reúne las condiciones necesarias para su defensa.

Lo que firmo, en León a ____ de ____ de 2018

Los Directores de la Tesis Doctoral

Dr. Javier González Gallego

Dr. José Luis Mauriz Gutiérrez

¹ Solamente para las tesis depositadas en papel.

² Si la Tesis está dirigida por más de un Director tienen que constar los datos de cada uno y han de firmar todos ellos.



ADMISIÓN A TRÁMITE DE LA TESIS DOCTORAL³

(Art. 13.2 del RD 99/2011)

La Comisión Académica del programa de doctorado en Biomédicina y Ciencias de la Salud en su reunión celebrada el día ___ de ___ de 2018 ha acordado dar su conformidad a la admisión a trámite de lectura de la Tesis Doctoral titulada “Modulación de la autofagia selectiva y no selectiva por melatonina en condiciones de normoxia e hipoxia: potencial interés en el tratamiento del HCC con sorafenib”, dirigida por el Dr. D. Javier González Gallego y el Dr. D. Jose Luis Mauriz Gutiérrez, elaborada por D. Néstor Prieto Domínguez, y cuyo título en inglés es el siguiente “Modulation of selective and non-selective autophagy by melatonin in conditions of normoxia and hypoxia: potential interest in the treatment of HCC with sorafenib”.

Lo que firmo, en León a ___ de _____ de 2018.

La Secretaria del Programa de Doctorado,

Fdo.: Dña. Maria Jose Cuevas González

Vº Bº

La presidenta de la Comisión Académica,

Fdo.: Dña Maria Jesús Tuñón González


³ Solamente para las tesis depositadas en papel.



PROGRAMA ESTATAL DE PROMOCIÓN DEL TALENTO
Y SU EMPLEABILIDAD

CERTIFICADO DEL CENTRO RECEPTOR TRAS LA ESTANCIA BREVE O TRASLADO
TEMPORAL

CERTIFICATE OF STAY IN A FOREIGN INSTITUTION

1. Beneficiario/ Applicant:
Nombre y apellidos/ Name: Néstor Prieto Domínguez
D.N.I./ National identity Card: 71554077L
Centro de adscripción de la beca/ Home Institución: Instituto de Biomedicina (IBIOMED) de la Universidad de León, España.
2. Centro en el que se ha realizado la estancia/ Host institution:
Nombre/ Name: Dental College of Georgia, Medical College of Georgia, Augusta University
Dirección/ Address: 1120 15th Street, Augusta, GA 30912
Localidad/ Country: United States of America
3. Investigador responsable en el centro de la estancia/ Responsible person in the Host
Institución/ Institution: Department of Oral Biology, Dental College of Georgia; Department of Biochemistry and Molecular Biology, Medical College of Georgia
Nombre/ Name: Yong Teng
Cargo/ Post: Assistant Professor at Augusta University
CERTIFICO: que el becario arriba mencionado ha realizado una estancia en este centro en las siguientes fechas: desde 16 / 09 / 2017 hasta 15 / 12 / 2017
THIS IS TO CERTIFY: that the above mentioned person has performed a stay in this Institution in the following dates: From: 09 / 16 / 2017 To: 12 / 15 / 2017
Lugar y fecha: Augusta, 15/12/2017 City and date: Augusta 12/15/2017
Firma y Sello/ Signature & Stamp
 12/15/2017

Parte de los resultados presentados en la presente memoria han sido objeto de las siguientes publicaciones:

Ceramide metabolism regulates autophagy and apoptotic cell death induced by melatonin in liver cancer cells.

Ordóñez R, Fernández A, Prieto-Domínguez N, Martínez L, García-Ruiz C, Fernández-Checa JC, Mauriz JL, González Gallego, J.

Journal of pineal research, 2015;59(2):178-89

Factor de impacto: 10,391; 7/138 en Endocrinología y metabolismo (Q1)

Melatonin-induced increase in sensitivity of human hepatocellular carcinoma cells to sorafenib is associated with reactive oxygen species production and mitophagy.

Prieto-Domínguez N, Ordóñez R, Fernández A, Méndez-Blanco C, Baulies A, García-Ruiz C, Fernández-Checa JC, Mauriz JL, González-Gallego J.

Journal of pineal research, 2016;61(3):396-407

Factor de impacto: 10,391; 7/138 en Endocrinología y metabolismo (Q1)

Melatonin enhances sorafenib actions in human hepatocarcinoma cells by inhibiting mTORC1/p70S6K/HIF-1 α and hypoxia-mediated mitophagy.

Prieto-Domínguez N, Méndez-Blanco C, Carbajo-Pescador S, Fondevila F, García-Palomo A, González-Gallego J, Mauriz JL.

Oncotarget, 2017;8(53):91402-14

Factor de impacto: 5,168; 44/217 en Oncología (Q1)

Parte de los resultados de la presente memoria han sido objeto de las siguientes comunicaciones a congreso:

12th Annual Biotechnology Congress (BAC)- Congress of the Spanish Federation of Biotechnologists (FEBiotec). Girona (España) 11-13/07/2018

Inhibition of HIF-1 α /BNIP3 axis and hypoxia-mediated mitophagy by melatonin addition enhances human hepatocellular carcinoma cells sensitivity to sorafenib treatment.

Fondevila F, Méndez-Blanco C, Prieto-Domínguez N, Fernández-Palanca P, García-Palomo A, González-Gallego J, Mauriz JL.

XLIII Congreso Anual de la Asociación Española para el Estudio del Hígado (AEEH). Madrid (España) 21-23/02/2018

La inhibición de los factores HIF-1 α y HIF-2 α por el tratamiento con la melatonina incrementa la sensibilidad al sorafenib en células de hepatocarcinoma humano en cultivo

Méndez-Blanco C, Fondevila F, Prieto-Domínguez N, Carbajo-Pescador S, Fernández-Palanca P, Mauriz JL, González-Gallego J.

11th Annual Biotechnology Congress (BAC)- Congress of the Spanish Federation of Biotechnologists (FEBiotec). León (España) 12-14/07/2017

Melatonin downregulates hypoxia-inducible factor 1 α through inhibition of the mTOR/p70S6K signaling pathway in human hepatocarcinoma cells.

Méndez-Blanco C, Prieto-Domínguez N, Fondevila F, Carbajo-Pescador S, Mauriz JL, González-Gallego J.

XLII Congreso Anual de la Asociación Española para el Estudio del Hígado (AEEH). Madrid (España) 15-17/02/2017

La modulación de la vía de HIF-1 α y de la mitofagia por acción de la melatonina reduce la resistencia al sorafenib en células de hepatocarcinoma en hipoxia.

Prieto-Domínguez N, Méndez-Blanco C, Ordóñez R, Fondevila F, Fernández A, García-Palomo A, Mauriz JL, González-Gallego J.

XLI Congreso Anual de la Asociación Española para el Estudio del Hígado (AEEH). Madrid (España). 17-19/02/2016.

La combinación de melatonina y sorafenib incrementa la mitofagia e induce procesos de muerte celular en líneas tumorales humanas.

Fernández A, Ordóñez R, Prieto-Domínguez N, Méndez-Blanco C, García-Palomo A, Mauriz JL, González-Gallego J.

XXXVIII Congress of the Spanish Society of Physiological Sciences (SECF) Zaragoza (España) 13-16/09/2016.

Melatonin increases sorafenib sensitivity in Hep3B liver cancer cells through mitophagy induction

Ordóñez R, Fernández A, Prieto-Domínguez N, Méndez-Blanco C, García-Palomo A, Baulies A, García-Ruiz C, Fernández-Checa JC, Mauriz JL, González-Gallego J.

Oxygen Club of California (OCC) World Congress 2015. Valencia (España). 24-26/06/2015.

Acid sphingomyelinase activity but not de novo ceramide synthesis is implicated in the pro-apoptotic actions of melatonin on HepG2 hepatoma cells.

Ordóñez R, Fernández A, Martínez L, Núñez S, Carbajo-Pescador S, Baulies A, Prieto-Domínguez N, García-Ruiz C, Fernández-Checa JC, Mauriz JL, González-Gallego J.

50th The International Liver Congress 2015 by the European Association for the study of the liver (EASL). Viena (Austria). 22-26/04/2015.

Melatonin-induced apoptosis of HepG2 cells is enhanced by autophagy suppression.

Ordóñez R, Fernández A, Martínez L, Núñez S, Carbajo-Pescador S, Baulies A, Prieto-Domínguez N, García-Ruiz C, Fernández-Checa JC, Mauriz JL, González-Gallego J.

**XL Congreso Anual de la Asociación Española para el Estudio del Hígado (AEEH).
Madrid (España). 24-27/02/2015.**

La modulación de la autofagia inducida por la melatonina potencia su efecto apoptótico en células de hepatocarcinoma humano.

Ordóñez R, Fernández A, Martínez L, Núñez S, Carbajo-Pescador S, Baulies A, Prieto-Domínguez N, García-Ruiz C, Fernández-Checa JC, Mauriz JL, González-Gallego J.

XXXVII Congress of the Spanish Society of Physiological Sciences (SECF). Granada (España). 24-26/09/2014.

Melatonin causes an early induction of autophagy followed by enhanced ceramide metabolism

Ordóñez R, Fernández A, Carbajo-Pescador S, Prieto-Domínguez N, Mauriz JL, González-Gallego J.

Financiación

Durante la ejecución de la presente Tesis Doctoral, Néstor Prieto Domínguez ha sido beneficiario del programa “*Formación del Profesorado Universitario*” (FPU) del Ministerio de Educación, Cultura y Deporte (FPU13/04173) dentro del Programa Estatal de Promoción del Talento y su Empleabilidad, en el marco del Plan Estatal de Investigación Científica y Técnica y de Innovación 2013-2016 en I+D+i.

Además, el doctorando ha sido beneficiario del programa de concesión de ayudas complementarias para la realización de estancias breves y de traslados temporales destinadas a becarios activos FPU del Ministerio de Educación Cultura y Deporte (ST16/00783) dentro del Programa Estatal de Promoción del Talento y su Empleabilidad, en el marco del Plan Estatal de Investigación Científica y Técnica y de Innovación 2013-2016 en I+D+i con el objetivo de realizar una estancia breve en el *Department of oral biology*, perteneciente al *Dental College of Georgia* de la Universidad de Augusta, GA, EEUU desde el 16/09/2017 al 15/12/2017.

Esta Tesis Doctoral se enmarca dentro de una línea de investigación que ha contado con financiación de la Fundación de Investigación Sanitaria en León mediante los siguientes contratos de investigación: “*Estudio del papel de diversos factores de transcripción en la carcinogénesis hepática*” y “*Estudio del efecto de inhibidores de tirosín quinasas en la modulación de la supervivencia y muerte celular en diferentes tipos de cáncer*”

“La ciencia no sabe de países, porque el conocimiento le pertenece a la humanidad y es la antorcha que ilumina al mundo”.

*“Science knows no country, because knowledge belongs to humanity,
and is the torch which illuminates the world”*

Louis Pasteur

A todos aquellos que han estado a mi lado todos estos años

En especial a mis padres y a mi hermano

Agradecimientos

Hoy se cierra un capítulo de mi vida, y por lo tanto ha llegado el momento de dar gracias a todas las personas que me han apoyado durante mis años de Doctorado.

En primer lugar, quiero dar las gracias a mis directores y amigos, Dres. José Luis Mauriz Gutiérrez y Javier González Gallego, por haberme dado la oportunidad de permitirme realizar esta Tesis Doctoral. Muchas gracias por la confianza puesta en mí durante estos años, por vuestros consejos y por vuestro apoyo incondicional sobre todo en los momentos más duros.

A todos mis compañeros del área de Fisiología del Departamento de Ciencias Biomédicas de la Universidad de León, gracias por aconsejarme en el terreno académico y por enseñarme a desenvolverme con soltura en el terreno profesional. Nunca olvidaré los buenos consejos que he recibido de vosotros durante estos años.

Agradezco también los consejos dados por mis compañeros y compañeras del Instituto Universitario de Biomedicina (IBIOMED) de la Universidad de León. A Sara, Raquel y Anna por enseñarme todo sobre el trabajo en el laboratorio. A Vicky por levantarme el ánimo cuando lo necesitaba. A Diana por sus clases de conversación en inglés y por las charlas que siempre te sacaban una sonrisa, aunque fueran las ocho de la mañana. A Bárbara e Irene por aportarme grandes momentos día a día. A Brisa, Ester y David por los buenos ratos que hemos pasado en el despacho. A las chicas y chicos del grupo de la Dra. Carmen Marín, y a Carla e Irene por aportarme nuevos enfoques durante mi investigación. A Susana, Juancho, Tomás, Carlos y Rebeca por darme toda la ayuda técnica que necesitaba. A todos los becarios que han pasado por el laboratorio y con los que he compartido experimentos y buenos ratos. Gracias por aportar nuevas ideas al instituto.

Gracias a mis compañeras de grupo Carolina, Flavia y Paula, por todo vuestro apoyo durante estos años, tanto en el laboratorio como fuera de él. Por todos los buenos ratos que hemos pasado entre cultivos, Western blots y PCRs. Por ayudarme a superar los momentos difíciles con palabras de ánimo y de apoyo. ¡Esta experiencia no habría sido la misma sin vosotras!

To every member that constitutes the Department of Oral Biology of Augusta University (GA, USA), especially my teammates Liwei, Lie Lie and Xiangdong, thanks for making every day at Augusta enjoyable and for considering me as a new member of

your group for the first time. Thanks to my boss Dr. Yong Teng for trusting me from the first day I arrived in Augusta, as well as for the assistance received during the three months that I was there.

Muchas gracias a todos los que me han acompañado durante esta etapa de mi vida. Gracias a mis compañeros de la Banda Municipal de Música “Sones de Órbigo” de Veguellina de Órbigo, por ayudarme a crecer como persona durante los diez años que llevo como miembro de la misma, así como por los buenos momentos que hemos pasado juntos. Gracias a mis compañeros de la Banda y de la Orquesta de Juventudes Musicales de la Universidad de León, por los grandes momentos que hemos pasado durante los ensayos y los conciertos. ¡Me habéis ayudado mucho durante todos estos años!

Por último, y no por ello menos importante, dar las gracias a toda mi familia por ayudarme a superar los momentos difíciles que han ido surgiendo en el día a día. Gracias a mis padres por su apoyo incondicional, así como soportarme en los peores momentos. Gracias a mi hermano Mario por los ratos de relax que me ha brindado, y por apoyarme cuando las cosas se torcían. Gracias a mi prima Sara por ayudarme tanto personal como profesionalmente. Gracias a mis abuelos por servir como modelo para afrontar y superar las dificultades del día a día. Gracias a mis tíos y primos por estar siempre ahí cuando os he necesitado.

Espero que, en este nuevo capítulo de mi vida, me lleve donde me lleve, siga contando con el apoyo de todos vosotros.

“La gratitud convierte lo que tenemos en suficiente. Es la señal de las almas nobles”.

Esopo.

“Gratitude turns what we have into enough. Gratitude is the sign of noble souls”

Aesop.

General index

<i>List of figures</i>	<i>vii</i>
<i>List of tables</i>	<i>xvii</i>
<i>List of abbreviations</i>	<i>xix</i>
<i>Introduction and aims</i>	<i>1</i>
<i>Literature review</i>	<i>5</i>
1. Hepatocellular carcinoma.....	7
1.1. Etiology.....	9
1.2. Diagnosis.....	12
1.2.1. Imaging techniques.....	12
1.2.2. Diagnostic markers.....	14
1.2.3. Liver biopsy.....	15
1.3. HCC staging.....	15
1.4. HCC treatment.....	17
1.4.1. Curative treatments in HCC.....	18
1.4.2. Palliative treatments in HCC.....	18
2. Sorafenib.....	20
2.1. Sorafenib pharmacodynamics in cancer.....	21
2.2. Sorafenib pharmacokinetics and safety.....	24
2.3. Sorafenib resistance.....	25
2.3.1. Primary resistance to sorafenib.....	26
2.3.2. Acquired resistance to sorafenib.....	26
2.3.3. Mechanisms to overcome sorafenib resistance.....	28
3. Microenvironment and hypoxia in cancer progression. Role of HIFs.....	29
3.1. HIFs isoforms and structure.....	30
3.2. Regulation of HIFs.....	32
3.2.1. Oxidative regulation of HIF- α subunits.....	32
3.2.2. Oxygen-independent regulation of HIF- α subunits.....	34

3.3. <i>The balance between HIF-1α and HIF-2α in cancer progression under hypoxia</i>	37
4. Autophagy.....	38
4.1. <i>Types of autophagy</i>	39
4.2. <i>Molecular mechanism of autophagy</i>	41
4.2.1. <i>The generation of a novel autophagosome membrane</i>	41
4.2.2. <i>The elongation and the closure of the autophagosome membrane</i>	43
4.2.3. <i>Autophagosome and lysosome fusion</i>	47
4.3. <i>Modulation of autophagy by extracellular and intracellular stimuli</i>	49
4.3.1. <i>Nutrients, growth factors and energy deprivation stresses</i>	49
4.3.2. <i>Hypoxia, ceramides, oxidative and reticulum stresses</i>	51
4.4. <i>Role of autophagy in human pathologies</i>	53
5. Mitochondrial dynamics and mitophagy.	56
5.1. <i>Mitochondrial fusion</i>	57
5.2. <i>Mitochondrial fission</i>	58
5.3. <i>Mitophagy</i>	60
5.3.1. <i>The PINK1/Parkin pathway</i>	61
5.3.2. <i>The BNIP3/Nix pathway</i>	63
5.3.3. <i>The FUNDC1 pathway</i>	66
5.3.4. <i>Novel inductors of the mitophagy pathway</i>	66
5.3.5. <i>Role of mitophagy in human pathologies</i>	67
6. Apoptosis and its interrelation with autophagy.	69
6.1. <i>Intrinsic apoptosis pathway</i>	70
6.2. <i>Extrinsic apoptosis pathway</i>	72
6.3. <i>Crosstalk between autophagy and apoptosis</i>	73
7. Melatonin: structure, synthesis and functions.....	74
7.1. <i>Regulation of circadian rhythms by melatonin</i>	76
7.2. <i>Other effects of melatonin</i>	79
Material and methods	81
1. <i>Workspace</i>	83

2. Cell culture and reagents.	83
2.1. Cell culture.	83
2.2. Cell treatment and reagents.	83
3. Determination of cell viability and apoptosis.	84
3.1. MTT assay.	84
3.2. Annexin V-propidium iodide assay.	85
4. Determination of protein expression.	86
4.1. Western blot.	86
5. Determination of nucleic acid levels.	89
5.1. Reverse transcription quantitative polymerase chain reaction (RT-qPCR).	89
5.2. Mitochondrial DNA content.	90
6. Determination of mitochondrial damage.	91
6.1. ROS measurement.	91
6.2. JC-1 staining assay.	91
7. Immunofluorescence and laser confocal imaging.	92
7.1. Acridine orange staining assay.	92
7.2. LAMP2 and Tom20 colocalization.	93
8. Gene silencing.	94
9. Statistical analysis.	95
Results.	97
1. Effect of melatonin on autophagy response in HCC cells.	99
1.1. Melatonin stimulates a transient and complete autophagy response in HCC cells.	99
1.2. Melatonin induction of autophagy is dependent on the JNK pathway, but not on mTORC1 inhibition.	102
1.3. Melatonin-induced autophagy response exerts a prosurvival behavior in HCC cells.	103
2. Modulation of HCC cell sensitivity to sorafenib by melatonin under normoxia.	105
2.1. Melatonin enhances sorafenib cytotoxicity in HCC cells under normoxia.	105
2.2. Sorafenib and melatonin coadministration induces apoptotic response in Hep3B cells.	108
2.3. Sorafenib and melatonin coadministration induces mitochondrial turnover through mitophagy in Hep3B cells.	108

2.4. Sorafenib and melatonin coadministration stimulates oxidative stress and membrane depolarization in Hep3B cells.	113
2.5. Combined-treatment-induced mitophagy exerts a prodeath role in Hep3B cells.	114
3. Modulation of HCC cell sensitivity to sorafenib by melatonin under hypoxia.	115
3.1. Melatonin enhances sorafenib cytotoxicity in HCC cells under hypoxia.	115
3.2. Melatonin and sorafenib coadministration modulates the expression and activity of both HIF-1 α and HIF-2 α , leading to reducing Hep3B viability.	116
3.3. Melatonin enhances HIF-1 α protein synthesis, but does not modify its transcription or its degradation.	119
3.4. Melatonin restrains HIF-1 α translation by downregulating mTORC1/p70S6K pathway.	121
3.5. Melatonin and sorafenib coadministration inhibits hypoxia-induced mitophagy, which ultimately reduces Hep3B viability.	123
3.6. Melatonin and sorafenib coadministration under hypoxia induces apoptosis in HCC cells.	127
Discussion	129
1. Effects of melatonin treatment alone on autophagy response in HCC cells.	133
2. Effects of melatonin and sorafenib cotreatment under normoxia in HCC cells.	136
3. Effects of melatonin and sorafenib cotreatment under hypoxia in HCC cells.	142
Conclusions	149
Resumen en español	153
1. Introducción.	159
1.1. El cáncer hepatocelular (HCC por sus siglas en inglés).	159
1.2. El sorafenib.	160
1.3. Hipoxia y microambiente celular en la progresión cancerígena, papel de los factores inducibles por hipoxia (HIF).	162
1.4. La autofagia.	164
1.5. Dinámica mitocondrial y mitofagia.	166
1.5.1. Los procesos de fusión y fisión celular.	166
1.5.2. La mitofagia.	167
1.6. La apoptosis.	169
1.6.1. Interrelación entre la apoptosis y la autofagia.	170

1.7. <i>La melatonina</i>	170
2. Objetivos	173
3. Material y métodos	175
3.1. <i>Ámbito de trabajo</i>	175
3.2. <i>Cultivo celular, tratamientos y reactivos</i>	175
3.2.1. <i>Cultivo celular</i>	175
3.2.2. <i>Tratamientos celulares y reactivos usados</i>	175
3.3. <i>Ensayos de viabilidad celular y apoptosis</i>	176
3.3.1. <i>Ensayo MTT</i>	176
3.3.2. <i>Ensayo Anexina V-yoduro de propidio</i>	177
3.4. <i>Western blot</i>	177
3.5. <i>Técnicas de análisis de ácidos nucleicos</i>	178
3.5.1. <i>Reacción en cadena de la polimerasa cuantitativa con transcripción reversa (RT-qPCR por sus siglas en inglés)</i>	178
3.5.2. <i>Medida del contenido mitocondrial de ADN por reacción en cadena de la polimerasa cuantitativa (qPCR por sus siglas en inglés)</i>	179
3.6. <i>Determinación del daño mitocondrial</i>	179
3.6.1. <i>Medida de la producción de ROS</i>	179
3.6.2. <i>Medida del potencial de la membrana mitocondrial</i>	180
3.7. <i>Técnicas de microscopia confocal de barrido laser</i>	181
3.7.1. <i>Tinción con naranja de acridina</i>	181
3.7.2. <i>Colocalización entre LAMP2 y Tom20</i>	181
3.8. <i>Silenciamiento génico</i>	182
3.9. <i>Análisis estadístico</i>	183
4. Resultados y discusión	184
4.1. <i>Efecto de la melatonina sobre la respuesta autofágica en las células de HCC</i>	186
4.1.1. <i>La melatonina induce una repuesta autofágica transitoria y completa en las células de HCC</i>	186
4.1.2. <i>La inducción de la autofagia por la melatonina es dependiente de la vía de JNK, pero no de la de mTORC1</i>	187

4.1.3. La autofagia inducida por la melatonina protege a las células tumorales frente a la muerte celular.....	188
<i>4.2. La melatonina es capaz de modular los efectos citotóxicos del sorafenib en las células de HCC mantenidas en normoxia.</i>	<i>189</i>
4.2.1. La melatonina estimula la capacidad citotóxica del sorafenib en las células HCC mantenidas en normoxia.....	189
4.2.2. La coadministración de sorafenib y melatonina induce la activación de la apoptosis en las células Hep3B.....	190
4.2.3. La coadministración de melatonina y sorafenib induce la degradación mitocondrial a través de la mitofagia en las células Hep3B.....	191
4.2.4. La mitofagia inducida por la coadministración de melatonina y de sorafenib induce la despolarización mitocondrial y la acumulación de ROS en las células Hep3B.....	194
4.2.5. La mitofagia inducida por la coadministración de melatonina y sorafenib potencia la muerte de las células Hep3B.....	195
<i>4.3. La melatonina es capaz de modular los efectos citotóxicos del sorafenib en las células de HCC mantenidas en hipoxia.....</i>	<i>196</i>
4.3.1. La melatonina estimula la capacidad citotóxica del sorafenib en las células HCC mantenidas en hipoxia.....	196
4.3.2. La coadministración de melatonina y de sorafenib modula la expresión y la actividad de HIF-1 α y HIF-2 α , lo cual reduce la viabilidad de las células Hep3B.....	197
4.3.3. La melatonina estimula la síntesis proteica de HIF-1 α , pero no es capaz de modificar ni su transcripción ni su degradación.....	199
4.3.4. La melatonina restringe la síntesis proteica de HIF-1 α al desregular la vía de mTORC1/p70S6K.....	199
4.3.5. La coadministración de melatonina y de sorafenib inhibe la mitofagia inducida por la hipoxia, lo cual lleva a la reducción de la viabilidad celular.....	201
5. Conclusiones.....	205
References	207

List of figures

-
- Figure 1:** Estimated age-standardized liver cancer incidence rate worldwide according to the results obtained by GLOBOCAN 2012 study. Copyright from World Health Organization (WHO), 2018. All Rights Reserved. Available from <http://gco.iarc.fr/today/home> (Consulted on 28/01/2018). 7
- Figure 2:** Sequential changes in liver during hepatic carcinogenesis and HCC progression. All chronic damage processes finish with the generation of a cirrhosis in the liver. In this environment, some cells can become carcinogenic and start to proliferate without control, generating a tumor. HCC passes for three different sequential steps: dysplastic nodule, early HCC and advanced HCC according to the number of genes mutated in those cells and to their grade of dedifferentiation. Concomitant with this process, there are an increment of neovascularization of tumor, which is more evident in advanced phases. Finally, advanced HCC cells are able to break the extracellular matrix and invade other organs, generating secondary tumors. The dashed arrow represents the little number of tumors that curse without previous cirrhosis. Retrieved from [13]. 8
- Figure 3:** Leading imaging techniques used for the diagnostic of HCC. **(A)** Abdominal transverse US sonogram shows a hypothetical tumor mass in the right lobe of the liver. **(B)** The late arterial phase of multi-detector computed tomography visualizes an HCC as an enhanced nodule (white arrows). **(C)** The arterial phase of dynamic MRI shows a tumor mass adjacent to portal vein (white arrow). **(D)** Detection of a hepatic tumor by hepatic angiography as a hyper-vascular zone into the liver. Retrieved from [44]. 13
- Figure 4:** The BCLC staging algorithm for HCC staging and diagnosis. BCLC scale divides liver tumors into 5 different stages, 0, A, B, C and D; depending on tumor size and on the liver functionality that remains in carcinogenic cells. Additionally, this scale also includes the first-line treatment recommended for each of the stages. LT means liver transplant; PS, performance status; and BSC, best supportive care. Retrieved from [64]. 17
- Figure 5:** Molecular mechanisms through sorafenib restrains HCC progression **(A)** Sorafenib is able to reduce cell proliferation in HCC cells through inhibiting Raf transduction ability, which in turn restrain MAPK/ERK1 pathway activation. This repression ultimately leads to diminishing cyclin D1 levels by Myc-1 inhibition. Otherwise, this drug can also induce the intrinsic pathway of apoptosis through impeding the translation of Myc-1 protein, an antiapoptotic agent which is in charge of restraining Bak activation. **(B)** Sorafenib can restrain tumor angiogenesis through impeding the substrate-induced autophosphorylation and activation of VEGFR-2, VEGFR-3 and PDGFR- β in tumor-associated vascular endothelial cells, which prevents the expression of proangiogenic genes through the induction of MAPK/ERK1 pathway. (Sor): sorafenib. Modified and retrieved from [81]. 22
- Figure 6:** Cellular pathways involved in the stimulation of autophagy by sorafenib. Sorafenib can induce autophagy pathway through the modulation of multiple mediators and pathways in tumor cells. This chemotherapeutic drug can induce AMPK pathway by the reduction of ATP content and the

increment of ROS, reducing mTORC1 phosphorylation by Raptor phosphorylation, which ultimately leads to induce autophagy pathway. Raptor could repress mTORC1 phosphorylation directly or indirectly through increasing the formation of mTORC2 (mammalian/mechanistic target of rapamycin complex 2). Furthermore, sorafenib could also stimulate autophagy pathway by inducing a misbalance between ceramide/S1P levels, as well as by enhancing UPR expression and calcium release from the ER (endoplasmic reticulum). Finally, sorafenib could also augments autophagy by decreasing miR30 α expression, which has been described as a Beclin1 repressor. Retrieved from [90]...... 23

Figure 7: Molecular mechanisms that reduce cell sensitivity to sorafenib in HCC cells. These mechanisms could be divided into two groups depending on the moment when their starting since the beginning of the treatment. Primary resistance mechanisms usually appear at the start of sorafenib administration and are related to changes in the expression of some proteins due to the genetic heterogeneity of HCC cells. The overexpression of JNK, VEGFA and EGFR; as well as the reduction of ERK phosphorylation are biomarkers of sorafenib primary resistance. On the other hand, the time-prolonged sorafenib administration generates an acquired resistance to that drug in HCC cells, due to the stimulation of cellular pathways and mechanisms which mask the action of sorafenib, such as autophagy, EMT, Akt/mTOR or JAK/STAT3. Retrieved from [108]. 27

Figure 8: Structure and domain organization of the main HIF subunits. Canonical HIF proteins are constituted by a bHLH domain, which recognizes the HRE sequence; two different PAS domains, which are responsible for HIF heterodimerization; two TAD zones, which activate HIF-related transcription and are intimately regulated by oxygen; as well as two different NLS sequences which import these transcriptional factors into the nucleus. Additionally, HIF- α subunits present a unique ODD domain that overlaps N-TAD, in which oxidative regulation of these factors is taken place. Finally, HIF-3 α does not have the C-TAD domain, while HIF-1 β lacks the N-TAD one. The percentages displayed under each domain indicates the degree of amino acid homology which exists between a domain and its equivalent in HIF-1 α . Retrieved from [144]. 31

Figure 9: Regulation of the transcriptional activity of the main oxygen-sensitive HIF subunits by PHDs and FIH. When the O₂ concentration is high in the medium, both PHDs and FIH are active, leading to the downregulation of the transcriptional activity of HIF- α subunits by the hydroxylation of some key proline and asparagine residues situated in the ODD domain and in the C-TAD domain of these transcription factors respectively. These modifications ultimately result in the proteolytic degradation of these oxygen-sensitive mediators through a pVHL-, ubiquitin-, proteasome-dependent process; as well as in the blockage of p300 and CBP recruitment, which are their specific transcriptional coactivators. Oppositely, when hypoxia is induced in the cell media, these HIF hydroxylases are inactive, thus HIF- α subunits can bind with their specific coactivators p300 and CBP and with the oxygen-independent HIF- β subunit, inducing finally the HIF transcriptional activity. Modified from [154]. 33

Figure 10: Oxygen-dependent and -independent regulation of the transcription, translation and degradation of the most important HIF- α subunits. The stimulation of the PI3K/Akt/mTOR and MAPK/ERK

pathways modulates the translation levels of HIF-1 α through inducing the overactivation of p70S6K and eIF-4E, whereas HIF-2 α is mainly activated through PI3K/mTORC2 pathway. On the other hand, HIF- α homologs are degraded in an oxygen-dependent manner through the dependent hydroxylation of some proline residues, leading to their elimination by the ubiquitin-proteasome system. Besides, p53 also triggers another degradation system of HIF-1 α by a proteasome-dependent, oxygen-independent mechanism, which might involve the Mdm2 protein. Otherwise, JNK promotes the stimulation of HSP90 protein, which in turn has been shown to stabilize the HIF-1 α protein in an oxygen-independent manner. Additionally, extracellular stimuli could induce the activation of MAPK/ERK, which in turn can stimulate the binding between HIF-1 α and p300, whereas FIH impedes this process through the hydroxylation of an asparagine residue in the C-TAD domain of both HIF- α proteins, but principally in HIF-1 α . Finally, SIRT1 deacetylase restrains HIF-1 α activation, but enhances HIF-2 α binding to p300 through the elimination of a specific acetyl posttranslational modification..... 36

Figure 11: Differences among the principal selective and non-selective autophagy variants. Macromolecules and organelles could be included into the lysosome through CMA, microautophagy (right pathways) or macroautophagy (left pathways). Non-selective microautophagy engulfs the cytoplasmic content through the generation of a membrane invagination that introduces the cargo into the lysosome. Selective micromitophagy, micropexophagy and piecemeal microautophagy of the nucleus insert little amounts of mitochondria, peroxisomes and nucleus respectively into the lysosome by microautophagy. On the other hand, CMA introduces specifically proteins with the domain KFERQ into the lysosome through the pore created by the protein LAMP2A in its membrane. Finally, macroautophagy carries macromolecules to its degradation through the formation of an additional vesicle, whose name is autophagosome, which subsequently fuses with the lysosomes. This pathway may be known as mitophagy, pexophagy, aggrephagy, reticulophagy or xenophagy, if respectively mitochondria, peroxisomes, protein aggregates, endoplasmic reticulum or pathogens undergoes macroautophagy. Retrieved from [204]..... 39

Figure 12: Molecular process involved in autophagosome formation, closure, docking and fusion with lysosomes. Different stimuli, such as hypoxia, ER stress, oxidative stress and nutrient depletion lead to the activation of the ULK1 complex which is responsible for autophagy induction. This activation is mainly inhibited by mTORC1, which is mainly activated by PI3K/Akt pathway. ULK1 complex phosphorylates AMBRA1, leading to the activation of the Beclin1/Vps34 system and to translocate it from the microtubules to the nascent autophagosome, where it starts to increase the content of PI3P in the membrane. Subsequently, this membrane starts to elongate by the action of the complexes Atg9-Atg18, which bring new vesicles to the formation site, and by the two ubiquitin-like systems Atg12-Atg5-Atg16L and LC3-II. In addition, LC3-II is also responsible for the cargo selection and for the autophagosome closure. Then, this structure fuses with a lysosome to achieve the degradation of the autophagosome content. Retrieved from <http://www.genetex.com/Web/Pathway/Autophagy-Pathway-39> (27/03/2018)..... 43

- Figure 13:** SNARE-dependent mechanism of lysosome and autophagosome fusion. STX17 is the main protein that mediates the fusion process between autophagosomes and lysosomes. This molecule arises in the mature autophagosome membrane through an unknown mechanism and catalyzes the binding of these two structures by associating through SNAP-29 to the lysosomal protein VAMP8. Atg14L joins to STX17 and stabilizes the whole complex. On the other hand, the fraction of Rab7 that is in the lysosome membrane can also bind to STX17 through RILP and HOPS, conforming a secondary tethering complex that approximates both vesicles prior to their fusion. Retrieved from [252]. 48
- Figure 14:** Role of autophagy in different human pathologies. Autophagy modulates the progression of many organ-specific and multi-systemic diseases. The pathologies in which primary autophagy defects has been reported are marked in red, whereas those in which autophagy deficiencies present a more secondary role or are generated by the disease are labeled in green. Autophagy-related gene mutations (m), polymorphisms (p) and haplo-insufficiencies (h) in each respective disease are labeled in blue. Retrieved from [288]. 54
- Figure 15:** Molecular mechanisms involved in mitochondrial fusion and fission processes. Tethering and fusion of the OMM are mediated by MFNs, whereas the heterodimer OPA1-CL mediates IMM fusion. Fission process is mainly mediated by the protein Drp1, which is recruited to the mitochondrion, where oligomerizes to form a helix structure that surrounds this organelle. Subsequently, the narrowing of this ring disrupts both mitochondrial membranes. Retrieved from [311]. 59
- Figure 16:** Description of the main pathways that induce the degradation of mitochondria in autophagosomes. **(A)** PINK1 is stabilized in the OMM after mitochondrial depolarization, where phosphorylates ubiquitin and MFN2. This process leads to the mitochondrial recruitment and activation of Parkin, which starts to ubiquitylate many OMM proteins. Subsequently, mitophagy receptors AMBRA1, p62 and OPTN, which are attracted to the OMM in response to the previous mechanism, interact with LC3 and target mitochondria to the nascent autophagosome. Moreover, it has been shown that OPTN and NDP52 can be recruited to the mitochondria by PINK1. **(B)** BNIP3 and Nix are induced under low oxygen conditions and are integrated to the OMM, where interact with LC3 at the nascent autophagosome and target mitochondria for degradation. In addition, BNIP3 activity is regulated at the post-transcriptional level by the phosphorylation of certain serine residues in its N-terminal region. **(C)** Under non-stress conditions, the OMM transmembrane protein FUNDC1 is inhibited through the phosphorylation of its T18 by Src. Hypoxia can revert this process, which allows its interaction with LC3 at the nascent autophagosome to introduce damaged mitochondria for degradation. Besides, CK2-dependent phosphorylation of FUNDC1 at S13 and its dephosphorylation by PGAM5 constitutes a secondary mechanism in the regulation of this mitophagy factor. **(D)** Bcl-2-L-13 induces Drp1-independent mitochondrial fission and targets mitochondria to the autophagosome by interacting with LC3. Retrieved from [331]. 65
- Figure 17:** Role of mitophagy in disease. Both PINK1/Parkin and BNIP3/Nix pathway collaborate in the induction of mitophagy pathway in response to different stress stimuli, such as mitochondrial

depolarization, hypoxia or nutrient deprivation. Mitophagy protects cells against several pathological processes, such as cancer, Parkinson's disease, aging-related type II diabetes (aging) and inflammation, through preventing ROS production, mitochondrial dysfunction, inflammasome activation and lipid accumulation amongst others. Retrieved from [347]. 68

Figure 18: Molecular mechanisms that induce extrinsic and intrinsic apoptosis pathways. In the extrinsic apoptotic pathway, death receptors, such as TRAILR1 and FAS can activate initiator caspases 8 and 10 when their specific death ligand is bounded. These initiator enzymes cleave the effector caspases 3 and 7, which ultimately leads to enhancing apoptosis. In the intrinsic apoptotic pathway, the activation of certain BH3-only proteins upon an intern stress triggers MOMP due to their ability to enhance the oligomerization of Bax and Bak in the OMM. This process is restrained by antiapoptotic Bcl-2 family members. The release of cytochrome c to the cytosol specifically activates APAF1, stimulating its oligomerization and the formation of the apoptosome. This complex enhances the action of caspase 9, which in turn activates effector caspases 3 and 7. Other secondary autophagy mediators, such as SMAC/Diablo, will prevent the caspase-inhibitory action of XIAP. Caspase 8-dependent cleavage of BH3-only protein BID to constitute tBID, which is its functional derivative, suggests the existence of a crosstalk between both pathways. Retrieved from [370]. 71

Figure 19: Mechanism that controls melatonin synthesis in mammals. The SCN detects changes in the amount of light that incides on the retina, sending an electrical signal to the pineal gland under dark conditions. This signal passes through the PVN, the upper thoracic intermediolateral cell column and the SCG to pineal noradrenergic (NA) receptors. This induction leads to increment the content of cAMP into the pinealocyte, which ultimately leads to increase melatonin synthesis by inducing the activity of AANAT. Retrieved from [384]. 77

Figure 20 Effects of melatonin administration on the expression of different autophagy markers and on the autophagic flux in HepG2 cells. **(A)** p62 and LC3-I/II levels were analyzed by Western blot at 2, 4, 8, 12, 18 and 24 h after 1 mM melatonin (Mel) administration. Immunoblots were quantified by using ImageJ software and the results were expressed as band density/ β -actin density vs control group (0 h). **(B)** Beclin1, LC3 and Atg3 mRNA levels were analyzed by RT-qPCR assay using the same conditions as Western blot technique. Data were expressed as mean values of arbitrary units (a.u.) \pm SD of three different experiments. * $p < 0.05$ vs control (0 h). **(C)** The effects of 2 mM melatonin administration for 8 h on autophagy flux was measured by adding either chloroquine 50 μ M (CQ) or bafilomycin A1 100 nM (Baf A1) 4 h before the end of the treatment. LC3 representative immunoblot was quantified by using ImageJ software and the results were expressed as band density/ β -actin density vs control group (0 h). 100

Figure 21: Effect of melatonin administration on autophagosome formation in HepG2 cells measured by acridine orange assay. Representative confocal images show the results of this technique after 4, 8, 12, 24 and 48 h of 1 mM melatonin (Mel) treatment. Red and green dot areas were measured by using ImageJ software, and the data were expressed as the R/GFIR vs control (0 h) of the representative confocal images. * $p < 0.05$ vs control (0 h). 101

Figure 22: Effects of melatonin on the principal inductors of the autophagy pathway. **(A)** mTORC1 and Beclin1 proteins levels were analyzed by Western blot technique at short time periods (until 120 minutes) after 2 mM melatonin (Mel) treatment. **(B)** The levels of these two proteins were also evaluated at long time periods (from 2 to 24 h) after the administration of this indoleamine. **(C)** grp78 and p-JNK protein levels were analyzed by Western blot assay from 0.5 to 8 h of 2 mM melatonin treatment. **(D)** The JNK phosphorylation repressor SP600125 (10 μ M) was added 1 h prior to the administration of 2 mM melatonin and cells were collected after 2, 4 and 8 h of treatment. LC3 protein levels were measured by Western blot. Representative immunoblots were quantified by using ImageJ software and the results were expressed as band density/ β -actin density vs control group (0 h)..... 102

Figure 23: Effect of Atg5 silencing on melatonin-induced autophagy. **(A)** The efficiency of Atg5 silencing was measured by RT-qPCR of this gene at 24 and 48 h after cell silencing. Data were expressed as a percentage of mean values of arbitrary units (a.u.) \pm SD of three different experiments. * p <0.05 vs non-silenced cells (siRNA control group). **(B)** Atg5, p62 and LC3 protein levels were measured by Western blot technique after 24 h of Atg5 silencing and/or 8 h of 2 mM melatonin (Mel) treatment. Representative immunoblots were quantified by using ImageJ software and the results were expressed as band density/ β -actin density vs non-silenced and non-treated cells (siRNA control group). 104

Figure 24: Effects of Atg5 silencing on melatonin-induced HCC cell death. **(A)** HepG2 cells were incubated with either 1 or 2 mM of melatonin (Mel) during 48 h in presence or absence of the specific siRNA against Atg5. Viability was analyzed by MTT. Data were expressed as a percentage of the mean value \pm SD of three different experiments. * p <0.05 vs non-treated and non-silenced cells, ** p <0.05 vs non-treated and silenced cells, # p <0.05 between non-silenced and silenced cells treated with the same melatonin concentration. **(B)** The effect of *Atg5* gene silencing on PARP cleavage was measured by Western blot technique after 8, 24, 36 and 48 h of 2 mM melatonin treatment. Representative immunoblots were quantified by using ImageJ software and the results were expressed as band density/ β -actin density vs non-silenced and non-treated cells..... 105

Figure 25: Effects of either melatonin or sorafenib single treatment on the viability of three different HCC cell lines. Variations in HepG2, Hep3B and Huh7 cell death were analyzed by using MTT assay after 48 h of melatonin (Mel) (0.1, 0.5, 1 or 2 mM) or sorafenib (Sfb) (0.01, 0.05, 0.1, 1, 2.5, 5, 10 and 50 μ M) treatment. Data were expressed as a percentage of the mean value \pm SD of three different experiments. * p <0.05 vs Control group. 106

Figure 26: Effects of melatonin and sorafenib combined treatment on the viability of three different HCC cell lines. Variations in HepG2, Hep3B and Huh7 cell death were analyzed by using MTT assay after 48 h of melatonin (Mel) (1 or 2 mM), sorafenib (Sfb) (2.5, 5, 10 μ M) or melatonin plus sorafenib treatment. Data were expressed as a percentage of the mean value \pm SD of three different experiments vs control. * p <0.05 vs Control group. 107

Figure 27: Effects of melatonin and sorafenib combined treatment on apoptotic cell death in Hep3B cells. **(A)** PARP and Bax protein levels were measured by Western blot assay after 12, 24 and 48 h of

2.5 μ M sorafenib (Sfb) treatment alone or in combination with 1 mM melatonin (Mel). Representative immunoblots were quantified by using ImageJ software and the results were expressed as band density/ β -actin density vs control cells (0 h group). **(B)** Flow cytometric analysis of cell viability was performed with a commercial Annexin V-IP kit at 48 h after 2.5 μ M sorafenib and/or 1 mM melatonin administration. **(C)** Annexin V-negative, PI-negative cells are represented as a percentage of the mean value \pm SD of three different experiments. * p <0.05 vs non-treated group..... 109

Figure 28: Effects of melatonin and/or sorafenib administration on mitochondria and lysosome colocalization. **(A)** Representative confocal images show colocalization between Tom20 and LAMP1 in Hep3B cells at 6, 12 and 24 h after 2 mM melatonin (Mel) and/or 2.5 μ M sorafenib (Sfb) treatment. **(B)** Average normalized mean deviation product (nMDP) value was obtained by using ImageJ software with the Colocalization Colormap plugin and was represented as a percentage of the mean value \pm SD of three different experiments. * p <0.05 vs control group, # p <0.05 vs melatonin-treated group at the same time point, † p <0.05 vs sorafenib-treated group at the same time point..... 110

Figure 29: Effects of sorafenib treatment alone or in combination with melatonin on the expression of the main autophagy and mitophagy markers. **(A)** Time course of PINK1 and Parkin were measured by Western blot technique at 3, 6, 12, 24 and 48 h after 2.5 μ M sorafenib (Sfb) treatment alone or in combination with 1 mM melatonin (Mel). **(B)** The variations in the expression of LC3 were analyzed by Western blot technique after 3, 6, 12 and 24 of sorafenib and sorafenib plus melatonin treatment. Representative immunoblots were quantified by using ImageJ software and the results were expressed as band density/ β -actin density vs control cells (0 h group). 111

Figure 30: Effects of melatonin and/or sorafenib treatment on mitochondrial dynamics and biogenesis. **(A)** MFN-2, OPA1 and Fis1 levels were measured by Western blot technique at 3, 6, 12 and 24 h after 2.5 μ M sorafenib (Sfb) alone or in combination with 1 mM melatonin (Mel). Representative immunoblots were quantified by using ImageJ software and the results were expressed as band density/ β -actin density vs control cells (0 h group). **(B)** mtDNA content was measured by using qPCR after 6, 12 and 24 h of treatment. mtDNA/ncDNA ratio was represented as a percentage of the mean value \pm SD of three different experiments. * p <0.05 vs control group. HSP60 levels were analyzed by using Western blot assay at 3, 6, 12 and 24 h after 2.5 μ M sorafenib alone or in combination with 1 mM melatonin. Representative immunoblots were quantified by using ImageJ software and the results were expressed as band density/ β -actin density vs control cells (0 h group). 112

Figure 31: Analysis of ROS production and membrane polarization statuses after sorafenib and/or melatonin administration. **(A)** The amount of harmful ROS was measured by DCF-DA quantification in Hep3B cells treated with sorafenib (Sfb) (2.5 μ M) and/or melatonin (Mel) (1 and 2 mM) for 1, 3 and 6 h. DCF-DA intensity was represented as a percentage of the mean value \pm SD of three different experiments. * p <0.05 vs 0 h groups in each treatment **(B)** Changes in mitochondrial membrane potential were measured using JC-1 fluorometric assay in Hep3B cells treated with

sorafenib (2.5 μ M) and melatonin (1 and 2 mM) for 1, 3 and 6 h. JC-1 aggregates /JC-1 monomers fluorescent ratio was represented as a percentage of the mean value \pm SD of three different experiments vs Control. * p <0.05 vs 0 h groups in each treatment..... 113

Figure 32: Effects of Parkin silencing on Hep3B viability and apoptosis after melatonin and/or sorafenib treatment. **(A)** Cell viability from silenced and non-silenced cells was analyzed by using MTT assay at 48 h after being treated with either 2.5 μ M sorafenib, 1 mM melatonin or combination of both compounds. Data were expressed as a percentage of the mean value \pm SD of three different experiments. * p <0.05 vs non-treated group, # p <0.05 vs non-silenced cells with the same treatment. **(B)** PARP and Bax protein levels were measured by Western blot technique after 24 and 48 h of treatment in presence or in absence of Parkin siRNA. Representative immunoblots were quantified by using ImageJ software and the results were expressed as band density/ β -actin density vs non-treated and non-silenced cells. 114

Figure 33: Effects of melatonin and/or sorafenib single and combined administration on Hep3B cell viability under basal and low oxygen conditions. Cells were maintained under normoxia (Nx) or hypoxia (Hx) for 48 h with or without sorafenib (Sfb) (2.5, 5 or 10 μ M) and/or melatonin (Mel) (1 or 2 mM). Cell viability was determined with MTT assay. Data were expressed as a percentage of the mean value \pm SD of three different experiments. * p <0.05 vs non-treated cells under the same oxygen concentration..... 116

Figure 34: Effects of melatonin and/or sorafenib treatment on HIF-1 α and HIF-2 α expression and activity. **(A)** Hep3B cells incubated under normoxia (Nx) or hypoxia (Hx) by adding 100 μ M CoCl₂ were treated with 5 μ M sorafenib (Sfb) and/or 2 mM melatonin (Mel) for 24 h. HIF-1 α , HIF-2 α and VEGF expression were measured by using Western blot technique. **(B)** Hep3B cells were preincubated with 100 μ M CoCl₂ to induce hypoxia for 3 h (lane 2), being subsequently treated with 2 mM melatonin for 1.5 and 3 h (lane 3 and 4). Finally, melatonin was removed and cells were maintained under hypoxic conditions for 1.5 and 3 h (lanes 5 and 6). Lane 1 shows cells under normoxia. HIF-1 α levels were measured by Western blot assay. Representative immunoblots were quantified by using ImageJ software and the results were expressed as band density/ β -actin density vs normoxia group (Nx)..... 117

Figure 35: Analysis of HIF-1 α repercussion on the cytotoxic effects of sorafenib and melatonin administered alone or in combination. **(A)** HIF-1 α and HIF-2 α expression levels were measured through Western blot technique at 48 h post-silencing. **(B)** HIF-1 α and BNIP3 expression were measured by Western blot assay at 48 h after 5 μ M sorafenib (Sfb) administration in absence or presence of 2 mM melatonin (Mel). Representative immunoblots were quantified by using ImageJ software and the results were expressed as band density/ β -actin density vs non-silenced cells under normoxia. **(C)** Cell viability from silenced and non-silenced cells was measured by using MTT assay 48 h after melatonin and/or sorafenib administration. Data were expressed as a percentage of the mean value \pm SD of three different experiments. * p <0.05 vs non-treated and non-silenced cells. 118

Figure 36: Effects of melatonin single administration on the transcription of HIF-1 α and on the release of ROS. **(A)** HIF-1 α mRNA levels were measured by RT-qPCR in Hep3B cells at 0, 1.5, 3 and 6 h

after normoxia (Nx), hypoxia (Hx) or hypoxia plus 2 mM melatonin (Mel). Data were expressed as a percentage of the mean values of arbitrary units (a.u.) \pm SD of three different experiments. * $p < 0.05$ vs cells under Nx at the same time point (siRNA control group). **(B)** ROS production was analyzed by DCF-DA quantification in Hep3B cells treated with melatonin (2 mM) and/or NAC (5 mM) for 0, 3 and 6 h. DCF-DA intensity was represented as a percentage of the mean value \pm SD of three different experiments vs Nx 0 h. * $p < 0.05$ at the same time point, # $p < 0.05$ vs Hx at the same time point..... 119

Figure 37: Effects of melatonin treatment on HIF-1 α protein synthesis and degradation. **(A)** Changes in HIF-1 α synthesis were analyzed by Western blot assay in Hep3B cultured under normoxia (Nx) and hypoxia (Hx) and treated with or without 2 mM melatonin (Mel) and either 10 μ M MG132 or 1 mM DMOG for 0, 1.5, 3 and 6 h. **(B)** Variations in HIF-1 α degradation were analyzed by Western blot assay in Hep3B cultured under normoxia (Nx) and hypoxia (Hx) and treated with or without 2 mM melatonin, 10 μ M MG132 and/or 100 mM CHX for 6 h. Representative immunoblots were quantified by using ImageJ software and the results were expressed as band density/ β -actin density vs Nx group..... 120

Figure 38: Effects of melatonin single treatment on the PI3K/Akt/mTORC1 pathway and its impact on HIF-1 α expression. **(A)** Hep3B cells were treated with 100 μ M CoCl₂ to mimic hypoxia (Hx) alone or in combination with 2 mM melatonin (Mel) for 1, 3 and 6 h. Lane 1 shows protein basal levels under normoxia (Nx) (B) and (C) 20 nM rapamycin or 50 μ M LY294002 alone or in combination with 2 mM melatonin were administered to Hep3B cells under hypoxia. Protein levels of HIF-1 α , p-mTORC1, p-mTORC2, p-Akt, p-RP-S6, and p-p70S6K were measured by Western blot. Representative immunoblots were quantified by using ImageJ software and the results were expressed as band density/ β -actin density vs Nx group..... 122

Figure 39: Effects of melatonin and/or sorafenib treatment on hypoxia-induced mitophagy and role of this response in sorafenib cell resistance. **(A)** BNIP3 and Nix protein levels were measured by Western blot assay at 24 h after 2 mM melatonin (Mel) and/or 5 μ M sorafenib (Sfb) treatment under hypoxia (Hx). Lane 1 shows basal protein levels under normoxia (Nx). Representative immunoblots were quantified by using ImageJ software and the results were expressed as band density/ β -actin density vs Nx group. **(B)** Cell viability from silenced and non-silenced cells was measured by using MTT assay 48 h after melatonin and/or sorafenib administration. Data were expressed as a percentage of the mean value \pm SD of three different experiments. * $p < 0.05$ vs non-treated control cells. # $p < 0.05$ vs non-silenced cells in each treatment..... 124

Figure 40: Effects of sorafenib treatment in presence or absence of melatonin under hypoxia on mitochondrial and lysosomal colocalization. **(A)** Representative confocal images show the colocalization between mitochondria and lysosomes in Hep3B cells at 6, 12 and 24 h after 2 mM melatonin (Mel) and/or 2.5 μ M sorafenib (Sfb) treatment under hypoxia (Hx). Basal levels of mitophagy response under normoxia (Nx) are used as control values **(B)** Average positive normalized mean deviation product (nMDP) value was obtained by using ImageJ software with the Colocalization Colormap plugin and was represented as a percentage of the mean value \pm SD of three different experiments.

*p<0.05 vs Nx group at the same time point, #p<0.05 vs Hx group at the same time point, † p<0.05 vs Sorafenib-treated group at the same time point. 125

Figure 41: Effects of sorafenib and/or melatonin treatment under hypoxia on the expression of main autophagosome markers, as well as on autophagy flux. **(A)** LC3-II and p62 protein levels were assessed by Western blot assay at 6, 12 and 24 h post-treatments with 5 µM sorafenib (Sfb) and/or 2 mM melatonin (Mel) under hypoxia (Hx). Lane 1 shows basal levels of these proteins under normoxia (Nx). **(B)** LC3 and p62 expression were measured by Western blot assay at 12 h for the indicated treatments in presence or absence of 5 µM bafilomycin A1 (Baf A1) for the last 3 h. Representative immunoblots were quantified by using ImageJ software and the results were expressed as band density/β-actin density vs Nx group. 126

Figure 42: Effects of melatonin and/or sorafenib administration under hypoxia on the main markers of the intrinsic apoptosis pathway. PARP and Bax levels were measured by Western blot technique at 6, 12, 24 and 48 h after 5 µM sorafenib (Sfb) and/or 2 mM melatonin (Mel) under hypoxia (Hx) conditions. Lane 1 shows basal protein expression levels under normoxia (Nx). Representative immunoblots were quantified by using ImageJ software and the results were expressed as band density/β-actin density vs Nx group. 127

Figure 43: Proposed model of melatonin induction of autophagy in HCC cells. Melatonin induced prosurvival autophagy response through inducing JNK phosphorylation and ER stress, which ultimately displaces Beclin1 and Bcl-2 binding. However, it does not stimulate this pathway by inhibiting mTORC1 signaling. 135

Figure 44: Proposed model of mitophagy induction after melatonin and sorafenib cotreatment under normoxia. Sorafenib addition to Hep3B cells induces the loss of the basal mitochondrial membrane potential, while melatonin administration enhances the accumulation of ROS species in the mitochondria. These two events stabilize PINK1 in the OMM, inducing the recruitment of the E3 ligase Parkin to this membrane. This system introduces the mitochondria in the autophagosome for its degradation by ubiquitinating multiple OMM substrates, such as MFN2. Besides, melatonin administration diminishes the expression of the main mitochondrial fusion proteins (OPA1 and MFN2) which leads to enhancing the activation of mitophagy response in HCC cells. 141

Figure 45: Proposed model of melatonin-dependent inhibition of hypoxia-induced mitophagy in sorafenib-treated cells. Melatonin restrains the synthesis of HIF-1α by reducing the activation of mTORC1 and its downstream effectors p70S6K and RP-S6. This process leads to the decrease of BNIP3 and Nix transcription, preventing the induction of prosurvival mitophagy and inducing HCC cell death. 147

List of tables

Table 1: List of the antibodies used for protein detection by Western blot. The source, dilution, host and type of each antibody is specified in the different columns.	87
Table 2: List of primers used for SYBR green RT-qPCR.	90
Table 3: List of primers used to analyze changes in mitochondrial DNA content by SYBR green qPCR. ..	90

List of abbreviations

5-LOX	5-lipoxygenase
a.u.	Arbitrary units
AAAD	Aromatic amino acid decarboxylase
AANAT	N-acetylated by N-acetyl transferase
AASLD	American Association for the Study of Liver Diseases
ABC	ATP-binding cassette
AFMK	N ¹ -acetyl-N ² -formyl-5-methoxyknuramine
AFP	α -fetoprotein
AFP-L3	Fucosylated AFP
AGO2	Argonaute 2
AIF	Apoptosis-inducing factor
AMBRA1	Beclin1-regulated autophagy protein 1
AMK	N-acetyl-5-methoxyknuramine
AML	Acute myeloid leukemia
AMP	Adenosine monophosphate
AMPK	AMP-activated protein kinase
ANOVA	Analysis of variance
APAF1	Apoptotic protease-activating factor 1
ARNT1	Aryl hydrocarbon receptor nuclear translocator 1
ATCC	American Type Culture Collection
ATF4	Activating transcription factor 4
Atg	Autophagy-related gene
ATP	Adenosine triphosphate
ATPase	Adenosine triphosphatase
AUROC	Area under the receiver-operating characteristic curve
BAD	Bcl-2-associated agonist of cell death
Baf A1	Bafilomycin A1
Bak	Bcl-2 homologous agonist killer
Bax	Bcl-2-associated X protein
Bcl-2	B-cell lymphoma protein-2
Bcl-2-L-13	Bcl-2-like protein 13
BCLC	Barcelona Clinic liver cancer
BH3	Bcl-2 homology 3 domain
bHLH	Basic helix-loop-helix
BID	BH3-interacting domain death agonist
Bif-1	Bax-binding protein-1
BIK	Bcl-2-interacting killer

BIM	Bcl-2-interacting mediator of cell death
BMAL1	Brain and muscle ARNT-like 1
BNIP3	Bcl-2/adenovirus E1B 19 kDa protein-interacting protein 3
BNIP3L	BNIP3-like protein
BRCA1	Breast cancer type 1 susceptibility protein
C/EBP β	CCAAT/enhancer binding protein β
CAMKK β	Ca ²⁺ /calmodulin-dependent protein kinase β
cAMP	Cyclic AMP
CBP	CREB-binding protein
CCA	Intrahepatic cholangiocarcinoma
CCD	Coiled-coil domain
CD4	Cluster of differentiation 4
CDK1	Cyclin-dependent kinase 1
cDNA	Complementary DNA
cAMP	Cyclic AMP
cGMP	Cyclic GMP
CHOP	C/EBP β homologous protein
CHX	Cycloheximide
CK2	Casein kinase
CL	Cardiolipin
CLIP	Cancer of the liver Italian program
CMA	Chaperone-mediated autophagy
COPD	Chronic obstructive pulmonary disease
CQ	Chloroquine
c-Raf	Normal cellular Raf gene
CREB	cAMP response element-binding
CRF	Cancer-related fatigue
CRY2	Cryptochrome-2
CSIC	Consejo Superior de Investigaciones Cientificas
C-TAD	COOH terminal TAD
CUPI	Chinese university prognostic index
CYP3A4	Cytochrome P450 3A4
CYP450	Cytochrome P450
DCF-DA	2',7'-dichlorodihydrofluorescein diacetate
DCP	Des- Γ -carboxyprothrombin
DFCP1	Double FYVE domain-containing protein 1
Diablo	Direct IAP binding protein with low pI
DISC	Death-inducing signaling complex
DMEM	Dulbecco's modified Eagle's medium

DMSO	Dimethyl sulfoxide
DNA	Deoxyribonucleic acid
DNase I	Deoxyribonuclease I
Drp1	Dynamin-related protein 1
EASL	European Agency for the Study of the Liver
ECL	Enhanced chemiluminescence
EDTA	Ethylenediaminetetraacetic acid
EGFR	Epidermal growth factor receptor
eIF-2 α	Eukaryotic translation initiation factor 2-alpha
eIF-4E	Eukaryotic translation initiation factor 4E
EMA	European Medicines Agency
EMT	Epithelial-mesenchymal transition
EPAS1	Endothelial PAS domain-containing protein 1
EPO	Eosinophil peroxidase
ERK1	Extracellular signal-regulated kinase 1
FADD	Fas-associated death domain
Fas	First apoptosis signal
FasL	First apoptosis signal ligand
FBS	Fetal bovine serum
FDA	Food and Drug Administration
FFA-BSA	Fatty acid-free bovine serum albumin
FIH	Factor inhibiting HIF
FIP200	Focal adhesion kinase family interacting protein of 200 kDa
Fis1	Mitochondrial fission protein 1
FITC	Fluorescein
FUNDC1	FUN14 domain-containing protein 1
FYCO1	FYVE and CCD-containing protein 1
GABA	Gamma-aminobutyric acid
GABARAP	Gamma-aminobutyric acid receptor-associated protein
GADD45 β	Growth arrest DNA damage-inducible gene 45 β
GAP	GTPase-activating protein
GATE-16	Golgi-associated ATPase enhancer of 16 kDa
GCD2	Granular corneal dystrophy type 2
GDP	Guanosine diphosphate
GIDEON	Global investigation of therapeutic decisions in HCC and of its treatment with sorafenib
GMP	Guanosine monophosphate
GPC-3	Glypican-3
GRETCH	Groupe d'Etude et de Traitement du Carcinome Hépatocellulaire
GTP	Guanosine triphosphate

GTPase	Guanosine triphosphatase
HBsAg	HBV surface antigen
HBV	Hepatitis B virus
HCC	Hepatocellular carcinoma
HCV	Hepatitis C virus
HDAC-1	Histone deacetylase-1
HDV	Hepatitis D virus
HFSR	Hand-foot skin reaction
HIF	Hypoxia-inducible factor
HIFU	High-intense focused ultrasound
HIOMT	Hydroxyindole-O-methyltransferase
HOPS	Homotypic fusion and protein sorting
HRE	Hypoxia responsible element
HRK	Activator of apoptosis harakiri
HRP	Horseradish peroxidase
hsc70	Heat shock-cognate protein of 70 kDa
HSP60	60 kDa heat shock protein
HSP90	90 kDa heat shock protein
HTRA2	High temperature requirement protein A2
Hx	Hypoxia
IAP	Inhibitors of apoptosis
IARC	International Agency of Cancer Research
IBIOMED	Instituto Universitario de Biomedicina
IDO	Indoleamine 2,3-dioxygenase
IFN2	Inverted formin 2
IFN- γ	Interferon- γ
IIB	Instituto de Investigación de Ciencias Biomédicas de Barcelona
IL	Interleukin
IMM	Inner mitochondrial membrane
IMS	Intramembrane mitochondrial space
IRE1	Inositol-requiring enzyme 1
JC-1	Tetraethylbenzimidazolylcarbocyanine iodide
JIS	Japan integrate staging
JAK	Janus kinase
JNK	c-Jun N-terminal kinase
KG	α -ketoglutarate
LAMP2A	Lysosome-associated membrane protein type 2A
LC3	Microtubule-associated proteins 1A/1B light chain 3B
LIR	LC3-interacting region

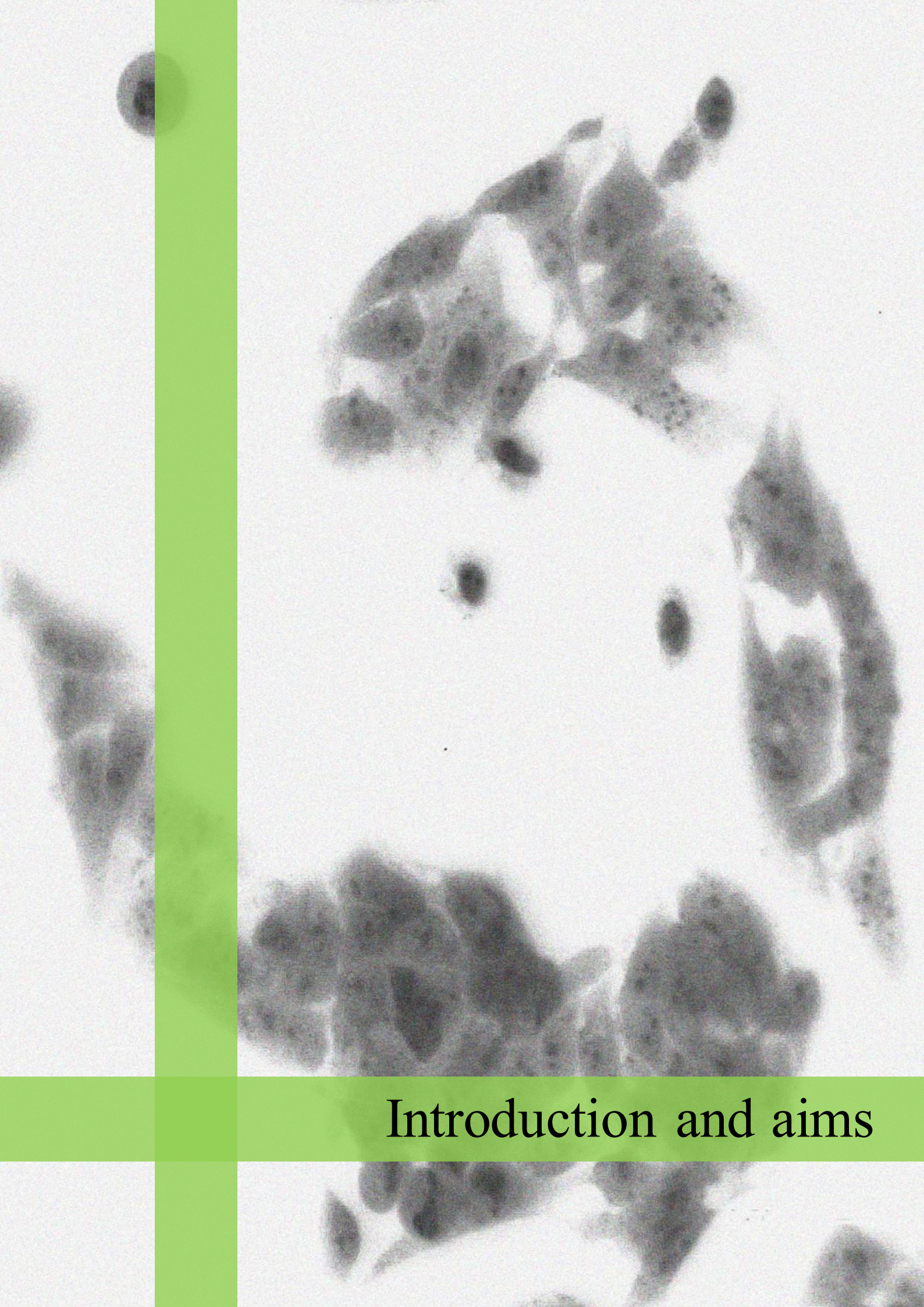
LKB1	Liver kinase B1
lncRNA	Long non-coding RNAs
L-OPA1	Membrane-anchored long OPA1
MAM	Mitochondria-associated membrane
MAPK	Mitogen-activated protein kinases
Mcl-1	Myeloid cell leukemia 1
mdivi-1	Mitophagy and mitochondrial inhibitor-1
mdm2	Murine double minute 2
Mel	Melatonin
Mff	Mitochondrial fission factor
MFN	Mitofusin
MHC II	Major histocompatibility complex type II
MHCT	Multi-detector helical computed tomography
MiD	N-terminally anchored mitochondrial dynamics protein
MIEF1	Mitochondrial elongation factor 1
MIF	Migration inhibitory factor
miRNA	MicroRNA
Miro	Small mitochondrial Rho GTPase
MMP9	Matrix metalloproteinase 9
MMT	3-(4,5-dimethylthiazol-2-yl)-2,5-diphenyltetrazolium bromide
MOC	Mechanisms of chemoresistance
MOMP	Permeabilization of the OMM
MPO	Myeloperoxidase
MRI	Magnetic resonance imaging
mtDNA	Mitochondrial DNA
mTOR	Mammalian or mechanistic target of rapamycin
mTORC1	Mammalian or mechanistic target of rapamycin complex 1
mTORC2	Mammalian or mechanistic target of rapamycin complex 2
NA	Noradrenergic
NAC	N-acetyl cysteine
NADPH	Nicotinamide adenine dinucleotide phosphate
NAFLD	Non-alcoholic fatty liver disease
N-BAR	Amino-terminal Bin-Amphiphysin-Rvs
ncDNA	Nuclear DNA
NDP52	Nuclear dot protein 52 kDa
NF-κB	Nuclear factor kappa-light-chain-enhancer of activated B cells
Nix	NIP-3-like protein X
NLS	Nuclear localization signal
nMDP	Normalized mean deviation product

NO	Nitric oxide
Nox	NADPH oxidase
Noxa1	NADPH oxidase activator 1
NQO2	Quinone reductase 2
NRB1	Neighbor of BRCA1 gene 1
NSF	N-ethylmaleimide sensitive
N-TAD	NH ₂ terminal TAD
Nup538	Nucleoporin 538
Nx	Normoxia
OCT1	Octapeptidyl aminopeptidase 1
ODD	Oxygen-dependent domain
OMA1	Overlapping with the m-AAA protease 1 homolog
OMM	Outer mitochondrial membrane
OPA1	Optic atrophy factor
OPN	Osteopontin
OPTN	Optineurin
OS	Overall survival
p70S6K	Ribosomal protein S6 kinase beta-1
PARL	Presenilins-associated rhomboid-like protein
PAS	Per-ARNT-Sim
PBS	Phosphate buffered saline
PBS-T	PBS supplemented with Tween-20 at 0.05%
PCD	Programmed cell death
PCR	Polymerase chain reaction
PD-1	Programmed cell death protein 1
PDGFR-β	Platelet-derived growth factor receptor
PE	Phosphatidylethanolamine
PEI	Percutaneous ethanol injection
PER	Period circadian clock
pERK	Phosphorylated ERK
PERK	PRKR-like endoplasmic reticulum kinase
PGAM5	Phosphoglycerate mutase family member 5
PGC-1α	Peroxisome proliferator-activated receptor gamma coactivator-1α
PHB-2	Prohibitin-2
PHD	Prolyl hydroxylase
PI	Propidium iodide
PI3K	Phosphatidylinositol 3-kinase
PI3P	Phosphatidylinositol 3-phosphate
PIASγ	Protein inhibitor of activated STAT protein gamma

PINK1	PTEN-induced putative kinase protein
PKA	Protein kinase A
PKC δ	Protein kinase C delta type
PLA2	Phospholipase A2
PP1/2A	Protein phosphatases 1 and 2A
PTEN	Phosphatase and tensin homolog
PUMA	p53-upregulated modulator of apoptosis
PVDF	Polyvinylidene fluoride
PVN	Paraventricular nucleus
qPCR	Quantitative PCR
R/GFIR	Red-to-green fluorescence intensity ratio
Rab-37	Ras-related protein in brain 37
RACK1	Receptor of activated protein kinase C1
Raf1	Rapidly accelerated fibrosarcoma 1
Rag	Ras-related GTP-binding protein
RanBP2	Ran-binding protein 2
Raptor	Regulatory-associated protein of mTOR
Ras	Rat sarcoma
Rb	Retinoblastoma-associated protein
RCC	Renal cell carcinoma
REDD1	Protein regulated in development and DNA damage response 1
Rheb	Ras-homologue enriched in brain
RILP	Rab-interacting lysosomal protein
RISC	RNA-induced silencing complex
RNA	Ribonucleic acid
RNAi	Interference RNA
RNS	Reactive nitrogen species
ROMO1	Reactive oxygen species modulator 1
RORs	Nuclear retinoid-related orphan receptors
ROS	Reactive oxygen species
RP-S6	Ribosomal protein S6
RSUME	RWD-containing sumoylation enhance
RT-qPCR	Reverse transcription quantitative polymerase chain reaction
RUBICON	RUN domain protein as Beclin1 interacting and cysteine-rich containing
S1P	Sphingosine 1-phosphate
SCG	Superior cervical ganglia
SD	Standard deviation
SDS	Sodium dodecyl sulfate
SDS-PAGE	SDS-polyacrylamide gel electrophoresis

SENP	SUMO-specific protease
Sfb	Sorafenib
SH3	Src-homology 3
SHARP	Sorafenib HCC assessment randomized protocol
siRNA	Small interference RNA
SIRT1	Sirtuin 1
SMAC	Second mitochondria-derived activator of caspases
SNAP-29	Synaptosome-associated protein 29 kDa (
SNARE	NSF-attachment protein receptor
SNC	Suprachiasmatic nucleus
SNX18	Sortin nexin-18
S-OPA1	Transmembrane region-free short OPA1
Sor	Sorafenib
STAT3	Signal transducers and activators of transcription type 3
STX17	Syntaxin-17
SUMO	Small ubiquitin-related modifiers
TACE	Transarterial chemoembolization
TAD	Transactivation domain
TARE	Transarterial radioembolization
TBC1D7	TBC domain family member 7
TCA	Tricarboxylic acids
TFEB	Transcription factor that specially recognizes and binds E-box sequences
TGF- α	Transforming growth factor alpha
TIMM	Translocase of the IMM
TIP60	Human immunodeficiency virus-1 Tat interactive protein
TNF	Tumor necrosis factor
TNF-R	Tumor necrosis factor receptor
TNM	Tumor-node metastasis
TOMM	Translocase of the OMM
TPH	Tryptophan-5-hydroxylase
TRAF6	TNF receptor-associated factor 6
TRAIL	TNF-related apoptosis-inducing ligand
TRAIL-R	TNF-related apoptosis-inducing ligand receptor
TRB3	Tribbles homolog 3
TSC	Tuberous sclerosis protein
UBA	C-terminal ubiquitin association domain
UDP	Uridine diphosphate
UGT1A9	UDP glucuronosyltransferase family 1-member A9
ULK1	Unc-51-like kinase

UPR	Unfolded protein response
US	Ultrasonography
UVRAG	Ultraviolet irradiation resistance-associated gene
VAMP8	Vesicle-associated membrane protein 8
VDAC	Voltage-dependent anion-selective channel protein
VEGF	Vascular endothelial growth factor
VEGFR	Vascular endothelial growth factor receptor
VHL	Von Hippel–Lindau protein
VMP1	Vacuole membrane protein 1
Vps34	Vacuolar protein sorting-associated protein 34
WHO	World health organization
WIPI1	WD repeat domain phosphoinositide-interacting protein 1
XIAP	X-linked inhibitor of apoptosis protein
YC-1	3-(50-hydroxy methyl-20-furyl)-1-benzylindazole
YME1	Yeast mitochondrial escape protein 1
YME1L	YME1 like 1 ATPase



Introduction and aims

Hepatocellular carcinoma (HCC) is the fifth most prevalent malignant disease, as well as the second cause of cancer-related death worldwide in men. Unfortunately, its prognosis is very poor and its incidence is increasing progressively worldwide owing to the difficulty of early diagnosis and to the lack of curative treatments to manage the late stages of this pathology. Therefore, the development of new therapeutic strategies should be essential to improve the survival of advanced HCC patients.

Sorafenib was the first drug approved to be used for the treatment of advanced HCC. This molecule has been reported to reduce cancer cell proliferation and angiogenesis, as well as to promote apoptotic cell death through restraining the activity of multiple serine/threonine and receptor tyrosine kinases. However, sorafenib sustained treatments lead to reducing the availability of oxygen inside the tumor mass due to the antiangiogenic properties that present this drug, which ultimately improves the arising of resistant HCC cells. Moreover, many tumors are not initially sensitive to this anticancer agent due to the great heterogeneity that present HCC cells. Recently, some new strategies, such as the use of new adjuvants or some second-line drugs, such as regorafenib or nivolumab, have been developed to address with this harmful situation or to be used after sorafenib failure respectively.

Imbalances between cell survival and death mechanisms have been reported to induce the appearance of chemotherapy resistant cells. Although both nonspecific and specific autophagy have been showed to be able to modulate these processes in HCC, this regulation seems to be highly dependent on the tumor progression stage and on its microenvironment. Indeed, these pathways hinder tumorigenesis by eliminating damaged organelles and preventing genomic instability at earlier stages, whereas they protect advanced tumors against chemotherapy and radiotherapy through degrading damaged organelles and preventing ROS release. Otherwise, autophagy is tightly interconnected with other programmed cell death (PCD) pathways, such as apoptosis, to manage cellular response against many stressful stimuli. Therefore, the fine tuning of autophagy response in HCC could lead to the control of chemotherapy sensitiveness.

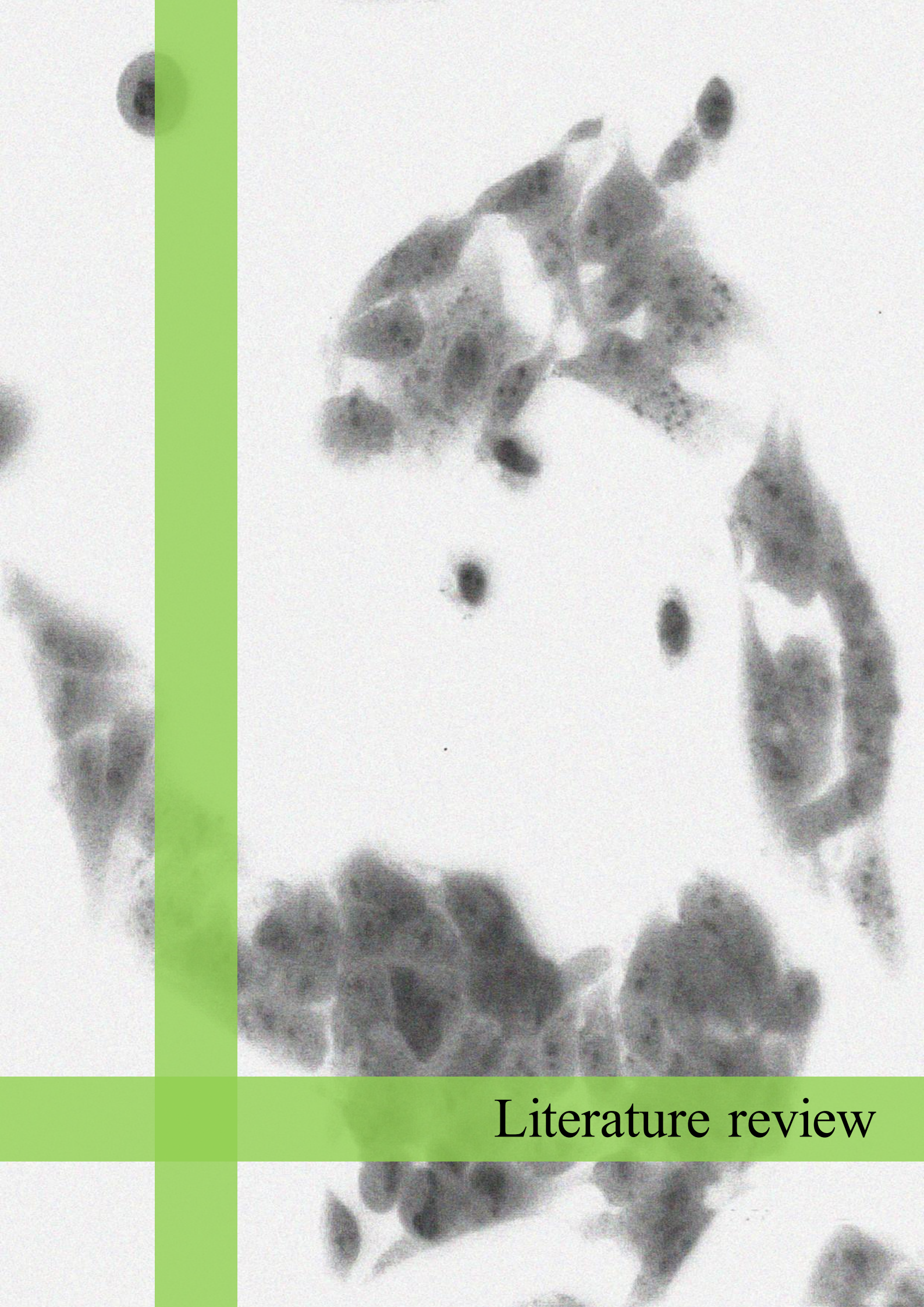
Melatonin is a serotonin-derived hormone whose main function in mammals is the adjusting of the circadian and seasonal rhythms to the light and dark fluctuations. Moreover, it has been also reported to present some protective local actions in many human tissues and organs. For instance, it can reduce depression, anxiety, inflammation, oxidative damage and tumorigenesis. More in detail, melatonin has been showed to exert a great

number of oncostatic activities in many human tumors, such as prevent tumor proliferation, angiogenesis, invasion and metastasis. Moreover, this indoleamine has been demonstrated to improve the cytotoxic effects of other chemotherapeutic drugs, such as doxorubicin or clofarabine. These data allow its potential use as an adjuvant for cancer therapy.

According to the previous data, the main purpose of this dissertation was the analysis of the melatonin ability to increase the cytotoxic effect of sorafenib and to reduce the arising of both innate and acquired cell resistance to this drug in HCC cells maintained under either normoxia or hypoxia conditions, through modulating both unspecific and specific autophagy, as well as apoptosis.

Besides, the following specific objectives were proposed:

- To determine whether melatonin treatment alone can induce autophagy cytotoxic response in HepG2 cells, as well as the behavior of this pathway on the reduction of cell viability observed after melatonin addition.
- To analyze the ability of melatonin to promote the cytotoxic effects of sorafenib by inducing pro-death mitochondrial autophagy, also known as mitophagy, in Hep3B cells under normoxia, as well as the underlying mechanism implicated in the activation of this pathway.
- To determine whether melatonin is able to improve sorafenib antiproliferative effects in Hep3B cells under hypoxia by reducing the expression and the activity of the main hypoxia-inducible factors (HIFs).
- To study the molecular mechanism through which melatonin reduces HIF-1 α steady-state protein levels in Hep3B cells under hypoxia.
- To analyze if melatonin and sorafenib coadministration in Hep3B cells under hypoxia is able to induce mitophagy response, as well as its biological role in apoptosis and cell viability.



Literature review

1. Hepatocellular carcinoma.

Liver cancer is the fifth most prevalent malignant disease in men and the ninth in women with an estimation of 841,000 new cases in 2018 [1]. Additionally, it is the fourth cause of cancer-related death globally with an estimation of 782,000 new deaths in 2018, being its prognosis poor and its 5-year survival rate about 5% [1,2]. Nevertheless, some differences in the incidence of this pathology are observed among the diverse world regions, being highest in South-Eastern Asia and in Northern and Western Africa and lowest in Northern, Central and Eastern Europe and South-Central Asia (Fig. 1) [1,3]. In fact, Mongolia is the country which has the highest HCC incidence and mortality rates worldwide (Fig. 1) [1]. Additionally, there are clear differences between developed and non-developed countries, being prevalence and mortality values higher in the countries with low monetary-resources, being prevalence and mortality values higher in the countries with low monetary-resources [2,4]. On the other hand, the southern zone of Europe presents the most elevated liver cancer incidence among the rest of the continent (Fig. 1) [2]. In Spain, there were 4,252 new cases in men and 1,610 in women in 2015 [5], being the incidence of hepatocellular carcinoma (HCC) in this country more elevated than the European average [6].

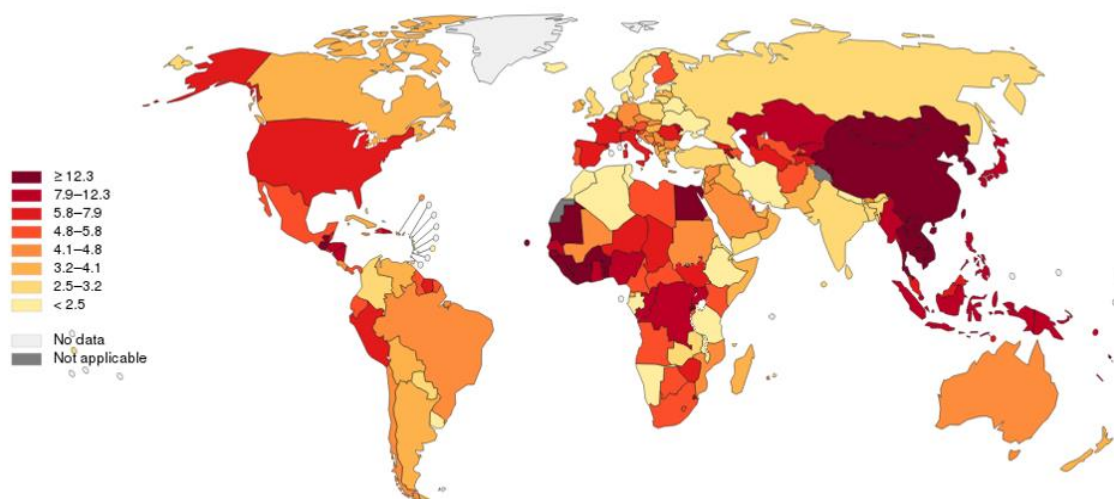


Figure 1: Estimated age-standardized liver cancer incidence rate worldwide according to the results obtained by GLOBOCAN 2012 study. Copyright from World Health Organization (WHO), 2018. All Rights Reserved. Available from <http://gco.iarc.fr/today/home> (Consulted on 28/01/2018).

Hepatobiliary cancers constitute a heterogeneous group of malignant pathologies with poor prognosis which includes HCC, hepatoblastoma, intrahepatic cholangiocarcinoma (CCA), bile duct cystadenocarcinoma and mixed hepatocellular cholangiocarcinoma [7,8]. Among them, HCC is the most prevalent type of liver cancer

[9], because it comprises from 75 % to 85% of all the new cases of this malignant pathology [1,9]. HCC is usually derived from hepatocytes [10,11], although the existence of some variants which express different gene patterns implied that these tumors could also come from hepatic progenitors cells [11,12]. These data would support the hypothesis of the existence of different HCC subtypes, depending on their cellular origin [11,12].

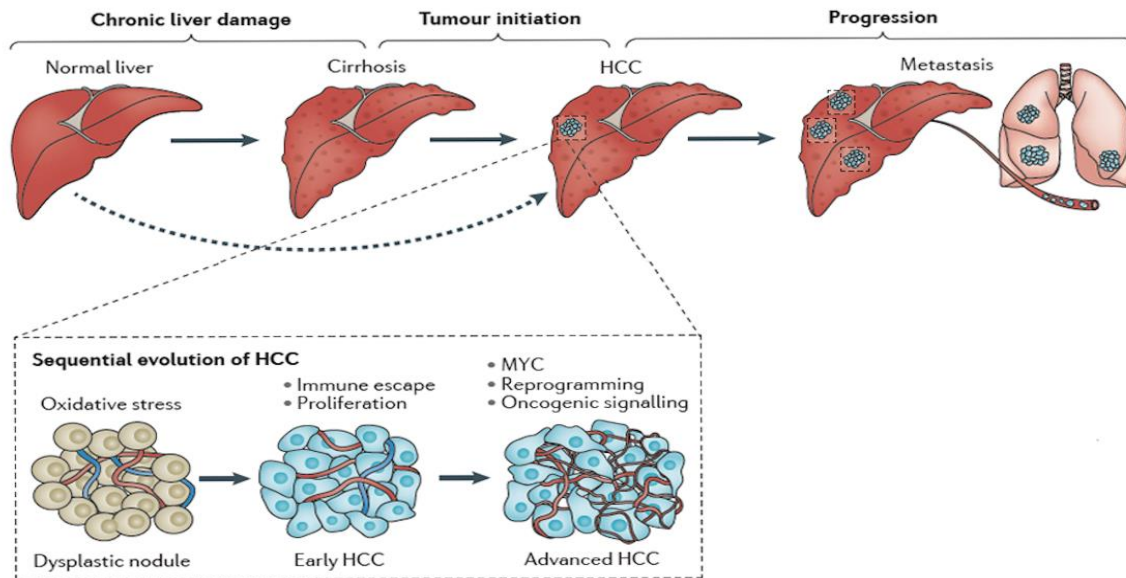


Figure 2: Sequential changes in liver during hepatic carcinogenesis and HCC progression. All chronic damage processes finish with the generation of a cirrhosis in the liver. In this environment, some cells can become carcinogenic and start to proliferate without control, generating a tumor. HCC passes for three different sequential steps: dysplastic nodule, early HCC and advanced HCC according to the number of genes mutated in those cells and to their grade of dedifferentiation. Concomitant with this process, there are an increment of neovascularization of tumor, which is more evident in advanced phases. Finally, advanced HCC cells are able to break the extracellular matrix and invade other organs, generating secondary tumors. The dashed arrow represents the little number of tumors that curse without previous cirrhosis. Retrieved from [13].

HCC progression is a multistep process that starts with the generation of a liver cirrhosis due to the maintenance of a chronic inflammatory status and to the induction of fibrosis in this organ, although there are some tumors that arise without previous cirrhosis (Fig. 2) [13]. As a result of the prolongation of this harmful status, high cellular turnover is induced in dysplastic nodules that finally results in the generation of several mutations due to the malfunction of the DNA-repairing systems, increasing hepatocyte carcinogenicity (Fig. 2) [13]. The progressive accumulation of chromosome aberrations increases genetic instability in HCC cells, decreasing progressively their hepatic features and increasing their malignant and invasive properties (Fig. 2) [14]. Some of the most commonly mutated genes in HCC cells are related to the regulation of telomere upkeep, such as telomerase; to DNA

repair, chromatin remodeling and cell cycle regulation, such as p53 or retinoblastoma-associated protein (Rb); and to the induction of epithelial-mesenchymal transition (EMT), such as β -catenin [13,15]. Concomitant with this process, new blood vessels are generated in the tumor milieu in order to avoid the lack of oxygen and nutrients in the center of this tissue (Fig. 2) [16]. Finally, this continuous process disrupts tumor cell matrix, which allows to HCC cells to escape from the primary site of the tumor and to generate secondary tumors in the liver or in other body organs (Fig. 2) [17].

1.1. Etiology.

HCC arises as the result of the incidence of multiple etiological factors in the liver with external or internal origin [18]. Therefore, the identification of these risk factors is essential to increment its early diagnosis and to improve its treatment [18].

The infection with hepatitis B virus (HBV) or hepatitis C virus (HCV) are the leading risk causes in HCC [18]. HBV is a double-stranded circular DNA virus which can induce an inflammatory status in the liver, generating ultimately hepatocarcinogenesis when this infection becomes chronic through the introduction of HBV DNA in the genome of the host cell [19,20]. HBV surface antigen (HBsAg) is the main blood marker for the risk of developing HBV-related HCC, although it has recently been claimed that the presence of some antibodies against other HBV antigens, like HBV core protein, could be also a key indicator of increasing carcinogenesis risk [19]. HBV infection is the main risk factor for HCC in South-East Asia and in Sub-Saharan Africa regions, where its genotype C, which is the most procarcinogenic one, is endemic [1,19]. Nevertheless, the progressive improvement of sanitation and the beginning of a global HBV vaccination program are reducing the probability of HBV-related hepatocarcinogenesis in these world areas [19,21]. For example, the implementation of this program in Taiwan since 1984 has been proven to have reduced the incidence of this cancer in more than 80% [21]. Additionally, the use of antiviral therapy can also restrain HBV-related hepatocarcinogenesis [22]. For instance, entecavir administration can reduce the HBV-related HCC cumulative 5-year incidence rate by more than 10% [22].

On the other hand, HCV is an enveloped, single-stranded RNA virus that can induce oxidative stress. This effect is related to the increase in the production of reactive oxygen and nitrogen species (ROS and RNS, respectively), repressing cell antioxidant defense and

overexpressing Nox enzymes [23]. This process increases the generation of an oxidative damage in the DNA and impairs the correct working of its repairing mechanisms, which finally stimulates the generation of carcinogenic cells through the appearance of some mutations in their genetic content [23]. Otherwise, this virus can also induce carcinogenesis through deregulating some programmed cell death pathways [24]. In contrast to HBV hepatocarcinogenesis, HCV-related HCC normally courses with a previous well-established cirrhosis in the liver [19] and it is more frequent in Europe, Japan, Latin America and North America [9]. Oppositely, the development of new HCV antiviral therapies and protocols have reduced the formation of HCC tumors more than 4,6% in these historic zones [25].

In addition, HBV and HCV mixed infections also stimulate the risk of hepatocarcinogenesis because their effects are additive and multiplicative, stimulating their coinfection a more severe process of hepatocarcinogenesis [18]. Otherwise, the coinfection of HBV and hepatitis D virus (HDV) also increases the risk of HCC because HDV proteins can alter hepatic cell epigenetics, enhancing the transcription of prosurvival proteins [26].

Even though VHC and VHB-related hepatocarcinogenesis are diminishing worldwide due to the progressive development of new antiviral treatments and vaccines, HCC incidence is still increasing in developed countries, which is due to the increment in the incidence of other non-viral risk factors, such as alcohol abuse, smoking, obesity or type II diabetes [1]. Alcohol abuse (the continuous drinking of more than 80 g per day) is the leading cause of hepatocarcinogenesis in Western countries, accounting for more than 40% of all its new cases in Europe [27]. This continuous process generates a liver fibrosis which is clearly associated with the deregulation of hepatic metabolizing systems, which can ultimately progress until the generation of HCC [28]. On the other hand, tobacco consumption has been claimed to increase HCC genesis both in current smokers and in former ones [19]. Otherwise, obesity increases until 4 times more the risk of develop liver cancer [19], because the accumulation of lipids in the liver induces a proinflammatory status in this organ whose name is non-alcoholic fatty liver disease (NAFLD), progressing this status to liver fibrosis, cirrhosis and ultimately HCC if it is not reversed [29]. In addition, hyperinsulinemia provoked by type II diabetes also performs a role as an independent risk factor of HCC, because it can increase until three times the incidence of this pathology due to the insulin-dependent overinduction of cell proliferation and

the inhibition of apoptosis [19]. Summarizing, all these data asseverates that the control of daily food intake could be essential to avoid hepatocarcinogenesis, as it is has been claimed in various studies, which demonstrate that the daily consumption of fruit, green vegetables, white meat, eggs, soya-derivatives, such as miso soup, and caffeinated coffee reduces the risk to develop new hepatic tumors [30–32].

Another important etiological factor which is related to liver cancer induction is the intake of food contaminated with aflatoxins [18]. These are a group of fungal toxins generated by some species of the genus *Aspergillus* that can appear in diverse cereal crops commodities which have been stored for a long time in a hot and humid environment [33,34]. Aflatoxin B1, which is the most potent one, can induce hepatocarcinogenesis through its metabolization into 8,9-exo-epoxide by phase 1 cytochrome P450 monooxygenases in hepatocytes, which ultimately leads to the generation of mutagenic lesions in the DNA of these cells and to become them into tumor cells [34,35]. One of the most described aflatoxin-derived mutations in hepatocytes affects the 249 codon of p53 gene [36]. Indeed, the relation between the intake of food poisoned with aflatoxin B1 and the appearance of tumors in the liver has been demonstrated in many etiological studies [37].

Furthermore, other external factors, such as pesticides exposure or *Helicobacter pylori* infection, can perform a less common role in the increment of hepatocarcinogenesis [18]. Some recent etiological studies have demonstrated a direct association between the direct exposure to organophosphate, organochlorine and carbamate pesticides and the increment of hepatocarcinogenesis in non-developed countries due to the induction of DNA mutations in hepatocytes [38]. Otherwise, the infection with *H. pylori* exhibits liver toxicity both *in vivo* and *in vitro*, inducing HCC as well as other chronic hepatic diseases [39]. Additionally, some of its genomic sequences have been founded in the livers of HCC patients and some liver proteins, such as integrin β -3 or Ras-related protein in brain 37 (Rab-37), are upregulated as a result of bacterial infection [40,41]. Summarizing, although it seems that *H. pylori* is a key etiological factor for the development of hepatic tumors, there are not many hypotheses which explain how this bacteria induces hepatocarcinogenesis [39].

Finally, sex, age and race are also main risk factors implicated in the modulation of liver carcinogenesis, because this disease occurs more frequent in men than women [42],

in age-advanced individuals than in young ones [43], and in Asian and Native American people than in black, white and Hispanic people [19].

1.2. Diagnosis.

Early HCC diagnosis is key to improve clinical treatment results, even achieving the total tumor remission [19]. However, patients are often diagnosed at late stages because HCC tumors do not present any clear symptoms or have the same ones as other concomitant liver diseases [9]. Therefore, the improvement of screening procedures is essential to stimulate the early detection of these tumors, especially in patients with a previous cirrhosis diagnostic [9]. The most used methods for HCC screening accomplish imaging techniques, molecular markers and liver biopsy techniques [44].

1.2.1. Imaging techniques.

Imaging techniques are very useful in HCC diagnosis due to its non-invasive and low-risk features [45]. Nevertheless, the detection of liver tumors is usually difficult owing to the heterogeneous environment which surrounds the HCC mass [45]. For these reasons, it is recommendable the use of an intravascular contrast media which augments the visibility of the tumor mass [45]. The most used imaging techniques for the detection of this disease are ultrasonography (US), multi-detector helical computed tomography (MHCT), magnetic resonance imaging (MRI) and angiography (Fig. 3) [46,47].

US is the most commonly used imaging technique for early HCC diagnoses due to its reliability, its great cost-effectiveness index and its low-invasiveness [48]. In fact, abdominal US permits the identification of tumor masses with at least 1 cm in diameter (Fig. 3A) [44]. However, the cirrhotic environment which surrounds the tumor can alter the US detection, which explains the low sensitivity of this technique for HCC detection ($\approx 70\%$) [49,50]. Recently, the addition of an intravascular contrast media and the precise application of ultrasound against liver tissue have led to the development of more sensitive variants, such as Doppler US, contrast-enhanced US or the endoscopic US [44].

MDCT is the most important imaging technique used in the detection of small HCC, as well as in the following of patients with cirrhosis and viral hepatitis, due to its high

capability to detect tumor mass in contrast to the cirrhotic milieu [44,46]. This technique normally presents two correlative phases, allowing the identification of the blood vessels that surround the tumor in the earliest phase, which could be important to plan a future surgery treatment; and the tumor mass in the latest one (Fig. 3B) [46]. However, the prolonged use of this technique could carry a significant radiation exposure risk, which ultimately limits its use for continuous HCC diagnosis [46].

MRI, which consists in getting liver images through magnetic resonance without the use of ionizing radiation or contrast media which could be poisonous by the kidney, present higher accuracy than the other two previous HCC diagnosis techniques and is also used for the estimation of tumor size (Fig. 3C) [44,46]. Nevertheless, its high cost and the extended duration required to get good quality HCC images make that most radiologists prefer the use of helical CT for the fast detection of this tumor, restricting the use of MRI when CT results are not very clear because of the presence of nodules in the liver [44,50].

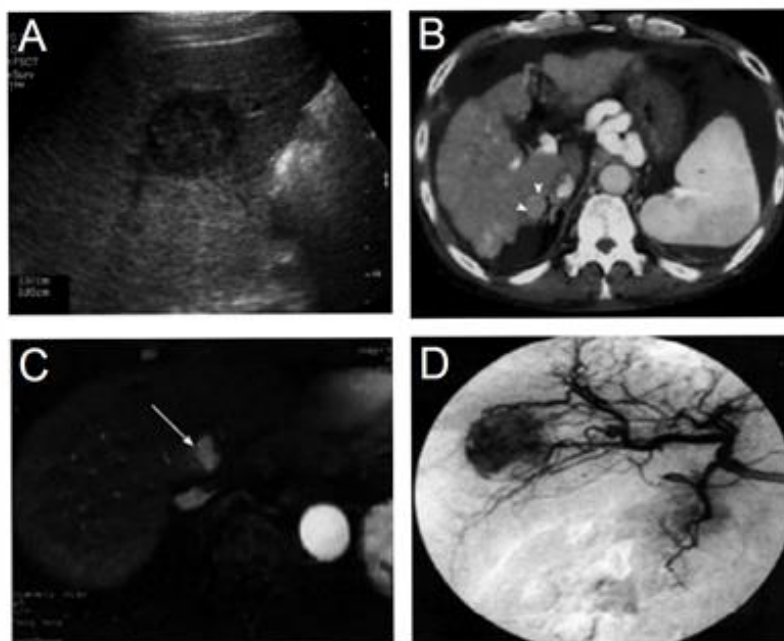


Figure 3: Leading imaging techniques used for the diagnostic of HCC. (A) Abdominal transverse US sonogram shows a hypothetical tumor mass in the right lobe of the liver. (B) The late arterial phase of multi-detector computed tomography visualizes an HCC as an enhanced nodule (white arrows). (C) The arterial phase of dynamic MRI shows a tumor mass adjacent to portal vein (white arrow). (D) Detection of a hepatic tumor by hepatic angiography as a hyper-vascular zone into the liver. Retrieved from [44].

Because the high vascular net which normally surrounds HCC tumors, the use of angiography, which consists in the injection of an intra-arterial contrast media into the hepatic region, instantly followed by a CT or MRI; could improve the detection and

characterization of HCC tumor masses (Fig. 3D) [44]. Nevertheless, this technique has only been restricted to detect bleeding during the disruption of focal HCCs, and to avoid complications during chemoembolization, due to the improvement of less-invasive methods, such as CT or Doppler US [44,47].

1.2.2. Diagnostic markers.

The first molecular marker that was described for HCC diagnosis was serum α -fetoprotein (AFP), which is a glycoprotein sensitized only in the first-trimester fetal livers, decreasing progressively its expression after birth, and increasing during hepatocarcinogenesis [51]. However, the use of its serum values as a diagnostic marker is controversial, because of its cut-off values (20 ng/ml) are not very sensitive to discriminate HCC patients. In this way, almost half of these individuals presents very low values (\approx 2 ng/ml) [52], and that more than one-third of HCC cases are not diagnosed due to the use of this biomarker [53]. Furthermore, up to 47% of liver cirrhosis patients without HCC also present high AFP levels [3]. Therefore, novel markers or AFP derivatives with better sensitivity and specificity than this factor has been developed to be used in HCC diagnostic [53], such as fucosylated AFP (AFP-L3), des- Γ -carboxyprothrombin (DCP), osteopontin (OPN) and glypican-3 (GPC-3). Recently, some microRNAs, such as miR122 and let-7b have also been claimed to be useful for earlier detection of HCC [44,53].

AFP-L3, which is a fucosylated form of AFP, could be also used in HCC diagnosis, replacing non-glycosylated AFP form [54]. Indeed, protein fucosylation increases during hepatocarcinogenesis in order to increase cell proliferation, since most of these fucosylated proteins are growth factor receptors [54]. Moreover, it has been proven that AFP-L3 is only detected in the plasma of HCC patients, on the contrary to AFP whose expression is induced also in benign diseases [55]. All these data enable its use in the early diagnosis of HCC.

DCP, which is a modified form of prothrombin that carries abnormal carboxylations in ten different N-terminal glutamic acid residues, is only produced in liver tumor cells, but not in normal hepatocytes [51,56]. This factor could promote the angiogenesis of liver carcinogenic cells by inducing the migration of vascular endothelial cells to the tumor milieu [56]. Serum DCP levels correlate with hepatic tumor size and are

undetected in patients with liver benign diseases, enabling its use as a diagnostic and a prognosis marker for patient survival and HCC recurrence [56].

OPN is an integrin-binding glycoprophosphoprotein that is constantly expressing in HCC and other carcinogenic tissues, but not in non-carcinogenic hepatocytes [3]. It has demonstrated that this molecule could be used in the detection of early HCC tumors with high sensitivity, remaining intact at least 1 year after sample collection, encouraging its future use in HCC diagnosis and prognosis [57].

GPC-3 is a protein which anchorages to the cell membrane, controlling from there cell growth by modulating the activation and repression of different growth factors [51]. In most HCC cells this factor is upregulated, being one of the first transcripts that arise during hepatocarcinogenesis, suggesting its use as an early biomarker in this disease [58]. In addition, it has found that the expression of this mRNA is practically absent in normal and cirrhotic livers [54]. Finally, it seems that the blood values of this mRNA are associated with the presence of extra-hepatic metastasis, enabling the use of GPC-3 as a prognostic marker of metastasis occurrence [59].

1.2.3. Liver biopsy.

Liver biopsy, which consists in the extraction of a small portion of the tumor mass for its analysis, presents a high number of risks for patients due to its elevated invasive features, implying that this method should be done by a trained specialist which asseverates the correct retrieve of the sample with the correct size [60]. In addition, there is a low risk of bleeding and tumor spreading through the track that has been followed by the biopsy needle [60]. For all these reasons, this technique is only used to analyze poor-defined HCCs which have not been detected by a previous imaging test [44].

1.3. HCC staging.

Correct and accurate staging of cancer patients is fundamental in oncology, owing to its significance in the management of clinical decisions, as well as for the development of cancer epidemiologic studies [61]. These staging systems should be reliable, reproducible and use data which could be easily obtained from clinical practice [61]. In

particular, cancer staging scales and scores become essential for the clinical management of HCC due to its high geographical and biological heterogeneity, as well as to its usual arising in damaged liver tissues [61,62]. Therefore, some different staging scales with different variables and markers have been developed for HCC management, thus the use of various scales simultaneously would asseverate the accurate patient staging [62].

The most important HCC staging index is Barcelona Clinic liver cancer (BCLC) being the only which connects the morphologic and pathologic characteristics of each tumor with its best first-line treatment (Fig. 4) [62]. Moreover, this rank is said to present the highest area under the receiver-operating characteristic curve (AUROC) for overall survival (OS), which basically, makes this scale as the most accurate for the staging of long-term treatment-naïve HCC staging [63]. Therefore, it is not strange that this scale has become the most used in clinical practice in Western countries since it has been included in the European Agency for the Study of the Liver (EASL) and American Association for the Study of Liver Diseases (AASLD) standard guidelines for HCC diagnostic [62]. BCLC rank divides HCC into 5 different types, from 0 to D, based on the stage where the tumor is and on the functionality that remains in the liver which is measured by Child-Pugh scale (Fig. 4) [62]. The characteristics of each stage, as well as the first-line treatment recommended are shown in Fig. 4.

Other staging scales used in HCC are:

- Tumor-node-metastasis (TNM) stage, which classifies tumors according to tumor size, nodal involvement and distant metastasis presence [61].
- Okuda score, which is now outdated because it only stages advanced HCCs, which is currently easier to do through imaging techniques [61].
- Cancer of the liver Italian program (CLIP) score, which is used for detect HCC recurrence, but it is not very precise in the detection of early cancers [61].
- Japan integrate staging (JIS) score, which is very accurate in the diagnosis of early HCC stages [61].
- Chinese university prognostic index (CUPI), which is great to classify patients with HBV-derived HCC [61].

- *Groupe d'Etude et de Traitement du Carcinome Hépatocellulaire* (GRETCH) index, which is only based on the levels of serum biomarkers and is used mainly for initial HCC diagnosis [61].

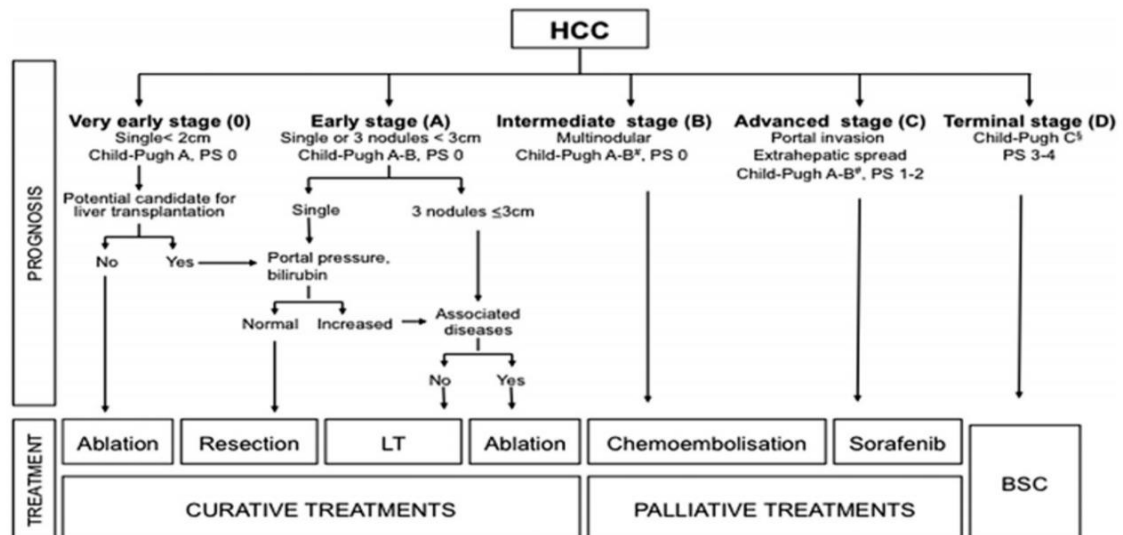


Figure 4: The BCLC staging algorithm for HCC staging and diagnosis. BCLC scale divides liver tumors into 5 different stages, 0, A, B, C and D; depending on tumor size and on the liver functionality that remains in carcinogenic cells. Additionally, this scale also includes the first-line treatment recommended for each of the stages. LT means liver transplant; PS, performance status; and BSC, best supportive care. Retrieved from [64].

1.4. HCC treatment.

Despite the improvement of diagnostic and staging methods, HCC continues being diagnosed at late stages, when the use of curative strategies are ineffective and only palliative techniques are possible [44,65]. Additionally, HCC is resistant to most chemotherapeutic drugs, and is not normally amenable to radiotherapy protocols, limiting even more the number of available treatments for this disease [65]. These features will explain its incredibly low 5-years survival rate, whose value is about 5% [3]. Fortunately, some new treatment modalities have arisen recently in order to increase HCC remission at later stages [66].

1.4.1. Curative treatments in HCC.

Curative treatments for HCC include liver transplantation, hepatic resection and ablation [67]. Liver transplantation is recommended by HCC patients with only a 5 cm lesion or up to 3 nodules of 3 cm in diameter each one and with a concomitant cirrhotic milieu [68,69]. This technique not only removes the primary tumor, but it also eliminates secondary liver tumors and underlying cirrhosis from the liver [70]. Unfortunately, the lack of organs for transplantation, the possible rejection of transplanted tissue by the immune system of the patient and the possibility of HCC recurrence after the transplantation are the main flaws of this technique [70]. Despite these problems, the 5-year overall survival of this technique is about 75%, and the recurrence rate is less than 15% [68,70,71]. Otherwise, surgical hepatic resection could be an alternative to liver transplantation in patients with a single small HCC which courses in a non-cirrhotic milieu, with the maintenance of normal liver function and without vascular complications [67,68]. Nevertheless, the main flaw of this therapeutic approach is its high recurrence, which appears in more than 30% of surgical resection patients due to intrahepatic metastasis and local invasion in early phases and to the *de novo* formation in later ones [72].

Liver ablation has recently become an interesting alternative to liver surgery due to its high safety profile, its low invasive features and its brief recovery period [69,73]. According to the agent used to induce the necrosis of carcinogenic cells, ablation is divided in radiofrequency ablation, microwave ablation, percutaneous ethanol injection (PEI) ablation, cryoablation and high-intense focused ultrasound (HIFU) ablation [73]. The ablation variants which are most broadly used are RFA and PEI, being the other variants currently under evaluation [67]. However, ablation techniques present an elevated risk of carcinogenic recurrence, as well as of generating severe complications such as liver failure, intraperitoneal bleeding, hepatic abscess, bile duct injury and gastrointestinal perforation [74]; which implies that this technique should be used carefully.

1.4.2. Palliative treatments in HCC.

Palliative HCC treatments, which are normally used at later stages, try to increase patients' survival and to improve their life quality without achieving the complete remission of the tumor mass [69]. This type of treatments includes transarterial

chemoembolization (TACE), transarterial radioembolization (TARE) and systemic treatment with sorafenib or regorafenib [64].

TACE is used in the treatment of multifocal HCC patients with 4 or more different tumor masses, or even in individuals which bears a single tumor mass, but in which the surgical resection and ablation are not possible due to the presence of anatomical problems or comorbidities [75]. Traditionally, this process consists in the injection into the hepatic artery of some chemotherapeutic drugs, such as doxorubicin or cisplatin, followed by embolization, which increases the load of cytotoxic agents in the tumor milieu and impedes the supply of blood to the carcinogenic tissue [69]. Although TACE efficiency varies depending on multiple prognostic factors (tumor burden, liver function and portal vein invasion grade by carcinogenic cells) [69], the mean overall survival rate of this strategy is 16 months [76]. So as to improve this technique, new TACE variants have recently been arisen, such as drug-eluting bead TACE, which combines the embolic material and the chemotherapeutic drug in the same bead, or balloon-occluded TACE, which consists in the use of a micro-balloon catheter to occlude the hepatic artery [75].

On the other hand, although radiotherapeutic tools are not very used for HCC treatment, TARE has recently been added to the available palliative therapies for HCC. This technique consists in the intra-arterial injection in the arterial milieu of excluding beads coating with a radioisotope, such as yttrium-90, iodine-131 or rhenium-188 [66,67]. It has been claimed to present an OS rate of 12.8 months, depending on the BCLC stage, number of nodules present and presence/absence of extrahepatic disease [77].

Otherwise, hardly any systemic chemotherapeutic drug, nor therapeutic agents, such as antiestrogens or interferon present any survival benefit for patients with advanced HCC [67]. Therefore, sorafenib was the first drug which has demonstrated a clear improvement in the overall survival of HCC patients, validating its use as primary therapy for HCC [78,79]. Moreover, some brand-new chemotherapy drugs, such as regorafenib, nivolumab and lenvatinib, are being developed to be used after sorafenib failure [80]. All these data are going to be described further more in detail.

2. Sorafenib.

Sorafenib (BAY 43-9006, Nexavar®) is a chemotherapeutic drug derived from a bi-aryl urea that was first described in 1995 by Bayer and Onyx to impede the effects that exert the oncogene rapidly accelerated fibrosarcoma 1 (Raf1) on the proliferation of carcinogenic cells [81]. It was the first chemotherapeutic drug approved by the American Food and Drug Administration (FDA) and by the European Medicines Agency (EMA) to be used as the first-line systemic treatment in advanced HCC [82]. Additionally, this drug has also been authorized for the treatment of radioiodine-resistant metastatic thyroid carcinoma and in renal cell carcinoma (RCC), improving OS rates as it is has been reported in various randomized clinical trials [83,84]. Moreover, sorafenib has also been tested, in some phase II clinical trials, for the treatment of prostate and esophageal cancer in which avoids carcinogenic progression, stabilizing the tumor, but without achieving a significant reduction in tumor volume [85,86].

Otherwise, two different phase III randomized clinical trials were performed in order to asseverate the anticarcinogenic effects of this drug in hepatic cancer: sorafenib HCC assessment randomized protocol (SHARP) trial, which was conducted mainly in Europe and America [78], and another similar one which was performed in the Asian-Pacific region [79]. In these studies, oral sorafenib administration into patients with advanced HCC was able to extend their OS media from 7.9 months to 10.7 months in SHARP trial and from 4.2 months to 6.5 months in Asia-Pacific study [78,79]. Subsequent analysis of SHARP trial patients demonstrated that vascular endothelial grown factor (VEGF) and angiopoietin 2 serum levels could predict the survival of advanced HCC patients, but not their response to sorafenib [87]. Finally, Global investigation of therapeutic decisions in HCC and of its treatment with sorafenib (GIDEON) phase IV clinical trial has recently been developed to assess the safety of sorafenib treatment [88]. In this study, sorafenib has been demonstrated to be well tolerated by all patients, even in patients with poor liver function, being the safety profile of this drug totally independent of age, initial sorafenib dose and BCLC and Child-Pugh scores [88].

2.1. Sorafenib pharmacodynamics in cancer.

Sorafenib is a multikinase inhibitor which can restrain the proliferation, angiogenesis and progression of HCC cells by inhibiting various serine/threonine kinases, as well as some receptor tyrosine kinases [89,90]. As indicated previously, sorafenib was originally developed to restrain the signal transduction activity of Raf1 [also called normal cellular Raf gene (cRaf)] and either wild-type or mutated RafB [91]. These processes ultimately inhibit the activation of mitogen-activated protein kinases (MAPK)/extracellular signal-regulated kinase 1 (ERK1) pathway, which is implicated in the malignant transformation of liver cells and in the induction of cancer cell proliferation (Fig. 5A) [81,91]. In addition, it seems that the inhibition of this pathway by sorafenib is correlated with the reduction of cyclin D1 expression in HCC cells, inducing aberrant cell cycle arrest as a result of this inhibition (Fig. 5A) [92]. Otherwise, sorafenib could also arrest the cell cycle progression in HCC cells through overexpressing the growth arrest DNA damage-inducible gene 45 β (GADD45 β) [93], which disrupts of cell cycle G2/M progression in response to different stress stimuli [94]. Curiously, this process is not dependent on MAPK/ERK1 pathway inhibition, but it seems to be associated with sorafenib-mediated c-Jun N-terminal kinase (JNK) overexpression [93].

Conversely, sorafenib can also modulate some pathways that stimulate programmed cell death programs in cancer [81,90]. In fact, it has been reported that this drug could sensitize cells to tumor necrosis factor (TNF)-related apoptosis-inducing ligand (TRAIL) apoptosis in RCC [95]. Since most of RCC and HCC tumors are resistant to this pathway, the development of agonists which activate TRAIL receptors could represent a promising therapeutic strategy in these cancer types [95,96]. Sorafenib can overcome the TRAIL resistance in HCC cells by reducing the T705 phosphorylation of signal transducers and activators of transcription type 3 (STAT3) as well as its related proteins myeloid cell leukemia 1 (Mcl-1), survivin and cyclin D1 [90,96]. Furthermore, sorafenib can downregulate Mcl-1 translation through a MAPK independent mechanism, which ultimately potentiates intrinsic apoptosis pathway by impeding that B-cell lymphoma protein- 2 (Bcl-2) homologous antagonist killer (Bak) can exert its proapoptotic effects (Fig. 5A) [81,90].

On the other hand, sorafenib is also able to reduce HCC angiogenesis through the inhibition of the tyrosine kinase activity of vascular endothelial growth factor receptor-2

(VEGFR-2), VEGFR-3 and platelet-derived growth factor receptor (PDGFR- β) in tumor-associated vascular endothelial cells (Fig. 5B) [81,89]. This drug is able to inhibit the substrate-mediated autophosphorylation of these receptors, impeding the transduction of the proangiogenic signal into the cell by MAPK/ERK1 pathway (Fig. 5B) [97]. This process generates the reduction in tumor vessel formation surrounding the tumor, which leads to enhancing cell death due to the lack of nutrient and oxygen supply [81]. Some studies have highlighted the role of VEGFR repression by sorafenib, which seems to be as essential as Raf inhibition in the induction of sorafenib antiproliferative effects [89].

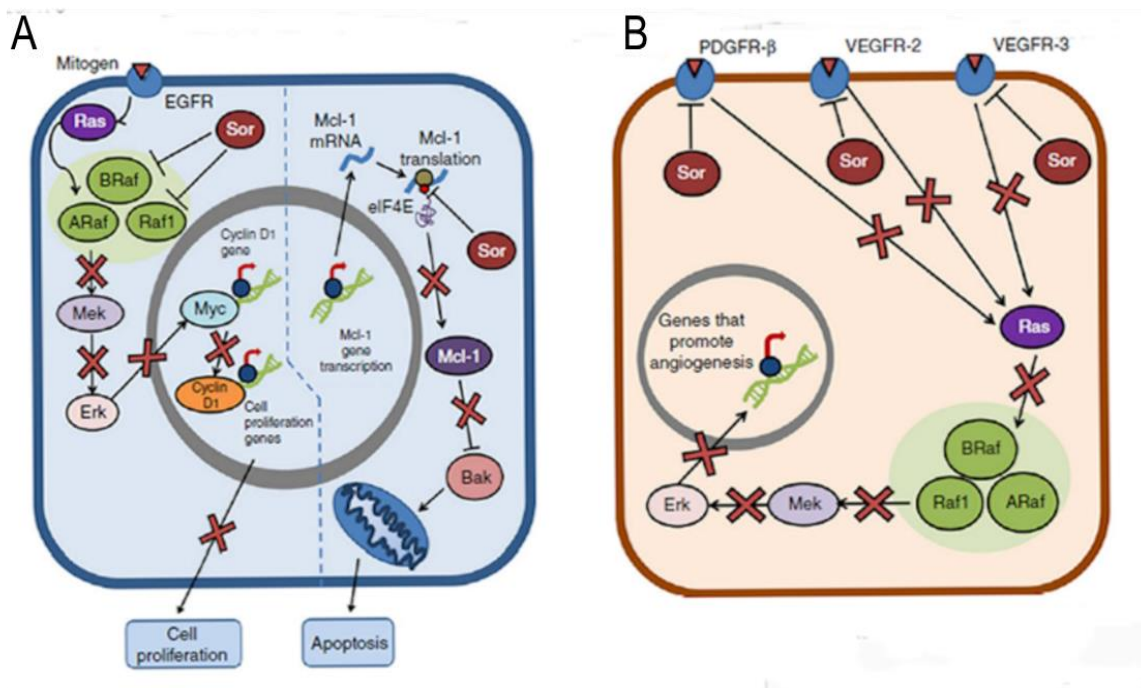


Figure 5: Molecular mechanisms through sorafenib restrains HCC progression **(A)** Sorafenib is able to reduce cell proliferation in HCC cells through inhibiting Raf transduction ability, which in turn restrains MAPK/ERK1 pathway activation. This repression ultimately leads to diminishing cyclin D1 levels by Myc-1 inhibition. Otherwise, this drug can also induce the intrinsic pathway of apoptosis through impeding the translation of Myc-1 protein, an antiapoptotic agent which is in charge of restraining Bak activation. **(B)** Sorafenib can restrain tumor angiogenesis through impeding the substrate-induced autophosphorylation and activation of VEGFR-2, VEGFR-3 and PDGFR- β in tumor-associated vascular endothelial cells, which prevents the expression of proangiogenic genes through the induction of MAPK/ERK1 pathway. (Sor): sorafenib. Modified and retrieved from [81].

Finally, it has recently been demonstrated that sorafenib can induce autophagy pathway in HCC cells, stimulating microtubule-associated proteins 1A/1B light chain 3B (LC3) lipidation, Beclin1, autophagy-related gene 5 (Atg5), and Atg12 expression [81,90]. Sorafenib-induced autophagy can exert a dual role in cancer cells because in a way, it can

promote cell death by collaborating with sorafenib-induced PCD mechanisms, but on another way, it can prevent its antiproliferative effects [90]. Induction of autophagy by sorafenib could be assessed by the modulation of multiple cellular pathways and mediators that include Akt/mammalian or mechanistic target of rapamycin complex 1 (mTORC1), AMP-activated protein kinase (AMPK), unfolded protein response (UPR) ceramide/sphingosine 1-phosphate (S1P) balance or miR30 α [90], which will be reviewed in Fig. 6.

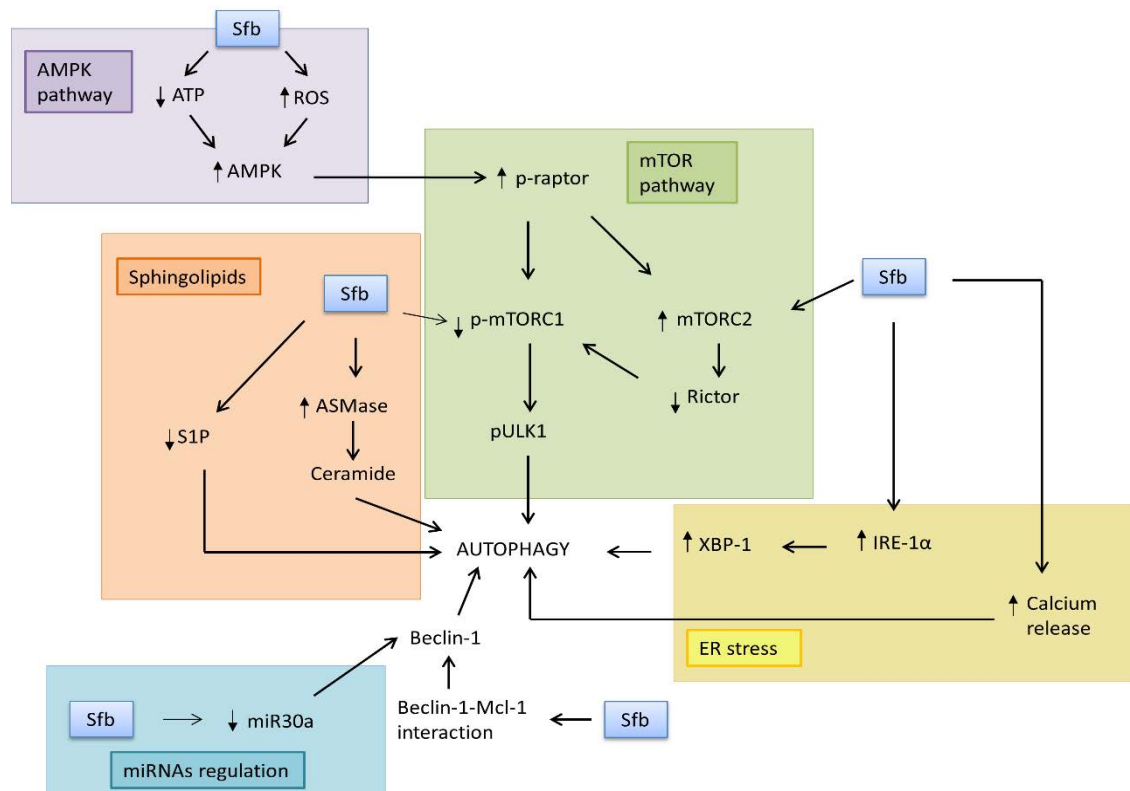


Figure 6: Cellular pathways involved in the stimulation of autophagy by sorafenib. Sorafenib can induce autophagy pathway through the modulation of multiple mediators and pathways in tumor cells. This chemotherapeutic drug can induce AMPK pathway by the reduction of ATP content and the increment of ROS, reducing mTORC1 phosphorylation by Raptor phosphorylation, which ultimately leads to induce autophagy pathway. Raptor could repress mTORC1 phosphorylation directly or indirectly through increasing the formation of mTORC2 (mammalian/mechanistic target of rapamycin complex 2). Furthermore, sorafenib could also stimulate autophagy pathway by inducing a misbalance between ceramide/S1P levels, as well as by enhancing UPR expression and calcium release from the ER (endoplasmic reticulum). Finally, sorafenib could also augments autophagy by decreasing miR30 α expression, which has been described as a Beclin1 repressor. Retrieved from [90].

2.2. Sorafenib pharmacokinetics and safety.

When sorafenib is orally administered at fasted state, it presents a relative bioavailability of 38-49 %, remaining these values similar when is administered with low-or-moderate-fat meals, but decreasing with high-fat meals [98]. This drug reaches to the peak plasma levels 3 h after administration, achieving the steady-state concentrations 7 days after its first dosage [98]. Sorafenib is metabolized oxidatively by the liver through cytochrome P450 3A4 (CYP3A4) and is subsequently glucuronidated by uridine diphosphate (UDP) glucuronosyltransferase family 1 member A9 (UGT1A9) [98]. Finally, it is excreted in feces and urine, oscillating its half-life of elimination between 25 and 48 h [98].

Although sorafenib appears to be well-tolerated, it is rather frequent the manifestation of some mild or moderate side-effects that could force to reduce its doses or to end its administration [88,99]. Fortunately, only the 9% of all patients treated with this drug during GIDEON phase IV trial study experimented life-threatening drug-related adverse events, being less frequent than the mild side-effects [88]. The most important adverse events derived from sorafenib treatment are cutaneous lesions, cancer-related fatigue, hypertension and other cardiac symptoms, diarrhea and anorexia [98,99].

Cutaneous lesions are the most frequent side effects of this drug, affecting to more than 90% of all sorafenib-treated individuals [100]. However, these lesions are normally mild or moderate and can be treated with an appropriate clinical management, being the incidence of severe dermatological lesions lower than 10% [101]. The most frequent dermatologic adverse event is hand-foot skin reaction (HFSR), which often arises dose-dependently during the first 6 weeks of drug treatment and is distinguished by the progressive necrosis of keratinocytes, which results in the generation of painful intradermal blisters in the palm, sole and fingertips [101]. Furthermore, the erythematous eruption in face, scalp and trunk, and alopecia are other frequent side effects that appear between 2 and 16 weeks after the start of sorafenib administration [101]. Finally, less common dermatologic problems are subungual splinter hemorrhages, scrotal eczemas, skin cysts, xerosis, areolar hyperkeratosis and eruptive melanocytic lesions [100,101].

Diarrhea affects to about 27.1% of the total sorafenib-treated HCC patients [102]. Loperamide administration, low-fiber diet assumption, elevated liquid intake and the disruption of lactulose treatment are some of the measures that are usually performed in

clinical practice to treat mild or moderate sorafenib-related diarrheas [99]. The reduction of sorafenib doses and the suppression of the treatment with this drug would be only necessary if severe diarrheas occurred [99].

Sorafenib has been reported to induce low-frequent moderate-to-severe cardiovascular side effects [103]. As it was reported in the SHARP study, about 5 % of all sorafenib-treated patients develop hypertension, being these effects severe or life-threatening in about the 2% of the whole total [78]. Therefore, the monitorization of blood pressure should be essential to reduce the appearance of these side-effects [103]. Moreover, sorafenib administration also rises significantly the risk of undergoing cardiac ischemia, infarction and bleeding regarding non-treated HCC patients, which would ultimately lead to interrupt sorafenib administration if these events persisted or worsened [103].

Finally, cancer-related fatigue (CRF), which is defined as a persistent status of tiredness that appears during cancer treatment [104], is also a common side effect during sorafenib treatment [98]. Although doses adjustment or treatment restriction should be used in clinical practice to prevent or reduce the severity of CRF, an appropriated clinical management could be enough to avoid the increase of this disease in sorafenib-treated patients [99].

2.3. Sorafenib resistance.

The appearance of some cells that are insensitive to sorafenib treatment and continue proliferating, even when this chemotherapeutic drug is present in their microenvironment, is a highly frequent limitation for HCC treatment [89,105]. Whereas the genetic heterogeneity of HCC could account for sorafenib primary resistance, the progressive overexpression of survival pathways and mechanisms, which could mask its antiproliferative and prodeath effects, leads to the arising of an acquired resistance to sorafenib in HCC (Fig. 7) [105]. These processes could explain the disappointing rate of responsiveness to sorafenib, which only generates a starting significantly beneficial response in 30% of all patients, decreasing progressively within the first 6 months of treatment [89,106]. Although some molecules have recently been developed to be used in combination with sorafenib treatment or as second-line therapy after sorafenib failure, this issue continues being a major challenge in the treatment of advanced HCC [107].

2.3.1. *Primary resistance to sorafenib.*

Due to the genetic heterogeneity of HCC cells, some of the sorafenib targets could be downregulated or totally absent. For this reason, sorafenib could not assess its antiproliferative effects, leading to the generation of a primary resistance against sorafenib [105,108]. This statement could explain the great variations showed in sorafenib sensibility among the different HCC immortalized cell lines [109]. Therefore, the identification of predictive biomarkers is essential to identify and manage sorafenib primary resistance [105]. Some of the proteins which can be used with this purpose, since their cellular levels are related with the sensitiveness to sorafenib treatment, are epidermal growth factor receptor (EGFR), phosphorylated ERK (pERK), JNK, VEGF and angiopoietin 2 (Fig. 7) [87,91,110,111]. Additionally, other non-protein molecules, such as some microRNAs (miRNAs) or long non-coding RNAs (lncRNAs), have recently been arisen as predictive markers for monitoring patients' response to sorafenib [112,113]. Despite these findings, it is necessary the discovery of more specific biomarkers which can be applied to classify HCC patients according to their sensitiveness to sorafenib and to select individualized treatments [108].

2.3.2. *Acquired resistance to sorafenib.*

Time-extended exposure to sorafenib can result in the deregulation of multiple cellular pathways which masks the prodeath actions of this drug, generating acquired resistance inside the tumor [105]. Some of these mechanisms include the activation of some compensatory pathways which disable sorafenib-related antiproliferative signals, the induction of EMT, the stimulation of autophagy and the modulation of cellular microenvironment (Fig. 7) [89,105,108].

Phosphatidylinositol 3-kinase (PI3K)/Akt/mammalian or mechanistic target of rapamycin (mTOR) pathway and Janus kinase (JAK)/STAT pathways are the main compensatory pathways that are usually overactivated in sorafenib resistant cells, leading to neutralize its antiproliferative actions [105,108]. It has been demonstrated that PI3K/Akt/mTOR signaling remains untargeted after sorafenib treatment [105], and that the inhibition of these pathways, either by a chemical compound or by a small interference RNA (siRNA), enhances sorafenib-related apoptotic processes [114], suggesting that the

upregulation of this pathway could have a role in the development of acquired sorafenib resistance (Fig. 7). Indeed, PI3K, Akt and mTOR, as well as their downstream targets, were overexpressed in HCC sorafenib resistant-cells, and the induction of Akt ectopic expression in non-resistant cells can desensitize these cells to this drug (Fig. 7) [115]. In addition, Akt restriction in the resistant cells sensitizes them to sorafenib treatment [115]. On the other hand, sorafenib, as indicated previously, is able to restrain STAT3 phosphorylation [116], impeding the induction of JAK/STAT3 pathway [108]. Curiously, aberrantly high phosphorylation of JAK1, JAK2 and STAT3, as their downstream factors Mcl-1 and cyclin D₁, has been found in sorafenib resistant cells (Fig. 7) [117]. Therefore, the elimination of this singular situation overcomes sorafenib resistance [117], while the overinduction of STAT phosphorylation in sorafenib-sensitive HCC cells induces this resistance [118]. Summarizing, the use of Akt or JAK/STAT3 inhibitors in combination with sorafenib could partly avoid acquired sorafenib resistance [108].

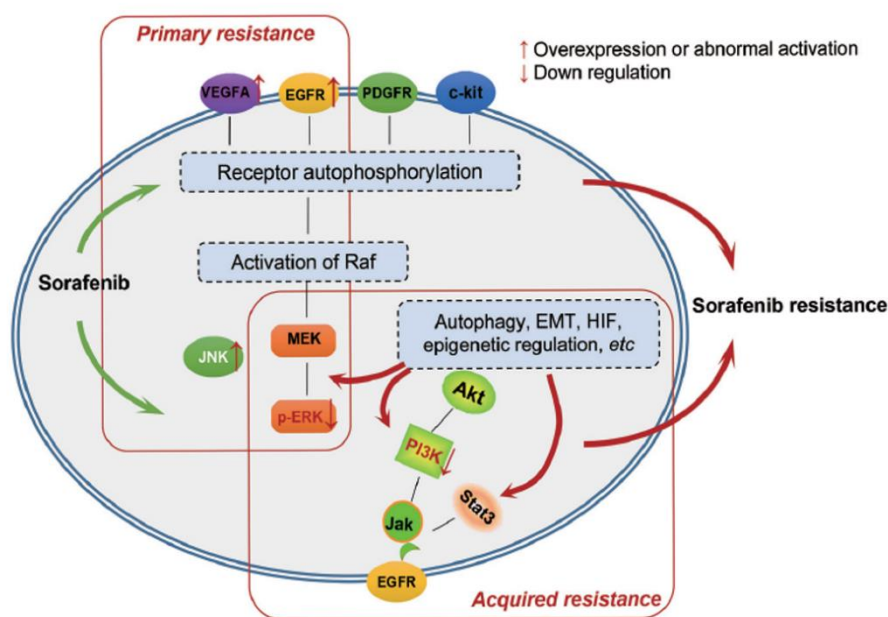


Figure 7: Molecular mechanisms that reduce cell sensitivity to sorafenib in HCC cells. These mechanisms could be divided into two groups depending on the moment when their starting since the beginning of the treatment. Primary resistance mechanisms usually appear at the start of sorafenib administration and are related to changes in the expression of some proteins due to the genetic heterogeneity of HCC cells. The overexpression of JNK, VEGFA and EGFR; as well as the reduction of ERK phosphorylation are biomarkers of sorafenib primary resistance. On the other hand, the time-prolonged sorafenib administration generates an acquired resistance to that drug in HCC cells, due to the stimulation of cellular pathways and mechanisms which mask the action of sorafenib, such as autophagy, EMT, Akt/mTOR or JAK/STAT3. Retrieved from [108].

EMT process is a transitional phenomenon from epithelial to mesenchymal phenotype which occurs not only in physiological processes, such as wound healing or embryonic development, but also in pathological situations, such as in cancer progression and metastasis [105]. EMT has recently been asseverated to be a hallmark in acquired sorafenib resistant cells, presenting a mesenchymal-like morphology due to the reduction in the expression of some epithelial markers, such as E-cadherin, and to the overexpression of mesenchymal ones, such as N-cadherin, vimentin or Snail (Fig. 7) [119].

Autophagy, which is a bulk degradation system that degrades both useless or damaged organelles and molecules, also seems to have a role in the acquisition of cellular resistance to sorafenib [107]. It has been described that sorafenib treatment can induce autophagosome formation and enhance the expression of the autophagy-related genes [90]. Nevertheless, sorafenib-induced autophagy could unexpectedly work as a prosurvival pathway because of the dual role that this pathway presents in cancer management (Fig. 7) [90,107]. Therefore, it has been proven that Atg7 knockdown stimulates sorafenib-related HCC cell apoptosis by inducing the activity of caspase 3 and 7 [120]. To sum, it seems that the induction of prosurvival autophagy could play a key role in the desensitization of HCC cells to sorafenib treatment.

Finally, HCC cell microenvironment also performs a fundamental role in the induction of cell resistance to sorafenib [89]. Although many factors which surround the cell could affect to HCC sorafenib sensibility, such as liver inflammatory status, oxidative stress, fibrosis grade or viral reactivation; hypoxia is probably the most important of them [89]. This cellular harmful status is characterized by the lack of oxygen in the tumor milieu, which finally leads to inducing different prosurvival pathways, such as EMT or PI3K/Akt, avoiding tumor cells death, increasing ultimately the cellular resistance to sorafenib chemotherapy (Fig. 7) [121,122].

2.3.3. Mechanisms to overcome sorafenib resistance.

Due to the great number of different extracellular and intracellular factors with the ability to modulate sorafenib effectiveness in HCC, it is necessary to develop new strategies which can extend the use of sorafenib or replace this drug after its failure [107]. For this reason, many brand-new drugs are being proven either as therapeutic adjuvants or as second-line therapy to overcome this situation or to continue inducing antiproliferative

signals when sorafenib action has been neutralized [80,107]. This process peaked on 2017 with the approval of regorafenib by the FDA and the EMA and nivolumab only by the FDA, as the first second-line chemotherapeutic drugs available to be used in the treatment of HCC after sorafenib failure [123]. Regorafenib, which present the same mechanism of action as sorafenib, with the ability to restrain carcinogenesis, angiogenesis and metastasis, can extend the OS of sorafenib-resistant patients from 7.8 to 10.6 months [124,125]. On the other hand, nivolumab, which is a monoclonal antibody developed against programmed cell death protein 1 (PD-1), leading to the reactivation of the antitumor immune response, has demonstrated in a phase II trial that it is able to increase the mean OS rate in sorafenib-resistant patients with a manageable safety profile [126]. Nevertheless, its FDA approval is contingent until the development of a phase III trial which confirms its safety and clinical benefit [127].

3. Microenvironment and hypoxia in cancer progression. Role of HIFs.

Hypoxia is a physiological situation that occurs when oxygen supply is not enough to satisfy cellular demand, which may normally occur due to the generation of changes in the tissue vasculature or malfunctions of the hemoglobin protein [128]. Indeed, chronic hypoxia is a common feature that arises during the advanced stages of cancer development [16,128], because of the great proliferative and metabolic rates that present carcinogenic cells [129]. The progressive expansion of the tumor due to uncontrolled cancer proliferation leads to increasing the distance from the microvasculature to the tumor core, exhausting both nutrient and oxygen supply, and generating the arising of hypoxic tumor areas [129,130]. Therefore, in an advanced tumor tissue has been shown to coexist re-oxygenation, mild hypoxic and severe hypoxic areas where carcinogenic cells are death by necrosis [130]. Tumor cells under hypoxia present a more aggressive phenotype, a higher likelihood to develop secondary tumors and a greater resistance to chemotherapy and radiotherapy [128].

Carcinogenic cells treat to counteract hypoxia-related death signaling through the induction of multiple prosurvival processes which include cell immortalization, metabolic reprogramming, tumor vascularization, tumor invasion and metastasis [131]. For example, hypoxia switches tumor cell metabolism from oxidative to fermentative by downregulating glucose flux to acetyl coenzyme A and tricarboxylic acid (TCA) cycle and by increasing

glucose flux to lactic fermentation [132,133]. Additionally, this condition also stimulates cellular glucose intake and glycogen synthesis [132,133]. Otherwise, hypoxia induces the sprouting of new vessels towards the tumor [134]. Nevertheless, these capillaries are usually morphologically and functionally aberrant due to the extensive and continuous liberation of proangiogenic factors, which ultimately could lead to impairing drug delivery and to easing cell dissemination and metastasis [135]. Finally, recent evidence has demonstrated that hypoxia induction is fundamental to achieve all steps of tumor invasion, since it is necessary to provoke EMT, extracellular matrix breakdown, tumor cell intravasation/extravasation, and metastasis [136]. All these responses are modulated by a group of transcriptional factors known as HIFs that act as oxygen sensors inside the cells [131].

3.1. HIFs isoforms and structure.

HIFs factors are composed by α -subunits that are oxygen-sensitive, and β -subunits which are constitutive expressed independently of the oxygen concentration [137]. All these factors recognize a specific five-nucleotide DNA sequence (5'-RCGTG-3'), which is known as hypoxia responsive element (HRE) and is situated in the promoter or enhancer regions of the target genes of these proteins [138]. Otherwise, three different HIF- α proteins, HIF-1 α , HIF-2 α /endothelial PAS domain-containing protein 1 (EPAS1) and HIF-3 α has currently been described [139]. The HIF-1 α and HIF-2 α structure, functions and activity are well-known [137], whereas the less-known HIF-3 α seems to negatively regulate the hypoxic response in an opposed way in relation with the others [139,140]. Indeed, the splicing variants of HIF-3 α are able to interact with the rest of HIF- α homologs, impeding their nuclear translocation and activity [140,141]. Unexpectedly, it has recently been reported that the overexpression of some HIF-3 α variants leads to the upregulation of different HIF target genes, suggesting that these proteins could perform a more versatile role in the regulation of hypoxia response [140]. On the other hand, three different HIF- β subunits, HIF-1 β /aryl hydrocarbon receptor nuclear translocator 1 (ARNT1), ARNT2 and ARNT3 have been currently described [137].

HIF factors belong to the basic helix-loop-helix (bHLH)-Per-ARNT-Sim (PAS) family [142–144], which is a subgroup of human transcriptional factors that are characterized by presenting two contiguous repetitions of the PAS domain, PASA and

PASB, behind the NH₂-terminal bHLH domain (Fig. 8) [143]. These PAS structures are not only implied in the heterodimerization of these factors, but also prevent the formation of odd interactions with non-PAS containing proteins. Moreover, PASB performs a clear role as a metabolic and environmental sensor due to its ability to interact directly with proteins that bring either external or internal information (Fig. 8) [143]. Otherwise, bHLH domain is responsible for the recognition and joining to their specific binding sequence in the DNA, which is the HRE domain in the case of HIF factors [142]. Additionally, these proteins usually present two transactivation domains (TADs) that are responsible for triggering their transcriptional activity [145]. The first TAD is situated in the COOH-terminal region (C-TAD), which is absent in all HIF-3 α splicing variants [140,145]. However, the second TAD is situated near the NH₂-terminal region (N-TAD), being included in HIF- α subunits in the oxygen-regulation site, which is also known as oxygen-dependent degradation (ODD) domain (Fig. 8) [145,146]. Finally, these proteins also present two nuclear localization signal (NLS) which allow their translocation into the nucleus (Fig. 8) [146,147].

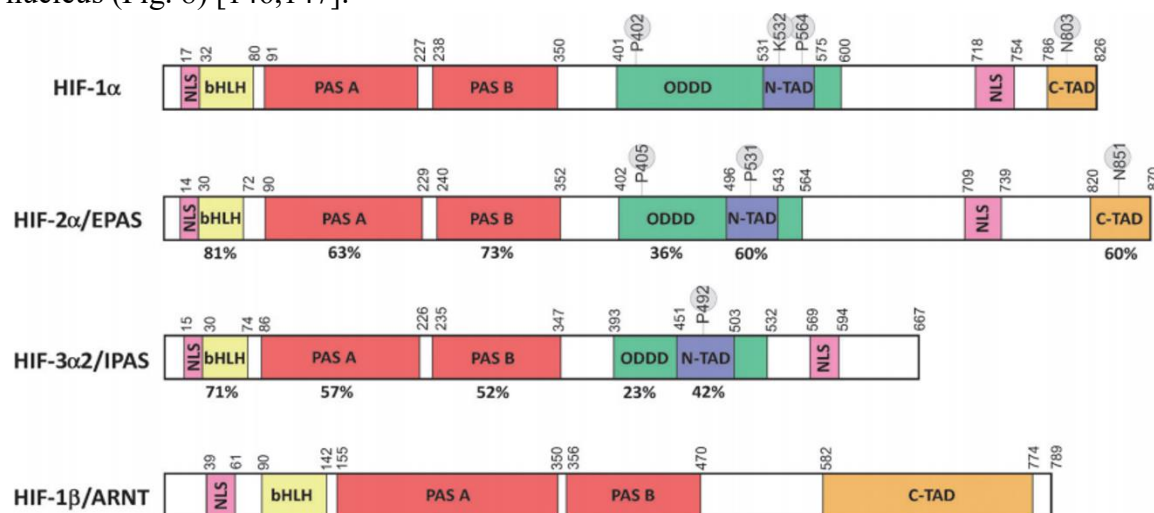


Figure 8: Structure and domain organization of the main HIF subunits. Canonical HIF proteins are constituted by a bHLH domain, which recognizes the HRE sequence; two different PAS domains, which are responsible for HIF heterodimerization; two TAD zones, which activate HIF-related transcription and are intimately regulated by oxygen; as well as two different NLS sequences which import these transcriptional factors into the nucleus. Additionally, HIF- α subunits present a unique ODD domain that overlaps N-TAD, in which oxidative regulation of these factors is taken place. Finally, HIF-3 α does not have the C-TAD domain, while HIF-1 β lacks the N-TAD one. The percentages displayed under each domain indicates the degree of amino acid homology which exists between a domain and its equivalent in HIF-1 α . Retrieved from [144].

3.2. Regulation of HIFs.

Although the main factor that affects to HIF-1 α and HIF-2 α activation levels is the external concentration of O₂, other anaerobic stimuli, such as the presence of certain growth factors in the surrounding medium, are also able to modulate the transcription, translation and stability of these transcription factors [145,148]. These oxygen-independent signals usually provoke HIF-1 α accumulation and activation through the stimulation of either MAPK or PI3K/Akt/mTOR pathways [145].

3.2.1. Oxidative regulation of HIF- α subunits.

When oxygen is present in the media, both HIF-1 α and HIF-2 α undergoes a progressive hydroxylation in some certain proline residues located in the ODD domain by a specific group of enzymes known as prolyl hydroxylases (PHDs) (Figs. 8, 9 and 10) [148]. Basically, there are four different PHD enzymes that modulate the activation of these factors [149], being PHD2 the main enzyme that mediates the hydroxylation of HIF-1 α , and PHD3 which mediates HIF-2 α modification [150,151]. These enzymes require Fe²⁺, ascorbic acid, O₂ and α -ketoglutarate (KG) to exert their function, being tightly regulated by metabolic cellular status, since KG belongs to the TCA cycle, and by ROS, which can oxidize the Fe²⁺ ion to Fe³⁺ deactivating them [152]. Subsequently, hydrolyzed HIF- α subunits are recognized by von Hippel–Lindau protein (VHL), an E2 substrate recognition enzyme for an E3 ubiquitin ligase module, which polyubiquitinates HIF- α driving this factors into degradation in the proteasome complex (Figs. 9 and 10) [153,154]. When oxygen is absent in the media, PHDs are inactive and both HIF-1 α and HIF-2 α do not suffer degradation, thus they can translocate into the nucleus; heterodimerize with HIF-1 β through their PAS domains; and ultimately, bind to the HRE sequence of their target genes in combination with some transcriptional coactivators, such as cAMP response element-binding (CREB)-binding protein (CBP) and p300, inducing the expression of their target genes (Figs. 9 and 10) [146,154].

Although the pathway which involves PHDs and pVHL is the most representative process, is not the only oxygen-dependent mechanism that modulates HIF- α degradation under normoxia [144]. For example, factor inhibiting HIF (FIH), which is a Fe²⁺-, KG-, ascorbate-dependent (as PHDs) asparagine hydroxylase, specific hydroxylates N803 in

HIF-1 α and N851 in HIF-2 α , both located in their C-TAD region (Figs. 9 and 10) [144], acting as a secondary oxygen sensor and preventing the binding of the transcriptional coactivators CBP and p300 to the HIF heterodimers in normoxia (Figs. 9 and 10) [144,146,154]. In addition, it has demonstrated that this hydroxylase presents more affinity for HIF-1 α than HIF-2 α , being this last mediator almost insensitive to this inhibition [155]. On the other hand, the small ubiquitin-related modifiers (SUMO)ylation of HIF-1 α also seems to perform a key role in the oxidative-dependent degradation of this protein [148]. Indeed, it has been reported that HIF-1 α undergoes some SUMOylations in the proximities of its ODD domain through different SUMO E3 ligases, such as protein inhibitor of activated STAT protein gamma (PIAS γ) or Ran-binding protein 2/ nucleoporin 538 (RanBP2/Nup538), preventing its activation; and ultimately, driving into its degradation by the ubiquitin-proteasome system [156,157]. In addition, the SUMO deconjugation enzymes known as Sentrin/SUMO-specific proteases (SENPs) have been

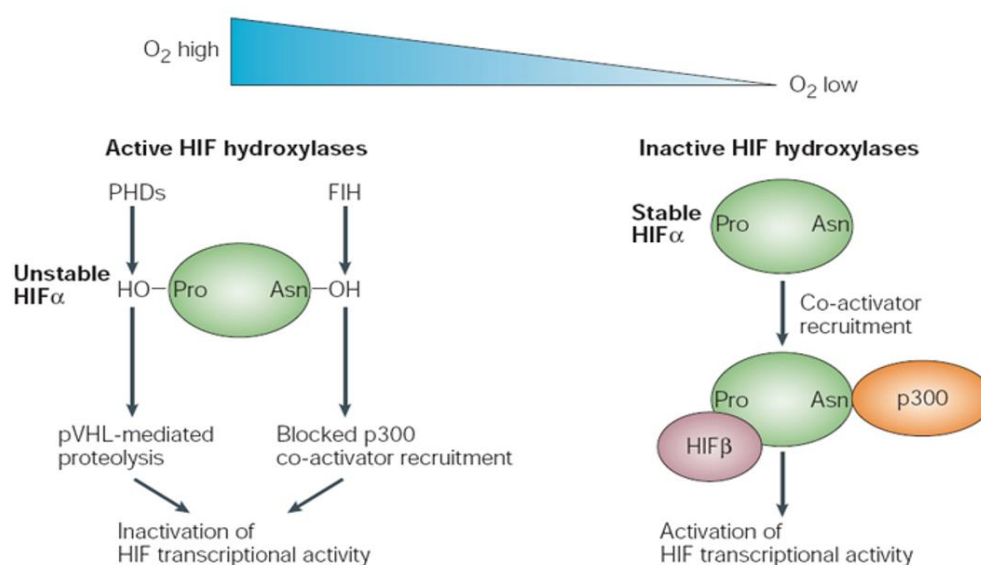


Figure 9: Regulation of the transcriptional activity of the main oxygen-sensitive HIF subunits by PHDs and FIH. When the O_2 concentration is high in the medium, both PHDs and FIH are active, leading to the downregulation of the transcriptional activity of HIF- α subunits by the hydroxylation of some key proline and asparagine residues situated in the ODD domain and in the C-TAD domain of these transcription factors respectively. These modifications ultimately result in the proteolytic degradation of these oxygen-sensitive mediators through a pVHL-, ubiquitin-, proteasome-dependent process; as well as in the blockage of p300 and CBP recruitment, which are their specific transcriptional coactivators. Oppositely, when hypoxia is induced in the cell media, these HIF hydroxylases are inactive, thus HIF- α subunits can bind with their specific coactivators p300 and CBP and with the oxygen-independent HIF- β subunit, inducing finally the HIF transcriptional activity. Modified from [154].

shown to be able to increase the translocation, stability and activity of HIF-1 α , being these enzymes accumulated when oxygen is deprived [158]. Oppositely, it has also been reported that SUMOylation promotes the stabilization and the transcriptional activity of HIF-1 α under hypoxic conditions through other different SUMOylation enhancers, such as RWD-containing SUMOylation enhancer (RSUME) [159]. Therefore, further studies should be developed to assess the fine regulation of HIF-1 α by SUMOylation.

3.2.2. Oxygen-independent regulation of HIF- α subunits.

Besides oxygen-dependent mechanisms that regulate the transcriptional activity of the different HIF- α subunits, there are also other non-oxygen-dependent pathways that can stimulate the accumulation of activated HIF- α under hypoxic conditions [145]. These cellular routes, which are depending on growth factors, cytokines and other molecular signals, induce the accumulation of these subunits through the modulation of different cellular proteins, such as 90 kDa heat shock protein (HSP90) or p53/murine double minute 2 (Mdm2); or pathways, such as MAPK or PI3K/Akt/mTOR (Fig. 10) [144,145].

HSP90 collaborates in the control of the folding and the stabilization of misfolded proteins due to its ATP-directed chaperone activity [160]. This molecule has been reported to attach to the PASA domain of HIF-1 α , stabilizing this protein in an oxygen-independent manner through displacing its binding to the receptor of activated protein kinase C1 (RACK1), which can disturb HIF-1 α through an O₂/PHD/pVHL-independent, but proteasome-dependent degradation mechanism (Fig. 10) [160,161]. Additionally, it has recently been demonstrated that HSP90-dependent HIF-1 α accumulation is dependent on JNK activation by phosphorylation [162], suggesting that this process is also modulated by the growth factors that can activate MAPK/JNK pathway (Fig. 10).

Otherwise, it has been assessed that the tumor suppressor protein p53 is able to promote the oxygen-independent degradation of HIF-1 α through the ubiquitin-proteasome system in a PHD-, pVHL- and p300-independent manner when there is a severe stress situation outside the cell (Fig. 10) [163,164]. Besides, Akt and macrophage migration inhibitory factor (MIF) seems to act as negative regulators of this process [164]. Oppositely, this protein only induces a lesser reduction in HIF-1 α activity without affecting its protein levels in milder conditions, as a result of the competition of this two proteins for attaching to the same transcriptional coactivator [164,165]. Curiously, p53 also can reduce the

transcriptional levels of the constitutive-activated HIF-1 β subunit through the upregulation of miR-107, inhibiting the translation of this protein by targeting its 3'-UTR region [166]. On the other hand, the implications of Mdm2 in p53-dependent HIF-1 α regulation are still controversial, because it seems to vary according to the model used and to the severity of the hypoxia stimulus which has previously been induced in the cells [164]. Indeed, Mdm2 has been reported either to be necessary to induce the degradation of HIF-1 α by p53, not to affect to this process or even to prevent it through inducing the transcriptional activity of HIF-1 α [163,167,168]. Summarizing, some new comparative studies should be done to understand the role of Mdm2 in the degradation of HIF-1 α by p53.

Conversely, other amino acid modifications different from hydroxylation could also modify the transcriptional activity of HIF- α subunits, which in turn might include a transcriptional skew towards one of the two oxygen-dependent sensors [169]. In this way, the deacetylation of a lysine residue located in the N-TAD domain of HIF-1 α and HIF-2 α by the protein sirtuin 1 (SIRT1) can alter their capacity to binding to p300 (Fig. 10) [169]. Curiously, this process increases the activity of HIF-2 α while decreases the HIF-1 α , indicating the existence of a differential regulation between both subunits (Fig. 10) [169]. Moreover, it has also been shown that other proteins of the sirtuin family can modify the activity of HIF- α subunits [169]. For instance, both SIRT6 and SIRT3 restrain the expression of HIF-1 α , although the mechanisms underlying these processes have not been clearly defined yet [169,170].

On the other hand, the control of HIF-1 α and HIF-2 α activity could also be performed through the modulation of their translation levels [146]. This process is usually mediated by growth factors, cytokines and oncoproteins, which ultimately achieve the transduction of the signal through the activation of PI3K/Akt/mTOR pathway (Fig. 10) [171]. Indeed, the chemical repression of this pathway by YC-1 [3-(50-hydroxy methyl-20-furyl)-1-benzylindazole] reduces the accumulation of HIF-1 α without affecting to its transcription or to its half-life [172]. This process is mediated by the mTORC1-related direct upregulation of ribosomal protein S6 kinase beta-1 (p70S6K) and eukaryotic translation initiation factor 4E (eIF-4E), which are responsible for initiating eukaryotic protein synthesis (Fig. 10) [173]. Moreover, it has also been shown to be triggered through MAPK/ERK pathway, which in turn stimulates the binding of the nuclear HIF-1 heterodimer to its transcriptional coactivator p300 (Fig. 10) [174]. Conversely, it has recently been reported that HIF-2 α expression could be modulated by the PI3K-dependent

induction of mammalian or mechanistic target of rapamycin complex 2 (mTORC2) signaling instead of Akt/mTORC1 pathway; in contrast to the PI3K-dependent HIF-1 α modulation, which seems to rely mainly on mTORC1 (Fig. 10) [175]. This differential regulation could be essential to achieve the fine tuning between both HIF- α subunits

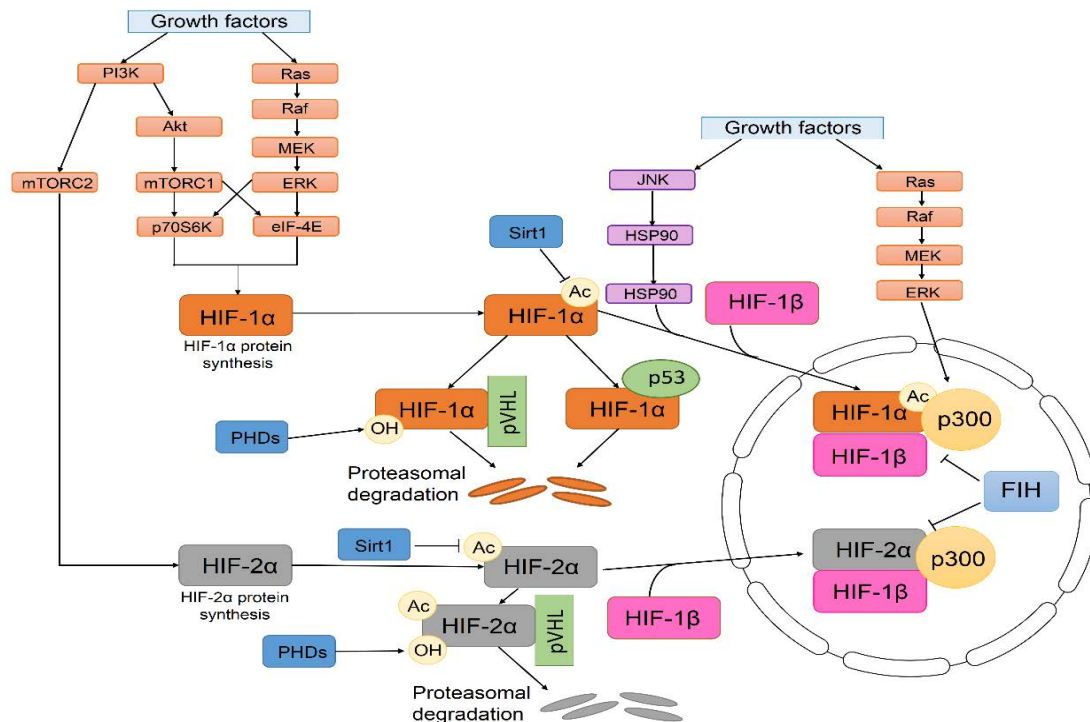


Figure 10: Oxygen-dependent and -independent regulation of the transcription, translation and degradation of the most important HIF- α subunits. The stimulation of the PI3K/Akt/mTOR and MAPK/ERK pathways modulates the translation levels of HIF-1 α through inducing the overactivation of p70S6K and eIF-4E, whereas HIF-2 α is mainly activated through PI3K/mTORC2 pathway. On the other hand, HIF- α homologs are degraded in an oxygen-dependent manner through the dependent hydroxylation of some proline residues, leading to their elimination by the ubiquitin-proteasome system. Besides, p53 also triggers another degradation system of HIF-1 α by a proteasome-dependent, oxygen-independent mechanism, which might involve the Mdm2 protein. Otherwise, JNK promotes the stimulation of HSP90 protein, which in turn has been shown to stabilize the HIF-1 α protein in an oxygen-independent manner. Additionally, extracellular stimuli could induce the activation of MAPK/ERK, which in turn can stimulate the binding between HIF-1 α and p300, whereas FIH impedes this process through the hydroxylation of an asparagine residue in the C-TAD domain of both HIF- α proteins, but principally in HIF-1 α . Finally, SIRT1 deacetylase restrains HIF-1 α activation, but enhances HIF-2 α binding to p300 through the elimination of a specific acetyl posttranslational modification.

Finally, there are other cellular mechanisms that can alter HIF- α levels by modulating their *de novo* synthesis [176,177]. For example, the aberrant demethylation of CpG dinucleotide islands in the HIF-1 α gene induces its overexpression through a

mechanism of autoregulation including its direct binding to its own promoter, which is normally overmethylated, and inducing a HIF-1 α positive feedback series in response to hypoxia stimuli [178]. Besides, the hypermethylation of this gene has shown to stimulate the opposite process [179]. Otherwise, there are some miRNAs that are implied in HIF-1 α and HIF-2 α gene regulation, such as miR-17-92, which is responsible for c-Myc-mediated HIF-1 α repression [180]; miR-20a, miR-199a-5p, miR-22, miR-138, which can also reduce HIF-1 α *de novo* synthesis [181–183]; and miR-185, which in turn diminishes HIF-2 α expression [184]. On the other hand, STAT3 can upregulate the transcription of HIF-1 α gene in carcinogenic cells, conferring to these organisms a great set of benefits against extracellular death signals [185].

3.3. The balance between HIF-1 α and HIF-2 α in cancer progression under hypoxia.

Although HIF-1 α and HIF-2 α have an elevated homology and a similar oxygen-dependent degradation, they do not actually present neither the same time activation pattern, nor activate the transcription of the same amount of genes under oxygen deprivation in tumor cells [169,186]. Although HIF-1 α is expressed nearly in all human organs and tissues, HIF-2 α expression is restricted to some specific non-carcinogenic cell types, such as hepatocytes, cardiomyocytes, endothelial cells, glial cells or interstitial cells of the pancreas and duodenum [186], as well as to certain types of tumors, such as pancreatic cancer, HCC or RCC [187–189]. Besides, some different time-dependent stabilization patterns have been reported for HIF- α subunits, since HIF-1 α is usually activated after acutely hypoxia stimuli, whereas HIF-2 α modulates chronic and time-extended oxygen-deprivation response [190]. These temporal variations extend the cellular hypoxic response, preventing its decline throughout the time [190].

On the other hand, it has also been demonstrated that the specific amount of genes that these two HIF- α proteins regulate are totally different, even being able to exert completely opposite functions [186]. For instance, HIF-1 α modulates more significantly vascular cell proliferation, migration and sprouting in tumor angiogenesis process, whereas HIF-2 α is more responsible for the regulation of vascular morphogenesis, integrity and assembly; thus both proteins act together to achieve a better blood vessel formation [191]. Besides, these two isoforms present antagonistically roles in the induction of tumor growth, being this process retarded by HIF-1 α upregulation and promoted by HIF-2 α overactivation

in RCC [192]. This phenotype might be associated with a specific response of some tumorigenic genes, such as cyclin D1, transforming growth factor alpha (TGF- α) and VEGF, to HIF-2 α signaling and of some proapoptotic factors, such as BNIP3 and Nix, to HIF-1 α [192]. Nevertheless, this process seems to be highly dependent on the cellular model used in the study, because opposite results have been obtained in colorectal carcinoma in which HIF-1 α depletion restrained tumor growth while HIF-2 α deficiency stimulates carcinogenic cell proliferation [193]. Since the levels of HIF-1 α and HIF-2 α are more elevated in metastatic than in non-metastatic cancers, it has been suggested that both subunits could collaborate in the modulation of cell metastasis [186]. Nevertheless, the mechanisms through these two proteins enhance the generation of secondary tumors are rather different, being possible that they could even act in an antagonistic manner [194]. For example, it has been reported that HIF-1 α can develop nitric oxide (NO)-dependent lung metastasis, whereas HIF-2 α completely delay this situation [194]. Finally, it seems that HIF-2 α upregulation could perform a clear role in the induction of cell resistance to diverse chemotherapeutic drugs, such as paclitaxel, mitomycin C, imatinib and sorafenib [186]. Indeed, time-extended treatments with some antiangiogenic chemotherapeutic drugs, such as sorafenib, could switch hypoxic signaling from HIF-1 α - to HIF-2 α -dependent pathways, inducing some cellular mechanism, such as ATP-binding cassette (ABC) proteins or the TGF- α /EGFR pathway, which ultimately leads to desensitizing carcinogenic cells against this drug [195,196]. Summarizing, although these HIF- α subunits seem to present totally different functions under hypoxia in carcinogenic cells, both proteins collaborate together to increase cancer malignancy and to induce cancer progression.

4. Autophagy.

Autophagy consists in a bulk degradation system that is in charge of the degradation of dysfunctional, damaged or useless macromolecules and organelles to upkeep cell homeostasis against different stressful situations [197,198]. This is a multistep process that has been conserved throughout all eukaryotic organisms [199]. Although autophagy normally protects cells against either extracellular or intracellular stresses, the prolonged activation of this pathway could lead to induce cell death since many vital components are eliminated [198]. This type of cell death is also known as type II PCD in contrast to apoptosis, which is type I [200]. Nevertheless, it is not currently very clear whether

autophagy is the promoter of type II PCD, or if it tries to avoid it, emerging cell death when this system has been overwhelmed [201].

4.1. Types of autophagy.

Three major types of autophagy have currently been reported in human cells: microautophagy, chaperone-mediated autophagy (CMA) and macroautophagy (Fig. 11) [202]. These three pathways act together and coordinately to maintain cellular homeostasis in human cells since they are completely interdependent among them [203].

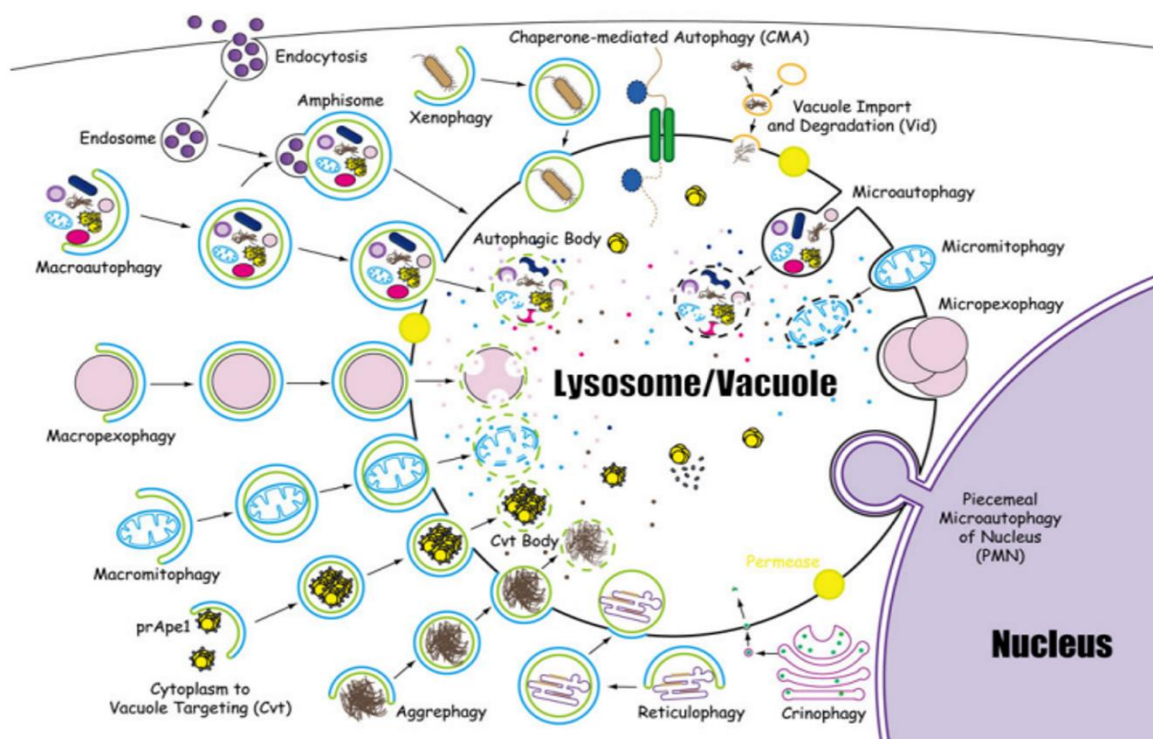


Figure 11: Differences among the principal selective and non-selective autophagy variants. Macromolecules and organelles could be included into the lysosome through CMA, microautophagy (right pathways) or macroautophagy (left pathways). Non-selective microautophagy engulfs the cytoplasmic content through the generation of a membrane invagination that introduces the cargo into the lysosome. Selective micromitophagy, micropexophagy and piecemeal microautophagy of the nucleus insert little amounts of mitochondria, peroxisomes and nucleus respectively into the lysosome by microautophagy. On the other hand, CMA introduces specifically proteins with the domain KFERQ into the lysosome through the pore created by the protein LAMP2A in its membrane. Finally, macroautophagy carries macromolecules to its degradation through the formation of an additional vesicle, whose name is autophagosome, which subsequently fuses with the lysosomes. This pathway may be known as mitophagy, pexophagy, aggrephagy, reticulophagy or xenophagy, if respectively mitochondria, peroxisomes, protein aggregates, endoplasmic reticulum or pathogens undergoes macroautophagy. Retrieved from [204].

Microautophagy is a non-selective degradation system that is characterized by the direct engulfment of degradation cargo through the formation of a membrane invagination which is subsequently disintegrated into the lumen of the vesicle (Fig. 11) [204]. This process normally occurs in the lysosomes, in which the invaginated vesicle is degraded by the luminal hydrolases [203]. Although this pathway was thought to be a bulk system, three different selective types of microautophagy named micropexophagy, piecemeal microautophagy of the nucleus and micromitophagy have recently been discovered (Fig. 11) [204]. They differ from non-selective micromitophagy in how the lysosomes introduce the cargo to its degradation (Fig. 11) [204]. In bulk pathways, the cargo insertion occurs through the generation of tubular invaginations, whereas the formation of arm-like protrusions that embrace the organelle that will be degraded is typical from selective systems (Fig. 11) [204].

In contrast with microautophagy, which could be a non-selective pathway, CMA always involves the recognition of a specific motif in the protein by the heat shock-cognate protein of 70 kDa (hsc70) (Fig. 11) [205]. This five-amino-acidic sequence is always constituted by a glutamine residue, as well as by a positive-charged, a hydrophobic and a negative-charged amino acid, being KFERQ the most frequent arrangement [205]. After the recognition process, hsc70 conducts its cargo to the lysosomes, where it interacts with lysosome-associated membrane protein type 2A (LAMP2A), a transmembrane protein with the ability to multimerize, generating a pore in the lysosome membrane which allows the translocation of the substrate into this vesicle for degradation [205,206]. In addition, hsc70 is also responsible for unfolding the substrate to achieve its crossing through the pore [206,207]. Some chaperones located in the lysosomal lumen, such as HSP90, can maintain the stability of LAMP2A complex, whereas others, such as lysosomal-hsc70, assists in the substrate translocation through the lysosomal membrane [207].

On the other hand, macroautophagy (hereafter referred to as autophagy) constitutes the most important of these mechanisms in eukaryotic cells [208]. This process is characterized by the sequestration of the macromolecules and proteins that will be subjected to degradation in a double-membrane vacuole, also known as autophagosomes, that has been generated *de novo* from an isolated membrane (Fig. 11) [209,210]. Subsequently, this vesicle fuses with a lysosome to form an autolysosome, where the autophagosome content will be degraded by the lysosome enzymes (Fig. 11) [209,210]. Similarly to microautophagy, cargo could enter into the autophagosomes in a bulk or a

selective manner (Fig. 11) [208]. There is an increasing interest in the study of selective autophagy due to the progressive discovering of the sensors that decide what organelles should be entered into the autophagosomes, as well as the disorders which are related to their deregulation [211]. Some of the most frequent types of selective autophagy are pexophagy, ribophagy, xenophagy, aggrephagy, reticulophagy and mitophagy, in which peroxisomes, ribosomes, pathogens, aggregated proteins, ER and mitochondria are respectively degraded (Fig. 11) [211].

4.2. Molecular mechanism of autophagy.

Autophagy is a multistep process that involves the sequential activation of at least five protein complexes in mammals, which constitutes the core machinery that regulates the autophagosome membrane generation, elongation and closure [209,212]. These are the unc-51-like kinase (ULK1) complex, the Beclin1/vacuolar protein sorting-associated protein 34 (Vps34) complex, the mAtg9/WD repeat domain phosphoinositide-interacting protein 1 (WIPI1) system, the Atg12 conjugation system and the LC3 ubiquitin-like conjugation system [209,210].

4.2.1. The generation of a novel autophagosome membrane.

The first step that occurs during autophagosome formation is the generation of a novel isolated membrane, which is also known as phagophore [212]. This is a double-membrane structure that starts engulfing the cargo and further elongates until it closes, generating a functional autophagosome [213]. Although the determination of its cellular origin has been highly controversial, the main hypothesis which has recently arisen is that the phagophore is generated in the ER-mitochondrion contact site through the formation of an omega-shape structure known as omegasome [214]. Conversely, it seems that the vesicles derived from Golgi apparatus, plasma membrane and endosomes only contribute to the expansion of phagophore, but not to its generation [214]. Although it has demonstrated the existence of a phagophore assembly site in yeast, which is essential for autophagosome nucleation, a similar structure has not been discovered in mammals yet [213].

ULK1 is temporally the first complex that modulates the assembly of autophagosomes (Fig. 12) [209,212]. It is constituted by the serine/threonine kinase ULK1, the regulator protein Atg13, as well as Atg101 and focal adhesion kinase family interacting protein of 200 kDa (FIP200), which modulate the stability of the whole complex (Fig. 12) [209,210]. The coordinated and differential phosphorylation of ULK1 and Atg13, by both mTORC1 and AMPK, adjusts the activation of this complex in response to certain stimuli, such as energy or nutrient depletion (Fig. 12) [215]. In nutrient-replete conditions, mTORC1, but not mTORC2, directly binds to the ULK1 complex in an Atg13-independent manner, which ultimately leads to its inactivation through the hyperphosphorylation of both Atg13 and ULK1, as well as by the disruption of the interaction between this complex and AMPK1 (Fig. 12) [215,216]. Otherwise, mTORC1 detaches from it when the nutrient concentration in the medium is low, allowing the dephosphorylation of ULK1 [216]. This process activates ULK1, inducing the phosphorylation of Atg13 and FIP200, which ultimately leads to the organization of the new autophagosome membrane by the retrieval of proautophagic proteins to the phagophore, such as mAtg9, or by the direct stimulation of Beclin1/Vps34 complex [212,216,217]. In addition, ULK1 has recently been reported to be also induced by human immunodeficiency virus-1 Tat interactive protein, 60 kDa (TIP60)-dependent acetylation and by AMPK1-dependent phosphorylation of S317 and S777 (Fig. 12) [215,218]. Moreover, ULK1 can directly phosphorylate raptor to restrain mTORC1 signal in a fast forward feedback mechanism that ensures the restraint of the activity of this mediator under starvation conditions [219]. Finally, activating molecule in Beclin1-regulated autophagy protein 1 (AMBRA1) stimulates ULK1 self-association through promoting its polyubiquitylation in its K63 by TNF receptor-associated factor 6 (TRAF6) [220,221].

Conversely, the Beclin1/Vps34 complex is constituted by Beclin1, p150 and by the class III PI3K protein Vps34 (Fig. 12) [212]. This complex is inactivated in non-fasting conditions by AMBRA1 due to its ability to tether this structure to the microtubules [220,222]. Under starvation, activated ULK1 phosphorylates AMBRA1, which results in its release from dynein and in its translocation, together with Beclin1/Vps34 complex, to the mitochondria-ER contact sites (Fig. 12) [214,222]. The location of this complex is also mediated by ULK1, because it can promote the binding between syntaxin-17 (STX17) and Atg14L, enhancing their translocation to the mitochondria-ER contact sites where Beclin1 interacts by its coiled-coil domain (CCD) with Atg14L, attaching the complex to these

zones [223]. This interaction augments the activity of Vps34, leading to altering the lipid composition of the mitochondria-associated membrane (MAM) by increasing of phosphatidylinositol 3-phosphate (PI3P) (Fig. 12) [214,223]. This process finally results in the generation of an ER deformation that creates the omegasome [214,223].

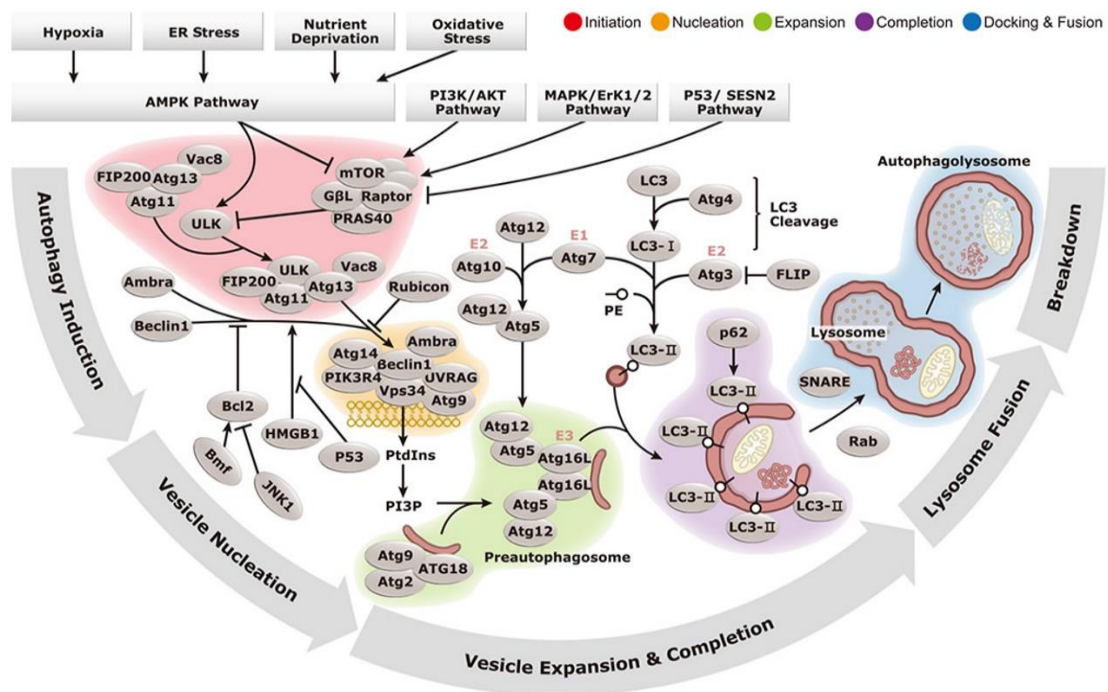


Figure 12: Molecular process involved in autophagosome formation, closure, docking and fusion with lysosomes. Different stimuli, such as hypoxia, ER stress, oxidative stress and nutrient depletion lead to the activation of the ULK1 complex which is responsible for autophagy induction. This activation is mainly inhibited by mTORC1, which is mainly activated by PI3K/Akt pathway. ULK1 complex phosphorylates AMBRA1, leading to the activation of the Beclin1/Vps34 system and to translocate it from the microtubules to the nascent autophagosome, where it starts to increase the content of PI3P in the membrane. Subsequently, this membrane starts to elongate by the action of the complexes Atg9-Atg18, which bring new vesicles to the formation site, and by the two ubiquitin-like systems Atg12-Atg5-Atg16L and LC3-II. In addition, LC3-II is also responsible for the cargo selection and for the autophagosome closure. Then, this structure fuses with a lysosome to achieve the degradation of the autophagosome content. Retrieved from <http://www.genetex.com/Web/Pathway/Autophagy-Pathway-39> (27/03/2018).

4.2.2. The elongation and the closure of the autophagosome membrane.

After the phagophore isolation, the new membrane generated starts to elongate and to curve, until it closes, constituting a new autophagosome (Fig. 12) [209,210].

The elongation and curving processes are primarily modulated by the Beclin1/Vps34/Atg14L complex, which is able to translocate from the MAM surface to the isolated membrane (Fig. 12) [224,225]. There, Beclin1 interacts through its CCD with other proteins to resume autophagosome formation, being ultraviolet irradiation resistance-associated gene (UVRAG) the most important of them [224]. However, the binding of the Beclin1 core complex to Atg14L or to UVRAG is mutually exclusive, mainly because of the overlapping of their binding zones [226,227], suggesting that more Beclin1/Vps34 complexes should be attracted to the phagophore during this phase. Furthermore, it has been reported that Beclin1-UVRAG complex is more stable and lasting than Beclin1-Atg14 [224]. This complex induces the nucleation of the new isolated membrane through the further stimulation of Vps34 activity, which leads to increasing exponentially the concentration of PI3P in a specific membrane zone [228]. This process enables the recruitment of proteins that will be essential for the following processes, such as WIPI and double FYVE domain-containing protein 1 (DFCP1), mAtg9 or Atg2 [228]. Furthermore, the interaction of Bcl-2-associated X protein (Bax)-binding protein-1 (Bif-1) with Beclin1 through UVRAG generates a growing force that deforms the isolated membrane, achieving eventually the correct curvature of the autophagosomes [229]. This process seems to be mediated by two different Bif-1 domains, the amino-terminal Bin-Amphiphysin-Rvs (N-BAR) and the carboxy-terminal Src-homology 3 (SH3) since they can join to the phagophore and bend it [229]. Moreover, the interaction of Beclin1 to vacuole membrane protein 1 (VMP1) stimulates the conversion of LC3-I to LC3-II, an essential step for achieving the final maturation of the autophagosome [230]. Oppositely, RUN domain protein as Beclin1 interacting and cysteine-rich containing (RUBICON), which binds to Beclin1 core complex through UVRAG, can regulate negatively autophagy induction (Fig. 12) [225,231]. This factor has been shown to impede the kinase activity of Vps34, working in the opposite way to Beclin1-UVRAG complex to prevent excessive inositide phosphorylation [231].

mAtg9 is the only transmembrane membrane protein among all autophagy-related mediators, thus it has been suggested to be responsible for the elongation of the phagophore (Fig. 12) [232]. This protein is located in the *trans*-Golgi regions under non-fasting conditions, being redistributed by the ULK1 complex after nutrient deprivation [214]. Curiously, it is thought that only a very small percentage of this mediator accumulates in the milieu of the isolated membrane, suggesting that mAtg9 is able to shift among this

compartment and the Bif-1-positive recycling vesicles that will contain the lipids and the proteins necessary for the expansion of the nascent membrane [232,233]. In fact, these vacuoles are grabbed by this protein to the autophagosome milieu, where will fuse with the phagophore, leading to its elongation until the generation of the whole vesicle (Fig. 12) [232]. mAtg9 is never included in the autophagosome, but it is shuffling continuously around the cell to bring new components [234]. Apart from mAtg9, some other factors have also been reported to contribute to this process [214]. For instance, the endosomal protein sortin nexin-18 (SNX18), which is able to attach to the PI3Ps that remains in Rab11-positive endocytic structures, induces the tubulation of late endosomes, as well as their fusion with the growing autophagosome [214,235]. Curiously, SNX18 protein has also been found in Golgi-derived vesicles, suggesting that this protein may be involved in the driving of these vacuoles to the autophagosome milieu [214].

Conversely, WIPI1 remains in the cytoplasm in non-fasting conditions, being relocalized to the PI3P-positive membranes of the autophagosomes through labile microtubules upon nutrient deprivation [236]. This specific joining, which is totally abolished when the ion Ca^{2+} is chelated, is responsible for the attraction of the two ubiquitin-like conjugation systems to the nascent autophagosome [236,237]. Moreover, this protein has recently been shown to likely present a crucial role in xenophagy and aggrephagy, since it colocalizes with p62 during autophagosome maturation [236,238]. In addition, WIPI2 has also been shown to participate in the recruiting of the Atg12-Atg5-Atg16L complex to the autophagosome, which implies that this protein exerts a similar role than its paralogue WIPI1 [239].

As previously claimed, two ubiquitin-like protein conjugation systems participate in the expansion and closure of the autophagosome vesicle (Fig. 12) [212]. The first pathway includes Atg12, a protein which presents the same folding structure and activation process as ubiquitin [240]. Indeed, the C-terminal G186 of this protein must be firstly activated by the E1-like enzyme Atg7, prior to be transferred to the E2-like enzyme Atg10, as well as to be conjugated with the K149 of Atg5 (Fig. 12) [240]. Subsequently, Atg12-Atg5 associate with the protein Atg16L, translocating to the autophagosome formation site (Fig. 12) [241]. In addition, the homo-oligomerization of Atg16L through its CCD, generating a bigger complex that includes four different sets of the Atg5-Atg12-Atg16L system, seems to be essential to amplify its signal [242]. This complex attaches to WIPI2 in the autophagosome PI3P-positive membrane during the initial phases of

elongation [239], dissociating from this structure during the process of closure (Fig. 12) [240]. Besides, it has been reported that the Atg5-Atg12-Atg16L system colocalizes with Atg14L during autophagosome elongation, suggesting that this protein could also perform a role in achieving the binding of Atg5-Atg12-Atg16L to this structure [227]. Basically, its main function is the stimulation of LC3 conjugation (Fig. 12) [240]. This process is accomplished due to its capability to not only stimulate the activity of Atg3, but to also work as the LC3-specific E3-like enzyme, inducing its attachment to phosphatidylethanolamine (PE) [240]. Moreover, Atg12 has recently been reported to perform a fundamental role in the regulation of mitochondrial homeostasis, since it can induce mitochondrial fusion and intrinsic apoptosis [243].

Opposite to other ubiquitin-like protein, which usually conjugate with proteins, LC3 and its paralogue gamma-aminobutyric acid (GABA) receptor-associated protein (GABARAP)/Golgi-associated adenosine triphosphatase (ATPase) enhancer of 16 kDa (GATE-16) subfamily bind specifically to the phospholipid PE (Fig. 12) [244]. Although the activation and autophagosome integration process are rather similar between all mammalian LC3 paralogues, the functions that they exert during autophagosome formation are quite different (Fig. 12) [245]. LC3 is synthesized as a precursor protein, being cleaved in its C-terminus by the cysteine protease Atg4B, originating the mediator known as LC3-I (Fig. 12) [240]. Additionally, it has recently been reported that this inactive form can be stored in the nucleus by its acetylation, being necessary the action of the nuclear enzyme Sirt1 to revert this modification and to return to the cytoplasm to exert its function (Fig. 12) [246]. Subsequently, it is activated in its C-terminal glycine by the E1-like enzyme Atg7, prior to being conjugated with Atg3, which is its specific E2-like enzyme (Fig. 12) [240]. Then, it is transferred to the autophagosome milieu, where interacts with the complex Atg5-Atg12-Atg16L, leading to generating an amide bond between this protein and the phospholipid (Fig. 12) [240]. The lipidated form of LC3, which is also called LC3-II, is rapidly integrated into the inner and outer membranes of the autophagosome (Fig. 12) [247]. Conversely, LC3-II is cleaved after the autophagosome and lysosome fusion, being degraded on the autophagosome outer membrane by the proteolytic enzyme Atg4, and by lysosomal enzymes on the inner membrane [247]. LC3 subfamily has been shown to be essential for the elongation of the phagophore membrane, whereas GABARAP family performs a fundamental role in the closure of this vesicle (Fig. 12) [244]. In addition, GABARAP protein seems to act as scaffolds of the ULK1 complex, promoting its

activation in non-hierarchical autophagy [245]. Besides, LC3-II is also involved in the regulation of the autophagosome size [248], as well as in the cargo recognition during selective autophagy, because most of the proteins that carry macromolecules or organelles to the autophagosome, such as p62, Bcl-2/adenovirus E1B 19 kDa protein-interacting protein 3 (BNIP3) or BNIP3-like protein (BNIP3L)/Nix, interact with this protein [245] (Fig. 12).

Finally, it has recently reported the existence of a new factor of the Atg family in mammals, which has been called Atg2 due to the high homology that shares with this yeast protein [249]. Besides, it has been reported to be attracted to PI3P-positive membranes by WIPI4, even though it has also been shown to colocalize with WIPI1 in these structures [236]. Although it seems to act downstream LC3-II in autophagosome formation, since its knockdown leads to accumulating p62-positive unclosed vesicles, its function in the autophagosome generation has not been specified yet [249].

4.2.3. Autophagosome and lysosome fusion.

After the closure of the autophagosome and the selection of the degradation cargo, the fusion between this vacuole and the lysosome will occur to form an acidic vesicle called autolysosome (Figs. 12 and 13). Subsequently, all the intra-autophagosomal content is degraded in this structure by different hydrolases, such as cathepsins, glycolytic enzymes and lipases, being all the products derived from this process recycled in order to generate new cellular structures (Figs. 12 and 13) [209]. Finally, the reactivation of mTOR after the degradation of autolysosomal content leads to reducing autophagy initiation and to the generation of proto-lysosomal vesicles and tubules from autolysosomes that will mature into new functional lysosomes [250].

Soluble N-ethylmaleimide sensitive (NSF)-attachment protein receptor (SNARE) family has recently been reported to be the molecular machinery that allows the fusion between these two vacuoles (Fig. 13) [251]. Curiously, it seems that the ER SNARE protein STX17, which locates the Beclin1/Vps34 complex in the mitochondria-ER contact sites during the earliest phase of autophagosome formation [214], is also in charge of this process (Fig. 13) [251]. Nevertheless, it has been reported that STX17 only appears on mature autophagosomes in a non-membrane-fusion fashion, although its specific mechanism of integration has not been discovered yet (Fig. 13) [251]. In addition, it is surmised that this

recruitment is also dependent on LAMP2, which implies that lysosomes would control the fusion process [252]. Once STX17 has been anchored on the membrane of that vesicle, it recruits synaptosome-associated protein 29 kDa (SNAP-29), which interacts with the lysosomal transmembrane protein vesicle-associated membrane protein 8 (VAMP8), leading to moving both vesicles closer until that their membranes fuse (Fig. 13) [251,252]. Atg14L also seems to perform a fundamental role in the stabilization of the joining between STX17 and SNAP-29 (Fig. 13) [252].

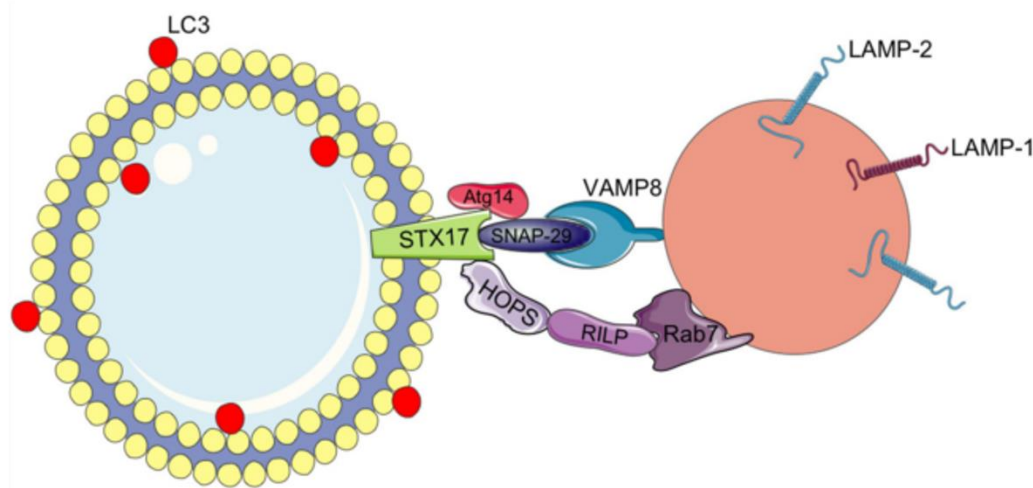


Figure 13: SNARE-dependent mechanism of lysosome and autophagosome fusion. STX17 is the main protein that mediates the fusion process between autophagosomes and lysosomes. This molecule arises in the mature autophagosome membrane through an unknown mechanism and catalyzes the binding of these two structures by associating through SNAP-29 to the lysosomal protein VAMP8. Atg14L joins to STX17 and stabilizes the whole complex. On the other hand, the fraction of Rab7 that is in the lysosome membrane can also bind to STX17 through RILP and HOPS, conforming a secondary tethering complex that approximates both vesicles prior to their fusion. Retrieved from [252].

It has been reported that this process is clearly dependent on the presence of the protein Rab7 in its GTP-bound stage in the membrane of the late autophagosome [253]. The recruitment of this protein to the vacuole seems to be mediated by the fusion of autophagosomes with Rab7-positive late endosomes to constitute a hybrid vesicle called amphisome [214]. Moreover, the lumen of this hybrid vacuole undergoes a progressive acidification to prepare the cargo before its degradation by lysosome hydrolases [253]. Conversely, it has also been claimed that Rab7 protein has a main role in amphisome transport and in its tethering with the lysosome. FYVE and CCD-containing protein 1 (FYCO1) is a cellular mediator that interact both with Rab7 and LC3 in the surface of amphisomes, promoting their movement to the microtubules plus-end by their direct binding with kinesin motor proteins [254]. Moreover, the specific binding of Rab7 with

Rab-interacting lysosomal protein (RILP) promotes endosomes and likely amphisomes movement to the microtubules minus-end, since they are able to associate with dynein-dynactin motor proteins [255]. On the other hand, Rab7-RILP complex acts as a secondary anchoring system between autophagosomes and lysosomes (Fig. 13) [252,255]. This interaction leads to the recruitment of homotypic fusion and protein sorting (HOPS) complex, which specifically binds with STX17, inducing the tethering of both vesicles before their association and facilitating the binding of the SNARE complexes (Fig. 13) [252,255].

Finally, autophagosome and lysosome fusion are also tightly regulated by the complexes UVRAG/Beclin1/Vps34 and Rubicon/UVRAG/Beclin1/Vps34 [209]. Indeed, UVRAG protein has been reported to induce the activity of the HOPS complex, which is necessary for the tethering of the two vacuoles, whereas RUBICON impedes this process by suppressing UVRAG function [256].

4.3. Modulation of autophagy by extracellular and intracellular stimuli.

Autophagy basal levels are modulated in human cells by a broad scope of extracellular and intracellular stimuli (Fig. 12) [212]. These stressful conditions lead to the activation of multiple transduction pathways with overlapping functions that eventually alter the expression or the activity of the core machinery that regulates autophagosome formation (Fig. 12) [212,257].

4.3.1. Nutrients, growth factors and energy deprivation stresses.

The lack of nutrients and energy in the cell, as well as growth factors in the medium, are the most potent physiological stimulators of autophagosome formation in human cells [212]. The induction of this pathway generates an internal source of both nutrients and energy that normally avoids cellular death when the supplied nutrition is extremely low [258]. Nevertheless, glucose deprivation has been shown to induce prodeath instead of prosurvival autophagy [259]. The two main pathways that are responsible for the sensing and translocation of these signals are the mTORC1 and the AMPK cellular routes [257].

mTOR, which is also known as the master regulator of cellular metabolism, is a serine/threonine kinase that is able to shift from catabolic to anabolic responses when there are sources of nutrients, oxygen and energy in the cellular microenvironment, or in response to growth factor signaling [260,261]. mTOR protein constitutes two different complexes, mTORC1 and mTORC2, which exert different outcomes in the modulation of cell metabolism [260,261]. Autophagy modulation is mainly dependent on mTORC1, but mTORC2 activation could indirectly suppress this cellular response, since this mediator is able to induce mTORC1 [261]. As claimed before, mTORC1 is able to abolish autophagy by the hyperphosphorylation of ULK1 and Atg13, restraining ULK1 kinase activity, as well as by impeding its AMBRA1-dependent stabilization (Fig. 12) [216,220,261]. Moreover, this complex reduces Vps34 activity by phosphorylating Atg14L and UVRAG, which increases its affinity for RUBICON [256,261]. Besides, it can also prevent the expression of multiple autophagy- and lysosome-related genes by phosphorylating the transcription factor that specially recognizes and binds E-box sequences (TFEB), retaining it in the cytoplasm [260,261]. Curiously, mTORC2, but not mTORC1, is thought to inhibit CMA through reducing the stabilization of LAMP2A multimer [262], which clearly suggests that each complex is in charge of restraining different types of autophagy.

mTORC1 responds to multiple incoming cellular signals that include hypoxia, growth factors, energy and nutrient status [260]. Most of these stimuli disturb the activity of the tuberous sclerosis 2 protein (TSC2), hindering its binding with tuberous sclerosis 1 protein (TSC1) and TBC domain family member 7 (TBC1D7) [260]. This inhibition leads to the induction of mTORC1, since these proteins act as the guanosine triphosphatase (GTPase)-activating protein (GAP) enzyme of the mTORC1 activator Ras-homologue enriched in brain (Rheb) [260]. The main transduction pathway that restrains TSC2 activity in response to growth factor signals is PI3K/Akt, whereas MAPK/ERK1, protein regulated in development and DNA damage response 1 (REDD1) and AMPK1 are also able to modulate its activity in response to different stimuli [260,263]. Conversely, amino acids induce mTORC1 activity by a TSC2-independent mechanism that involves Ras-related GTP-binding proteins (Rags) [260,263]. The activation of these mediators enables the translocation and tethering of mTORC1 to the lysosome membrane, increasing its interaction with Rheb and its phosphorylation [260,263].

On the other hand, AMPK is the major sensor of the energy level in the cell, being activated by a reduction in ATP/AMP ratio [257]. Indeed, the binding of AMP or ADP

to the regulatory subunit of AMPK induces its phosphorylation by liver kinase B1 (LKB1), and Ca^{2+} /calmodulin-dependent protein kinase β (CaMKK β), and protects this posttranscriptional modification from the action of phosphatases, being these effects antagonized by ATP [264]. As previously described, AMPK can induce autophagosome formation by the induction of TSC2 activity, which in turn impedes mTORC1 induction of autophagy (Fig. 12) [265]. Besides, it can also directly inhibit mTORC1 signaling by the phosphorylation of the regulatory-associated protein of mTOR (Raptor), which is a key part of this complex, inducing its sequester by the 14-3-3 protein (Fig. 12) [265]. Conversely, the AMPK-induced phosphorylation of ULK1 at S317 and S777 induces autophagy, being this process antagonized by the mTORC1-induced phosphorylation at S757, leading to reducing the interaction between AMPK and ULK1 (Fig. 12) [215]. Otherwise, this protein has been reported to modulate the stability of the different Beclin1/Vps34 complexes, stimulating proautophagic intermediaries with Atg14L and UVRAG, but repressing antiautophagic complexes without these proteins [266].

Finally, it has recently been demonstrated that protein kinase A (PKA) can reduce autophagosome formation in response to a glucose withdrawal in the medium [257,266]. Indeed, this enzyme prevents autophagosome elongation by phosphorylating LC3, which ultimately leads to reducing its ability to translocate to the membrane of this vesicle [266,267]. Finally, it can also prevent selective autophagy by preventing the interaction between p62 and the specific cargo [266]. However, this point should be addressed more in detail, since this protein is also implied in the management of metabolic stress [266]

4.3.2. Hypoxia, ceramides, oxidative and reticulum stresses.

Oxygen deprivation in the media is also one of the leading causes that can alter physiological basal levels of autophagy in human cells (Fig. 12) [268]. However, the molecular mechanisms that induce autophagy in response to oxygen deprivation are greatly dependent on the duration and severity of the stimulus [268]. Indeed, chronic and moderate hypoxia stimuli induce autophagosome formation mainly through HIF-1 α and protein kinase C delta type (PKC δ)-JNK pathways [268]. HIF-1 α -dependent induction of autophagy is regulated by its target genes BNIP3 and Nix, which increase autophagosome formation through directing mitochondria to this vesicle for their selective degradation [269]. Besides, these mitophagy factors can displace the interaction between Beclin1 and

Bcl-2 through attaching to this antiapoptotic protein by its Bcl-2 homology 3 domain (BH3), allowing autophagy induction by the release of Beclin1 [270]. Conversely, PKC δ increases the formation of LC3-positive vacuoles by inducing the JNK-dependent phosphorylation of Bcl-2, leading to the dissociation of Beclin1 from this antiapoptotic factor [271]. On the other hand, if hypoxia is acute and severe, autophagy is usually induced through mTORC1-dependent, HIF-1 α -independent cellular routes, due to their coupling with energy and glucose profound deprivation stimuli [268]. Therefore, the induction of REDD1 expression under severe hypoxia conditions leads to the overactivation of TSC2 by allowing its dissociation of 14-3-3 [272].

Ceramides, one of the most important constituents of the sphingolipid family, are a family of signal lipids with the ability to regulate a cell fate by modulating apoptosis and autophagy responses [273,274]. These lipids have recently been reported to induce either prosurvival or prodeath autophagy, depending on the cellular context, which would seem to be a bit paradoxical [273]. Amino acid depletion could induce autophagy through the augment of ceramide levels, leading to restrain the activation of mTORC1 through the induction of protein phosphatases 1 and 2A (PP1/PP2A), whereas the increment on S1P levels, a ceramide degradation product, antagonizes ceramide-dependent effects by overactivating this mTOR complex [275]. In contrast, ceramides can also prevent the entrance of nutrients into the cell, promoting cell death through necrosis and prosurvival autophagy through AMPK [276]. Conversely, ceramide also induces the activation of the kinase JNK, stimulating the liberation of Beclin1 and the formation of autophagosomes through the phosphorylation of Bcl-2 [277], as well as increasing the expression of both Beclin1 and LC3 by c-Jun phosphorylation [278]. Besides, the ceramide-induced Beclin1 expression has also been reported to be mediated by the subunit p65 of the nuclear factor kappa-light-chain-enhancer of activated B cells (NF- κ B) [279]. Finally, both ceramides and S1P can indirectly increase autophagy by stimulating ER stress [274].

Furthermore, ROS/RNS damaged proteins usually accumulates in the cytoplasm, being normally degraded by the ubiquitin-proteasome system or by autophagy to maintain cellular homeostasis (Fig. 12) [280]. Therefore, it is not strange that mild oxidative stress triggers autophagosome formation to protect cells against this harmful situation, while more severe stimuli enhance autophagy to accomplish cell death [280]. Indeed, it has been demonstrated that the production of H₂O₂ in the mitochondria induces the inactivation of Atg4 homologs, which in turn prevent the delipidation of LC3 and GATE-16 [281].

Moreover, H₂O₂ production has been associated with different oxidative modifications, including S-glutathionylation, in certain cysteine residues of the α and β subunits of AMPK that eventually increases its kinase activity independently from the value of the ATP/AMP ratio [282].

Otherwise, autophagy participates in the degradation of unfolded protein aggregates that are not efficiently eliminated by the ER-associated degradation machinery (Fig. 12) [283]. Therefore, the arising of ER stress leads to enhance autophagosome formation through the activation of the UPR [283]. For instance, the UPR specific pathway PRKR-like endoplasmic reticulum kinase (PERK)/eukaryotic translation initiation factor 2- α (eIF-2 α)/activating transcription factor 4 (ATF4), together with their downstream protein CCAAT/enhancer binding protein β (C/EBP β)-homologous protein (CHOP), reduce the translation of most mRNAs, but favor the expression of certain proteins that can alleviate ER stress [284]. Indeed, eIF-2 α , ATF4 and CHOP enhance the expression of certain autophagy genes, such as Atg16L, LC3, Atg12, Atg3, Beclin1, p62, Atg7, Atg5, Atg10, GABARAP or Tribbles homolog 3 (TRB3), which restrains Akt/mTORC1 activation [284]. Conversely, the activation of the JNK by the UPR constituent inositol-requiring enzyme 1 (IRE1) can disrupt the binding between Bcl-2 and Beclin1 [285]. Finally, the release of Ca²⁺ from the ER leads to induce the phosphorylation and activation of AMPK by CAMKKB and to stimulate the action of calpain proteases, inducing the autophagosome formation [286].

4.4. Role of autophagy in human pathologies.

Since the importance that present autophagy response in cell homeostasis, it is not strange that its deregulation has been linked with the pathogenesis of different human diseases, such as cancer, neurodegenerative, metabolic, cardiovascular and infectious diseases (Fig. 14) [287,288].

Autophagy presents a changing role in the different phases of tumorigenesis [287,289]. In this way, it acts as a tumor suppressor pathway at earlier stages, preventing genomic instability and removing damaged organelles, mainly mitochondria, that can promote genotoxic stress by releasing ROS/RNS (Fig. 14) [289]. Oppositely, autophagy can protect tumor cells against oxygen and nutrient factor deprivation stresses in later phases by inducing the breakdown of cellular components to obtain energy and nutrients

(Fig. 14) [287,289]. In addition, it can also promote the survival of advanced tumor cells by reducing their sensitiveness to either chemotherapy or radiotherapy (Fig. 14) [287]. This process is accomplished by the degradation of the macromolecules and organelles that have been damaged as a result of the use of antitumor therapies [287]. Therefore, the combination of chemotherapeutic drugs with autophagy inhibitors could be a great strategy for improving tumor sensitivity [287].

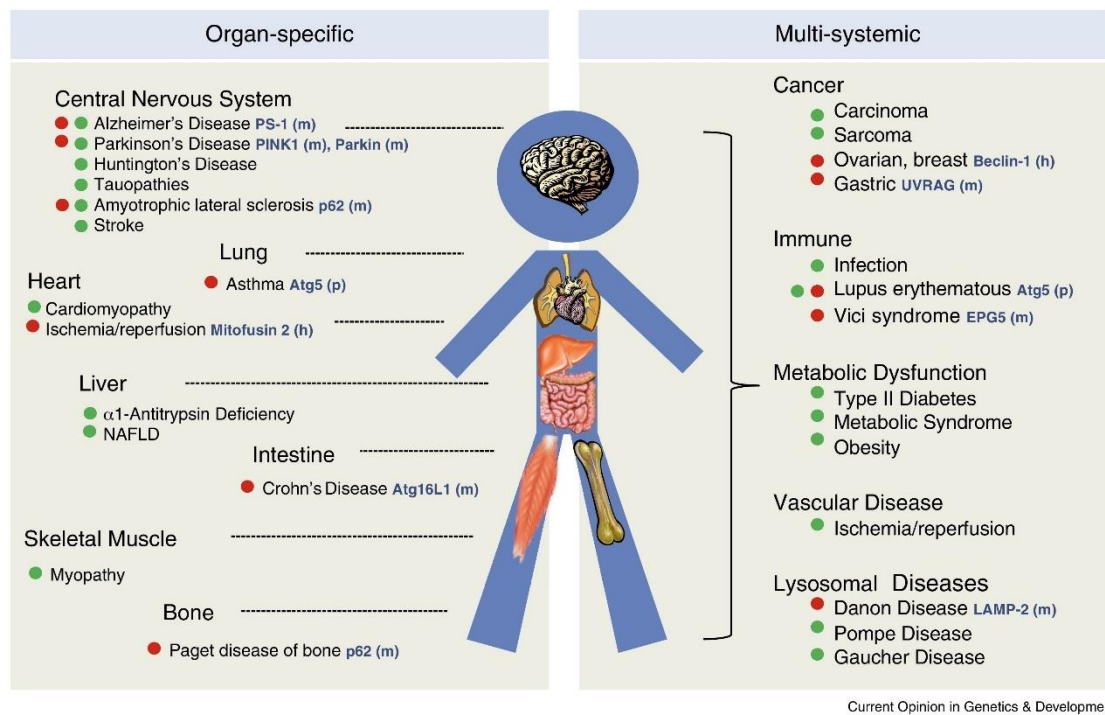


Figure 14: Role of autophagy in different human pathologies. Autophagy modulates the progression of many organ-specific and multi-systemic diseases. The pathologies in which primary autophagy defects has been reported are marked in red, whereas those in which autophagy deficiencies present a more secondary role or are generated by the disease are labeled in green. Autophagy-related gene mutations (m), polymorphisms (p) and haplo-insufficiencies (h) in each respective disease are labeled in blue. Retrieved from [288].

Otherwise, most of the neurodegenerative disorders, such as Alzheimer's disease, Parkinson's disease, Huntington's disease and amyotrophic lateral sclerosis are characterized by the deposition of misfolded proteins into the neuron cytoplasm [287,288]. Therefore, the abolishment of the cellular systems that are responsible for degrading these aggregates, including autophagy, triggers disease progression (Fig. 14) [290]. Indeed, the generation of deficiencies in autophagosome formation in a mouse model induces various age-dependent neurodegenerative disorders due to the accumulation of protein aggregates, indicating that basal levels of autophagy are indispensable to maintain neuron homeostasis (Fig. 14) [291]. Summarizing, pharmacological stimulation of autophagy could help to delay the progression of these pathologies [290].

On the other hand, autophagy sustains cell metabolism by regenerating the precursors that will be used for either catabolic or anabolic reactions (Fig. 14) [289,290]. Therefore, it is not strange that the deregulation of this process could aggravate some metabolic disorders (Fig. 14) [289,290]. For instance, a diminution in hepatic autophagy has been reported in some *in vivo* models of insulin resistance associated with central obesity, being this harmful phenotype reverted when this pathway is restored to basal levels [292]. Additionally, it seems that physical exercise could protect against glucose intolerance and leptin resistance by inducing autophagosome formation in certain human tissues, which values the fundamental role that presents physical exercise in the treatment of obesity and in the avoidance of its derived complications [293]. Finally, alterations in the selective degradation of ubiquitinated proteins by autophagy due to mutations in the *p62* gene have been reported to aggravate Paget's disease of bone [294].

Conversely, basal levels of autophagy are essential to maintaining cardiomyocyte homeostasis and function, due to its ability to avoid the accumulation of harmful macromolecules for these cells [287,295]. Therefore, defects in baseline autophagy could lead to inducing many cardiac diseases, such as cardiomyopathies, cardiac hypertrophy, ischemic heart disease, ischemia/reperfusion injury and myocardial infarction [290]. For instance, autophagy is thought to be induced in both acute and chronic phases of myocardial infarction to limit cell injury, thus its abolishment could lead to aggravating the progression of this disease [295]. Curiously, it has also been reported that excessive induction of autophagy pathway in cardiomyocytes during ischemia/reperfusion injury could lead to inducing their death by type II PCD [287]. Otherwise, autophagy also performs a role in the stabilization of atherosclerosis plaques, by avoiding their disaggregation by macrophages (Fig. 14) [290]. Summarizing, pharmacological regulation of autophagy seems to be useful in the treatment of multiple cardiac diseases [290].

Autophagy protects lung cells from a broad scope of stressful situations that include hypoxia, inflammation, ER stress, drugs or inhaled xenobiotics [290,296]. However, the chronic exposure to these xenobiotic agents, such as cigarette smoke or air pollution, induces prodeath autophagy pathway (Fig. 14) [296]. This prolonged stimulation generates a proapoptotic and propathogenic status into the lung tissue which is also known as chronic obstructive pulmonary disease (COPD) (Fig. 14) [290,296]. Besides, increased autophagy pathway has also been shown in some types of emphysema that are not related to particle inhalation, thus it seems that autophagy overinduction is a hallmark process in COPD

progression [296]. In addition, an augment in autophagosome formation, which is clearly associated with an increment in Atg5 expression, has been reported in asthma patients, although the effect of this pathway on airway fibrosis is still under discussion [297]. Conversely, dysfunctions in autophagosome and lysosome binding contribute to enhancing the sustained inflammatory response observed in the airways of cystic fibrotic patients [298].

Autophagy is one of the most important cellular mechanisms implicated in the defense against pathogens, since it modulates the function of either innate or adaptive immune responses (Fig. 14) [290,299]. Indeed, a great number of human pathogens, including bacteria, viruses and parasites, are degraded by a specific type of autophagy known as xenophagy (Fig. 14) [300]. Conversely, this pathway is also implicated in the processing of extracellular antigens by the major histocompatibility complex type II (MHC II) in macrophages and dendritic cells to be recognized by cluster of differentiation 4 (CD4)⁺ T cells, which in turn stimulates the production of antibodies against these pathogens (Fig. 14) [301]. Therefore, autophagy malfunctions have been associated with increments on the pathogen load, which leads to generating a chronic inflammatory status which occasions the arising of many pathologies, such as Crohn's disease [302]. Oppositely, certain viruses, such as Dengue virus or poliovirus, can use the host autophagy machinery to induce their maturation into a proinfectious particle or to stimulate their replication (Fig.14).[300]. Besides, some bacteria, such as *Porphyromonas gingivalis* or *Brucella abortus*, can escape from host immune mechanisms by invading cell autophagosomes and preventing their binding with lysosomes [287]. Summarizing, autophagy seems to exert a dual role in the defense against pathogen infections (Fig. 14).

5. Mitochondrial dynamics and mitophagy.

Mitochondria are not quiescent organelles, since their morphology and distribution are highly changeable [303]. These alterations are tightly regulated by the processes of mitochondria fusion and fission, which are in turn regulated by a group of proteins located both in the outer (OMM) and inner mitochondrial membranes (IMM) [303]. The coordinated activation of all these proteins modulates mitochondrial dynamics during cell proliferation [303].

5.1. Mitochondrial fusion.

Mitochondrial fusion is mediated at the OMM level by the proteins mitofusin 1 (MFN1) and 2 (MFN2), as well as by the optic atrophy factor 1 (OPA1) at the IMM level (Fig. 15) [303,304]. All these proteins work together in a GTP-dependent and coordinated mechanism that approach and ultimately fuse two neighboring mitochondria (Fig. 15) [304]. Nevertheless, the mechanism that coordinates the fusion between both mitochondrial membranes has not been elucidated yet [305].

MFN1 and MFN2 are transmembrane GTPases which are required for OMM fusion since *Mfn1/2* null cells present small and fragmented mitochondria due to their inability to achieve mitochondria fusion [306]. These proteins can constitute homo- or hetero-dimers through the specific interaction of their cytosolic HR2 regions, which leads to the tethering of two neighboring organelles (Fig. 15) [304,305]. Subsequently, the hydrolysis of GTP generates a conformational change in both mitofusins, approaching the membranes of both mitochondria to fuse [307]. Finally, it is surmised that the release of the GDP molecule induces OMM fusion, but this process has not been elucidated yet [307]. Although MFN1 and MFN2 present great homology and similar function in mitochondrial fusion, some differences have been detected between these two transmembrane proteins [305]. For instance, MFN1 presents higher enzymatic activity than MFN2, whereas this second mediator has more affinity for GTP [305].

On the other hand, IMM fusion in mammals is mainly regulated by the protein OPA1, since its down-regulation leads to generating large clusters of only superficial fused mitochondria with serious defects in their cristae [308]. In mammals, OPA1 undergoes alternative splicing and post-translational cleavage, generating a broad scope of variants that can be divided in membrane-anchored long OPA1 (L-OPA1) and transmembrane region-free short OPA1 (S-OPA) proteins [305]. The cleavage from L-OPA1 to S-OPA1 is mediated by the membrane-associated metalloproteases yeast mitochondrial escape protein 1 (YME1) like 1 (YME1L) ATPase and overlapping with the m-AAA protease 1 homolog (OMA1) [305]. L-OPA1 variants are the responsible for the achievement of IMM fusion, whereas S-OPA1 variants do not perform a role in mitochondrial fusion *per se*, but they increase the activity of L-OPA proteins [309]. It has recently been reported that L-OPA1 binds specifically to cardiolipin (CL) in the other IMM to tether both membranes, leading to the fusion of these structures by the subsequent hydrolysis of the GTP molecule that is

bounded to L-OPA1 (Fig. 15) [310,311]. Otherwise, L-OPA1 homodimers do not induce membrane fusion, but generate the formation of invaginations in the IMM that will constitute the mitochondrial cristae [310].

This process is tightly regulated by a certain group of proteins, such as peroxisome proliferator-activated receptor gamma coactivator-1 α (PGC-1 α), mitochondrial elongation factor 1 (MIEF1), reactive oxygen species modulator 1 (ROMO1), Bax, Parkin or BNIP3 [303]. For instance, PGC-1 α has been shown to enhance mitochondrial fusion by promoting the expression of MFN1 and MFN2 [312]. Otherwise, MIEF1 promotes fusion by inhibiting the GTPase activity of Drp1, which is the main protein that mediates mitochondrial fission [313]. Besides, ROMO1, which is fundamental for the upkeep of mitochondrial cristae integrity, induces fusion by enhancing the oligomerization and processing of OPA1 [314]. Additionally, the proapoptotic mediator Bax seems to induce this pathway through directly interacting with MFN2, but not with MFN1, which leads to augmenting its GTPase activity [315]. On the other hand, BNIP3 is able to bind to OPA1, preventing mitochondrial fusion and inducing their fragmentation during mitophagy [316]. Moreover, phosphatase and tensin homolog (PTEN)-induced putative kinase protein 1 (PINK1)/Parkin pathway induces the degradation of MFN1 and MFN2 by the ubiquitin-proteasome system, preventing mitochondria fusion during mitophagy [317]. Summarizing, multiple factors seems to modulate the mitochondrial fusion basal levels.

5.2. Mitochondrial fission.

The main factor that regulates mitochondria fission process in mammals is the dynamin-related protein 1 (Drp1) (Fig. 15) [303]. This cytosolic protein is able to associate to the OMM in response to fission signals and to oligomerize in a ring-like structure that surrounds the mitochondria (Fig. 15) [303,305]. Subsequently, the hydrolysis of the GTP molecule that is associated to this protein induces the narrowing of the Drp1 structure, generating eventually the scission of both mitochondrial membranes (Fig. 15) [305]. Consequently, two new organelles are formed from only one mitochondrion (Fig. 15):

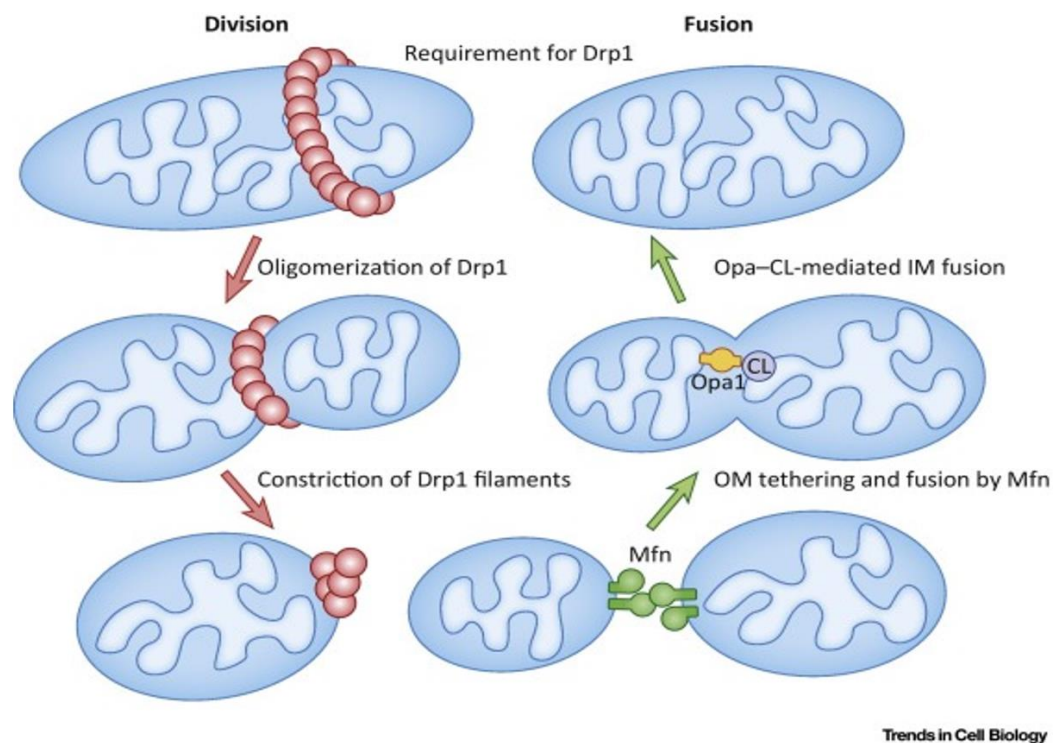


Figure 15: Molecular mechanisms involved in mitochondrial fusion and fission processes. Tethering and fusion of the OMM are mediated by MFNs, whereas the heterodimer OPA1-CL mediates IMM fusion. Fission process is mainly mediated by the protein Drp1, which is recruited to the mitochondrion, where oligomerizes to form a helix structure that surrounds this organelle. Subsequently, the narrowing of this ring disrupts both mitochondrial membranes. Retrieved from [311].

Conversely, the process of translocation from the cytosol, where Drp1 remains inactive, to the mitochondria in response to fission signals is mediated through some OMM receptor proteins that anchor Drp1 to this structure [305]. Although mitochondrial fission protein 1 (Fis1) has previously been suggested to be the main Drp1 receptor in mitochondria, it has been recently claimed that this protein presents a less important role in mitochondrial fission since its downregulation only generates mild defects in this pathway [318]. Besides, it is currently asseverated that Drp1 recruitment to the mitochondria is mediated by the tail-anchored mitochondrial fission factor (Mff) and the N-terminally anchored mitochondrial dynamics proteins of 49 and 51 kDa (MiD49 and MiD51 respectively) [305]. These three proteins can recruit independently Drp1 to the MAM, where all these receptors function in a cooperative way to generate the Drp1 oligomer [319,320]. Additionally, Mff has recently been shown to recruit Drp1 to MAM before to MiD49/51, which suggests the existence of a temporal differential in Drp1-dependent recruitment activity [321]. Otherwise, Fis1 seems to be in charge of connecting Mff-Drp1 to some proteins that are located in the ER-mitochondria interface [318].

On the other hand, it has recently been demonstrated that the ER also plays a key role in the determination of mitochondrial fission sites [307]. Indeed, it seems that Drp1-dependent fission requires a previous phase of mitochondrial constriction since the size of its oligomer is much smaller than mitochondrial diameter [322]. Recently, it has been reported that this contractile process is mediated by the rolling of an ER tubule around the fission site, which has also been shown to work as a scaffold for fission machinery [322]. The contractile force required to achieve this compression is performed by the inverted formin 2 (IFN2)-dependent recruitment of actin and myosin II proteins in the mitochondria-ER interface [323].

Similarly to the fusion process, mitochondrial fission is also tightly regulated by certain mitochondrial factors [303]. For instance, the proapoptotic protein Bax induces Drp1 SUMOylation, which in turn increases its activity by stabilizing its association with the mitochondrial membrane [324]. Besides, BNIP3 induces this process by promoting the translocation of Drp1, which in turn enhances mitophagy process [325]. Conversely, PKA prevents this process by phosphorylating Drp1 at S656, which prevents its capability to induce the scission of OMM and IMM [326]. This phenotype is easily reverted by calcineurin, a Ca^{2+} -dependent phosphatase, which implies that the cytoplasmic concentration of this ion also performs a role in the regulation of mitochondrial fission [326]. Moreover, mitochondrial fission is also enhanced during the mitosis process, since the cyclin B-cyclin-dependent kinase 1 (CDK1) complex, which is the key factor that induces cell division, stimulates Drp1 phosphorylation, augmenting its affinity for its OMM binding sites [327]. Finally, Aurora A, which is another kinase that is implied in mitosis process, triggers RalA-dependent recruitment of Drp1 to the mitochondria [328].

5.3. Mitophagy.

During cellular lifespan, mitochondrial homeostasis can be compromised by a high number of extracellular and intracellular stressful situations, such as ROS accumulation, hypoxia or nutrient starvation [329]. Under mild conditions, mitochondria are able to activate a group of molecular mechanisms that progressively eliminate dysfunctional macromolecules, such as the ubiquitin-proteasome system [329]. However, severe and prolonged stress induces the turnover of entire non-functional mitochondria by the autophagosomes in a process known as mitophagy (Fig. 17) [330,331]. This process

of degradation is normally preceded by the loss of mitochondrial membrane potential, and the segregation from healthy mitochondria by increasing its fragmentation through inducing the fission machinery (Fig. 16 and 17) [332]. Curiously, mitochondrial fusion process has been reported to protect healthy and functional mitochondria from mitophagy by inducing an increment of their size, which prevents their engulfment by the autophagosome [332,333]. This process seems to be mediated by PKA, which inhibits Drp1 when starvation conditions do not provoke mitochondrial damages [333].

Conversely, three main different protein pathways are in charge of the selective insertion of damaged mitochondrial into the autophagosome (Fig. 16 and 17) [330,331]. These are the PINK1/Parkin, the BNIP3/Nix and the FUN14 domain-containing protein 1 (FUNDC1) pathways, which can induce this degradation pathway in a non-overlapping manner (Fig. 16 and 17) [330,331].

5.3.1. *The PINK1/Parkin pathway.*

The mitophagy system constituted by the serine/threonine kinase PINK1 and the E3 ligase Parkin is responsible for targeting depolarized mitochondria to the autophagosome (Figs. 16A and 17) [331]. Therefore, this harmful status is detected by PINK1, since this protein is unable to accumulate in the OMM of the mitochondria that are correct polarized [331]. Indeed, PINK1 is rapidly guided in healthy organelles to the IMM through the translocase of the OMM (TOMM) and the translocase of the IMM (TIMM) [334]. In this location, PINK1 is cleaved by the presenilins-associated rhomboid-like protein (PARL) to form a 52 kDa subproduct that subsequently returns to the cytoplasm, where is degraded by the ubiquitin-proteasome system [335]. Additionally, this PINK1 derivative can also impede the translocation of the protein Parkin to the mitochondria, preventing the activation of mitophagy in this organelle [336]. When the mitochondrial membrane potential is lost, this protein is unable to translocate to the IMM, being stabilized by TOMM complex and integrated into this multiprotein system, increasing ultimately the PINK1 content in the OMM (Fig. 16A) [335].

Subsequently, Parkin is recruited from the cytosol and activated in response to PINK1 accumulation in the OMM of depolarized mitochondria (Fig. 16A) [330,331]. Although the mechanism through the translocation and activation of this protein is induced has not been totally elucidated yet, it seems to be dependent on PINK [331,337]. Indeed, if

the translocation of Parkin is forced in absence of PINK1, this mediator will not exert its function, remaining inactive in the surface of these organelles [337]. Currently, two different mechanisms have been reported to be in charge of the translocation of Parkin to the mitochondria (Fig. 16A) [331]. On the one hand, PINK1 has been shown to induce the phosphorylation of MFN2 at T111 and S442, which could initiate the recruitment of the Parkin to the OMM (Fig. 16A) [338]. On the other hand, PINK1 has been also reported to phosphorylate the ubiquitin-like domain of Parkin, as well as the ubiquitin protein (Fig. 16A) [330,331]. It seems that the PINK1-dependent phosphorylation of the ubiquitin basal levels at the OMM acts as an attraction and activator system for Parkin (Fig. 16A) [330]. Moreover, it has also been suggested the existence of a positive feedback mechanism that involves the E3-ligase activity of Parkin (Fig. 16A) [339]. Indeed, the increment of ubiquitin levels at the OMM allows the targeting of more Parkin molecules to this organelle due to the increase of PINK1-phosphorylation substrates [339].

Once activated, Parkin starts to ubiquitylate numerous OMM proteins, leading to the increase of the ubiquitin concentration in this membrane (Fig. 16A) [330,331]. Some of the proteins that are modified by this factor are the voltage-dependent anion-selective channel proteins 1, 2 y 3 (VDAC1, 2 and 3), TOMM, the fusion proteins MFN1 and MFN2 and the small mitochondrial Rho GTPase (Miro), which is implicated in the regulation of the movement of these organelles [330]. As a result of these post-translational modifications, the fusion of the Parkin-targeted mitochondria is totally abolished, as well as their movement through the microtubules [340,341]. Recent studies using microarrays have discovered a broad spectrum of mitochondrial proteins that present potential sites of Parkin-dependent ubiquitination, such as Fis1, FUNDC1, Bax or Mcl-1, which indicates that this factor could regulate more mitochondrial functions [342]. Moreover, it has also been demonstrated that all identified Parkin-dependent ubiquitination sites are situated towards the cytoplasm, which could suggest that this factor could also restructure the OMM proteome [342].

Subsequently, Parkin-ubiquitylated substrates associates to LC3-interacting proteins, such as p62, Optineurin (OPTN), neighbor of breast cancer type 1 susceptibility protein (BRCA1) gene 1 (NBR1), AMBRA1 and nuclear dot protein 52 kDa (NDP52), which are in charge to target depolarized mitochondria to the autophagosome (Figs. 16A and 17) [330,331]. All these proteins contain a LC3-interacting region (LIR) and a C-terminal ubiquitin association domain (UBA), which are responsible for the achievement

of the connection between the autophagosome and the mitochondria (Figs. 16A and 17) [343]. However, it has recently been assessed that only OPTN and NDP52 are indispensable to achieve this process, whereas p62 and NBR1 present more dispensable activities, such as the formation of damaged mitochondria clusters that will increase mitophagy efficiency [344,345]. Moreover, it has also been reported that the PINK1-dependent phosphorylation of mitochondrial basal levels of ubiquitin is sufficient to achieve the translocation of OPTN and NDP52 to the mitochondria, which likely suggest that Parkin will only work as a signal amplifier (Fig. 16A) [339]. Summarizing, more studies should be done to improve our comprehension of PINK/Parkin mitophagy process.

5.3.2. The *BNIP3/Nix* pathway.

BNIP3 and Nix are atypical BH3-only proteins that can induce apoptosis by suppressing the action of the antiapoptotic Bcl-2-family proteins [346]. Nevertheless, it has been claimed that their BH3-domain present redundant functions and is weakly conserved, which suggests that these proteins are not able to induce apoptosis in human tissues [347]. Although these proteins share the 56 % of their amino acid sequence, they present different cellular and temporal expression patterns [330,331]. For instance, these proteins present different expression among the diverse human organs, being BNIP3 more greatly expressed in heart, liver and muscle, whereas Nix is more present in hematopoietic tissues and testes [330]. Conversely, BNIP3 is normally more rapidly induced in response to stress stimuli than Nix [330]. Because of these discrepancies, Nix has usually been more associated with the control of mitochondria clearance in many physiological processes, such as the maturation of reticulocytes or spermatozoon, whereas BNIP3 has been associated with the management of stress stimuli in liver and muscle [330].

Both BNIP3 and Nix are direct targets of HIF-1 α , since they have multiple HRE in their promoter region (Figs. 16B and 17) [348]. Nevertheless, these two proteins present different induction patterns, since BNIP3 is stimulated at milder hypoxia levels than Nix, principally due to the differential dependence of these proteins on the different HIF-1 α TAD domains [349]. However, it has recently been reported that HIF-1 α -dependent expression of the *BNIP3* gene could be reduced by displacing HIF-1 α binding to the promoter or by epigenetic mechanisms [350–352]. Indeed, the pRb/E2F complex can associate to the *BNIP3* promoter, attenuating the hypoxia-dependent induction of this

gene and switching hypoxia-dependent cell death from autophagic to necrotic [350]. Moreover, it seems that the recruitment of histone deacetylase-1 (HDAC-1) to the *BNIP3* promoter by p65 also prevents the hypoxia-dependent expression of this gene [351]. On the other hand, the presence of a large CpG island in *BNIP3* promoter could lead to the silencing of this gene by hypermethylation, which clearly prevents hypoxia-dependent induction of BNIP3 expression since the HRE is located inside this region [352]. Moreover, the tumor cells that present methylations in the BNIP3 promoter are less sensitive to chemotherapy and present more aggressive features [352].

Oppositely to the PINK1/Parkin route, BNIP3 and Nix directly target damaged mitochondria to autophagosome to achieve their degradation (Figs. 16B and 17) [347]. Indeed, these mitophagy mediators integrate into the OMM and homodimerize through their C-terminal domain, maintaining their N-terminal region towards the cytoplasm (Figs. 16B and 17) [330,331]. This cytosolic region contains a LIR motif that directly interacts with LC3-II in the nascent autophagosome, introducing mitochondria into this vesicle for degradation (Figs. 16B and 17) [347]. In addition, it has recently been demonstrated that the phosphorylation of certain serine residues located around the LIR domains of BNIP3 and Nix increase their affinity by LC3 and GATE-16 (Fig. 16B) [331]. These data suggest the existence of a secondary post-transcriptional regulation that could stimulate the mitophagy in response to more severe stresses (Fig. 16B) [347].

Furthermore, BNIP3 and Nix can also trigger early autophagosome formation [331]. For instance, these two mitophagy mediators can displace the binding between Bcl-2 and Beclin1, since they can capture Bcl-2 by their non-canonical BH3 domain, which leads to the release of Beclin1 and the induction of autophagy [270]. Moreover, these proteins can also abolish the activation of mTORC1 by sequestering Rheb in the mitochondria and reducing the levels of its active form, leading to the increase of autophagosome formation [353]. On the other hand, BNIP3 and Nix proteins also induce mitochondrial fragmentation by inhibiting their fusion and inducing their fission [330]. It has been reported that BNIP3 can prevent the formation of OPA1 complexes, whereas it can promote the translocation of Drp1 to the mitochondria [316,325]. Therefore, the overexpression of mitochondrial fusion-related proteins, such as MFN1, or the reduction in the expression of fission-related proteins, such as Drp1, impair the induction of BNIP3-related mitophagy [330].

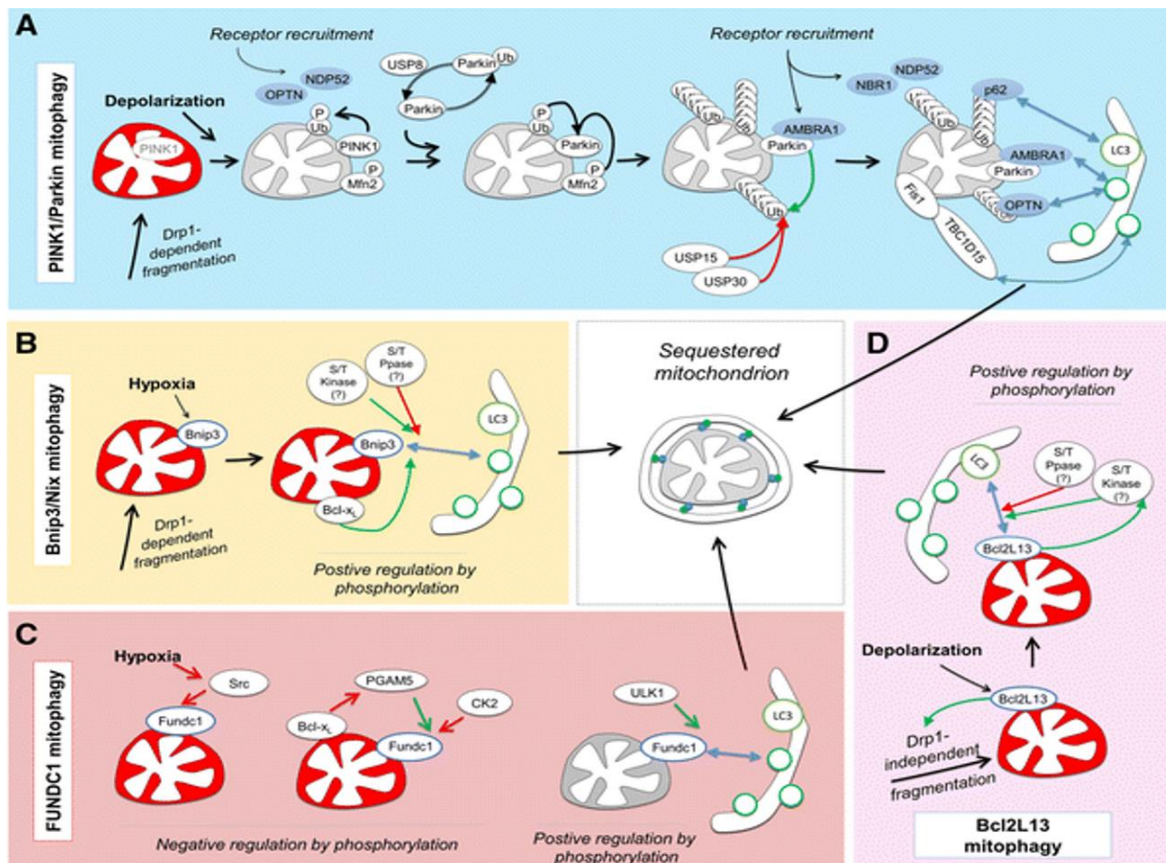


Figure 16: Description of the main pathways that induce the degradation of mitochondria in autophagosomes. (A) PINK1 is stabilized in the OMM after mitochondrial depolarization, where phosphorylates ubiquitin and MFN2. This process leads to the mitochondrial recruitment and activation of Parkin, which starts to ubiquitylate many OMM proteins. Subsequently, mitophagy receptors AMBRA1, p62 and OPTN, which are attracted to the OMM in response to the previous mechanism, interact with LC3 and target mitochondria to the nascent autophagosome. Moreover, it has been shown that OPTN and NDP52 can be recruited to the mitochondria by PINK1. (B) BNIP3 and Nix are induced under low oxygen conditions and are integrated to the OMM, where interact with LC3 at the nascent autophagosome and target mitochondria for degradation. In addition, BNIP3 activity is regulated at the post-transcriptional level by the phosphorylation of certain serine residues in its N-terminal region. (C) Under non-stress conditions, the OMM transmembrane protein FUNDC1 is inhibited through the phosphorylation of its T18 by Src. Hypoxia can revert this process, which allows its interaction with LC3 at the nascent autophagosome to introduce damaged mitochondria for degradation. Besides, CK2-dependent phosphorylation of FUNDC1 at S13 and its dephosphorylation by PGAM5 constitutes a secondary mechanism in the regulation of this mitophagy factor. (D) Bcl-2-L-13 induces Drp1-independent mitochondrial fission and targets mitochondria to the autophagosome by interacting with LC3. Retrieved from [331].

5.3.3. *The FUNDC1 pathway.*

The OMM-located protein FUNDC1 constitutes the most newly discovered mechanism that induces mitophagy (Fig. 16C) [331]. FUNDC1 present three hydrophobic transmembrane domains and a LIR motif that modulates the binding of this protein to LC3 and GABARAP to target mitochondria into autophagosomes [354]. Similarly to BNIP3 and Nix, FUNDC1 affinity for LC3 homologs is tightly regulated by the phosphorylation of certain amino acid situated around its LIR domain (Fig. 16C) [331]. For instance, the phosphorylation of the T18 of FUNDC1, which is part of its LIR motif, by Src kinase abolishes its interaction with LC3 (Fig. 16C) [331,355]. This process is returned by the phosphorylation of the adjacent S17 by ULK1 in response to hypoxia, which suggests that FUNDC1 activity is also modulated by the cellular oxygen status (Fig. 16C) [355]. Otherwise, the phosphorylation and dephosphorylation of the S13 of FUNDC1 by casein kinase 2 (CK2) and phosphoglycerate mutase family member 5 (PGAM5) respectively act as a secondary mechanism to regulate its activity (Fig. 16C) [355]. Indeed, the phosphorylation of this serine residue reduces FUNDC1 and LC3 affinity, whereas its dephosphorylation promotes this interaction (Fig. 16C) [355].

Similarly to BNIP3 and Nix, FUNDC1 can also promote mitochondrial fragmentation by modulating some proteins implicated in the fusion and fission of this organelle [356]. Therefore, it has recently been reported that the hyperphosphorylated form of FUNDC1 can associate to OPA1 in the intermembrane space [356]. However, the dephosphorylation of this mitophagy factor reduces the FUNDC1 affinity of OPA1, while it induces Drp1 recruitment to the mitochondria, which induces the fission of the candidate mitochondria for mitophagy [356].

5.3.4. *Novel inductors of the mitophagy pathway.*

Although PINK1/Parkin, BNIP3/Nix and FUNDC1 are the main molecular mediators that modulate mitophagy, new alternative mechanisms have been proposed in the last few years [355].

Bcl-2-like protein 13 (Bcl-2-L-13) is an atypical Bcl-2 family member that remains binding to the OMM and does not associate to other prodeath or prosurvival constituents of this family (Fig. 16D) [331]. Nevertheless, it is able to induce mitochondrial

fragmentation and mitophagy by targeting these organelles to the autophagosome since they have a LIR motif in its sequence (Fig. 16D) [357]. Curiously, it has been recently shown that Bcl-2-L-13 fragmentation is independent of Drp1, which likely suggests the existence of a secondary mechanism that modulates mitochondrial fission (Fig. 16D) [357].

Otherwise, C₁₈-ceramide has been shown to target mitochondria to the autophagosome by directly interacting with LC3 protein at the membrane of this vesicle [358].

Conversely, it has recently been reported that certain IMM components can also induce mitophagy in response to extremely severe stresses [359,360]. For instance, the IMM-located phospholipid CL is able to switch to the OMM in these situations [359]. The incorporation of CL marked organelles into the autophagosome has been reported to be mediated by the direct binding of CL to the N-terminal domain of LC3 [359].

Finally, the cristae homeostasis promoter prohibitin-2 (PHB-2) is able to attract Parkin to the OMM, which ultimately leads to the proteasome-dependent disaggregation of this membrane [360]. Besides, this molecule is also able to introduce mitochondria into the autophagosome after this rupture by directly associating with the protein LC3 by its LIR domain [360].

5.3.5. Role of mitophagy in human pathologies.

The deregulation of the mitophagy pathway, stimulating the loss of mitochondria functionality in certain human tissues, has been associated with the aggravation of many pathologies, such as cancer, Parkinson's disease, muscle atrophy and type II diabetes (Fig. 17) [347]. Furthermore, cell sensitivity to treatment can also be reduced as a result of the arising of defects in this pathway [361].

Similarly to autophagy, mitophagy also presents a changing role during the different phases of tumorigenesis [361]. In earlier steps, mitophagy protects cells from malignant transformation by maintaining ROS and RNS levels stables and avoiding the stabilization of HIF- 1 α (Fig. 17) [361]. In addition, this process also upkeeps basal mitochondrial oxidative metabolism and prevents the induction of the Warburg effect, which ultimately leads to promoting tumor progression [361]. On the other hand, mitophagy promotes tumor cell survival at later steps of carcinogenesis by alleviating the damage induced by

the excessive formation of ROS and RNS [361]. Besides, this process can protect tumor cells against conventional chemotherapy, thus the use of mitophagy repressors as therapeutic adjuvants could be a worthy strategy to avoid the loss of cellular sensitivity [361].

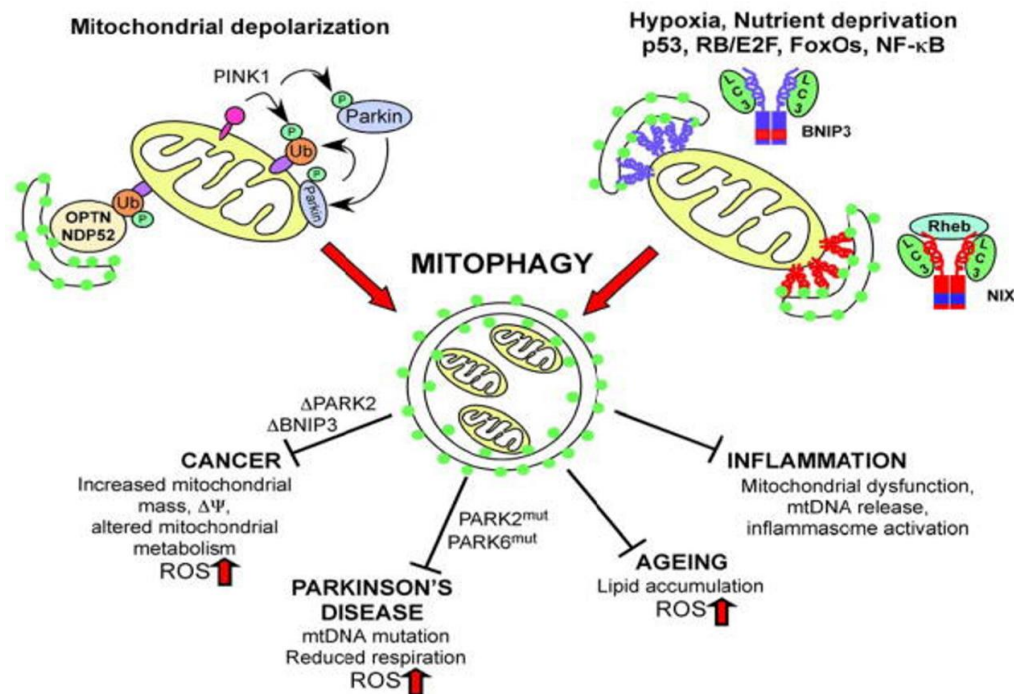


Figure 17: Role of mitophagy in disease. Both PINK1/Parkin and BNIP3/Nix pathways collaborate in the induction of mitophagy in response to different stress stimuli, such as mitochondrial depolarization, hypoxia or nutrient deprivation. Mitophagy protects cells against several pathological processes, such as cancer, Parkinson's disease, aging-related type II diabetes (aging) and inflammation, through preventing ROS production, mitochondrial dysfunction, inflammasome activation and lipid accumulation amongst others. Retrieved from [347].

Conversely, it has been shown that mitochondrial dysfunction is a pathogenic mechanism in Parkinson's disease (Fig. 17) [362]. Indeed, many mitochondrial processes are altered in this pathology, such as their dynamics, their trafficking, their metabolism and their degradation, which is accompanied by a reduced membrane potential and an elevated ROS and RNS concentration (Fig. 17) [362]. Otherwise, it has been shown that mitophagy dysfunctions are also linked with the pathogenesis of this disease, since the underexpression of either Parkin or PINK1 in dopaminergic neurons is responsible for the onset of a specific familiar type of Parkinson's disease (Fig. 17) [347,362]. Moreover, mitophagy is also indirectly inhibited as a result of the formation of α -synuclein aggregates, which impedes the generation of autophagosome vesicles [347].

On the other hand, dysfunctions on mitophagy are linked with the induction of a reduction in skeletal muscle mass, which is also known as muscle atrophy or wasting, due to the accumulation of non-functional mitochondria that produce high levels of ROS [347,363]. Moreover, recent studies have linked these mitophagy defects with the loss of Parkin expression in skeletal muscle, underscoring its critical function in the upkeep of muscle homeostasis [363]. Otherwise, the accumulation of age-related mitochondria dysfunction due to the impairment of mitophagy is related to the appearance of type II diabetes [347]. This effect seems to be related to the accumulation of lipid droplets in liver and muscle due to the reduction of fatty acid oxidation in dysfunctional organelles (Fig. 17) [347]. Finally, mitophagy restricts the induction of proinflammatory processes by limiting the formation of ROS and RNS in damaged mitochondria, thus its deregulation can promote the hyperactivation of these systems, leading to inducing proinflammatory cell death (Fig. 17) [347].

6. Apoptosis and its interrelation with autophagy.

PCD is constituted by a group of physiological mechanisms that control the natural elimination of non-functional, damaged or marked cells during non-pathogenic processes, such as embryonic development or after a cell injury that could not be solved by the mechanisms of reparation [364]. Currently, up to 15 different types of PCD has been described, being apoptosis, autophagy and necroptosis (programmed necrosis) the most common classes [364].

Apoptosis, or type I PCD, is characterized by the generation of a specific group of morphological and biochemical changes in the dying cells [365]. Some of these apoptosis-related morphological alterations are nuclear shrinkage (pyknosis), chromatin condensation in the periphery of the nuclear membrane, membrane blebbing, loss of membrane integrity and detachment from neighbor cells [365,366]. The main apoptosis-related biochemical alterations are the activation of cysteine-aspartic proteases (caspases), the rupture of chromatin and protein and the switching of phosphatidylserine from the inner layer to the outer layer of the cellular membrane [366]. This last process allows the recognition and subsequent engulfment of the dying cells by macrophages [366].

Caspases are the central enzymes that modulate the process of apoptosis, working either as initiators, by inducing the activation of downstream effectors, or as executioners, by cleaving certain cellular substrates and inducing the cellular morphological changes that are characteristic of apoptosis (Fig. 18) [366,367]. Indeed, the process of apoptosis could be defined as the progressive and sequential activation of these proteins [367]. At least four different caspase activation pathways have been described currently, being intrinsic (or mitochondrial) and extrinsic (or death receptor) pathways the most commonly induced routes (Fig. 18) [366]. These two cellular mechanisms converge in the activation of the executioner caspases (Fig. 18) [366]. Other pathways that also induces type I PCD under certain conditions are intrinsic endoplasmic reticulum pathway and perforin-granzyme route [366,368].

6.1. Intrinsic apoptosis pathway.

In intrinsic apoptosis, caspase activation is induced by the specific release of proapoptotic mediators from the intramembrane mitochondrial space (IMS), such as cytochrome c, second mitochondria-derived activator of caspases (SMAC), direct inhibitors or apoptosis (IAP), binding protein with low pI (Diablo) and high temperature requirement protein A2 (HTRA2) (Fig. 18) [369]. The permeabilization of the OMM (MOMP) in response to certain internal stress stimuli, such as irreparable genetic damage, severe oxidative stress, prolonged hypoxia and extremely elevated concentrations of Ca^{2+} in the cytoplasm allows the discharge of these mediators from the IMS (Fig. 18) [366,369]. Following this discharge, cytochrome c attaches to the apoptotic protease-activating factor 1 (APAF1), stimulating its oligomerization to form a platform known as apoptosome that enhances the activation of initiator caspase 9 (Fig. 18) [364,369,370]. Subsequently, this enzyme cleaves and activates the effector caspases 3, 6 and 7, enhancing the appearance of the morphological changes that are characteristics of apoptosis (Fig. 18) [364,369,370]. Conversely, secondary apoptotic mediators SMAC/Diablo and HTRA2 impede the action of X-linked inhibitor of apoptosis protein (XIAP), as well as increases the activity of endonuclease G and apoptosis-inducing factor (AIF), which are responsible for the apoptosis-dependent DNA breakdown (Fig. 18) [364].

Conversely, the MOMP is induced by the proapoptotic effectors Bax and Bak (Fig. 18) [364,369]. These proteins belong to the Bcl-2 family and are not inserted in the OMM

under basal conditions, being this process triggered after a proapoptotic stimulus [364]. Subsequently, Bax and Bak undergo a series of conformational changes that will lead to inducing the transient exposure of the BH3-domain [369,371]. This process allows the formation of symmetrical Bax and Bak homodimers by the reciprocal hydrophobic interaction of their BH3 domains, leading to the generation of membrane pores since these dimers can associate with each other to form oligomers [369,371]. Bax and Bak pores disrupt OMM, permitting the discharge of primary and secondary apoptotic adaptors contained in the IMS (Fig. 18) [369,371].

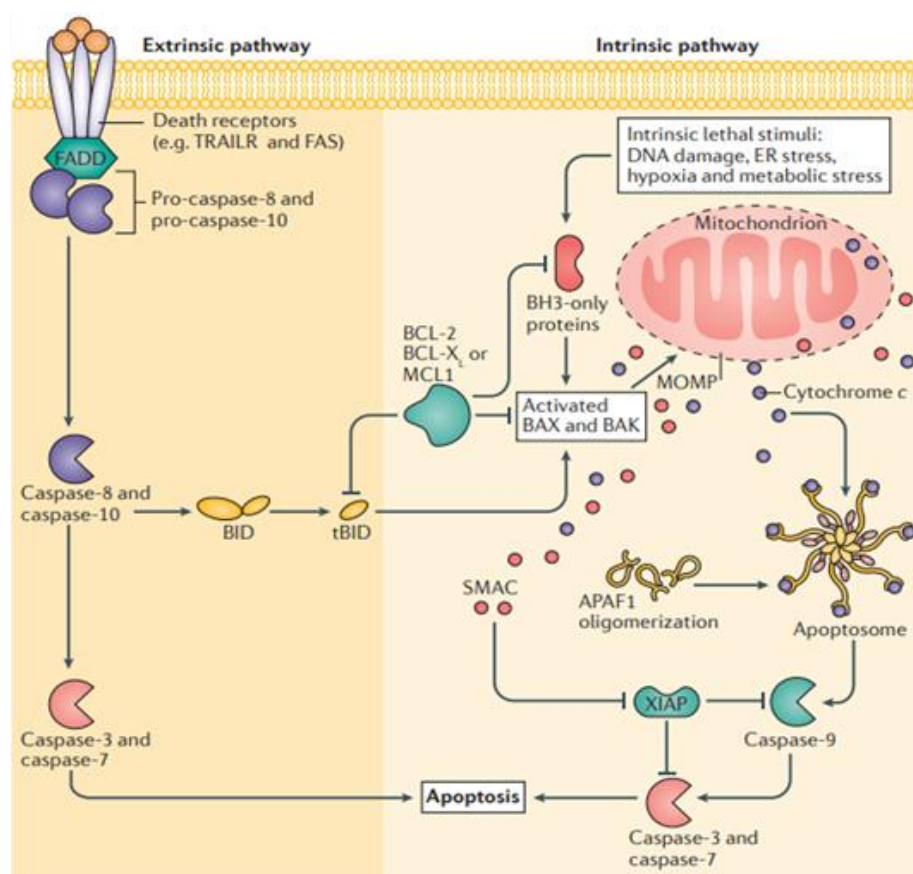


Figure 18: Molecular mechanisms that induce extrinsic and intrinsic apoptosis pathways. In the extrinsic apoptotic pathway, death receptors, such as TRAILR1 and FAS can activate initiator caspases 8 and 10 when their specific death ligand is bound. These initiator enzymes cleave the effector caspases 3 and 7, which ultimately leads to enhancing apoptosis. In the intrinsic apoptotic pathway, the activation of certain BH3-only proteins upon an intern stress triggers MOMP due to their ability to enhance the oligomerization of Bax and Bak in the OMM. This process is restrained by antiapoptotic Bcl-2 family members. The release of cytochrome c to the cytosol specifically activates APAF1, stimulating its oligomerization and the formation of the apoptosome. This complex enhances the action of caspase 9, which in turn activates effector caspases 3 and 7. Other secondary autophagy mediators, such as SMAC/Diablo, will prevent the caspase-inhibitory action of XIAP. Caspase 8-dependent cleavage of BH3-only protein BID to constitute tBID, which is its functional derivative, suggests the existence of a crosstalk between both pathways. Retrieved from [370].

The activation of Bax and Bak proteins is tightly regulated by the interaction of a great number of antiapoptotic and proapoptotic members of the Bcl-2 family [369,371]. The main proteins that promote Bak and Bax oligomerization upon a proapoptotic stimulus are the BH3-only proteins Bcl-2-interacting mediator of cell death (BIM) and BH3-interacting domain death agonist (BID) (Fig. 18) [369,371]. Indeed, it has been reported that the binding between these BH3-only proteins and the autophagy effectors induces some conformational changes that lead to the exposure of the BH3-domain of Bax and Bak [369,371]. Apart from BIM and BID, other BH3-only protein, such as Bcl-2-associated agonist of cell death (BAD), Bcl-2-interacting killer (BIK), activator of apoptosis harakiri (HRK), nicotinamide adenine dinucleotide phosphate (NADPH) oxidase activator 1 (Noxa1), and p53-upregulated modulator of apoptosis (PUMA) also induce apoptosis by preventing the action of anti-apoptotic proteins without directly binding with Bax and Bak (Fig. 18) [371]. Currently, three different hypotheses have been suggested based on the consequences that originate the association between BH3-only proteins and the antiapoptotic Bcl-2 proteins [371]. The sensitization model proposes that these proapoptotic proteins act as a sensitizer that sequesters Bcl-2, inducing MOMP by preventing the inhibitory action of this protein on BIM [371]. Besides, the derepressive hypothesis suggests that BH3-only proteins can displace the joining between BIM and Bcl-2, releasing this proapoptotic protein and inducing MOMP [371]. Finally, the neutralization model proposes that the oligomerization of Bax and Bak is prevented by their direct binding to the antiapoptotic Bcl-2 protein [371]. When apoptosis is induced, BH3-only proteins sequesters BCL-2, which ultimately enhances MOMP [371].

6.2. Extrinsic apoptosis pathway.

In contrast to the intrinsic pathway, extrinsic apoptosis is induced by an external death signal that is recognized by a transmembrane protein which is called as death receptor (Fig. 18) [366]. Currently, up to 40 different death ligand-receptors pairs have been detailed, being the first apoptosis signal ligand (FasL) selective binding to first apoptosis signal (Fas), the TRAIL to TNF-related apoptosis-inducing ligand receptors 1, 2 and 3 (TRAIL-R1, TRAIL-R2 and TRAIL-R3) and TNF- α to tumor necrosis factor receptors 1 and 2 (TNF-R1 and TNF-R2) the most common couples that are responsible for triggering cell death [364]. Once activated, each receptor can recruit certain proteins,

such as Fas-associated death domain (FADD) and procaspases 8 and 10 to constitute the death-inducing signaling complex (DISC) (Fig. 18) [372]. This complex activates these initiator caspases, triggering finally apoptosis by cleaving and activating executor caspases 3, 6 and 7 (Fig. 18) [372]. Besides, DISC can also induce MOMP by enhancing the caspase-8-dependent cleavage of BID to its active form tBID, suggesting that this pathway recruits intrinsic response to amplify the apoptotic signal (Fig. 18) [370,372].

6.3. Crosstalk between autophagy and apoptosis.

Autophagy and apoptosis mechanisms are tightly interconnected to develop a well-balanced cellular response against multiple stress signals [373]. Moreover, it seems that this crosstalk is essential to regulate cell fate [374]. Indeed, autophagy can avoid apoptotic cell death by inducing cell survival under mild or brief stress stimuli, but it can enhance PCD in concert with apoptotic pathway under very severe or prolonged stress stimuli [374]. The mechanism that crosstalk these cellular responses are very complex owing to the great number of mediators of both pathways that are involved in this regulation [373].

Apoptosis regulation by autophagy can be subdivided into three different subclasses, according to their mechanistic features [373]. Firstly, many autophagy proteins, such as Atg5-Atg12 or Beclin1 can work in a similar way to BH3-only proteins, sequestering antiapoptotic mediators of the Bcl-2 family and inducing apoptosis by releasing the proapoptotic proteins of this group [373]. Curiously, UVRAG exerts the opposite action, since it prevents the translocation of Bax to the mitochondria, which inhibits apoptosis induction [375]. Secondly, autophagosome vesicles can be used as platforms for the activation of certain protein caspases [373]. Indeed, autophagosomal membrane proteins LC3 and Atg5 can bind p62 and FADD respectively, which induces the recruitment and activation of caspase 8 in absence of the whole DISC complex [373]. Finally, the capability of autophagy to control the organelle function, the protein turnover and the energy availability modulate the apoptotic response in an indirect manner [373].

On the other hand, autophagy regulation by apoptosis can be also subdivided into two different subclasses [373]. Firstly, the antiapoptotic Bcl-2 protein can impede autophagy by sequestering Beclin1, whereas some BH3-only proteins can displace this binding, leading to the release of Beclin1 and inducing autophagy [373,376]. Otherwise, caspases are able to cleave a great number of autophagic proteins, such as Beclin1, Atg5,

Vps34, Atg3, Atg4 or AMBRA1, which prevents the activation of this prosurvival pathway during the final process of apoptosis [373]. Additionally, the Beclin1 and Atg5 cleavage products are translocated to the mitochondria, where enhance the discharge of cytochrome c to the cytoplasm [376].

Finally, some mitophagic adaptors can also crosstalk with apoptosis pathway, because BNIP3 and Nix can act as BH3-only proteins with the ability to induce apoptosis by sequestering antiapoptotic members of the Bcl-2 family [346].

7. Melatonin: structure, synthesis and functions.

Melatonin (N-acetyl-5-methoxytryptamine) is a serotonin-derived hormone that has been reported to be produced in at least three different groups of bacteria, including alphaproteobacteria and cyanobacteria, as well as in all kingdoms of the domain Eukaryote, including dinoflagellates, algae, fungi, plants and animals [377,378]. Indeed, the presence of this ancient molecule in such phylogenetically distant organisms, suggests that melatonin should have arisen with a primary role at the basis of evolution, acquiring during the evolution process the other additional functions [377,378]. Curiously, it has recently been demonstrated that this hormone is synthesized into the mitochondria to prevent the discharge of ROS, surmising that the scavenging of this harmful molecules was the initial role of this molecule at the start of eukaryotic evolution [377,379].

In mammals, melatonin is mainly synthesized and secreted by the pinealocytes of the pineal gland [380]. This is a diencephalic-derived organ that is situated in the center of the cerebral mass [381,382]. More in detail, it is located on the superior colliculi of the mesencephalon and under the third ventricle, just between the two cerebral hemispheres [382]. Besides, this gland is not included in the blood-brain barrier, since it is surrounded by an extensive capillary bed, allowing pineal-derived secretion of melatonin both into blood supply and cerebrospinal fluid [382].

Curiously, it has recently been reported that melatonin is also produced at low concentrations in the mitochondria of almost all corporal organs and tissues in response to oxidative stress by using the same enzymatic system than in the pineal gland [379,383]. However, the synthesis of extrapineal melatonin does not follow the circadian rhythm (excepting in retina cells) and it is unable to spread through the blood supply [379,383].

These data suggest that extrapineal melatonin present a local function to avoid the generation of elevated oxidative damage in the cell due to the high discharge of ROS/RNS [379]. Some of the extrapineal sites in which melatonin seems to be synthesized are neurons, Harderian gland, retina, lens, cochlea, immune system, lung, gut, liver, kidney, thyroid, pancreas, thymus, spleen, hematopoietic cells, reproductive tract, skin, platelets, bone marrow and oocytes [377,381]. In hepatocytes, it has been demonstrated that melatonin levels in their mitochondria and in their plasmatic membrane can rise after suffering a pinealectomy [379,383]. Besides, the levels of this hormone in bile are incredibly high to protect the biliary tree epithelium from the highly toxic constituents that could be carried by this fluid [379,383]. All these data surmise the hypothesis that the hepatocytes are able to produce melatonin to avoid oxidative damage [379,383].

Melatonin is synthesized from tryptophan in a four-reaction pathway which firstly includes the 5-hydroxylation of tryptophan by tryptophan-5-hydroxylase (TPH) to form 5-hydroxytryptophan (Fig. 19) [384,385]. Then, this molecule undergoes a decarboxylation by aromatic amino acid decarboxylase (AAAD) to form 5-hydroxytryptamine (serotonin), which is N-acetylated by N-acetyl transferase (AANAT) to N-acetylserotonin and O-methylated by hydroxyindole-O-methyltransferase (HIOMT) to constitute melatonin (Fig. 19) [384,385]. It has been reported that melatonin synthesis should be at least partly mitochondrial since the limiting enzyme AANAT is only located in the lumen of this organelle and it needs coenzyme A as a cofactor [386].

In mammals, melatonin is degraded in different tissues by iron-containing hemoproteins, such as cytochrome P450 (CYP450), indoleamine 2,3-dioxygenase (IDO), myeloperoxidase (MPO) and eosinophil peroxidase (EPO) [385]. CYP450 degrades circulating melatonin into 6-hydroxymelatonin and N-acetylserotonin in the liver and other peripheral organs such as gut or skin [387]. Subsequently, these melatonin derivatives are excreted as sulfate or glucuronide conjugates [387]. Conversely, it has also been showed that IDO also degrades this compound into N¹-acetyl-N²-formyl-5-methoxykynuramine (AFMK) in the brain, whereas MPO and EPO execute this process at inflammatory sites [385]. On the other hand, the non-enzymatic metabolism of melatonin by its coordination with certain ROS and RNS to form many different metabolites, such as AFMK or N-acetyl-5-methoxykynuramine (AMK), is another relevant mechanism that achieves its degradation under oxidative stress conditions [385,387].

Melatonin is a nonpolar molecule with the ability to cross lipid bilayers, which implies that this molecule can directly bind to certain protein located inside the cell to exert its characteristic functions [388]. Certainly, a nuclear, a cytoplasmic and two transmembrane melatonin receptors have currently been described in mammal cells [383]. Besides, it has recently been proven that this hormone modulates cytoskeleton assembly by directly interacting with calmodulin and calreticulin, suggesting the existence of more binding sites of this molecule inside the cell [383]. Melatonin surface receptors MT1 and MT2 belong to the guanine nucleotide-binding regulatory protein (G protein)-coupled receptors superfamily [383]. MT1 activation restrains the generation of cAMP and PKA activity, as well as induces Ca^{2+} release to the cytosol, leading to enhance most of the reproductive and metabolic functions of this molecule [383]. Otherwise, MT2 activation by melatonin mainly manages the control of circadian rhythms by inhibiting the production of both cAMP and cyclic GMP (cGMP) [383]. On the other hand, the activation of the melatonin cytoplasmic receptor MT3, or quinone reductase 2 (NQO2), protects cells against severe oxidative stress by preventing the action of this enzyme [389]. Finally, nuclear retinoid-related orphan receptors (RORs), especially ROR α subtype c and ROR γ , act as nuclear receptors of melatonin, increasing the transcription and transactivation of many of its specific targets [383,390].

7.1. Regulation of circadian rhythms by melatonin.

Pineal-derived melatonin presents photosensitivity, which means that this hormone is only synthesized and secreted during darkness periods, maintaining at low levels during light periods [381,391]. These variations have not been shown in the secretion of extrapineal melatonin (excepting in retina cells) [379,383]. These light/dark fluctuations suggest that the main function of pineal-derived melatonin is the chemical control of circadian and seasonal rhythms [381,391]. Indeed, this hormone synchronizes the daily activities of animals, such as sleep, feeding, metabolism or reproduction with the daily fluctuations of light and dark [381]. Conversely, it has also been reported that melatonin can also modify seasonal rhythms since the darkness period is longer in winter than in summer, thus the peak of this molecule will be more extended in the first than in the second season [385]. Therefore, these fluctuations lead to adjusting the reproductive

activity of many animals to the right season, as well as to determine their hibernation behavior [381,385].

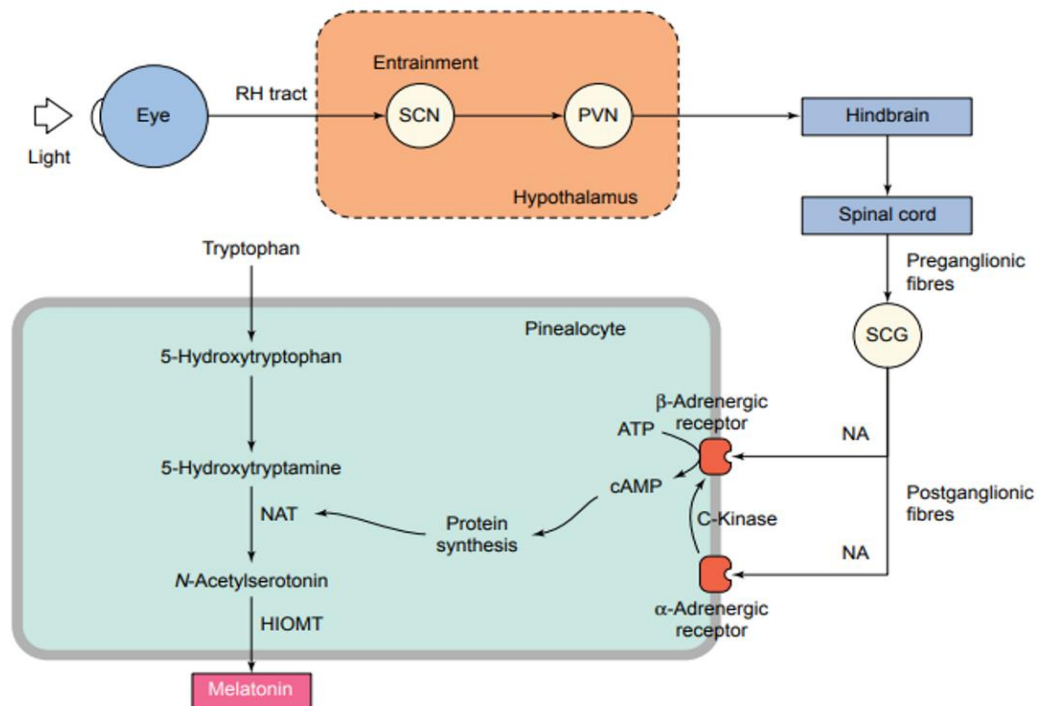


Figure 19: Mechanism that controls melatonin synthesis in mammals. The SCN detects changes in the amount of light that incides on the retina, sending an electrical signal to the pineal gland under dark conditions. This signal passes through the PVN, the upper thoracic intermediolateral cell column and the SCG to pineal noradrenergic (NA) receptors. This induction leads to increment the content of cAMP into the pinealocyte, which ultimately leads to increase melatonin synthesis by inducing the activity of AANAT. Retrieved from [384].

Melatonin production in the pineal gland under darkness conditions is regulated by the suprachiasmatic nucleus (SCN) (Fig. 19) [383,384]. This hypothalamic region integrates all the physical and the chemical signals that modulate light/dark cycles, leading to coordinating circadian rhythms in other cerebral zones and corporal tissues [391]. Retina photoreception is the principal mechanism through SCN detects light variations (Fig. 19) [391]. During the night, SCN sends a signal to the pineal gland through a complex pathway that involves the paraventricular nucleus (PVN), the intermediolateral nucleus of the spinal cord and the superior cervical ganglia (SCG), which ultimately sends sympathetic fibers to this endocrine organ (Fig. 19) [383,384]. The stimulation of the SCG during the night induces the release of norepinephrine by these sympathetic fibers, stimulating the generation of cyclic AMP (cAMP) in the pinealocyte through the specific binding of this neurotransmitter to the α_1 - and β_1 -adrenergic receptors [383,384]. The increase in intracellular cAMP concentrations in the pinealocyte stimulates the

expression and activity of AANAT and HIOMT, two key enzymes to accomplish melatonin synthesis [383,384].

Conversely, melatonin synthesis has recently been shown to be limited by dopamine. Certainly, the specific heterodimerization of the activated dopaminergic receptor D₄ and the α_1 - and β_1 -adrenergic receptors reduces the norepinephrine-dependent synthesis of melatonin during the dawn, acting as a secondary mechanism that limits the generation of this hormone during this period [392].

Pineal-derived melatonin produced during darkness periods has been shown to regulate the expression of the principal genes that modulate circadian rhythms [381,393]. Indeed, melatonin regulates the SCN activity, being this feedback essential to interpret correctly the photoperiodic changes that occur in the environment and to synchronize its activity to the fluctuations in the light/dark cycle [381]. To achieve these process, melatonin increases the expression of the clock genes period circadian clock 1 and 2 (PER1 and 2) during dark periods [381]. Otherwise, melatonin also enhances the expression of the genes PER1, cryptochrome-2 (CRY2) and brain and muscle ARNT-like 1 (BMAL1) in adrenal cortex [393]. Finally, this hormone synchronizes the circadian rhythm in cardiomyocytes by modulating the transcription levels of *Per2* and *Bmall* genes in the darkness and the light periods [393].

The disruption of circadian cycles due to disturbances in pineal-derived melatonin levels leads to the appearance of many severe disorders, such as neurodegenerative diseases, mood disorders, cardiomyopathies and cancer [385]. These disruptions have been associated with the incidence of artificial illumination during the night and are very common at night or shift workers [385,394]. Certainly, it has been demonstrated that the prevalence of breast and prostate cancers is higher in people that have been exposed to permanent circadian disruption during their job, such as nurses, airplane crews or miners [385,394]. In fact, the continued exposition of light during night period has been classified as a probable carcinogen by the International Agency of Cancer Research (IARC) [385,394]. On the other hand, the alteration of the circadian cycles due to changes in melatonin synthesis rhythms can disturb mood, originating some severe behavior pathologies, such as bipolar disorder, major depressive disorder or seasonal affective disorder [395]. Therefore, it is surmised that the restoration of the correct melatonin rhythms with bright light therapy or chronobiotic drugs with may be essential in the control of these mood disorders [395].

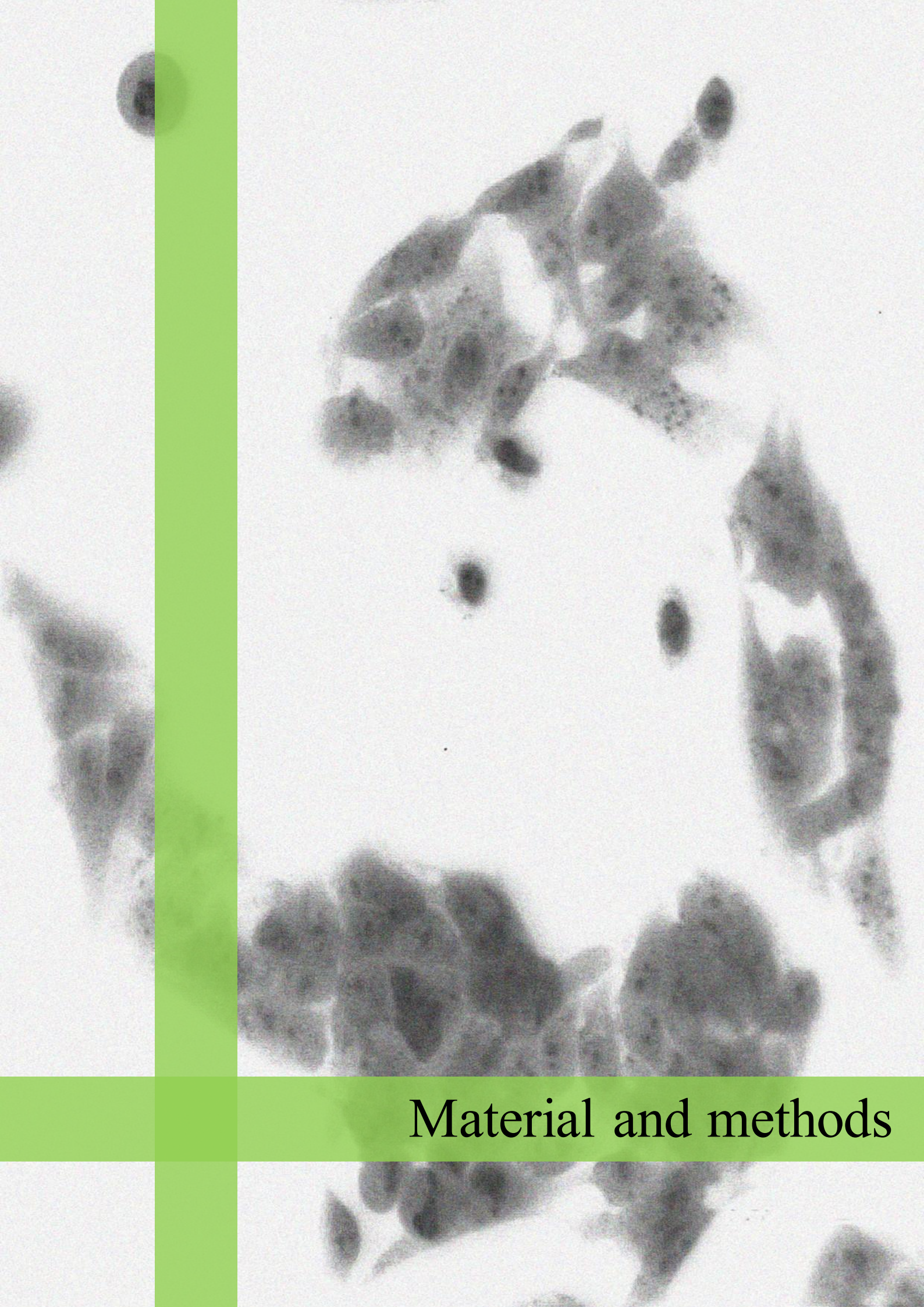
7.2. Other effects of melatonin.

Apart from the regulation of circadian and seasonal rhythms, melatonin has been reported to present hypnotic, antinociceptive, anticonvulsant, analgesic, anxiolytic, antidepressive, neuroprotector, anti-inflammatory, immunomodulatory and antitumor properties [396]. Therefore, more potent pharmacological analogs of this molecule are being developed to be used as an adjuvant for the treatment of multiple human disorders [397].

Melatonin is essential to maintain brain function and neuron homeostasis, so its deregulation generates multiple neuropsychiatric disorders such as depression, anxiety, or behavioral changes [397]. For instance, melatonin has been showed to improve neuron proliferation and neurogenesis in the subventricular zone and the adult hippocampus in a MT1-dependent mechanism and to attenuate the harmful effects that present stress-induced glucocorticoids on these processes [398]. Indeed, these melatonin beneficial features prevent the apparition of stress-related depression, a neuronal condition in which hippocampus neurogenesis is impaired [398]. Besides, the supplementation of melatonin alone or in combination with other antidepressants seems to be potentially effective in the remission of this disorder, indicating that this hormone could be useful for the treatment of depression [398]. On the other hand, melatonin reduces anxiety through stimulating the GABAergic system in a MT2-dependent mechanism [397]. This process leads to increasing the concentration of GABA in several brain zones, such as the hypothalamus, the cerebellum and the cerebral cortex, which ultimately reduces neuronal excitability and anxiety [397]. Conversely, melatonin induction of GABAergic and reduction of glutamatergic systems reduce excessive electrical activation of neurons, attenuating the arising of seizures in epileptic patients [399]. Indeed, some metabolites of this hormone, such as kynurenic acid, have been demonstrated to also present this anticonvulsant activity [399]. Finally, melatonin reduces the intensity and duration of chronic pain in multiple human disorders, such as migraines, fibromyalgia, cluster headaches, chronic back pain, rheumatoid arthritis and irritable bowel syndrome [400]. It has been reported that this molecule reduces pain perception in the brain by modulating the activation of several receptors in these neurons, such as GABA-B receptors, opioid μ -receptors or NO-arginine pathway in a MT2-dependent process [400].

Otherwise, melatonin also modulates the response of both the innate and the adaptive immune systems by modulating the levels of cytokines and leukocytes [401]. However, the immunomodulatory properties of this hormone are highly dependent on the activation status of the immune system [401]. Certainly, melatonin stimulates this response under basal or immunosuppressive conditions by inducing the generation of monocytes, macrophages and natural killer cells, as well as through increasing the production of interleukin-2, 6, 12 (IL-2, IL-6, IL-12) and interferon- γ (IFN- γ) [401,402]. Otherwise, melatonin controls the activation of exacerbated immune response by limiting chronic inflammation [401,402]. This mechanism seems to be mediated through the downregulation of certain proinflammatory mediators, such as 5-lipoxygenase (5-LOX), phospholipase A2 (PLA2), IL-1 and TNF- α [401,402].

Melatonin also presents a great number of oncostatic activities in a broad scope of human tumors, such as melanoma, breast, ovarian, endometrial, prostate, liver and colon cancers [403]. Indeed, this molecule is able to induce tumor cell apoptosis and antitumor immune response, as well as to prevent inflammation, angiogenesis, invasion and metastasis [16,17,403]. Conversely, melatonin can also synergize with other chemotherapeutic drugs, which leads to enhancing their antiproliferative and their proapoptotic features and to reducing their off-target toxicity [404,405]. In HCC cells, it has been demonstrated that melatonin can inhibit cancer cell proliferation and promote their apoptosis both in vitro and in vivo by upregulating MAPK and PI3K/Akt pathways [406–408]. Moreover, it presents antiangiogenic activities, since it is able to disturb VEGF release under hypoxia [16], and antimetastatic properties, due to its capability of inhibiting matrix metalloproteinase 9 (MMP9) through reducing NF- κ B signaling [17]. Summarizing, all these data allow the use of this molecule in the treatment of different cancers.



Material and methods

1. Workspace.

The experiments of this doctoral thesis were accomplished in the facilities of the *Instituto Universitario de Biomedicina (IBIOMED)* of the *Universidad de Leon*. Otherwise, the confocal microscopy analyses were performed in the *Servicio de Microscopia* of the *Universidad de Leon* and in the *Departamento de Muerte Celular y Proliferación* of the *Instituto de Investigación de Ciencias Biomédicas de Barcelona (IibB)* and of the *Consejo Superior de Investigaciones Científicas (CSIC)* of Barcelona.

2. Cell culture and reagents.

2.1. Cell culture.

Three different human HCC cell lines, Hep3B, HepG2 and Huh7 were used during the experimental procedure. All these cellular lines were obtained from the American Type Culture Collection (ATCC) (Manassas, VA, USA). Cells were grown as monolayer cultures in Dulbecco's modified Eagle's medium (DMEM) (Sigma-Aldrich, St Luis, MO, USA) supplemented with 10% fetal bovine serum (FBS) and 100 U/mL penicillin/streptomycin (Gibco, Grand Island, NY, USA). Besides, they were cultured under controlled CO₂ atmosphere (5%), temperature (37°C) and humidity (95%).

Cells were subcultured when their confluence was over 75 % using trypsin at 0.05% (Life Technologies, Carlsbad, CA, USA). After remaining at 37°C for approximately 1.5 minutes for Hep3B and Huh7 and 5 minutes for HepG2, this enzyme was neutralized by adding fresh complete media. Subsequently, cells were centrifuged at 1,100 rpm for 3 minutes at room temperature and the medium with trypsin was discarded, being replaced by fresh complete medium. Finally, about 2·10⁶ cells of each HCC line were plated in T75 flasks (BD Falcon, Franklin Lakes, NJ, USA).

2.2. Cell treatment and reagents.

For treatments, cells were seeded in 9.6 cm² culture dishes at a density of 2.5-3·10⁵ cells/well. 24 h after this process, plating media were replaced by fresh media containing different concentrations of melatonin (0.1, 0.5, 1 and 2 mM) (Sigma-Aldrich) with or

without sorafenib (0.01, 0.05, 0.1, 1, 2.5, 5, 10 and 50 μM) (Santa Cruz Biotechnology, Dallas, TX, USA). These two compounds were dissolved in dimethyl sulfoxide (DMSO) (Sigma-Aldrich) to increase its solubility in water, being 0.2% the residual concentration of this compound that remained in each plate. 100 μM CoCl_2 (Panreac AppliChem, Barcelona, Spain) was used to induce hypoxia since it can prevent HIF-1 α degradation through antagonizing Fe^{2+} -dependent PHD activity [409]. Additionally, the lysosomal acidification inhibitors bafilomycin A1 (Baf A1) (100 nM and 5 μM) (Tocris Bioscience, Bristol, UK) and chloroquine (CQ) diphosphate salt (50 μM) (Sigma-Aldrich) were added 3 h before the end of certain experiments to analyze the autophagy flux status. Moreover, cells were also treated in particular experiments either with the MAPK/JNK inhibitor SP600125 at 10 μM , with the PI3K/Akt repressor LY294002 at 50 μM , with the protein synthesis repressor cycloheximide (CHX) at 100 μM , with the PHD repressor DMOG at 1 mM, with the proteasome inhibitor MG132 at 10 μM (Tocris Bioscience) or with the mTORC1 inhibitor rapamycin at 20 nM (VWR, Radnor, PA, USA).

3. Determination of cell viability and apoptosis.

Two different procedures were performed to detect variations in cell viability and in apoptosis induction among the different experimental groups, the 3-(4,5-dimethylthiazol-2-yl)-2,5-diphenyltetrazolium bromide (MTT) assay and the Annexin V-propidium iodide assay.

3.1. MTT assay.

This colorimetric assay uses MTT to compare cell viability among the different treatments [410]. This compound forms yellowish aqueous solutions, but it is reduced into a water-insoluble violet-blue compound known as formazan in the cells that are metabolically active [410]. This reduced molecule precipitates, forming lipid-soluble crystals in the bottom of the plate, which can be dissolved in many organic solvents, such as ethanol and DMSO [410]. The color intensity of formazan dissolution is directly proportional to the number of living cells and could be quantified with a fluorescence spectrophotometer at a wavelength range of 540 to 580 nm [410].

MTT assay was carried out according to Denizot and Lang guidelines [410]. Confluent Hep3B, HepG2 and Huh7 cells were seeded in 96-well plates (Thermo Fisher Scientific, Waltham, MA, USA) at a density of 5,000 cells/well. 48 h after treatments, culture media were replaced by free-serum media containing MTT (Sigma-Aldrich) dissolved in phosphate-buffered saline (PBS) (Sigma-Aldrich) at 0.5 mg/ml. Cells were incubated with this compound for 3 h at 37°C. Subsequently, free-serum media was discarded and MTT precipitates were dissolved in DMSO. Finally, the optical densities of each well were measured at 560 nm spectral wavelength by using a microtiter plate reader (SynergyTM HT Multi-Mode Microplate Reader; BioTek Instruments, Inc.; Winooski, VT, USA).

3.2. Annexin V-propidium iodide assay.

This technique allows the determination of the percentage of cells that are suffering apoptosis or necrosis through analyzing the composition and integrity of their plasma membrane by using two different fluorochromes, annexin V conjugated with fluorescein (FITC) and propidium iodide (PI) [411]. On the one hand, annexin V can detect variations in the phospholipid distribution in the plasmatic membrane that occurs in the earlier steps of apoptosis [411]. Otherwise, PI is able to intercalate into the DNA and RNA of the cells that present defects in the integrity of both plasmatic and nuclear membranes [411]. Therefore, live cells are those that are negatively stained for the two fluorochromes, while early-apoptotic cells are only dyed with annexin V [412]. On the other hand, annexin V-positive, PI-positive cells are in late-apoptotic stages [412].

This procedure was assessed according to the Alexa Fluor 488 annexin V/Dead apoptosis kit (Invitrogen, Carlsbad, CA, USA) manufacturer's instructions. Hep3B cells were seeded in a 6-well plate at a density of $2.5 \cdot 10^5$ cells/well and were treated with 1 mM melatonin and 2.5 μ M sorafenib alone or in combination for 48 h. After this period, cell pellets were resuspended in 100 μ l of the 1x annexin-binding buffer with 5 μ l of annexin V and 1 μ l of PI and incubated for 15 minutes at room temperature under dark conditions. Subsequently, the volume of each sample was adjusted to 500 μ l by adding 400 μ l of 1x annexin-binding buffer. Cells were instantly analyzed with the SCAN flow Cytometer (Becton-Dickinson, San Jose, CA, USA) by acquiring a total of 10,000 cells per sample.

The percentage of cell death in each sample was assessed with the Cell Quest software (Becton-Dickinson).

4. Determination of protein expression.

4.1. Western blot.

Western blot, which is also known as immunoblotting or protein blotting, is a technique that allows detecting and comparing the expression of certain proteins among the different samples [413]. This assay normally starts with the extraction of all the proteins contained in the cell lysate [413]. Subsequently, a spectrophotometer technique is usually performed to equalize the protein concentration among all samples, ensuring that the same amounts of protein from all experimental groups are going to be used in the following steps [413]. Then, the protein mixture is separated by size and charge through electrophoresis in a gel matrix and transferred to an adsorbent membrane, which is going to be incubated with the antibody that detects the protein of interest [413]. The main method that allows the signal detection in this technique is the incubation with an enzyme-linked secondary antibody that recognizes the primary antibody and generates a chemiluminescence response that is going to be captured in a film by using a photographic development process [413]. The intensity and size of each stain are directly proportional to the amount of the protein of each sample [413].

After treatments, cultured cells were washed with ice-cold PBS and scraped off from the plate surface by adding 100 µl of an ice-cold homogenization buffer that contains 0.25 mM sucrose, 10 mM Tris and 1 mM ethylenediaminetetraacetic acid (EDTA), as well as commercial protease and phosphatase inhibitors (Roche Diagnostics, Basel, Switzerland). Samples were lysed by sonication during 2 pulses of 20 s at 60% amplitude with a compact ultrasonic processor (Hielscher-Ultrasound Technology, Teltow, Germany) and were centrifuged for 10 minutes at 14,000 g. Protein concentration was measured by using the Bradford protein assay (Bio-Rad, Hercules, CA, USA) according to manufacturer's instructions. Equal amounts of protein were mixed with Laemmli buffer 4x, which contains 40% glycerol, 8% 2-mercaptoethanol, 8% sodium dodecyl sulfate (SDS), 0.25 M Tris-HCl at pH 6.8 and 0.004% bromophenol blue and were heated up for 5 minutes at 100°C to ensure the correct denaturalization of the proteins.

Table 1: List of the antibodies used for protein detection by Western blot. The source, dilution, host and type of each antibody is specified in the different columns.

Antibody	Host and type	Dilution used in WB	Code	Source
p62	Rabbit, polyclonal	1:1,000	#5114	Cell signaling
LC3	Rabbit, monoclonal	1:1,000	PM036	MBL international
Beclin1	Rabbit, polyclonal	1:100	sc-11427	Santa Cruz Biotechnology
Atg5	Rabbit, monoclonal	1:1,000	#12994	Cell signaling
grp78	Rabbit, polyclonal	1:1,000	ab21685	Abcam
p-JNK (T183/Y185)	Rabbit, polyclonal	1:1,000	#9251	Cell signaling
PARP-1	Rabbit, polyclonal	1:100	sc-7150	Santa Cruz Biotechnology
Bax	Rabbit, polyclonal	1:100	sc-493	Santa Cruz Biotechnology
PINK1	Rabbit, polyclonal	1:1,000	ab23707	Abcam
Parkin	Rabbit, polyclonal	1:1,000	ab15954	Abcam
BNIP3	Mouse, monoclonal	1:200	sc-56167	Santa Cruz Biotechnology
Nix	Rabbit, monoclonal	1:1,000	ab109414	Abcam
OPA1	Rabbit, polyclonal	1:1,000	ab42364	Abcam
MFN2	Mouse, monoclonal	1:1,000	ab56889	Abcam
Fis1	Rabbit, polyclonal	1:1,000	ab71498	Abcam
HSP60	Mouse, monoclonal	1:100	sc-376240	Santa Cruz Biotechnology
HIF-1α	Rabbit, polyclonal	1:500	ab2185	Abcam
HIF-2α	Rabbit, polyclonal	1:500	ab20654	Abcam

Table 1: List of the antibodies used for protein detection by Western blot. The source, dilution, host and type of each antibody is specified in the different columns (continuation).

Antibody	Host and type	Dilution used in WB	Code	Source
p-Akt (S473)	Rabbit, monoclonal	1:1,000	#4060	Cell Signaling
p-p70S6K (T389)	Mouse, monoclonal	1:1,000	#9206	Cell Signaling
p-RP-S6 (S240/S244)	Rabbit, monoclonal	1:1,000	#5364	Cell Signaling
p-mTORC1 (S2448)	Rabbit, monoclonal	1:1,000	ab109268	Abcam
p-mTORC2 (S2481)	Mouse, monoclonal	1:100	sc-293132	Santa Cruz Biotechnology
VEGF	Rabbit, polyclonal	1:1,000	ab46154	Abcam

Denaturalized samples were loaded in a SDS-polyacrylamide gel electrophoresis (SDS-PAGE) gel and subsequently transferred to a polyvinylidene fluoride (PVDF) membrane (Bio-Rad) by using the Trans-Blot® Turbo™ Transfer System (Bio-Rad) according to the manufacturer's instructions. Then, membranes were blocked with 5% nonfat milk in PBS supplemented with Tween-20 at 0.05% (PBS-T) for 1 hour at room temperature and incubated overnight at 4°C with the primary antibodies listed in Table 1. Mouse monoclonal β -actin antibody (1:50,000; A3854, Sigma-Aldrich) conjugated with horseradish peroxidase (HRP) was used as loading control. After washing three times with PBS-T, membranes were incubated with the anti-rabbit (1:20,000; 31460, Thermo Fisher Scientific) or the anti-mouse (1:5,000; P0260, Dako, Glostrup, Denmark) secondary antibodies for 1 hour at room temperature. Proteins were visualized by using Pierce enhanced chemiluminescence (ECL) Western blot substrate (Thermo Fisher Scientific). The density of each band was measured with ImageJ software (National Institute of Mental Health, Bethesda, MD, USA).

5. Determination of nucleic acid levels.

5.1. Reverse transcription quantitative polymerase chain reaction (RT-qPCR).

RT-qPCR allows the comparison of mRNA levels among the different samples to identify patterns of gene expression [414]. This procedure starts with the isolation of the cellular RNA from the whole cell lysate and with the elimination of the residual genomic DNA with the deoxyribonuclease I (DNase I) [414]. Subsequently, RNA template is reverse transcribed to form its complementary DNA (cDNA), which are going to be amplified in a PCR reaction [414]. The addition of a fluorescent probe during the exponential phase of this reaction permits the absolute or relative quantification of the mRNA content in each sample [414]. This probe can be a fluorescent dye that only associates with double-stranded DNA molecules, such as SYBR green, or some type of special primers that will emit fluorescence when they are being utilized as a template for DNA replication, such as TaqMan™ probes [414].

Hep3B and HepG2 cells were seeded in 6-well culture plates at a density of $2.5 \cdot 10^5$ cells/well. After treatments, cells were scraped off from the plate and total RNA was isolated by using TRIzol® Reagent (Applied Biosystems, Carlsbad, CA, USA) according to the manufacturer's instructions. Isolated RNA was quantified by spectrophotometry by using Nanodrop 1000 (Thermo Fisher Scientific) and residual DNA was eliminated with RQ1 RNase-free DNase kit (Promega, Madison, WI, USA). Equal amounts of RNA were subjected to retrotranscription by using the High Capacity cDNA reverse transcription kit (Applied Biosystems). The RT-qPCR analysis was performed utilizing SYBR Green Master Mix (Invitrogen) with the primers listed in Table 2. β -actin was used as an endogenous control. Otherwise, RT-qPCR for Atg5 and HIF-1 α genes were performed utilizing FastStart TaqMan™ Probe Master (Roche Diagnostics GmbH, Mannheim, Germany). TaqMan™ probes and primers for *HIF1A* gene (NM_001243084.1 and Hs00153153_m1) and *ATG5* (NM_001286106.1 and Hs00169468_m1) were derived from commercially available ones (Thermo Fisher Scientific). *GADPH* gene probe (NM_002046.3 and 4326317E) was used as the endogenous control. Relative changes in gene expression levels were detected by the $2^{-\Delta\Delta CT}$ method [415].

Table 2: List of primers used for SYBR green RT-qPCR.

Gen	Forward primer (5'→3')	Reverse primer (5'→3')
Beclin1	AGGTTGAGAAAGGCGAGACA	AATTGTGAGGACACCCAAGC
Atg3	CTGGCGGTGAAGATGCTATT	GTGGCAGATGAGGGTGATTT
LC3	CCACACCCAAAGTCCTCACT	CACTGCTGCTTTCCGTAACA
β-actin	TTGCCGACAGGATGCAGAA	GCCGATCCACACGGAGTACT

5.2. Mitochondrial DNA content.

The analysis of the variations of mitochondrial DNA (mtDNA) content with respect to nuclear DNA (ncDNA) levels by quantitative polymerase chain reaction (qPCR) allows the detection of both mitochondria dysfunction and their clearance by mitophagy [416]. The main advantage of this assay is that permits the direct monitoring of mtDNA levels from total DNA lysate, without the previous requirement of purifying mitochondria from cells [416].

After treatments, total DNA was isolated from Hep3B cell lysate with 250 µl of 25:24:1 phenol:chloroform:isoamyl alcohol (Sigma-Aldrich) and was subsequently precipitated with absolute ethanol (Merck Millipore, Burlington, MA, USA) in presence of sodium acetate 0.3 M (Merck Millipore). DNA concentration was measured by spectrophotometry with Nanodrop 1000 (Thermo Fisher Scientific). The qPCR analysis was performed utilizing SYBR Green Master Mix (Invitrogen) with the primers enumerated in Table 3. Relative changes in mitochondrial DNA content were also detected by the $2^{-\Delta\Delta CT}$ method [415].

Table 3: List of primers used to analyze changes in mitochondrial DNA content by SYBR green qPCR.

Gen	GenBank code	Forward primer (5'→3')	Reverse primer (5'→3')
mtDNA	NC_012920	CTAAATAGCCCACACGTTCCC	AGAGCTCCCCTGAGT GGTTA
ncDNA	NT_010194.17	GCTGGGTAGCTCTAAACAATGT ATTCA	CCATGTACTAACAAA TGTCTAAAATGGT

6. Determination of mitochondrial damage.

Two different experimental techniques were performed to analyze mitochondrial status, the measurement of ROS production in this organelle by using 2',7'-dichlorodihydrofluorescein diacetate (DCF-DA) and the analysis of the integrity of their membrane potential by using 5,5',6,6'-tetrachloro-1,1',3,3'-tetraethylbenzimidazolylcarbocyanine iodide (JC-1).

6.1. ROS measurement.

The most sensitive techniques for the measurement of mitochondrial production of ROS and RNS in live cells involve the use of fluorescent probes that only emit fluorescence when these harmful species are generated [417]. DCF-DA is the most used fluorescent indicator of ROS generation since it only emits fluorescence when it is oxidized by these free radicals [417]. This emission can be monitored by confocal immunofluorescence microscopy or by a fluorescence reader [417].

Hep3B cells were plated in 96-well plates at a density of 5,000 cells/well and were treated with CoCl₂, sorafenib and/or melatonin. Right after treatment, cells were incubated with 20 μM DCF-DA (Sigma-Aldrich) and 15 mM Hepes (Sigma-Aldrich), which was added to buffer disturbances in cellular pH. Fluorescence was immediately measured in a microplate fluorescence reader (BioTek Instruments Inc.) at 1, 3 and 6 h by using 485 nm and 520 nm as excitation and emission wavelengths respectively. 5 mM of N-acetyl cysteine (NAC) (Sigma-Aldrich) was added as a ROS quencher, while hydrogen peroxidase (H₂O₂) (Merck Millipore) was used as a positive control of ROS generation.

6.2. JC-1 staining assay.

The lipophilic and cationic dye JC-1 is broadly used for the assessment of disruptions in mitochondria membrane potential [418]. This colorant accumulates in the lumen of non-damaged mitochondria due to their higher membrane potential, generating aggregates with intense red fluorescent [418]. However, this molecule is unable to form these complexes in depolarized mitochondria, remaining in its green fluorescent monomeric form [418].

To perform this experiment, Hep3B cells were seeded in 24-well plates at a density of $6 \cdot 10^4$ cells/well and were treated with sorafenib and/or melatonin for 1, 3 and 6 h. After these periods, they were stained with JC-1 (Mitochondrial membrane potential assay kit, Cayman Chemical, Ann Arbor, MI, USA) dissolved in fresh medium for 20 minutes following the manufacturer's recommendations. Fluorescence was measured in a microplate fluorescence reader (BioTek Instruments Inc.) using 550/600 nm and 485/535 nm of excitation/emission wavelengths to respectively detect red and green fluorescence. Results are shown as the ratio of red to green fluorescence since the value of this quotient is directly proportional to the number of mitochondria that have not undergone any alterations in their membrane potential. Fluorescence microscopy was performed as a positive control in parallel with microplate reading to validate the results of this procedure.

7. Immunofluorescence and laser confocal imaging.

Immunofluorescence procedures are widely used for the analysis of the different steps of the autophagy pathway, such as the autophagosome formation, the selective engulfment of the mitochondria and the lysosome fusion with the autophagy vesicle [247]. Therefore, these techniques are progressively displacing the use of electron microscopy assays since they are easier, faster and more widely accessible [247]. In this dissertation, two different confocal microscopy procedures are going to be performed for the analysis of autophagy and mitophagy, LAMP2/Tom20 colocalization and acridine orange staining.

7.1. Acridine orange staining assay.

Acridine orange is a membrane-permeable metachromatic fluorochrome that can shift from green to red fluorescence according to the concentration stored in the different cellular organelles [419]. Besides, this dye also presents acidotropic properties, inducing its aggregation in the vesicles at low pH, such as autophagolysosomes and lysosomes [419]. This accumulation ultimately leads to staining autophagy-derived acidic vacuoles in red, whereas the rest of the cytoplasm remains green-colored [419]. Therefore, this assay provides a quick and reliable method to measure the amount and size of

autophagolysosomes, as well as to monitor autophagy flux through calculating the red-to-green fluorescence intensity ratio (R/GFIR) [419].

HepG2 cells were plated in 24-well plate at a density of 10,000 cells/well and were treated with 1 mM melatonin for 4, 8, 12, 24 and 48 h. After these periods, treatment media was discarded and plates were washed twice with PBS (Sigma-Aldrich). Subsequently, cells were incubated with 5 $\mu\text{g/ml}$ of acridine orange (Sigma-Aldrich) for 15 minutes at room temperature under dark conditions. Then, the excess stain was discarded by washing the cells twice with PBS and samples were air-dried. Briefly, they were visualized in a Leica SPE confocal laser scanning microscope (Leica Microsystems, Wetzlar, Germany). Red and green dot areas were quantified with ImageJ software (National Institute of Mental Health) and R/GFIR was calculated by dividing the red and the green stained areas.

7.2. LAMP2 and Tom20 colocalization.

The analysis of the colocalization between the late lysosomal marker LAMP2 and the mitochondrial marker Tom20 permits the visualization of the number of mitochondria that are delivered to the lysosomes [420]. The quantification of the degree of colocalization between these two markers supplies a numeric index that could be used to compare the degree of mitophagy among the different samples time-dependently [420].

To perform this experimental technique, Hep3B cells were seeded on 24-well plates with glass coverslips at a density of $1 \cdot 10^4$ cells/well and were treated with the indicated concentrations of CoCl_2 , sorafenib and/or melatonin for 6, 12 and 24 h. Subsequently, cells were fixed with 4% paraformaldehyde (Thermo Fisher Scientific) for 15 min, washed twice with PBS, as well as permeabilized with 0.2% saponin (Sigma-Aldrich) and 1% fatty-acid-free bovine serum albumin (FFA-BSA) (Sigma-Aldrich) in PBS for 15 min at room temperature. Then, cells were washed twice with PBS and incubated overnight at 4°C with a mouse monoclonal anti-LAMP2 [H4B4] antibody (ab25631, Abcam), and a rabbit polyclonal Tom20 (FL-145) antibody (sc-11415, Santa Cruz Biotechnology) diluted both 1:300 in PBS with 1% FFA-BSA. After washing twice with PBS, cells were stained for 1 hour at room temperature with Alexa-488-conjugated secondary anti-mouse (1:1,000, Z25002, Molecular Probes, Eugene, OR, USA) and Alexa-647-conjugated secondary anti-rabbit (1:500, Z25308, Molecular Probes) IgG antibodies. Afterward, coverslips were

washed twice with PBS and mounted on glass slides using the Fluoroshield™ medium with DAPI (Sigma-Aldrich). Briefly, they were visualized in a Zeiss LSM 800 confocal laser scanning microscope (Zeiss AG, Jena, Germany) and samples were analyzed with ZEN software (Zeiss AG). The Colocalization Colormap plugin (Polish Academic of Science, Warsaw, Poland) of ImageJ software (National Institute of Mental Health) was used to determinate the degree of overlapping between the two fluorophores in each sample.

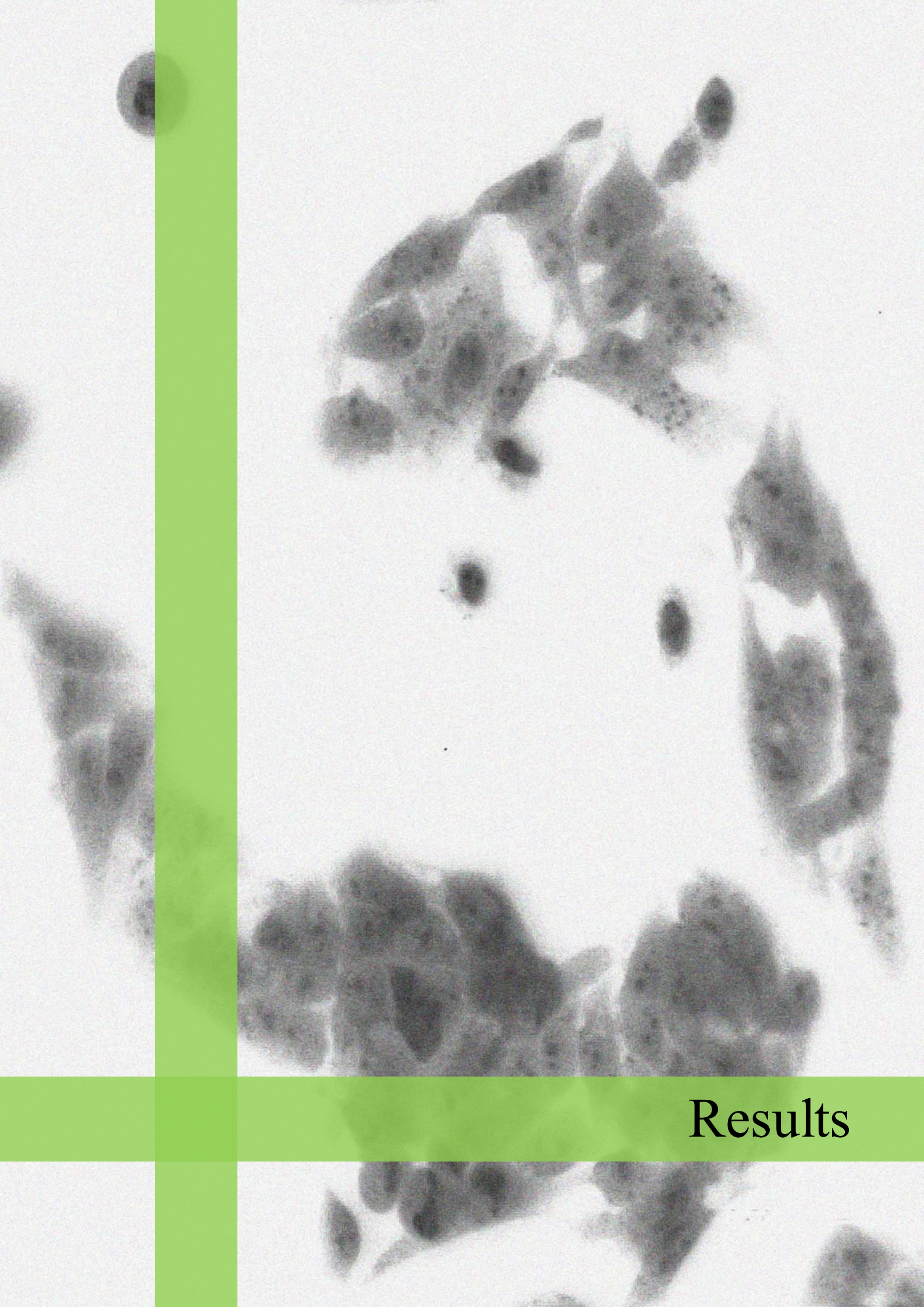
8. Gene silencing.

siRNAs are widely used in biomedical research due to its ability to induce a potent post-transcriptional restraint in the expression of a specific gene, mimicking a loss-of-function mutation [421,422]. This process is mediated by the proteins Argonaute 2 (AGO2) and RNA-induced silencing complex (RISC), which bind, unroll and separate the two siRNA strands to form a complex that is able to recognize and cleave a mRNA, blocking its translation by the ribosome [421]. Otherwise, siRNA transfection protocol usually incorporates a delivery agent, such as lipofectamine or oligofectamine, that facilitates its crossing through the plasmatic membrane [422]. Double-stranded siRNA vectors are able to inhibit gene expression in a faster and more convenient way than single-stranded interference RNA (RNAi) vectors since they are less recognized by the endogenous machinery that degrades RNA [421,422].

Commercial siRNAs against HIF-1 α (sc-35561), BNIP3 (sc-37451), Parkin (sc-42158), Atg5 (sc-41445) and control siRNA encoding a non-targeting sequence (sc-37007), which were purchased from Santa Cruz Biotechnology, were introduced into Hep3B and HepG2 cells by using Lipofectamine® RNAiMAX reagent (Thermo Fisher Scientific) according to manufacturer's instructions. 5 h after transfection, cell media were replaced by fresh complete DMEM. 16 h after this procedure, cells were treated with CoCl₂, sorafenib and melatonin and were subjected to MTT and western blot assays to determinate their viability and their protein expression levels.

9. Statistical analysis.

Results were expressed as mean values \pm standard deviation (SD) of at least three different experiments. Results were analyzed using the statistical package GraphPad Prism 6 (GraphPad Software, San Diego, CA, USA). Kolmogorov-Smirnov test was used to check the normality of data, whereas one-way analysis of variance (ANOVA) followed by Bonferroni post-hoc test was used to determinate significant differences among the mean values of the different treated groups, considering $p < 0.05$ as significant.



Results

1. Effect of melatonin on autophagy response in HCC cells.

1.1. Melatonin stimulates a transient and complete autophagy response in HCC cells.

We have previously reported that melatonin can reduce the viability of the HCC tumor cells in both *in vivo* and *in vitro* models [407,408]. Nevertheless, only the role that performs the apoptotic pathway on this inhibitory process has been analyzed, omitting the potential function that exerts other PCD types, such as autophagy. Therefore, the analysis of the melatonin ability to modulate this pathway could be interesting to improve its use in HCC therapy.

Firstly, the potential modifications induced by melatonin on autophagy basal levels were studied by analyzing the variations observed in the expression of some specific markers of this pathway. As shown in Fig. 20A, 1 mM melatonin increased gradually LC3 lipidation over time until reaching to a maximum between 8 and 12 h, decreasing progressively until 24 h after melatonin treatment. This process was associated with the increase observed in the accumulation of p62 in the autophagosomes until 8 h after the start of the experiment, decreasing thereafter (Fig. 20A). Subsequently, RT-qPCR assay was performed to complement the information obtained through the Western blot assay. As it is shown in Fig. 20B, 1 mM melatonin administration augmented gradually the levels of Beclin1 and LC3 mRNAs over time, peaking respectively at 8 and 12 h after the onset of the experiment. Then, the levels of the two mRNAs progressively decreased until 24 h after the administration of this indoleamine, being this effect more sharply in Beclin1 than in LC3 (Fig. 20B). Otherwise, Atg3 mRNA levels only increased significantly after 8 h of melatonin administration, undergoing non-significant variations regarding to control levels in the other experimental groups. These data indicate that melatonin is able to initiate the formation of autophagosomes in HepG2 cells.

However, the changes in the expression showed in these markers after melatonin administration does not asseverate that this molecule can induce the degradation of the autophagosomal content [247]. Indeed, this effect could be associated with the accumulation of defective autophagosomes that are unable to associate to the lysosomes [247]. Therefore, an autophagy flux assay was performed to discern between these two possible situations by adding chloroquine (50 μ M) or Baf A1 (100 nM) to melatonin-treated HepG2 cells [247]. These compounds evaluate the integrity of the autophagy flux

by blocking the endosomal acidification, which prevents the degradation of autophagosomal content by avoiding the fusion between autophagosomes and lysosomes [423]. Melatonin-induced LC3-II protein levels at 8 h after melatonin treatment, being this effect enhanced after either CQ or Baf A1 addition (Fig. 20C). Conversely, the lipidation of this protein was also stimulated after the treatment of control cells with either CQ or Baf A1 (Fig. 20C). Therefore, melatonin not only induced the onset of autophagy, but it also triggers the degradation of autophagosomal content.

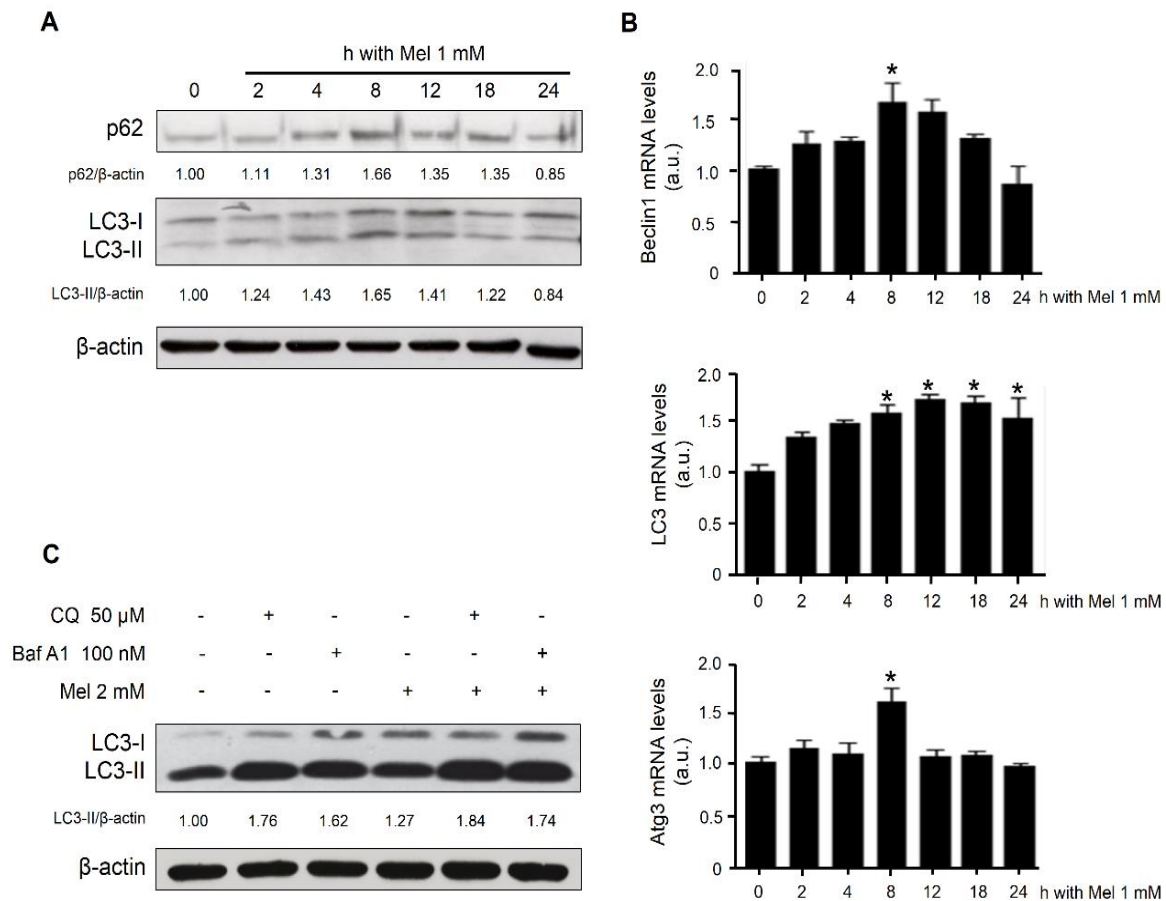


Figure 20 Effects of melatonin administration on the expression of different autophagy markers and on the autophagic flux in HepG2 cells. **(A)** p62 and LC3-I/II levels were analyzed by Western blot at 2, 4, 8, 12, 18 and 24 h after 1 mM melatonin (Mel) administration. Immunoblots were quantified by using ImageJ software and the results were expressed as band density/ β -actin density vs control group (0 h). **(B)** Beclin1, LC3 and Atg3 mRNA levels were analyzed by RT-qPCR assay using the same conditions as Western blot technique. Data were expressed as mean values of arbitrary units (a.u.) \pm SD of three different experiments. * p <0.05 vs control (0 h). **(C)** The effects of 2 mM melatonin administration for 8 h on autophagy flux was measured by adding either chloroquine 50 μ M (CQ) or bafilomycin A1 100 nM (Baf A1) 4 h before the end of the treatment. LC3 representative immunoblot was quantified by using ImageJ software and the results were expressed as band density/ β -actin density vs control group (0 h).

Furthermore, the metachromatic dye acridine orange was used to confirm the induction of autophagosome formation and autophagy flux in response to melatonin administration. This colorant stains acidic vesicles in red, remaining the cell cytoplasm in green color since it is slightly basic. As shown in Fig. 21, melatonin treatment increased significantly the extent of red-colored areas and the R/GFIR ratio until 12 h, diminishing progressively at 24 and 48 h after 1 mM melatonin administration. Besides, some apoptotic morphologic features, such as cell shrinkage, were displayed in the cells treated for 48 h with this molecule (Fig. 21). Therefore, these data support that melatonin induces an early, transient and complete autophagy response in HepG2 cells.

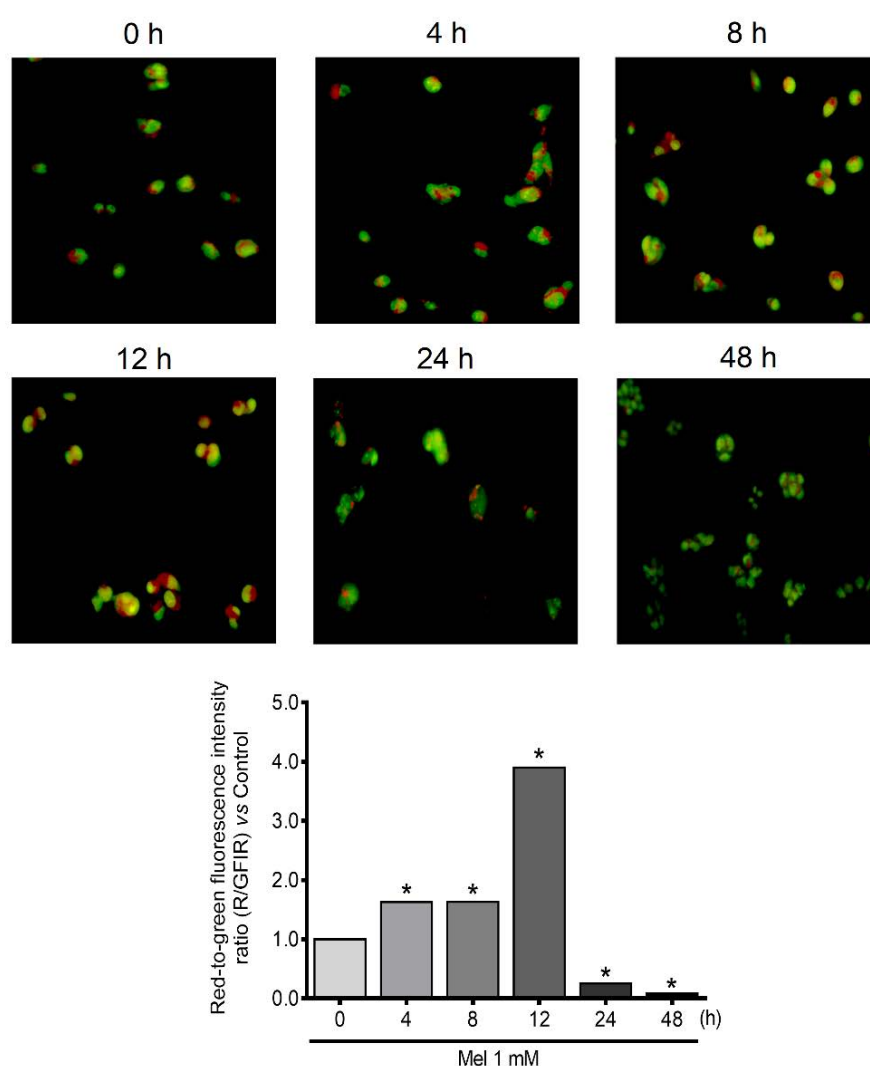


Figure 21: Effect of melatonin administration on autophagosome formation in HepG2 cells measured by acridine orange assay. Representative confocal images show the results of this technique after 4, 8, 12, 24 and 48 h of 1 mM melatonin (Mel) treatment. Red and green dot areas were measured by using ImageJ software, and the data were expressed as the R/GFIR vs control (0 h) of the representative confocal images. * $p < 0.05$ vs control (0 h).

1.2. Melatonin induction of autophagy is dependent on the JNK pathway, but not on mTORC1 inhibition.

Multiple transduction cell pathways can modify the basal levels of autophagy in response to internal or external stimuli, such as MAPK or PI3K/Akt/mTORC1 pathways [258]. For this reason, we first decided to identify the cellular mechanism that is responsible for the induction of autophagy in response to melatonin treatment, evaluating the mTORC1 pathway. Indeed, this intermediate is the main repressor of autophagy in response to growth factors and hormone signaling [260,261]. 2 mM Melatonin failed to decrease mTORC1 phosphorylation both at long and short time periods, even leading to its activation from 2 to 8 h (Figs. 22A and 22B). Moreover, this process was concomitant with the increase of Beclin1 expression (Figs. 22A and 22B). On the other hand, mTORC1 phosphorylation and Beclin1 levels dropped sharply at 18 and 24 h after the beginning of the experiment (Figs. 22A and 22B). These data suggest that mTORC1 is probably not implied in the induction of autophagy by melatonin.

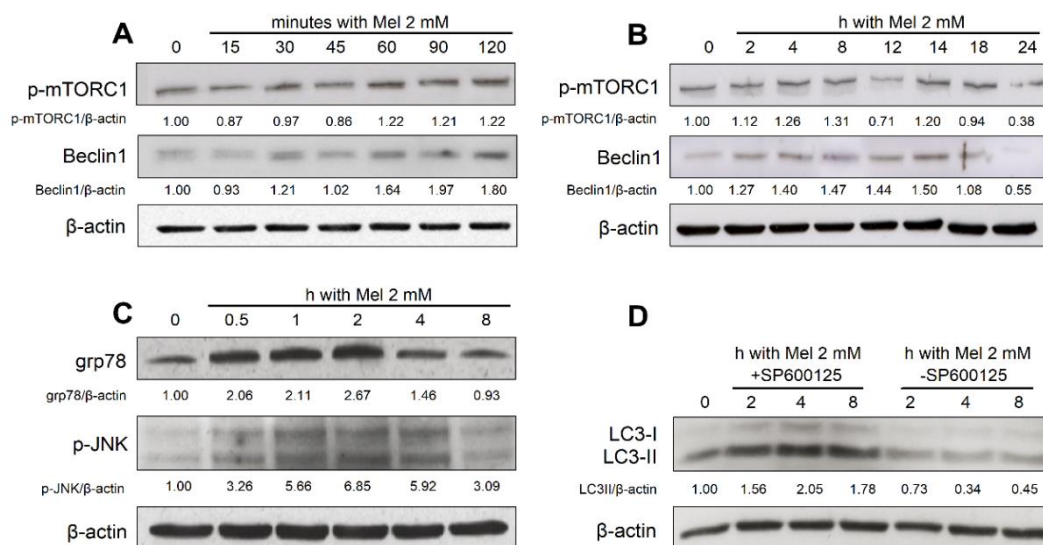


Figure 22: Effects of melatonin on the principal inductors of the autophagy pathway. **(A)** mTORC1 and Beclin1 proteins levels were analyzed by Western blot technique at short time periods (until 120 minutes) after 2 mM melatonin (Mel) treatment. **(B)** The levels of these two proteins were also evaluated at long time periods (from 2 to 24 h) after the administration of this indoleamine. **(C)** grp78 and p-JNK protein levels were analyzed by Western blot assay from 0.5 to 8 h of 2 mM melatonin treatment. **(D)** The JNK phosphorylation repressor SP600125 (10 μ M) was added 1 h prior to the administration of 2 mM melatonin and cells were collected after 2, 4 and 8 h of treatment. LC3 protein levels were measured by Western blot. Representative immunoblots were quantified by using ImageJ software and the results were expressed as band density/ β -actin density vs control group (0 h).

Otherwise, MAPK/JNK has been claimed to induce autophagy in many stressful situations, such as ER stress or oxygen deprivation [271]. Therefore, we analyzed if melatonin could induce mitophagy by stimulating UPR and enhancing JNK signaling. As shown in Fig. 22C, grp78 levels were enhanced from 1 to 4 h after 2 mM melatonin administration. Besides, this situation was clearly associated with a concomitant augment in JNK phosphorylation, which suggests that melatonin could induce autophagy response through the activation this MAPK (Fig. 22C). In order to asseverate this capability, the specific JNK phosphorylation inhibitor SP600125 was added at a concentration of 10 μ M, 1 h before melatonin administration. As shown in Fig. 22D, this repressor prevented melatonin-dependent lipidation of LC3, suggesting that this molecule can enhance autophagy in HCC cells through inducing the UPR system and the JNK pathway.

1.3. Melatonin-induced autophagy response exerts a prosurvival behavior in HCC cells.

Autophagy could exert a dual role in tumor cells since it can either promote or restrain tumorigenesis in the different cell phases of cancer progression [287,289]. Indeed, this cellular response acts as a tumor suppressor mechanism at the onset of cancer, whereas it prevents cell death at later phases of tumor progression [287,289]. Additionally, autophagy response has been reported to be able to increase the resistance to chemotherapy and radiotherapy in later steps of tumorigenesis [287], thus the prevention of the induction of this cellular response could be a useful strategy to increase the sensitiveness to these antitumor agents. In our experiments, Atg5 translation was restrained with a commercial siRNA. As shown in Fig. 23, Atg5 mRNA transcription and protein levels were clearly abolished after 24 and 48 h of gene silencing, demonstrating that this technique presents great efficiency in the inhibition of Atg5 gene expression. Besides, Atg5 silencing suppressed autophagy levels at 24 h through reducing LC3-II expression and p62 degradation both in non-treated and in 2 mM melatonin-treated cells (Fig. 23B). These data endorse the use of this siRNA to evaluate changes in autophagy response in HCC cells.

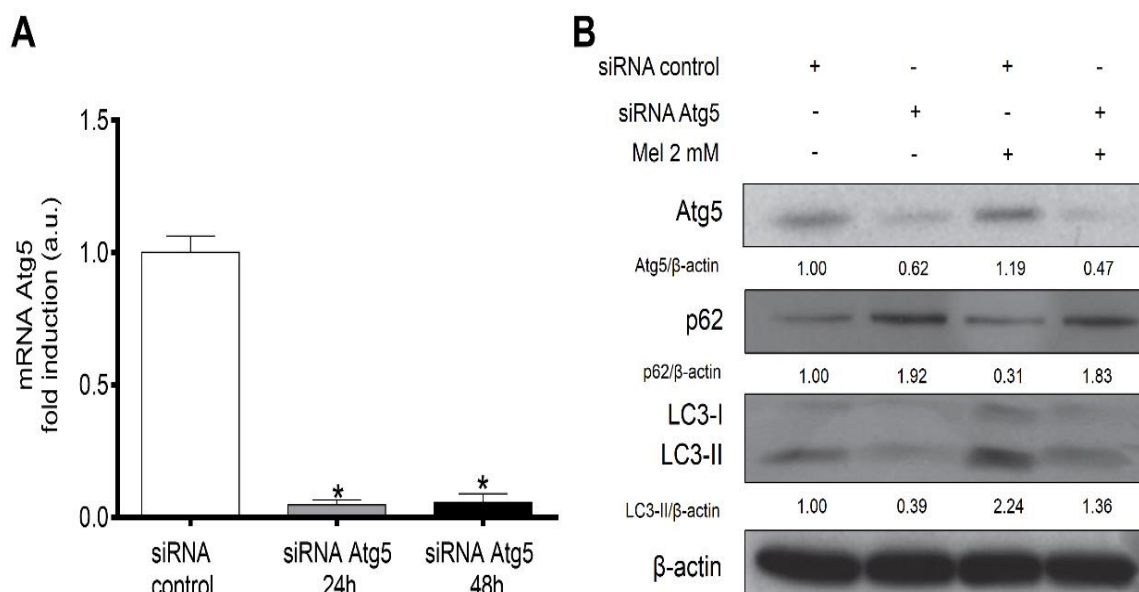


Figure 23: Effect of Atg5 silencing on melatonin-induced autophagy. **(A)** The efficiency of Atg5 silencing was measured by RT-qPCR of this gene at 24 and 48 h after cell silencing. Data were expressed as a percentage of mean values of arbitrary units (a.u.) \pm SD of three different experiments. * $p < 0.05$ vs non-silenced cells (siRNA control group). **(B)** Atg5, p62 and LC3 protein levels were measured by Western blot technique after 24 h of Atg5 silencing and/or 8 h of 2 mM melatonin (Mel) treatment. Representative immunoblots were quantified by using ImageJ software and the results were expressed as band density/ β -actin density vs non-silenced and non-treated cells (siRNA control group).

Subsequently, the effect of melatonin-induced autophagy on the viability of HepG2 cells was assessed. As shown in Fig. 24A, the inhibition of this cellular response in 1 mM melatonin-treated cells for 48 h induced slightly, but non-significantly, the cytotoxic effect of this hormone. Otherwise, this trend became significant when Atg5-silenced HepG2 cells were treated with higher doses of this hormone for the same time span (Fig. 24A). The reduction in cell viability showed after the silencing of Atg5 was accompanied with an increment in the processing of PARP, which is a caspase 3 target that is cleaved after apoptosis induction [364], at 24, 36 and 48 h after the start of the experiment (Fig. 24B). Summarizing, it seems that autophagy is induced in HepG2 cells in response to melatonin treatment in order to partly restrain the antiproliferative effects of this indoleamine.

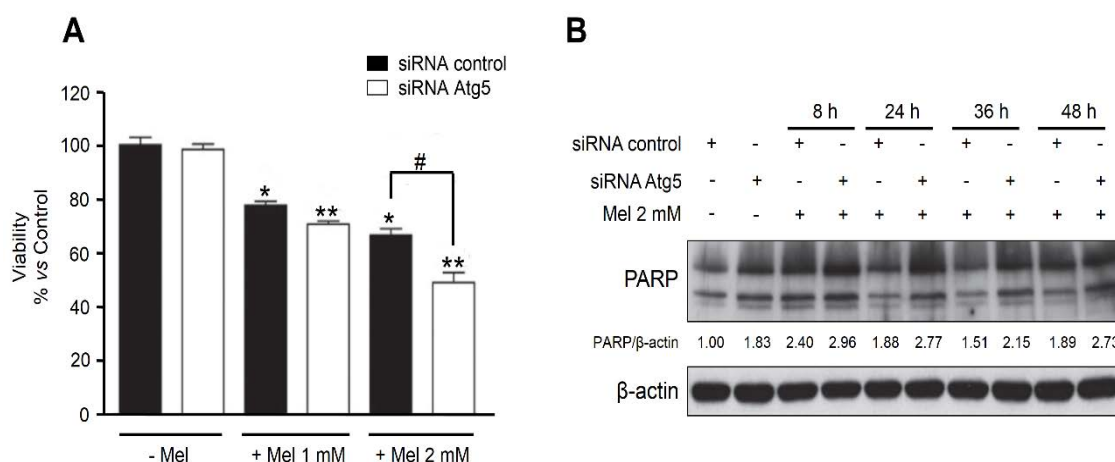


Figure 24: Effects of Atg5 silencing on melatonin-induced HCC cell death. **(A)** HepG2 cells were incubated with either 1 or 2 mM of melatonin (Mel) during 48 h in presence or absence of the specific siRNA against Atg5. Viability was analyzed by MTT. Data were expressed as a percentage of the mean value \pm SD of three different experiments. * $p < 0.05$ vs non-treated and non-silenced cells, ** $p < 0.05$ vs non-treated and silenced cells, # $p < 0.05$ between non-silenced and silenced cells treated with the same melatonin concentration. **(B)** The effect of *Atg5* gene silencing on PARP cleavage was measured by Western blot technique after 8, 24, 36 and 48 h of 2 mM melatonin treatment. Representative immunoblots were quantified by using ImageJ software and the results were expressed as band density/ β -actin density vs non-silenced and non-treated cells.

2. Modulation of HCC cell sensitivity to sorafenib by melatonin under normoxia.

2.1. Melatonin enhances sorafenib cytotoxicity in HCC cells under normoxia.

Although sorafenib exerts antitumoral effects in advanced HCC tumors [78,79], sustained treatments with this molecule have been reported to be ineffective due to the appearance of resistant cells that are insensitive to this chemotherapeutic drug [108]. Melatonin prevents cancer cell proliferation by inducing apoptosis, arresting cell cycle progression and preventing angiogenesis and metastasis [16,17,407]. Moreover, it has been showed that this indoleamine can sensitize tumor cells to some chemotherapeutic drugs, such as doxorubicin or clofarabine, by enhancing the cytotoxic effect of these molecules [404,405]. Accordingly, we decided to analyze if this indoleamine could overcome cellular resistance to sorafenib by potentiating the oncostatic effects of this drug in an HCC *in vitro* model.

Firstly, MTT assay was performed to evaluate the variations in cell viability that exert single treatment with melatonin or sorafenib for 48 h in three different HCC cell lines, HepG2, Huh7 and Hep3B. These established HCC cell lines are genetically heterogeneous, which signifies that they probably present different sensitivity to drug administration [105]. As shown in Fig. 25, the pharmacological concentration of melatonin (1 mM) reduced significantly the viability of HepG2 and Huh7 cells but failed to induce this phenotype in Hep3B cells. Indeed, this cell line was only sensitive to the highest concentration of this indoleamine (2 mM) (Fig. 25). On the other hand, nanomolar doses of sorafenib did not affect to the viability of any of the three HCC cell lines tested (Fig. 25). However, higher doses of sorafenib (from 1 to 50 μ M) induced a significant reduction in the viability of HepG2 and Huh7, but not in Hep3B cells (Fig. 25). Similar to melatonin, only the highest concentration of sorafenib was lethal for Hep3B cells (Fig. 25). Therefore, these data suggest that Hep3B cells have an innate resistance to either melatonin or sorafenib treatment, whereas HepG2 and Huh7 cells are more sensitive to these compounds.

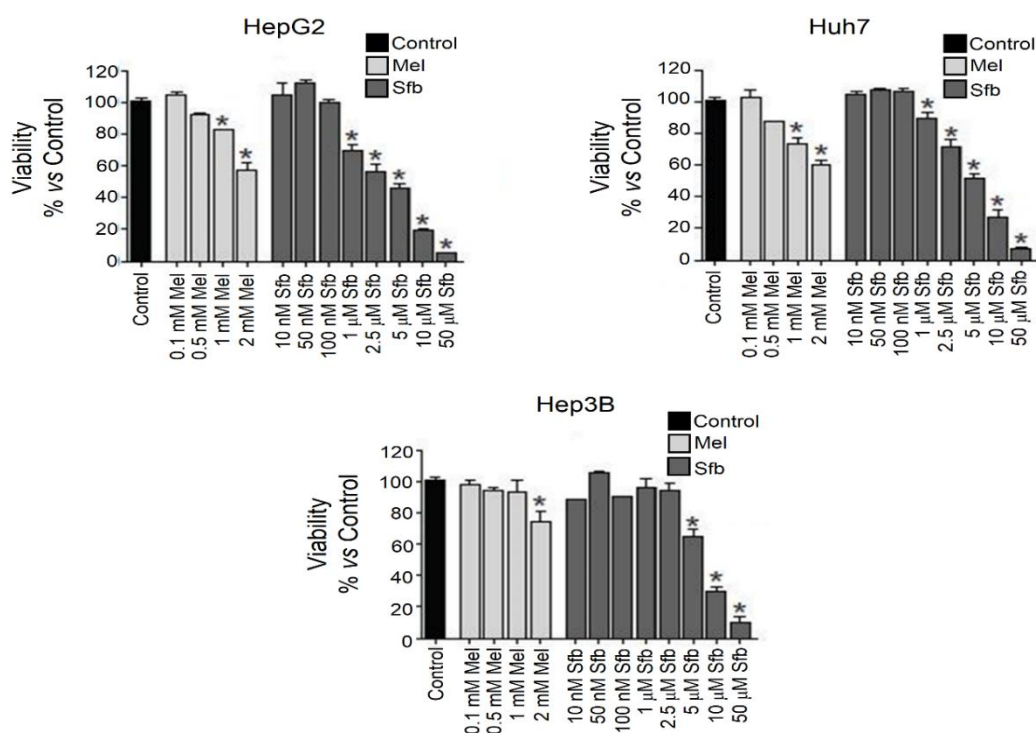


Figure 25: Effects of either melatonin or sorafenib single treatment on the viability of three different HCC cell lines. Variations in HepG2, Hep3B and Huh7 cell death were analyzed by using MTT assay after 48 h of melatonin (Mel) (0.1, 0.5, 1 or 2 mM) or sorafenib (Sfb) (0.01, 0.05, 0.1, 1, 2.5, 5, 10 and 50 μ M) treatment. Data were expressed as a percentage of the mean value \pm SD of three different experiments. *p<0.05 vs Control group.

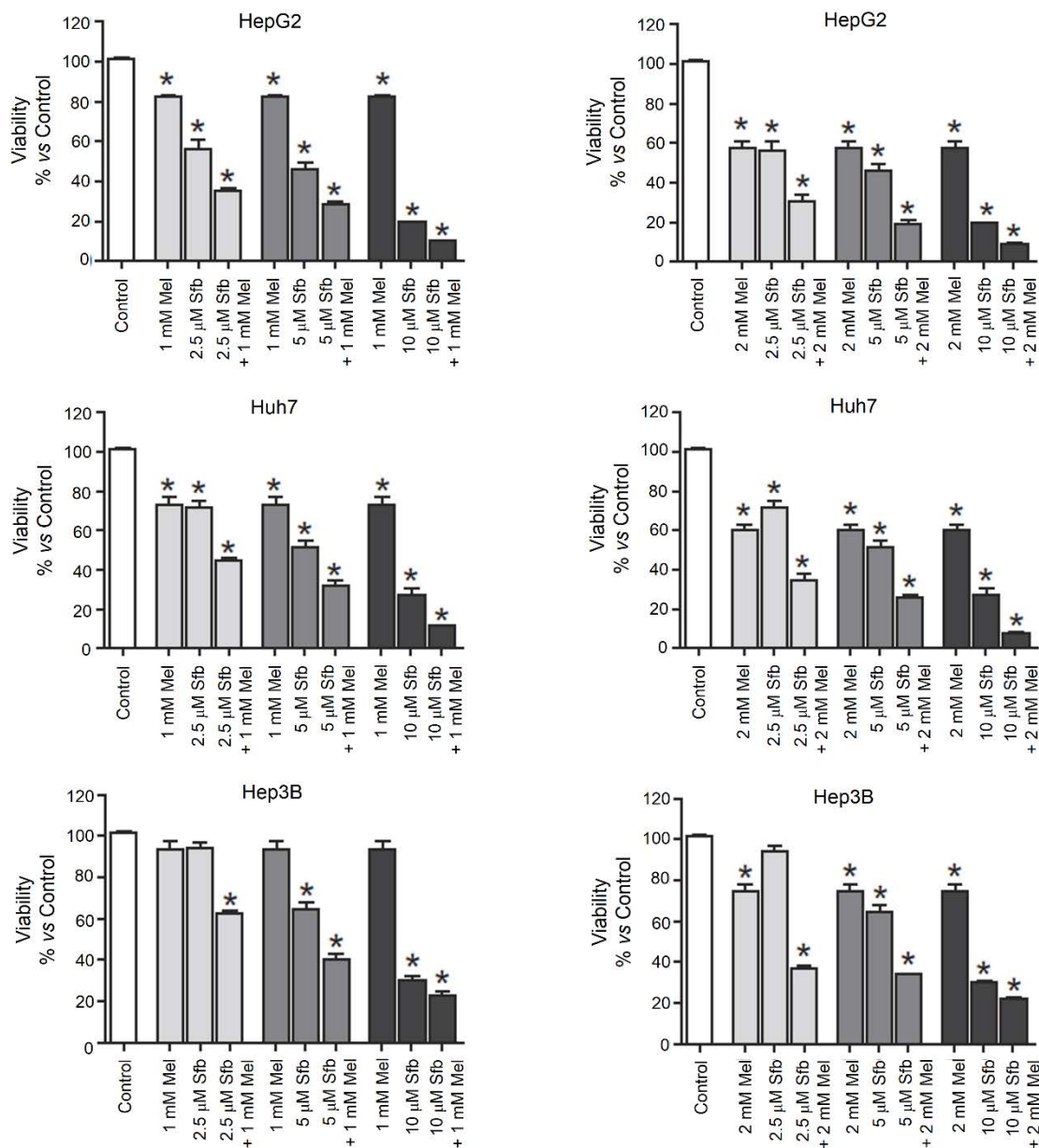


Figure 26: Effects of melatonin and sorafenib combined treatment on the viability of three different HCC cell lines. Variations in HepG2, Hep3B and Huh7 cell death were analyzed by using MTT assay after 48 h of melatonin (Mel) (1 or 2 mM), sorafenib (Sfb) (2.5, 5, 10 µM) or melatonin plus sorafenib treatment. Data were expressed as a percentage of the mean value \pm SD of three different experiments vs control. * $p < 0.05$ vs Control group.

Subsequently, 1 mM and 2 mM of melatonin and 2.5, 5 and 10 µM of sorafenib were coadministered to the three HCC cell lines to analyze cell death in normoxia. As shown in Fig. 26, both concentrations of melatonin stimulated sorafenib ability to reduce the viability of the three HCC cell lines. Moreover, combined treatment was able to diminish Hep3B innate resistance to this chemotherapeutic drug, since it decreased significantly their viability at doses in which sorafenib administration alone did not exert

any effect (Fig. 26). Due to the promising results obtained in this HCC cell line, it was used to carry out the next experiments in normoxia with 2.5 μ M and 1 mM doses of sorafenib and melatonin respectively. These concentrations did not present any deleterious effects when used alone, but it induced significantly Hep3B cell death when combined (Fig. 26).

2.2. Sorafenib and melatonin coadministration induces apoptotic response in Hep3B cells.

It has been previously reported that melatonin presents a clear proapoptotic role in HCC cells since this molecule is able to enhance both the intrinsic and the extrinsic pathways [407,408]. Therefore, the induction of the intrinsic apoptosis pathway by melatonin could be partly responsible for sensitizing Hep3B cells to sorafenib. 2.5 μ M sorafenib administration neither induced PARP cleavage nor stimulated Bax expression in Hep3B cells (Fig. 27A). However, 1 mM melatonin and 2.5 μ M sorafenib cotreatment stimulated PARP cleavage and Bax expression after 24 and 48 h of treatment (Fig. 27A). On the other hand, annexin V-PI assay was used to measure apoptosis and cell death after single or combined treatments. As shown in Fig. 27B and 27C, annexin V-positive, PI-positive cell fraction only increased significantly after melatonin and sorafenib coadministration, but not after the single treatments. These data are similar to those obtained in the MTT assay (Fig. 26). These results suggest that melatonin induces intrinsic apoptosis in sorafenib-treated cells.

2.3. Sorafenib and melatonin coadministration induces mitochondrial turnover through mitophagy in Hep3B cells.

Mitochondrial homeostasis is fundamental to maintain cell metabolism and survival due to the ability of these organelles to limit ROS release and apoptotic cell death [347]. Mitophagy is the main mechanism implicated in managing the integrity of these organelles due to its ability to degrade damaged or useless mitochondria [347]. Indeed, the modification of mitophagy basal levels during the earlier stages of tumorigenesis has been related with the promotion of cancer progression and aggressiveness [347]. Therefore, the restoration of mitophagy responses in cancer cells for treatment purposes could be useful to restrain cancer growth and progression.

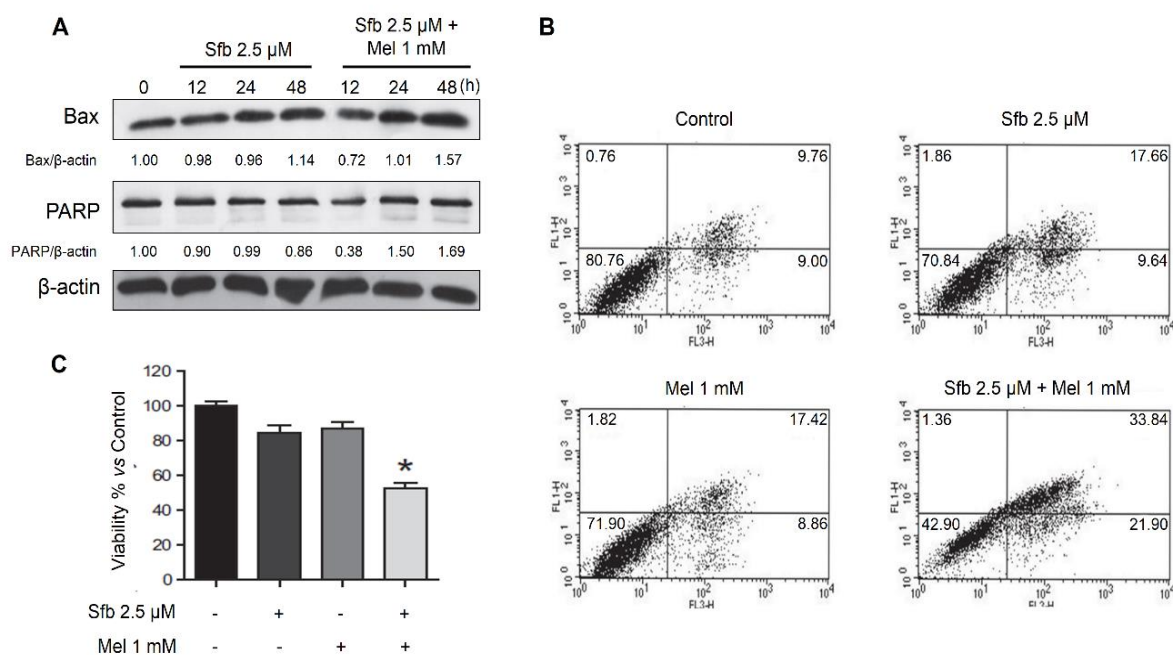


Figure 27: Effects of melatonin and sorafenib combined treatment on apoptotic cell death in Hep3B cells. **(A)** PARP and Bax protein levels were measured by Western blot assay after 12, 24 and 48 h of 2.5 μ M sorafenib (Sfb) treatment alone or in combination with 1 mM melatonin (Mel). Representative immunoblots were quantified by using ImageJ software and the results were expressed as band density/ β -actin density vs control cells (0 h group). **(B)** Flow cytometric analysis of cell viability was performed with a commercial Annexin V-IP kit at 48 h after 2.5 μ M sorafenib and/or 1 mM melatonin administration. **(C)** Annexin V-negative, PI-negative cells are represented as a percentage of the mean value \pm SD of three different experiments. * $p < 0.05$ vs non-treated group.

The colocalization of the mitochondrial marker Tom20 and the lysosomal protein LAMP2 was performed to measure changes in mitophagy induction over time among the different treatments. Confocal images showed that combined treatment increased greatly mitochondrial and lysosome colocalization at 6 and 12 h, whereas this process dropped off at 24 h until lower levels than the control group (Figs. 28A and 28B). Melatonin or sorafenib administration alone also induced slightly this colocalization at 12 h, but at a lesser extent than the combined treatment (Figs. 28A and 28B). Additionally, mitochondria and lysosome continued colocalizing after 24 h of melatonin single treatment, whereas this interaction diminished in sorafenib-treated cells until control levels (Figs. 28A and 28B). In order to corroborate the data obtained with the colocalization assay, PINK1 and Parkin protein levels were measured over time in response to either sorafenib treatment alone or in combination with melatonin. 2.5 μ M sorafenib failed to increase PINK1 protein levels, whereas a transient elevation in the expression of this factor from 3 to 12 h, was showed when 1 mM melatonin was added to

sorafenib-treated cells, returning to basal levels at 24 h (Fig. 29A). Protein levels of Parkin experienced a similar tendency since they were not modified with sorafenib treatment, but they experienced a transient increase from 3 to 6 h with combined administration, returning to basal levels at 12 h (Fig. 29A). These variations were probably connected with the increased shown after 6 and 12 h of sorafenib and melatonin cotreatment on LC3 lipidation levels (Fig. 29B). Summarizing, melatonin can induce PINK1/Parkin mitophagy response when it was coadministered with sorafenib.

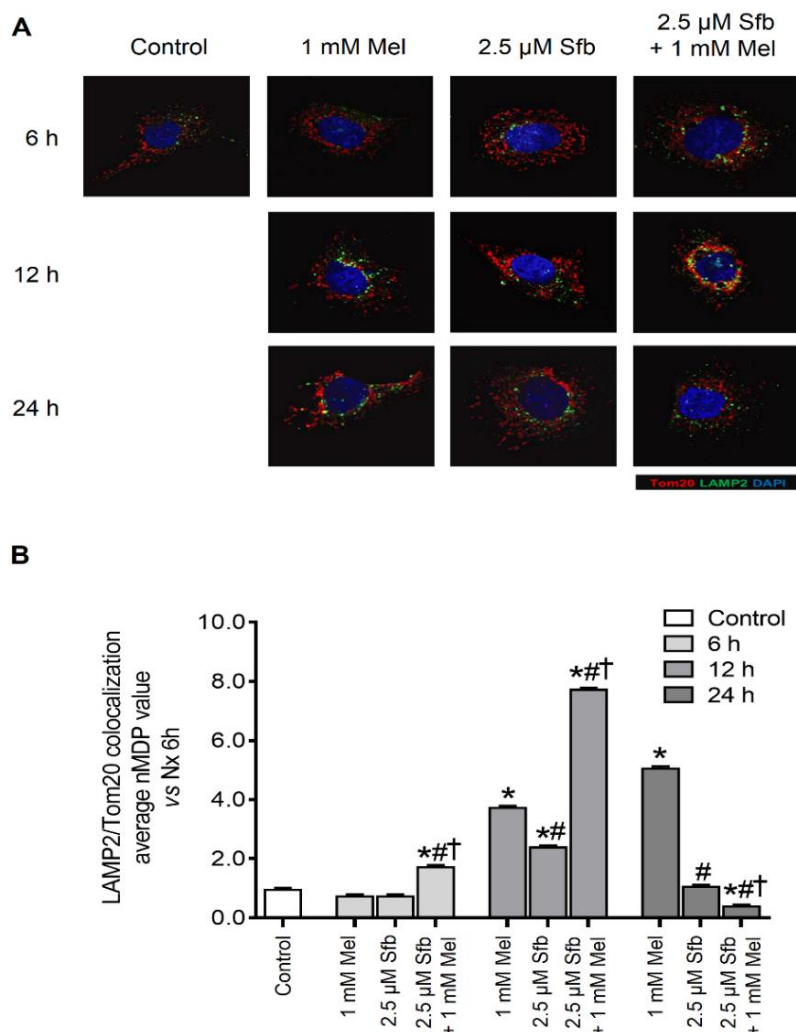


Figure 28: Effects of melatonin and/or sorafenib administration on mitochondria and lysosome colocalization. **(A)** Representative confocal images show colocalization between Tom20 and LAMP1 in Hep3B cells at 6, 12 and 24 h after 2 mM melatonin (Mel) and/or 2.5 μ M sorafenib (Sfb) treatment. **(B)** Average normalized mean deviation product (nMDP) value was obtained by using ImageJ software with the Colocalization Colormap plugin and was represented as a percentage of the mean value \pm SD of three different experiments. * $p < 0.05$ vs control group, # $p < 0.05$ vs melatonin-treated group at the same time point, † $p < 0.05$ vs sorafenib-treated group at the same time point.

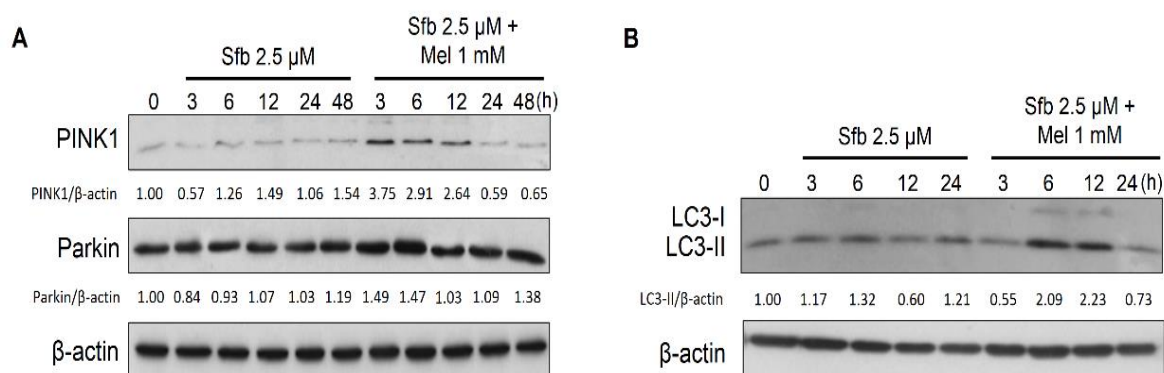


Figure 29: Effects of sorafenib treatment alone or in combination with melatonin on the expression of the main autophagy and mitophagy markers. **(A)** Time course of PINK1 and Parkin were measured by Western blot technique at 3, 6, 12, 24 and 48 h after 2.5 μ M sorafenib (Sfb) treatment alone or in combination with 1 mM melatonin (Mel). **(B)** The variations in the expression of LC3 were analyzed by Western blot technique after 3, 6, 12 and 24 of sorafenib and sorafenib plus melatonin treatment. Representative immunoblots were quantified by using ImageJ software and the results were expressed as band density/ β -actin density vs control cells (0 h group).

As previously claimed, mitophagy and mitochondria dynamics are closely related each other [332,333]. Indeed, mitochondrial fission stimulates the segregation and fragmentation of damaged organelles, which ultimately facilitates their engulfment by the autophagosome [332]. However, mitochondria fusion prevents mitophagy by inducing the aggregation of these organelles, hindering their integration into the autophagic vesicle [333]. Therefore, changes in the expression levels of MFN2, OPA1 and Fis1 were measured by Western blot assay in order to analyze the role of mitochondrial fusion and fission on the mitophagy induced after sorafenib and melatonin coadministration. Fusion proteins did not experiment any significant variations after sorafenib single treatment, whereas they diminished at 3, 6 and 12 h after sorafenib and melatonin coadministration, being OPA1 more sharply inhibited than MFN2 (Fig. 30A). Conversely, Fis1 protein levels remained unaltered after sorafenib administration, but a progressive reduction over time was found in combined treatment (Fig. 30A). Therefore, melatonin addition to sorafenib treatment seems to restrain transiently mitochondrial fusion and gradually mitochondrial fission.

In order to corroborate the extent of treatment-induced mitophagy in Hep3B cells, the modifications in mtDNA copy number were measured by qPCR. As shown in Fig. 30B, sorafenib or melatonin treatment alone did not alter mitochondrial levels, whereas combined treatment induced a clear diminution in mtDNA copy number from 12 to 24 h.

Besides, 60 kDa heat shock protein (HSP60) protein levels, which is a mitochondrial chaperone that is necessary to achieve the correct folding of mitochondrial proteins [424], diminished from 12 to 24 h of combined treatment (Fig. 30B). These results clearly suggest that melatonin and sorafenib coadministration was able to induce mitochondrial degradation and to prevent their biogenesis.

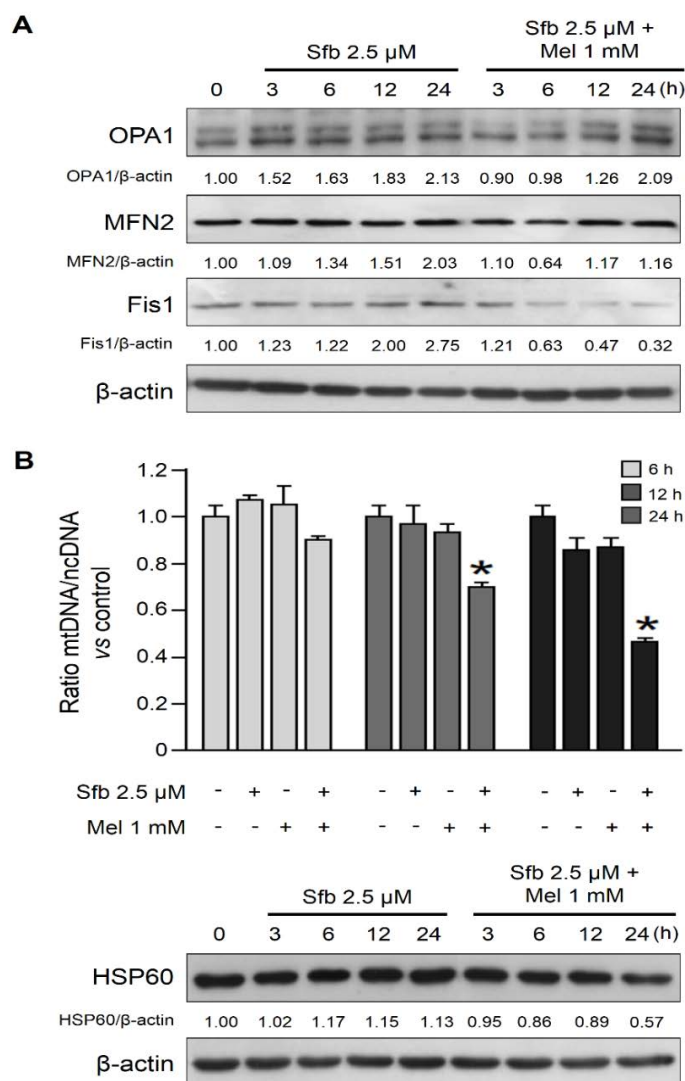


Figure 30: Effects of melatonin and/or sorafenib treatment on mitochondrial dynamics and biogenesis. **(A)** MFN-2, OPA1 and Fis1 levels were measured by Western blot technique at 3, 6, 12 and 24 h after 2.5 μ M sorafenib (Sfb) alone or in combination with 1 mM melatonin (Mel). Representative immunoblots were quantified by using ImageJ software and the results were expressed as band density/ β -actin density vs control cells (0 h group). **(B)** mtDNA content was measured by using qPCR after 6, 12 and 24 h of treatment. mtDNA/ncDNA ratio was represented as a percentage of the mean value \pm SD of three different experiments. * p <0.05 vs control group. HSP60 levels were analyzed by using Western blot assay at 3, 6, 12 and 24 h after 2.5 μ M sorafenib alone or in combination with 1 mM melatonin. Representative immunoblots were quantified by using ImageJ software and the results were expressed as band density/ β -actin density vs control cells (0 h group).

2.4. Sorafenib and melatonin coadministration stimulates oxidative stress and membrane depolarization in Hep3B cells.

Although melatonin normally exerts antioxidant actions at physiological concentrations, due to its ability to scavenge free radicals and induce the expression of detoxifying enzymes, it has been recently reported that pharmacological concentrations of this indoleamine (from μM to mM) can induce the opposite effect in both tumor and non-tumor cells [425]. In fact, the prooxidant actions of this hormone could be partly responsible for the alterations showed in mitochondria homeostasis after combined treatment. For these reasons, we assessed the capability of these molecules to induce ROS production at 1, 3 and 6 h after treatments by using DCF-DA, a ROS-sensitive fluorescent probe. Sorafenib failed to enhance ROS production, whereas melatonin alone or in combination with this drug induced ROS production in a dose- and time-dependent manner (Fig. 31A). Therefore, it seems that melatonin pro-oxidant effects could partly contribute to disturb mitochondria homeostasis and to induce mitophagy.

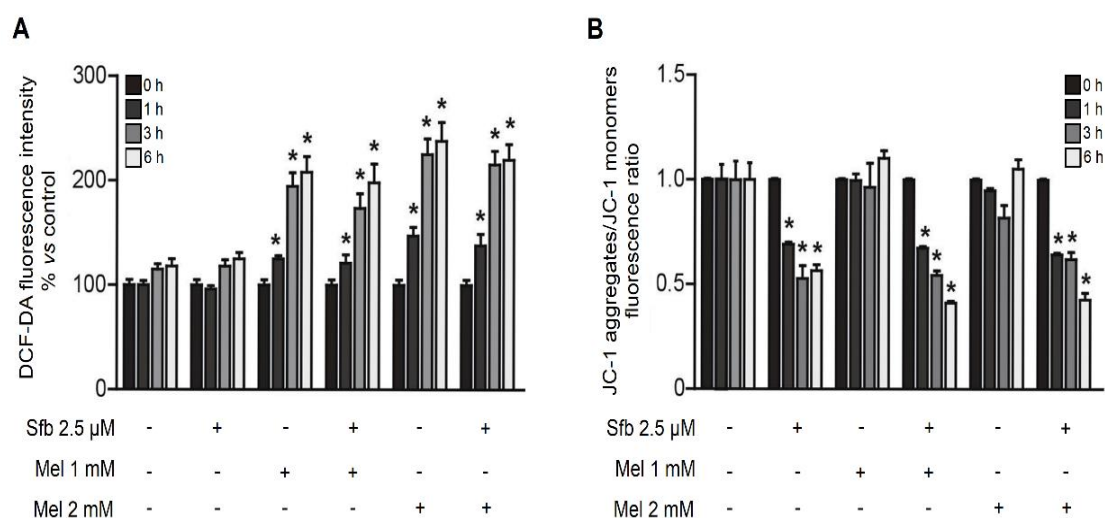


Figure 31: Analysis of ROS production and membrane polarization statuses after sorafenib and/or melatonin administration. **(A)** The amount of harmful ROS was measured by DCF-DA quantification in Hep3B cells treated with sorafenib (Sfb) (2.5 μM) and/or melatonin (Mel) (1 and 2 mM) for 1, 3 and 6 h. DCF-DA intensity was represented as a percentage of the mean value \pm SD of three different experiments. * $p < 0.05$ vs 0 h groups in each treatment **(B)** Changes in mitochondrial membrane potential were measured using JC-1 fluorometric assay in Hep3B cells treated with sorafenib (2.5 μM) and melatonin (1 and 2 mM) for 1, 3 and 6 h. JC-1 aggregates /JC-1 monomers fluorescent ratio was represented as a percentage of the mean value \pm SD of three different experiments vs Control. * $p < 0.05$ vs 0 h groups in each treatment.

Otherwise, loss of mitochondrial membrane potential is a key step for mitophagy induction, because PINK1 is only stabilized in the OMM of depolarized mitochondria [335]. Therefore, JC-1 staining assay was carried out to evaluate the capability of either melatonin, sorafenib or their combination to modulate mitochondrial membrane potential. Curiously, sorafenib administration alone or in combination with melatonin was able to reduce this membrane potential, which was not observed when this indoleamine was single added (Fig. 31B). These data suggest that the mitophagy response that is enhanced after sorafenib and melatonin coadministration is due to the combination of melatonin-induced ROS generation and sorafenib-induced mitochondrial membrane potential loss.

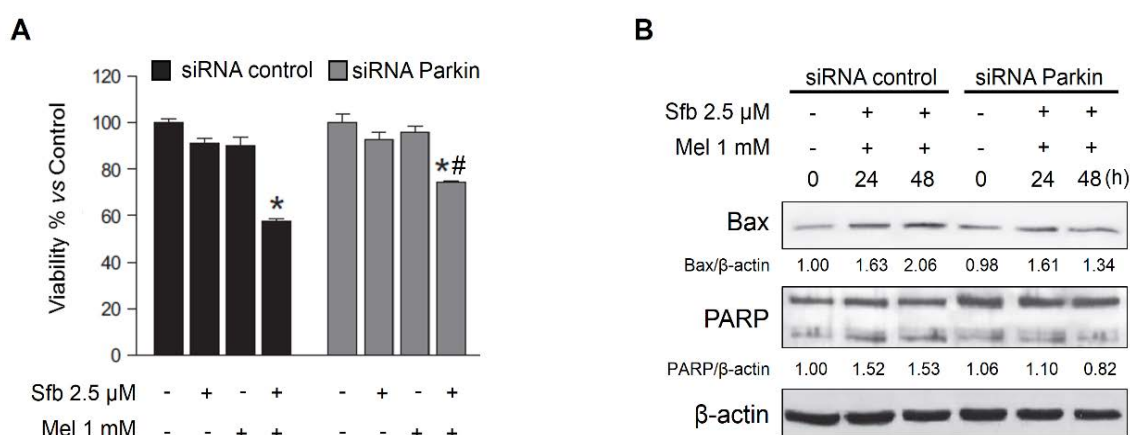


Figure 32: Effects of Parkin silencing on Hep3B viability and apoptosis after melatonin and/or sorafenib treatment. **(A)** Cell viability from silenced and non-silenced cells was analyzed by using MTT assay at 48 h after being treated with either 2.5 μM sorafenib, 1 mM melatonin or combination of both compounds. Data were expressed as a percentage of the mean value ± SD of three different experiments. * $p < 0.05$ vs non-treated group, # $p < 0.05$ vs non-silenced cells with the same treatment. **(B)** PARP and Bax protein levels were measured by Western blot technique after 24 and 48 h of treatment in presence or in absence of Parkin siRNA. Representative immunoblots were quantified by using ImageJ software and the results were expressed as band density/β-actin density vs non-treated and non-silenced cells.

2.5. Combined-treatment-induced mitophagy exerts a prodeath role in Hep3B cells.

Similarly to autophagy, mitophagy can also exert a dual role in cancer cells, since this cellular response avoids tumorigenesis in early steps of tumor progression, but promotes tumor cell survival in later phases [361]. In order to determinate the impact that presented mitophagy on the susceptibility of Hep3B cells to PCD after sorafenib and melatonin administration under normoxia, Parkin protein was silenced with a commercial

siRNA. As shown in Fig. 32A, cell viability increased significantly after Parkin inhibition when both compounds were coadministered, but not when melatonin or sorafenib were added alone. In addition, these findings were associated with a diminution in PARP cleavage and in Bax expression following 24 h and 48 h of melatonin and sorafenib treatment (Fig. 32B). Therefore, mitophagy response induced by melatonin in sorafenib-treated cells under normoxia potentiates cell death. These data suggest that this pathway is partly responsible for the melatonin ability to overcome sorafenib innate resistance of Hep3B cells.

3. Modulation of HCC cell sensitivity to sorafenib by melatonin under hypoxia.

3.1. Melatonin enhances sorafenib cytotoxicity in HCC cells under hypoxia.

As previously indicated, sorafenib has become one of the most important first-line treatment options for advanced HCC [82]. However, the arising of hypoxic zones in the tumor mass due to the high proliferative rate that present HCC cells, and/or to the sorafenib antiangiogenic effects, has been related to the loss of cell sensitiveness through the induction of several mechanisms, such as EMT [121,122,129]. Melatonin has been reported to reduce the activation of some hypoxia-dependent signals in HCC, such as the expression and release of VEGF [16]. Accordingly, the combination of this indoleamine with sorafenib could effectively overcome the appearance of acquired resistance to this chemotherapeutic drug in hypoxia zones.

To check this hypothesis, Hep3B cell viability was analyzed by using MTT assay at 48 h after melatonin (1 and 2 mM) and/or sorafenib (2.5, 5 and 10 μ M) administration and under either normoxia or hypoxia conditions. When administered alone, only the highest dose of sorafenib (10 μ M) was able to induce a significant reduction in cell viability under hypoxia, whereas 5 μ M was sufficient to induce HCC cell death under normoxia (Fig. 33). Moreover, only the 2 mM dose of melatonin was able to diminish Hep3B cell viability under normoxia, but not under hypoxia (Fig. 33). Interestingly, the combination of melatonin with all sorafenib concentrations tested stimulated HCC cell death under either basal or low oxygen conditions (Fig. 33). Therefore, melatonin administration sensitizes HCC cells to sorafenib treatment under both environmental conditions (Fig. 33).

In order to evaluate the molecular mechanisms that modulate this sensitization, 2 mM and 5 μ M doses of sorafenib and melatonin respectively were chosen to carry out the rest of the experiments under hypoxia.

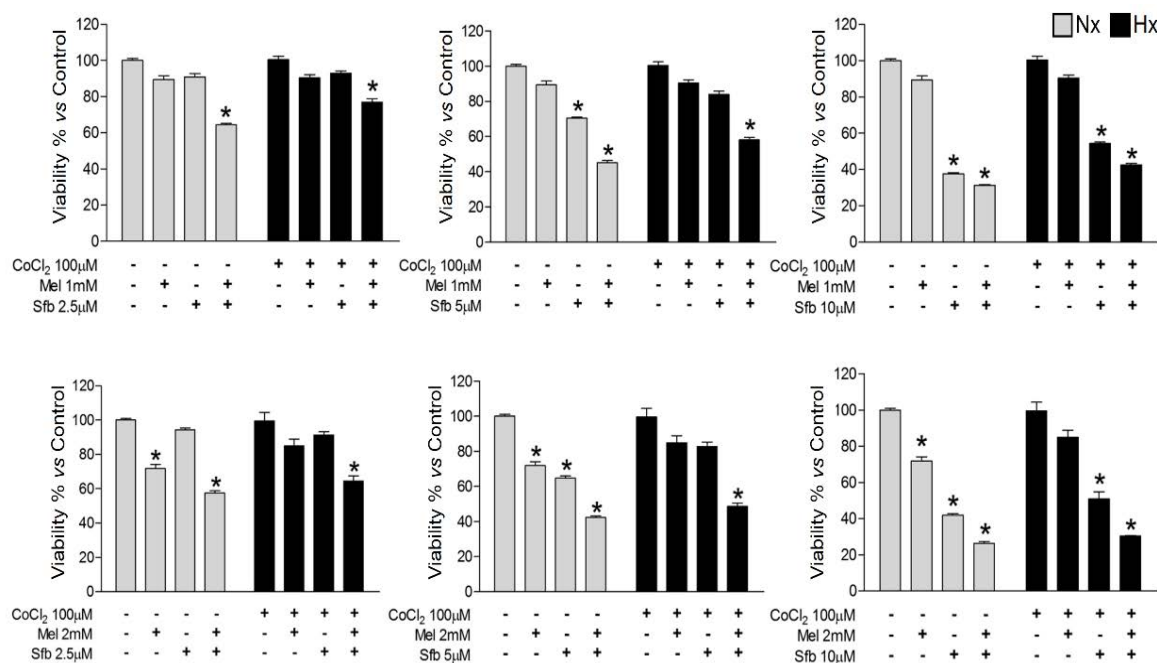


Figure 33: Effects of melatonin and/or sorafenib single and combined administration on Hep3B cell viability under basal and low oxygen conditions. Cells were maintained under normoxia (Nx) or hypoxia (Hx) for 48 h with or without sorafenib (Sfb) (2.5, 5 or 10 μ M) and/or melatonin (Mel) (1 or 2 mM). Cell viability was determined with MTT assay. Data were expressed as a percentage of the mean value \pm SD of three different experiments. * p <0.05 vs non-treated cells under the same oxygen concentration.

3.2. Melatonin and sorafenib coadministration modulates the expression and activity of both HIF-1 α and HIF-2 α , leading to reducing Hep3B viability.

HIF-1 α and HIF-2 α are the main cellular sensors of microenvironmental oxygen levels [131]. These proteins are usually overexpressed in different tumor tissues, which leads to cancer progression by the promotion of many cellular responses, such as cell immortalization, neovascularization, metastasis and immune evasion [131]. Moreover, HIF-1 α has also been related to the arising of sorafenib resistant cells [426]. Therefore, the addition of a sensitizer that can avoid this situation, by suppressing the expression of both HIF-1 α and HIF-2 α , seems to be a promising strategy to improve HCC therapy [122]. With the purpose of analyzing if melatonin could abolish hypoxia-mediated effects in

sorafenib-treated cells, HIF-1 α and HIF-2 α expression levels were measured at 24 h. As expected, the lack of oxygen-induced a robust increase in HIF-1 α and HIF-2 α expression (Fig. 34A). Although 5 μ M sorafenib treatment was able to diminish slightly HIF-1 α protein levels, it failed to alter the expression of HIF-2 α (Fig. 34A). Additionally, 2 mM melatonin alone or in combination with sorafenib abolished the expression of both oxygen sensors (Fig. 34A). Otherwise, VEGF protein levels were measured to analyze the activity of HIF-1 α and HIF-2 α after the different treatments, since it is a direct target shared by both sensors. As shown in Fig. 34A, the variations observed in its expression among the different experimental groups are close to those obtained in HIF-1 α protein levels, corroborating that melatonin was able to abolish its activity in sorafenib-treated cells under hypoxia. Therefore, these data suggest that melatonin administration to sorafenib-treated cells in hypoxia reduces HIF-1 α and HIF-2 α expression and activity in HCC cells.

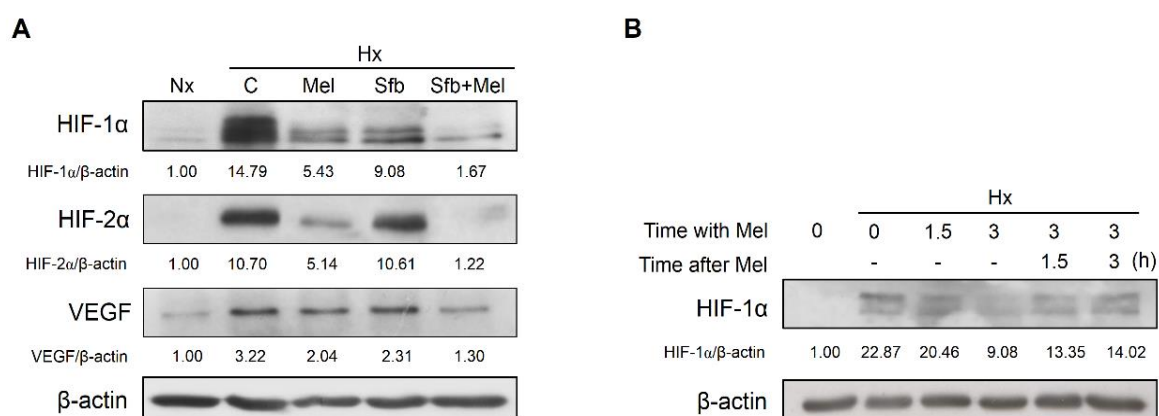


Figure 34: Effects of melatonin and/or sorafenib treatment on HIF-1 α and HIF-2 α expression and activity. **(A)** Hep3B cells incubated under normoxia (Nx) or hypoxia (Hx) by adding 100 μ M CoCl₂ were treated with 5 μ M sorafenib (Sfb) and/or 2 mM melatonin (Mel) for 24 h. HIF-1 α , HIF-2 α and VEGF expression were measured by using Western blot technique. **(B)** Hep3B cells were preincubated with 100 μ M CoCl₂ to induce hypoxia for 3 h (lane 2), being subsequently treated with 2 mM melatonin for 1.5 and 3 h (lane 3 and 4). Finally, melatonin was removed and cells were maintained under hypoxic conditions for 1.5 and 3 h (lanes 5 and 6). Lane 1 shows cells under normoxia. HIF-1 α levels were measured by Western blot assay. Representative immunoblots were quantified by using ImageJ software and the results were expressed as band density/ β -actin density vs normoxia group (Nx).

In order to explore the dynamic changes that experiment the expression of HIF-1 α in response to melatonin treatment, cells were preincubated with 100 μ M CoCl₂ to induce hypoxia for 3 hours before being treated with 2 mM melatonin for another 3 h. Finally, melatonin was withdrawn from the media for other additional 3 h to restore initial hypoxic conditions. As expected, melatonin addition diminished time-dependently HIF-1 α protein levels (Fig. 34B). Conversely, the expression of this mediator was progressively restored

after melatonin removal from media. Therefore, melatonin induces a reversible inhibition of HIF-1 α in Hep3B cells (Fig. 34B).

Subsequently, HIF-1 α was silenced to assess the role that performs this protein on the reduction of cell viability observed after melatonin and sorafenib coadministration under hypoxia. As shown in Fig. 35A, the silencing of HIF-1 α was greatly efficient, since the levels of this mediator dropped off $\approx 70\%$ after 48 h of silencing. Curiously, the levels of HIF-2 α increased significantly after HIF-1 α inhibition (Fig. 35A), suggesting the existence of a compensatory mechanism that overexpresses HIF-2 α in absence of HIF-1 α . Besides, this diminution in HIF-1 α expression was associated with a reduction in its activity, since the levels of its specific target BNIP3 decreased concomitantly with HIF-1 α (Fig. 35B). Although a slight decline in cell viability was observed in the silenced cells that have been treated with both compounds under hypoxia, non-significant differences were observed between all silenced and non-silenced groups (Fig. 35C), probably because of the compensatory mechanism existent between the two HIF isoforms. Therefore, the inhibition of HIF-1 α expression by melatonin seems to be partly responsible for sensitizing HCC cells to sorafenib in hypoxia.

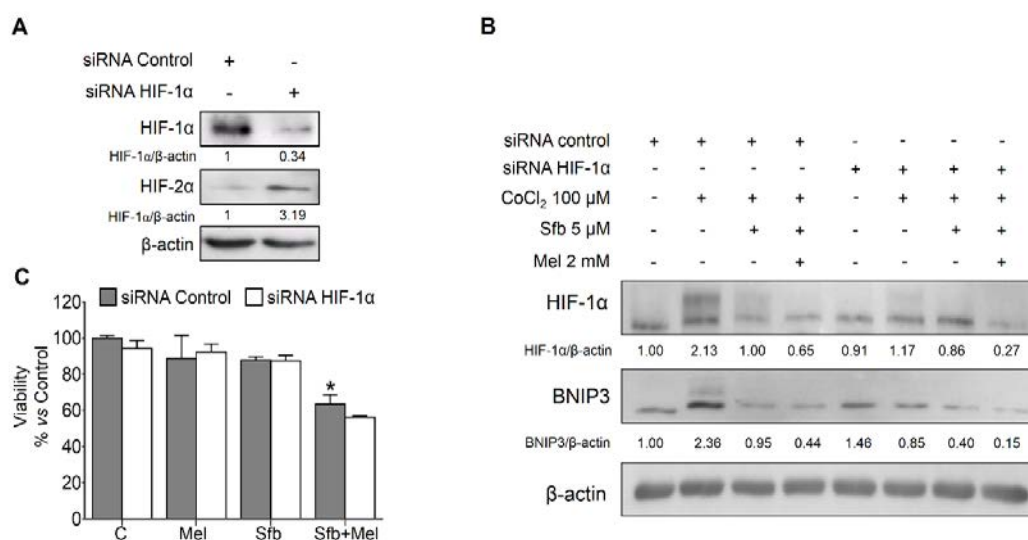


Figure 35: Analysis of HIF-1 α repercussion on the cytotoxic effects of sorafenib and melatonin administered alone or in combination. **(A)** HIF-1 α and HIF-2 α expression levels were measured through Western blot technique at 48 h post-silencing. **(B)** HIF-1 α and BNIP3 expression were measured by Western blot assay at 48 h after 5 μ M sorafenib (Sfb) administration in absence or presence of 2 mM melatonin (Mel). Representative immunoblots were quantified by using ImageJ software and the results were expressed as band density/ β -actin density vs non-silenced cells under normoxia. **(C)** Cell viability from silenced and non-silenced cells was measured by using MTT assay 48 h after melatonin and/or sorafenib administration. Data were expressed as a percentage of the mean value \pm SD of three different experiments. * $p < 0.05$ vs non-treated and non-silenced cells.

3.3. Melatonin enhances HIF-1 α protein synthesis, but does not modify its transcription or its degradation.

As reported previously, melatonin was able to reduce HIF-1 α levels in HCC cells alone or in combination with sorafenib. However, the variations observed in its expression could be associated with a modification in its transcription levels and/or in the balance between its protein synthesis and degradation [427]. Therefore, the determination of the mechanism through melatonin abolishes the expression of HIF-1 α could be useful to improve its use in the treatment of HCC tumors under hypoxia. As shown in Fig. 36A, the mRNA levels of HIF-1 α did not undergo any significant variations in normoxia, whereas they gradually diminished under hypoxia. Besides, melatonin administration to hypoxic cells did not alter significantly the levels of HIF-1 α mRNA (Fig 36A). These results suggest that melatonin is unable to alter HIF-1 α mRNA levels in hypoxia, exerting its action on the expression of this protein at a post-transcriptional level.

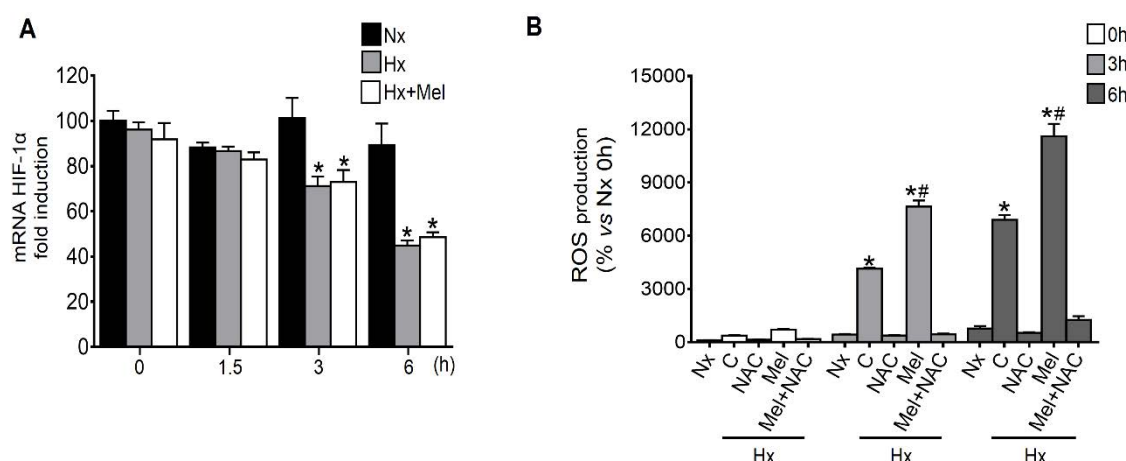


Figure 36: Effects of melatonin single administration on the transcription of HIF-1 α and on the release of ROS. **(A)** HIF-1 α mRNA levels were measured by RT-qPCR in Hep3B cells at 0, 1.5, 3 and 6 h after normoxia (Nx), hypoxia (Hx) or hypoxia plus 2 mM melatonin (Mel). Data were expressed as a percentage of the mean values of arbitrary units (a.u.) \pm SD of three different experiments. * p <0.05 vs cells under Nx at the same time point (siRNA control group). **(B)** ROS production was analyzed by DCF-DA quantification in Hep3B cells treated with melatonin (2 mM) and/or NAC (5 mM) for 0, 3 and 6 h. DCF-DA intensity was represented as a percentage of the mean value \pm SD of three different experiments vs Nx 0 h. * p <0.05 at the same time point, # p <0.05 vs Hx at the same time point.

Oxygen is the main mediator that regulates HIF-1 α degradation since PHDs require this molecule to induce the hydroxylation of this transcriptional factor, as well as its degradation by the proteasome [152]. Otherwise, ROS species can negatively regulate the activity of PHDs by oxidizing their Fe²⁺ cofactor to Fe³⁺ [152]. Although melatonin

presents a broad spectrum of antioxidant actions in human tissues at physiological doses, it can also promote ROS release at pharmacological doses (from μM to mM) [425]. This peculiar behavior suggests that this hormone should be considered as a conditional pro-oxidant in certain situations [425]. Therefore, ROS release after 3 and 6 h of treatment with melatonin under hypoxia was performed to address whether the potential antioxidant action of melatonin in HCC could induce the degradation of HIF-1 α by the proteasome. As shown in Fig. 36B, 2 mM melatonin treatment gradually stimulated the formation of ROS under low oxygen conditions. Indeed, the addition of 5 mM NAC prevented the melatonin-dependent release of these harmful species (Fig. 36B). Therefore, it seems really improbable that melatonin-dependent reduction in the expression of HIF-1 α could be associated with the ROS-dependent inhibition of PHDs.

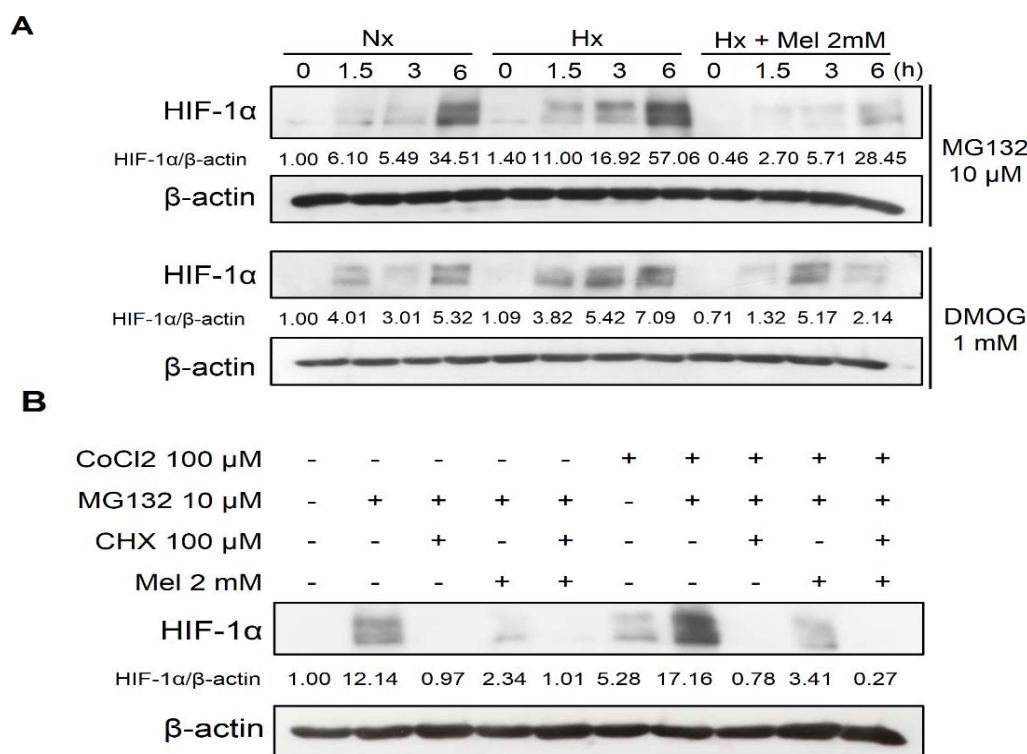


Figure 37: Effects of melatonin treatment on HIF-1 α protein synthesis and degradation. **(A)** Changes in HIF-1 α synthesis were analyzed by Western blot assay in Hep3B cultured under normoxia (Nx) and hypoxia (Hx) and treated with or without 2 mM melatonin (Mel) and either 10 μM MG132 or 1 mM DMOG for 0, 1.5, 3 and 6 h. **(B)** Variations in HIF-1 α degradation were analyzed by Western blot assay in Hep3B cultured under normoxia (Nx) and hypoxia (Hx) and treated with or without 2 mM melatonin, 10 μM MG132 and/or 100 mM CHX for 6 h. Representative immunoblots were quantified by using ImageJ software and the results were expressed as band density/ β -actin density vs Nx group.

With the intention of evaluating whether melatonin inhibits HIF-1 α protein synthesis in HCC cells, the specific proteasome repressor MG132 (10 μ M) or the specific PHD inhibitor DMOG (1 mM) were administered in combination with this indoleamine [427]. The blockage of either of the two systems of degradation induced a pronounced and time-dependently accumulation of HIF-1 α , being clearly diminished after 2 mM melatonin administration (Fig. 37A). Otherwise, 10 μ M MG132 in absence or presence of 100 μ M CHX, which blocks ribosomal translation by impeding the incorporation of amino acids to the proteins [428], were added to Hep3B cells to check the ability of melatonin to alter the half-life of HIF-1 α . The administration of both inhibitors for 6 h almost completely restrained the accumulation of HIF-1 α both in normoxia and hypoxia (Fig. 37B). Similarly, 2 mM melatonin combination with MG132 induced a significant reduction in the accumulation of this protein under both oxygen concentrations, which indicates that this indoleamine acts in a similar way to CHX (Fig. 37B). Therefore, these data suggest that melatonin prevents HIF-1 α protein synthesis and do not affect to its degradation.

3.4. Melatonin restrains HIF-1 α translation by downregulating mTORC1/p70S6K pathway.

PI3K/Akt/mTORC1 pathway is the main oxygen-independent mechanism that induces HIF-1 α protein synthesis in response to external stimuli, such as growth factors or hormones [145]. Therefore, melatonin could restrain the translation of this transcriptional factor by inhibiting this cellular pathway. As shown in Fig. 38A, 2 mM melatonin administration under low oxygen conditions decreased significantly the phosphorylation state of mTORC1, p70S6K and the ribosomal protein S6 (RP-S6) in a time-dependent manner. This diminution was concomitant with the melatonin-dependent reduction in HIF-1 α protein levels under hypoxia (Fig. 38A). Besides, mTORC2 and Akt phosphorylation levels increased at 3 and 6 h after melatonin administration under this microenvironmental condition (Fig. 38A).

In order to corroborate the role that presents this hormone on the activation of the PI3K/Akt/mTOR pathway, melatonin was combined with either rapamycin at 20 nM to restrain mTORC1 phosphorylation, or LY294002 at 50 μ M to prevent PI3K activation [173]. Rapamycin administration under hypoxia reduced mTORC1, p70S6K and RP-S6 phosphorylation/activation state both alone or in combination with melatonin, being this

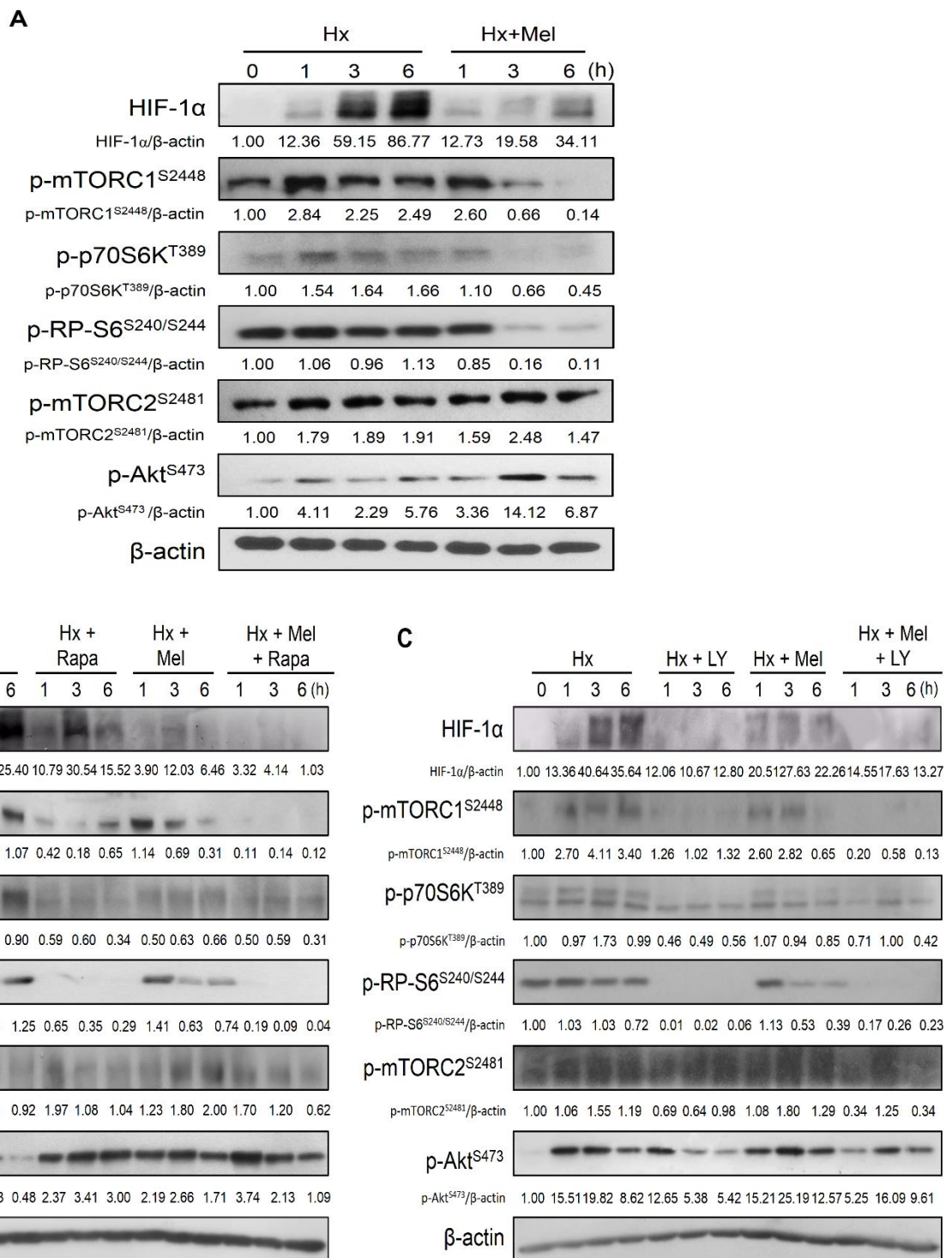


Figure 38: Effects of melatonin single treatment on the PI3K/Akt/mTORC1 pathway and its impact on HIF-1 α expression. (A) Hep3B cells were treated with 100 μ M CoCl₂ to mimic hypoxia (Hx) alone or in combination with 2 mM melatonin (Mel) for 1, 3 and 6 h. Lane 1 shows protein basal levels under normoxia (Nx) (B) and (C) 20 nM rapamycin or 50 μ M LY294002 alone or in combination with 2 mM melatonin were administered to Hep3B cells under hypoxia. Protein levels of HIF-1 α , p-mTORC1, p-mTORC2, p-Akt, p-RP-S6, and p-p70S6K were measured by Western blot. Representative immunoblots were quantified by using ImageJ software and the results were expressed as band density/ β -actin density vs Nx group.

phenotype concomitant with the reduction showed in HIF-1 α protein levels (Fig. 38B). Moreover, mTORC2 and Akt phosphorylation levels also increased after rapamycin administration alone or in combination with melatonin (Fig. 38B). Otherwise, LY294002 administration alone or in combination with this indoleamine under hypoxia downregulated the phosphorylation state of all the proteins of this pathway (Fig. 38C). The inhibition induced by LY2940002 lead to reducing more sharply the expression of HIF-1 α than melatonin (Fig. 38C). Summarizing, these data demonstrate that melatonin reduces HIF-1 α translation by downregulating PI3K/Akt/mTORC1/RP-S6 signaling in HCC cells.

3.5. Melatonin and sorafenib coadministration inhibits hypoxia-induced mitophagy, which ultimately reduces Hep3B viability.

As previously claimed, mitophagy is the main pathway that maintains mitochondrial homeostasis in response to a certain group of stresses [347]. Indeed, the lack of oxygen induces this pathway by enhancing the expression of BNIP3 and Nix, which are directly targeted by HIF-1 α [348]. Therefore, the expression of these two proteins were measured after sorafenib and/or melatonin administration under hypoxia conditions in order to analyze the effects that exert these molecules alone or in combination on the enhancement of mitophagy response. As expected, hypoxia stimulated the expression levels of both proteins regarding to normoxia (Fig. 39A). Moreover, 5 μ M sorafenib treatment alone decreased slightly the expression of both proteins, whereas 2 mM melatonin addition diminished more sharply the levels of these two proteins (Fig. 39A). In addition, the changes showed in BNIP3 and Nix expression after the different treatments correlated with HIF-1 α protein levels (Fig. 34A). These data seem to validate that melatonin reduces mitophagy response in HCC cells.

Although mitophagy prevents tumor progression at early stages of tumorigenesis, it has the opposite effect on later steps of this process, since it restrains tumor cell death by limiting mitochondrial oxidative stress [361]. Moreover, mitophagy can protect advanced tumors against chemotherapy by eliminating damaged mitochondrial and limiting the amount of ROS and RNS [361]. To evaluate the role that present mitophagy in HCC cells which has been treated with sorafenib and/or melatonin under hypoxia, cell viability was measured after the silencing of BNIP3 with a commercial siRNA. As shown in Fig. 39B,

the levels of this mitophagy mediator were almost suppressed after 48 h of silencing under hypoxic conditions. Otherwise, BNIP3 depletion induced a significant diminution in cell viability after single treatment with melatonin or sorafenib, but not after combined treatment (Fig. 39B). Therefore, hypoxia-induced mitophagy seems to exert a cytoprotective role in HCC cells under hypoxia.

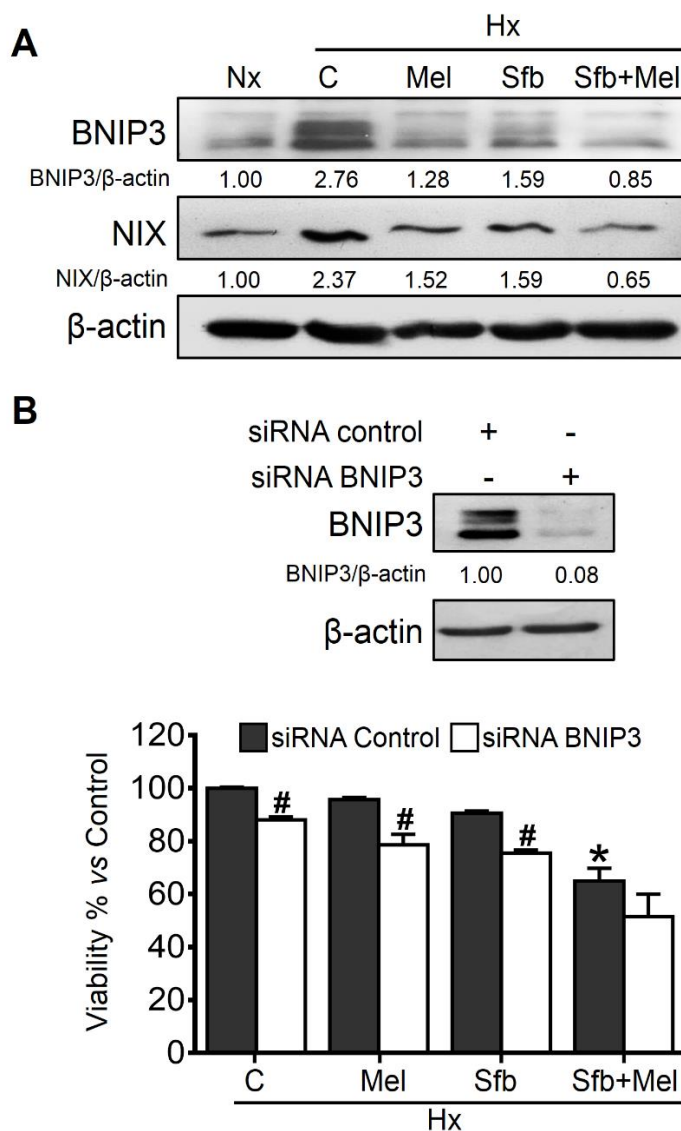


Figure 39: Effects of melatonin and/or sorafenib treatment on hypoxia-induced mitophagy and role of this response in sorafenib cell resistance. **(A)** BNIP3 and Nix protein levels were measured by Western blot assay at 24 h after 2 mM melatonin (Mel) and/or 5 μ M sorafenib (Sfb) treatment under hypoxia (Hx). Lane 1 shows basal protein levels under normoxia (Nx). Representative immunoblots were quantified by using ImageJ software and the results were expressed as band density/ β -actin density vs Nx group. **(B)** Cell viability from silenced and non-silenced cells was measured by using MTT assay 48 h after melatonin and/or sorafenib administration. Data were expressed as a percentage of the mean value \pm SD of three different experiments. * p <0.05 vs non-treated control cells. # p <0.05 vs non-silenced cells in each treatment.

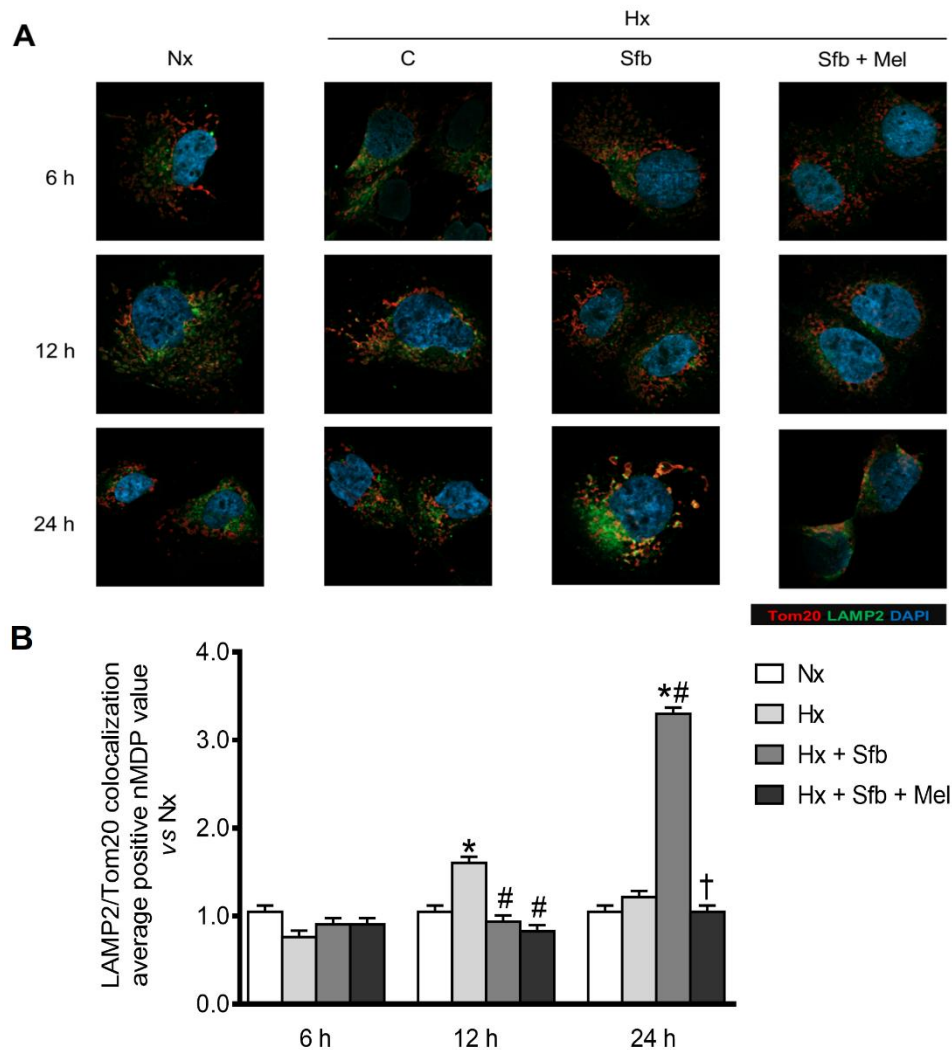


Figure 40: Effects of sorafenib treatment in presence or absence of melatonin under hypoxia on mitochondrial and lysosomal colocalization. **(A)** Representative confocal images show the colocalization between mitochondria and lysosomes in Hep3B cells at 6, 12 and 24 h after 2 mM melatonin (Mel) and/or 2.5 μ M sorafenib (Sfb) treatment under hypoxia (Hx). Basal levels of mitophagy response under normoxia (Nx) are used as control values **(B)** Average positive normalized mean deviation product (nMDP) value was obtained by using ImageJ software with the Colocalization Colormap plugin and was represented as a percentage of the mean value \pm SD of three different experiments. * $p < 0.05$ vs Nx group at the same time point, # $p < 0.05$ vs Hx group at the same time point, † $p < 0.05$ vs Sorafenib-treated group at the same time point.

BNIP3 and Nix proteins introduce damaged mitochondria into autophagosome for their degradation by interacting with LC3-II through their LIR domain [347]. Therefore, a colocalization assay between the mitochondrial marker Tom20 and the lysosomal protein LAMP2 was performed to analyze dynamically the variations observed on mitophagy induction in response to the different treatments. As shown in Fig. 40, hypoxia induced the colocalization between mitochondria and lysosome at 12 h after the beginning of the

treatment, whereas single 5 μ M sorafenib administration delayed this interaction until 24 h post-treatment. 2 mM melatonin addition to sorafenib-treated cells were able to completely prevent the colocalization between these organelles (Fig. 40). In order to confirm these dynamic changes observed after treatments, we evaluated the expression of the autophagosomal markers p62 and LC3-II at these time points. As expected, hypoxia induced the expression of both markers over time, peaking at 12 h after the experiment beginning and decreasing thereafter (Fig. 41A). Curiously, 5 μ M sorafenib treatment alone was only able to retard their maximum of expression from 12 to 24 h, while 2 mM melatonin addition to sorafenib-treated cells reduced LC3-II and p62 protein levels until normoxia basal levels (Fig. 41A). Summarizing, these data suggest that melatonin sensitizes HCC cells to sorafenib under hypoxia through restraining autophagosome synthesis.

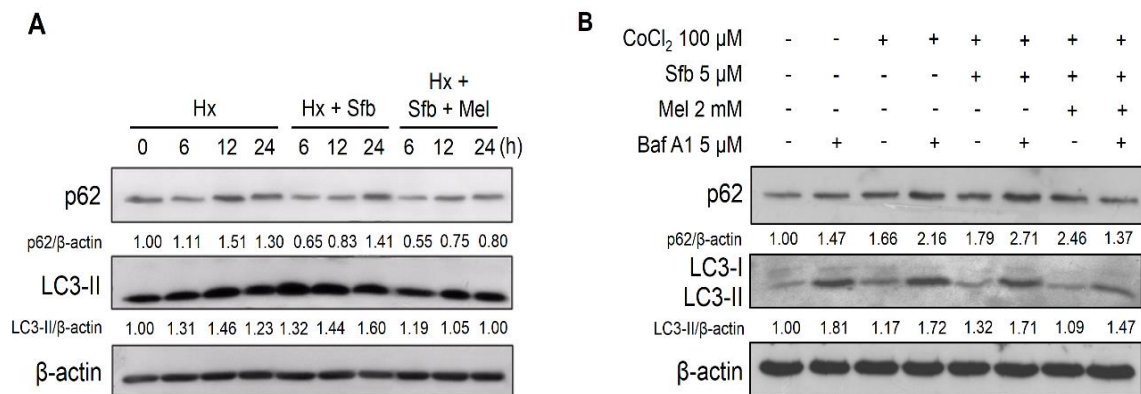


Figure 41: Effects of sorafenib and/or melatonin treatment under hypoxia on the expression of main autophagosome markers, as well as on autophagy flux. **(A)** LC3-II and p62 protein levels were assessed by Western blot assay at 6, 12 and 24 h post-treatments with 5 μ M sorafenib (Sfb) and/or 2 mM melatonin (Mel) under hypoxia (Hx). Lane 1 shows basal levels of these proteins under normoxia (Nx). **(B)** LC3 and p62 expression were measured by Western blot assay at 12 h for the indicated treatments in presence or absence of 5 μ M bafilomycin A1 (Baf A1) for the last 3 h. Representative immunoblots were quantified by using ImageJ software and the results were expressed as band density/ β -actin density vs Nx group.

In order to confirm the functional impact that presents this combination on hypoxia-induced mitophagy, autophagosome and lysosome fusion was blocked by using Baf A1 [423]. As expected, levels of p62 and LC3-II increased after Baf A1 administration as a result of the accumulation of non-fused autophagosomes (Fig. 41B). 5 μ M sorafenib administration alone to Baf A1-treated cells was unable to decrease the hypoxia-induced levels of LC3-II and p62 proteins, whereas the addition of 2 mM melatonin significantly diminished the accumulation of these two proteins (Fig. 41B). These data confirm the

ability of melatonin to restrain hypoxia-induced autophagosome formation in sorafenib-treated cells.

3.6. Melatonin and sorafenib coadministration under hypoxia induces apoptosis in HCC cells.

As reported previously, melatonin was able to induce the apoptotic pathway in sorafenib-treated HCC cells cultured under normoxia. In order to analyze whether this effect is similarly induced under low oxygen conditions, the levels of Bax expression and PARP excision were measured after sorafenib treatment in absence or in presence of melatonin. As shown in Fig. 42, the administration of 5 μ M sorafenib alone under hypoxia was not able to increment Bax expression levels regarding to hypoxia groups, whereas 2 mM melatonin addition to sorafenib-treated cells incremented Bax protein levels mainly after 6 and 24 h of treatment. Besides, PARP excision levels augmented slightly after sorafenib single treatment, but increased more sharply after melatonin and sorafenib coadministration. These data suggest that melatonin increases intrinsic autophagy response in sorafenib-treated cells under hypoxia.

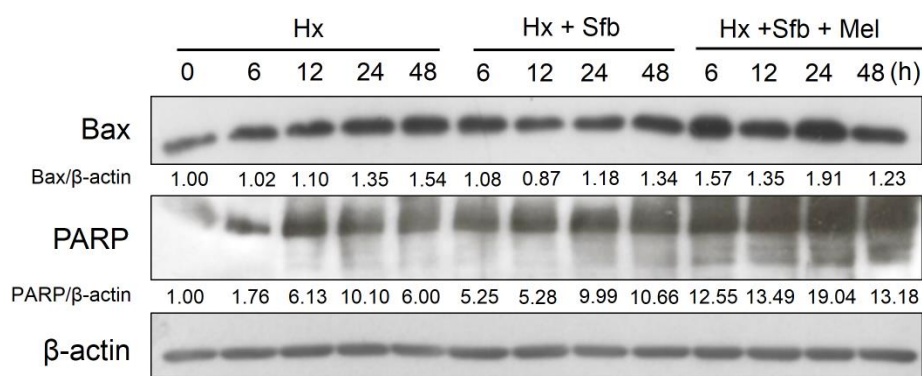
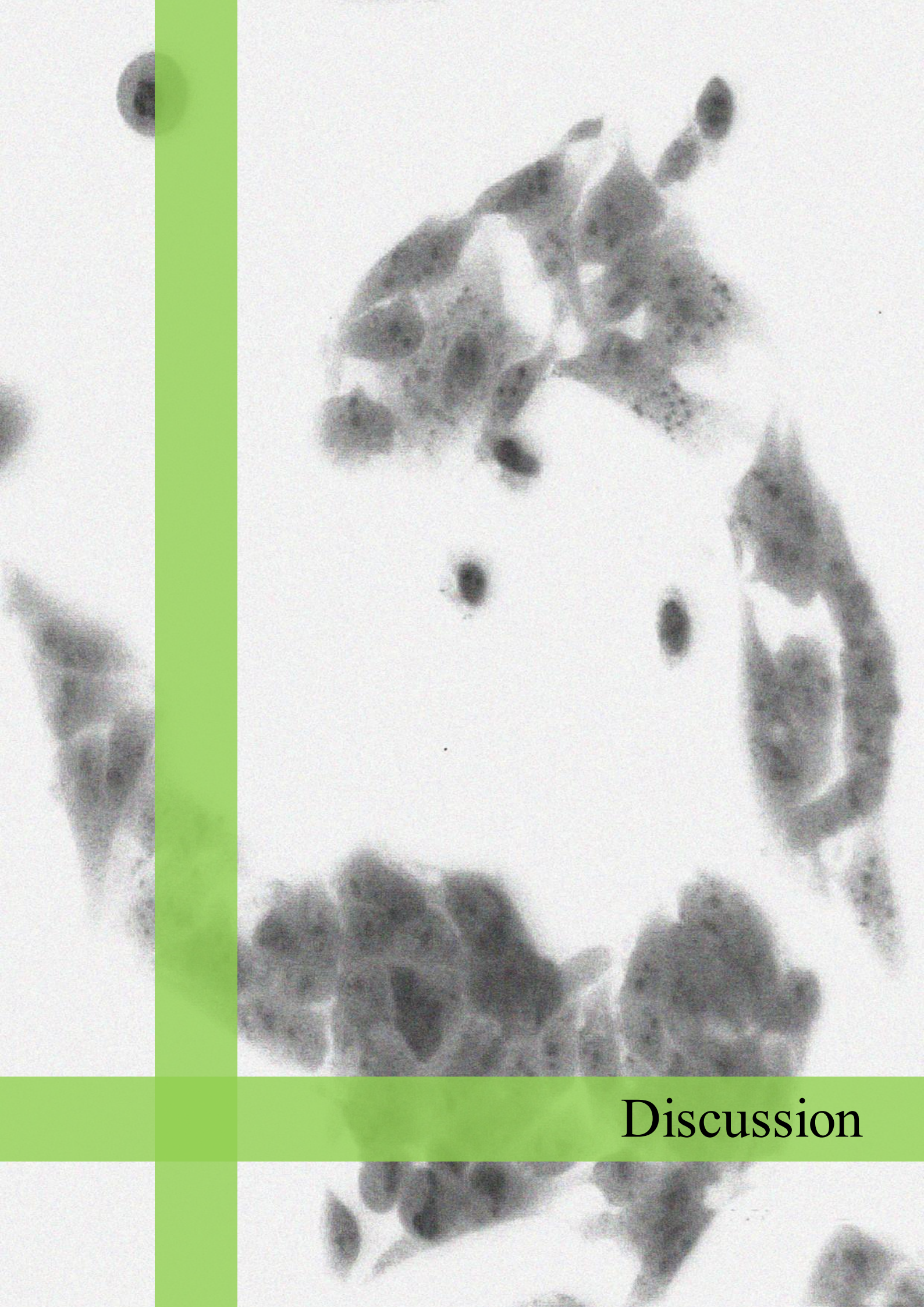


Figure 42: Effects of melatonin and/or sorafenib administration under hypoxia on the main markers of the intrinsic apoptosis pathway. PARP and Bax levels were measured by Western blot technique at 6, 12, 24 and 48 h after 5 μ M sorafenib (Sfb) and/or 2 mM melatonin (Mel) under hypoxia (Hx) conditions. Lane 1 shows basal protein expression levels under normoxia (Nx). Representative immunoblots were quantified by using ImageJ software and the results were expressed as band density/ β -actin density vs Nx group.



Discussion

Although the prevention, diagnosis and treatment of HCC, the most prevalent hepatobiliary cancer worldwide [9,429], has been gradually improved over time, its prognosis remains very poor [3,64]. This unexpected situation is partly owing to the fact that the early stages of HCC are asymptomatic or present the same symptoms as other hepatic pathologies, being this cancer normally diagnosed at advanced stages of tumor progression [9]. Despite some curative strategies have been developed for the treatment of this cancer, they are totally ineffective in the later stages, in which only palliative treatments are currently available [44,65]. Therefore, the development of more specific and selective therapeutic strategies for HCC treatment is essential to improve the life quality of patients and to induce its remission at advanced stages [66].

Despite many drugs have been tested for the treatment of HCC, most of them have failed at phase III trials owing to their high toxicity for the liver or to low antitumor potency [430]. Until last year, only the oral multikinase inhibitor sorafenib was authorized by FDA and EMA for the treatment of advanced HCC tumors [82] due to the promising improvement on OS achieved in both SHARP and Asia-Pacific phase III studies [78,79]. Nevertheless, sustained treatments with this chemotherapeutic drug are far from being satisfactory due to the arising of severe side-off effects and to the progressive loss of cell sensitivity [108]. Moreover, many HCC cells are initially resistant to sorafenib because of the genetic heterogeneity that presents this type of cancer, which could lead to the underexpression of some of its direct molecular targets [105,108]. As a result of the arising of these harmful situations, sorafenib administration must be prematurely discontinued due to the lack of response to this drug [431].

Adaptive desensitization of liver cancer cells to chemotherapy is mediated through the induction of a group of cellular pathways, which are also known as mechanisms of chemoresistance (MOC) [432]. These processes include the reduction of drug uptake or the increase of their export (MOC-1), the impairment of the transition to their active form (MOC-2), the underexpression of their molecular targets (MOC-3), the reparation of drug-induced modifications in the target molecules (MOC-4), the imbalance between prodeath and prosurvival mechanisms, which leads to favoring tumor survival (MOC-5), the disturbance of tumor microenvironment (MOC-6) and the transition between different cellular phenotypes (MOC-7) [432]. Sorafenib adaptive resistant cells have been reported to present diverse alterations in those mechanisms. For instance, the reduction of the levels of its main membrane carriers (MOC-1), such as octapeptidyl aminopeptidase 1

(OCT1), have been related with poorer response to this chemotherapeutic drug [433,434]. Moreover, the overactivation of some compensatory pathways, such as PI3K/Akt/mTOR and JAK/STAT, or the induction of prosurvival processes, such as autophagy can mask the antiproliferative effects of sorafenib in HCC cells (MOC-5) [90,114]. Besides, HCC cell microenvironment (MOC-6), including liver inflammation status, viral reactivation, oxidative stress and hypoxia, as well as EMT (MOC-7) also contribute to the loss of cell sensitivity to sorafenib [108,119,122].

Many therapeutic strategies have recently been developed to overcome sorafenib resistance [105]. On the one hand, some molecules, such as regorafenib or nivolumab, could continue reducing the proliferation of sorafenib-refractory cells after the failure of this drug [105,107]. On the other hand, combinational therapy could extend HCC patients' OS by reducing the incidence of sorafenib side effects and overcoming cell resistance. Indeed, many different compounds including anticancer drugs, such as celecoxib or fluvastatin [435,436], or natural substances, such as curcumin or silibinin [437,438], have been shown to enhance the action of sorafenib in several models *in vitro*. Moreover, some other compounds, such as 5-fluorouracil have demonstrated to stimulate the oncostatic effects of this drug in phase II clinical trials [439]. However, the perfect molecule that avoids the appearance of sorafenib-resistant cells has not been found yet.

Melatonin has been reported to exert a great number of beneficial effects in non-carcinogenic liver diseases, since it can attenuate apoptotic liver damage and reduce ER stress and UPR activation in an *in vivo* rabbit model of fulminant hepatic failure [440,441], while it can ameliorate NAFLD through decreasing the uptake of fat by the liver and its inflammatory status [442]. In HCC, melatonin has been reported to exert many antitumoral actions *in vitro*. For instance, this molecule can reduce cancer cell proliferation through enhancing both intrinsic and extrinsic apoptosis pathways [407]. These effects seem to be related to its ability to modulate both PI3K/Akt and MAPK pathways [443,444]. Otherwise, melatonin can prevent the migration of cancerous hepatocytes by restraining MMP9 expression and activity through NF- κ B inhibition, as well as impair cancer angiogenesis by reducing VEGF expression and release under hypoxia [16,17]. Besides, melatonin also reduces the size of HCC tumors *in vivo* by inducing apoptosis [408]. Because of the promising effects that this indoleamine has exerted in pre-clinical models, it is not strange that it has been associated with other chemotherapeutic drugs to potentiate its effects. For instance, this molecule can sensitize

two different established leukemic cell lines to clofarabine through increasing histone acetylation [405], stimulate the cytotoxic effect of doxorubicin in breast and liver cancer cells [404,445], as well as enhance the antiproliferative outcomes of 5-fluorouracil in colon cancer [446]. All these data encourage its use as an adjuvant in HCC therapy.

As previously claimed, imbalances between cell death and survival responses, including autophagy and its specific forms, such as mitophagy, might be associated with the increment of cell resistance to chemotherapy (MOC-5) [198,432]. These pathways present a dual behavior in cancer cells, since they can induce either tumor cell death or survival at different stages of this pathology [287,289]. Moreover, they protect advanced cancer cells from the cytotoxic effects induced by chemotherapy and radiotherapy, as well as induce Ras-dependent senescence, enhancing cancer cell progression and invasion [287]. Therefore, the development of compounds with the ability to alter this cellular response seems to be a promising, but a complex strategy to improve cancer treatment [287]. Consequently, we aimed to assess whether melatonin could improve sorafenib cytotoxic effects and overcome HCC cell resistance by modulating autophagy and mitophagy responses either under normoxic or hypoxic conditions.

1. Effects of melatonin treatment alone on autophagy response in HCC cells.

Firstly, we decided to assess the capability of melatonin to induce non-specific autophagy in HCC cells. This hormone was able to transiently increase LC3 lipidation and expression, as well as Beclin1 and Atg3 mRNA transcription. Moreover, this indoleamine was also able to temporally induce the formation of autophagosomes, as it was shown by the acridine orange assay. Melatonin administration has also been reported to induce autophagy in other tumor and non-tumor cells, such as HCT166 colorectal carcinoma or granular corneal dystrophy type 2 (GCD2) fibroblasts [447,448]. Moreover, this effect has also been shown in some *in vivo* models, such as hepatoma H22 tumor-bearing mice [449]. On the other hand, melatonin has been asseverated to restrain autophagy in some disease models. For instance, this hormone can enhance cell survival by preventing the activation of the autophagy response in a viral model of fulminant hepatic failure or in rat neurons treated with morphine [450,451]. Summarizing, melatonin-dependent modulation

of autophagy pathway seems to be highly context-dependently, since it can either induce or repress the activation of autophagy. Similar effects have also been reported after the addition of other natural molecules, such as quercetin or silibinin [198].

Additionally, in our experiments the integrity of the autophagy flux was measured by adding either Baf A1 or CQ. Melatonin induced a complete autophagy response since it was able to promote LC3-II accumulation in presence even of the lysosome and autophagosome fusion inhibitors. In addition, the diminution showed in p62 protein levels after LC3-II overexpression peak, as well as the decline observed in the number of autophagosomes at 24 and 48 h also indicates that melatonin induces the degradation of the content of this vesicle. This process has also been shown in some models of other pathologies, such as diabetic cardiomyopathy [452]. In this disease, autophagy complete response is stimulated by melatonin to prevent mitochondrial dysfunction and cardiomyocyte cell death [452]. Moreover, other natural compounds, such as quercetin or baicalein has also been shown to induce or even restore complete autophagy [198].

mTORC1 presents inhibitory effects on autophagy response when there are nutrients, oxygen or energy in the media, as well as in response to growth factors and hormones [261]. Accordingly, the variations observed in mTORC1 phosphorylated/activated state after the addition of melatonin were monitored both at short and extended time periods. Curiously, melatonin failed to diminish the phosphorylated levels of this mediator at all points tested, while the levels of Beclin1 increased in response to the administration of this molecule. These data surmise that melatonin is unable to induce autophagy through reducing the activity of mTORC1, thus this modulation might be done at an upstream point. This unexpected situation has also been founded in a brain ischemia model, in which the addition of this hormone does not alter the phosphorylation of this mediator [453]. Conversely, melatonin has been reported to induce autophagy by reducing the activation of mTORC1 in H22-tumor-bearing mice and in GCD2 cells [448,449]. Summarizing, it seems that the capability of melatonin to induce autophagy response by modulating the activity of mTORC1 is cell-type- and context-dependent.

On the other hand, some components of the MAPK, especially JNK, have been shown to modulate the autophagy pathway in response to different external and internal stimuli, such as UPR induction [285]. Indeed, this effect seems to be mediated by the phosphorylation of Bcl-2, which ultimately provokes the release of Beclin1 [271,285]. Melatonin addition to HCC cells induced the phosphorylation of JNK and simultaneously,

the expression of grp78, the main chaperone implied in the alleviation of ER stress [283]. These changes were concomitant with the increment showed in Beclin1 expression, suggesting that melatonin could induce autophagy through promoting the expression of JNK. In fact, the inhibition of this protein by the chemical inhibitor SP600125 resulted in the decrease of melatonin-derived induction of LC3-II protein levels, corroborating our previous hypothesis. Melatonin has also been claimed to induce JNK signaling in other cancer types, such as gastric cancer [454]. Moreover, the authors of this paper suggest that the activation of this cellular pathway could lead to enhance autophagy response in gastric cancer cells [454].

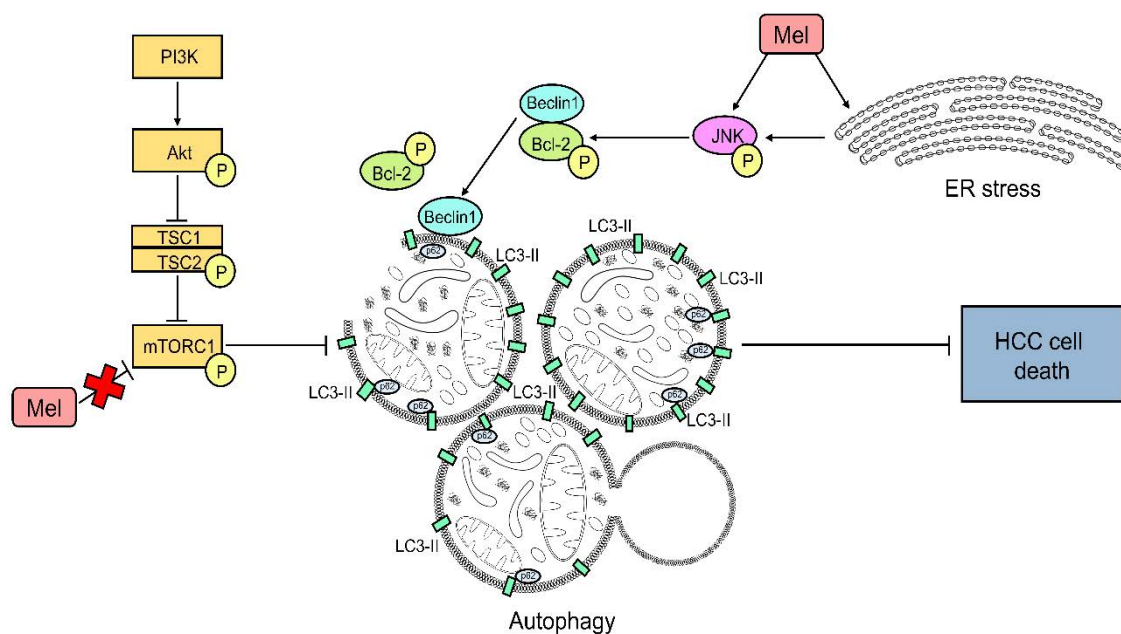


Figure 43: Proposed model of melatonin induction of autophagy in HCC cells. Melatonin induced pro-survival autophagy response through inducing JNK phosphorylation and ER stress, which ultimately displaces Beclin1 and Bcl-2 binding. However, it does not stimulate this pathway by inhibiting mTORC1 signaling.

As described previously, autophagy could exert different roles on cancer cells, since it can either promote cell survival or death according to their phase of tumorigenesis [287,289]. Therefore, it is essential to determine the contribution that presents this pathway to the melatonin antiproliferative effects in HCC cells. The inhibition of autophagosome formation by Atg5 silencing clearly augmented the cytotoxic effects of this hormone in HCC cells. Besides, this oncostatic phenotype was accompanied by the stimulation of apoptosis response, as shown by the enhancement of PARP cleavage. These data suggest that autophagy protects HCC cells against the cytotoxic action of melatonin. This protective behavior of melatonin-induced autophagy has also shown in hepatoma H22

cell line [449]. Besides, other natural molecules, such as quercetin or silibinin, has demonstrated analog effects on gastric and prostate cancer cells respectively [455,456].

Summarizing, melatonin is able to stimulate a prosurvival autophagy response in HCC cells by enhancing ER stress and JNK phosphorylation (Fig. 43). Therefore, the inhibition of this pathway could stimulate the anticancer actions of melatonin in hepatic tumors.

2. Effects of melatonin and sorafenib cotreatment under normoxia in HCC cells.

After the analysis of the capability that presents the single administration of melatonin to modulate autophagy in HCC cells, we decided to check the ability of this indoleamine to enhance the cytotoxic effects of sorafenib in HCC cells under normoxia. Our results reported a different response to sorafenib, melatonin and their combination among the three different cell lines tested. HepG2 and Huh7 were quite sensitive to sorafenib treatment, whereas only the highest dose of this drug was able to reduce significantly the viability of Hep3B. These data suggest the preexistence of an innate resistance to this chemotherapeutic drug in Hep3B cells, but not in HepG2 and Huh7 cells. This inherent resistance of Hep3B to sorafenib treatment has been recently corroborated by other authors [457,458], which clearly backs up our results. Curiously, HepG2 cells present higher innate resistance to paclitaxel than Hep3B cells [459], suggesting that the sensitivity of HCC cells to different anticancer agents may be highly dependent on their proteome. Melatonin and sorafenib combined treatment exerted a dose-dependent synergistic decrease in the viability of the three HCC lines. As expected, Hep3B cells were more resistant to combined treatment than the other two HCC lines. This additive effect has been recently corroborated in Huh7 cells [460], supporting the results obtained in the present study. In addition, melatonin has also been showed to enhance the cytotoxic action of other chemotherapeutic drugs, such as doxorubicin, clofarabine or 5-fluorouracil, in many different cancer types [404,405,446]. Similarly to melatonin, the administration of the flavonoid quercetin has demonstrated to reduce the viability of sorafenib-treated glioblastoma multiforme and anaplastic astrocytoma cells [461]. With the purpose of analyzing the pathways that could be responsible for the

modulation of the innate resistance to sorafenib in HCC, Hep3B cell line was selected to perform the rest of the experiments in the present thesis.

Apoptosis induces tumor cell death in response to the irreversible DNA damage that occurs during tumorigenesis, as well as after the administration of many anticancer drugs [365]. Indeed, it is not strange to note that the levels of this PCD response are reduced in the tumor cells that present resistance to chemotherapy [432]. Melatonin has demonstrated to decrease cell resistance to doxorubicin by enhancing apoptosis in hepatoma cells [404], suggesting that this pathway could be partly responsible for the reduction of HCC viability observed after the sorafenib and melatonin coadministration. PARP cleavage and Bax expression were significantly induced after this cotreatment, but not following sorafenib administration alone. Moreover, Annexin V-PI fluorometric assay corroborated these results, since apoptosis were only stimulated after the coadministration of the indoleamine and the chemotherapeutic drug. Otherwise, it has also been reported that the administration of quercetin to sorafenib-treated cells is able to enhance the activation of PCD type I response [461]. Summarizing, all these data suggest that melatonin partly reduces innate cell resistance to sorafenib by inducing apoptosis.

It has been demonstrated that sorafenib is able to induce autophagy pathway in Huh7 cells, but not in Hep3B [458], which suggests that the lack of this degrading response would be responsible for their low sensitivity to this drug. Besides, autophagy overinduction in cancer cells could enhance their death through type II PCD [365]. Similarly to non-specific autophagy, mitophagy has also been reported to prevent tumorigenesis and to restrain tumor cell proliferation and invasion [347]. Indeed, the loss of Parkin expression has been related with the spontaneous appearance of liver tumors, suggesting that this protein could exert a tumor-suppressive effect [347]. Our results demonstrated that melatonin and sorafenib cotreatment stimulated the expression of this mitophagy marker at 3 and 6 h post-treatment. Besides, this induction in Parkin expression after cotreatment was concomitant with an increment in the protein levels of PINK1, which is in charge of the recruitment of this protein to damaged mitochondria for inducing its degradation [331]. Moreover, the expression of LC3 was also induced following 6 and 12 h of melatonin and sorafenib coadministration, suggesting that the upregulation of PINK-Parkin pathway is inducing mitophagy response and not protein degradation by the proteasome. Besides, autophagosome and mitochondria colocalization corroborated the enhancement of mitochondrial degradation by mitophagy at 6 and 12 h

after melatonin and sorafenib coadministration, as well as the decline of this cellular response following 24 h since the start of the treatment. Besides, the significant diminution observed in the content of mtDNA after 12 and 24 h of cotreatment confirmed that melatonin addition to sorafenib-treated cells induces the degradation of mitochondria in HCC cancer cells. Subsequently, the levels of the mitochondrial chaperone HSP60, which participates in the biogenesis of this organelle by inducing the correct folding of its proteins [424], was measured to confirm the previous data. Melatonin addition to sorafenib-treated cells induced a significant reduction in the expression of this protein at 12 and 24 h post-treatment. Summarizing these data, it seems that the coadministration of melatonin and sorafenib can enhance mitochondrial degradation through PINK1/Parkin-dependent mitophagy. Otherwise, this molecule has also been reported to induce mitophagy in head and neck cancer cells either alone or in combination with rapamycin [462]. However, the stimulation of this degradative response by melatonin was not associated with a concomitant decrease in the mitochondrial DNA content, suggesting that this hormone could induce a defective mitophagy response in these cells [462]. Similarly to autophagy, melatonin-dependent induction of this pathway in cancer cells seems to be very dependent on cell context and type [463].

Mitochondrial dynamics are essential to regulate the shape, localization, function and degradation of these organelles [303]. Moreover, the balance between the opposing fusion and fission processes modulates transiently the extent of mitochondrial degradation by mitophagy [332]. For instance, mitochondrial fusion augments the size of these organelles, preventing their incorporation into the autophagosome [330]. On the other hand, mitochondrial fission fragments damaged mitochondria to be included into the autophagosome for its degradation [332]. Therefore the fine tuning of this processes might be essential for the regulation of mitophagy [332].

Mitochondrial fusion is mainly modulated by MFN1 and MFN2 at the OMM and OPA1 at the IMM [303,304]. It has been recently demonstrated that the protein MFN2 is implied in the PINK1/Parkin-dependent mitophagy pathway since its phosphorylation by PINK1 induces the translocation of Parkin to the OMM [338]. Besides, this protein serves as a substrate for Parkin-dependent ubiquitination, which ultimately induces the inhibition of mitochondrial fusion during mitophagy [332]. Our results showed a transient reduction in MFN2 expression after 6 h of melatonin and sorafenib cotreatment, which was restored at 12 h. This diminution was concomitant with the augment observed in Parkin protein

levels. Otherwise, the overexpression of MFN2 in HCC cells has been recently associated with the enhancement of apoptosis [464]. Therefore, the increase showed in the expression of this protein after extended cotreatment periods could be associated with the reduction of sorafenib innate resistance through inducing intrinsic apoptosis in Hep3B cells.

On the other hand, OPA1 has also been reported to be cleaved after the induction of mitophagy, reducing ultimately the IMM fusion during mitochondria degradation [316]. Our results also showed a transient reduction in OPA1 expression at 3 and 6 h, restoring after 12 h of cotreatment. This diminution was concomitant with the reduction observed in MFN2 levels and with the increase in Parkin levels. Otherwise, it has been recently described that Parkin overexpression induces transcriptionally the expression of this fusion protein through promoting NF- κ B signaling [465], which could explain the restoration of OPA1 levels showed in this experiment after the overexpression of Parkin.

Mitochondria fission is mainly modulated by Drp1, as well as by the tail-anchored Fis1, Mff, MiD49 and MiD51 proteins [305]. Fis1 overexpression has been related with the induction of Parkin-dependent mitophagy in acute myeloid leukemia (AML) stem cells [466]. Unexpectedly, levels of Fis1 diminished at 6 h after sorafenib and melatonin cotreatment, whereas it increased after sorafenib alone treatment. This strange reduction could explain the restoration of PINK/Parkin-related mitophagy basal levels showed after 24 h of cotreatment. Moreover, the abolishment of Fis1 expression through silencing has been related with the induction of cell cycle arrest and the reduction of cell viability [466], thus this reduction in Fis1 levels could be associated to the overcome of sorafenib innate resistance on HCC cells. Summarizing, these results suggest that melatonin administration to sorafenib-treated HCC cells could induce a temporal reduction in mitochondrial fusion during mitophagy induction and a constant decrease in mitochondrial fission when this cellular pathway has been completed.

Mitophagy can maintain mitochondrial homeostasis against several stressful situations, such as ROS overproduction or nutrient starvation [329]. Although melatonin has normally been described as an antioxidant molecule due to its ability to scavenge ROS, it has been recently demonstrated that the pharmacological concentrations of this indoleamine can induce the opposite effect in both tumor and non-tumor cells [425]. According to these data, melatonin-related induction of mitophagy response could be associated to the overproduction of these harmful species. Either melatonin treatments alone or in combination with sorafenib were able to increase ROS levels in Hep3B cells,

whereas sorafenib treatment alone was not able to induce the overproduction of these harmful species. Melatonin has previously demonstrated to induce this effect on ROS levels in multiple cancer types, such as liver cancer or leukemic T-cell lymphoblasts [467,468]. However, the induction of oxidative stress by sorafenib is very dependent on cell type and cellular context. For instance, this drug has been reported to enhance the production of ROS in HepG2 cells [469].

Otherwise, the loss of mitochondrial membrane potential is also a key modulator of PINK1/Parkin mitophagy, since PINK1 is only stabilized in the OMM of depolarized mitochondria [331]. Therefore, the induction of PINK1/Parkin expression after combined treatment could be associated with the stimulation of the depolarization of the membrane of these organelles. Sorafenib acted as a membrane uncoupler because of its ability to disturb the basal levels of mitochondrial membrane potential, despite it was not able to induce oxidative stress. However, melatonin treatment alone was not able to depolarize this structure, although it stimulated ROS overproduction. Furthermore, when the hormone and the chemotherapeutic drug were coadministered, these two mitochondrial effects were concomitantly induced, and only in this experimental group, effective PINK/Parkin-dependent mitophagy was activated. This double induction of ROS accumulation and mitochondrial membrane depolarization was also shown in pancreatic cancer cells after the coadministration of melatonin and a chemotherapy drug, such as 5-fluorouracil, doxorubicin and cisplatin [470]. Therefore, the coordinated activation of both specific mitochondrial responses seems to be necessary to induce this degradation pathway in Hep3B cells.

As previously claimed, mitophagy could present a dual behavior in tumor cells, since it can either restrain or induce the progression of this pathology accordingly to the cancer stage [361]. Therefore, it is essential to analyze the role that presents the mitophagy response induced by the cotreatment on Hep3B cell viability by abolishing the expression of Parkin. It has been demonstrated that Parkin presents a tumor suppressive role since its inhibition in non-carcinogenic tissues spontaneously induce tumorigenesis [347]. In addition, Parkin underexpression has been detected in more than 50% of primary liver tumors [471]. These data indicate that the loss of this factor could promote tumor progression and tumorigenesis in HCC. In our experiment, the silencing of Parkin in the cells that had been cotreated with sorafenib and melatonin increased cell viability and prevented apoptosis induction by reducing Bax expression and PARP cleavage.

These data suggest that melatonin-induced mitophagy contributes to the reduction of the innate resistance to sorafenib that presents the HCC.

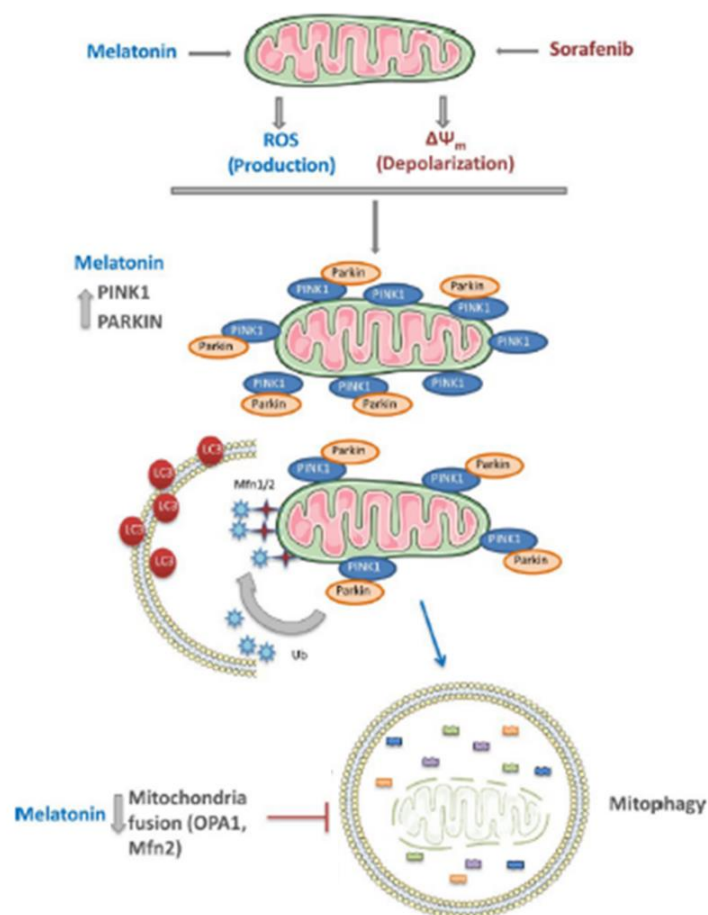


Figure 44: Proposed model of mitophagy induction after melatonin and sorafenib cotreatment under normoxia. Sorafenib addition to Hep3B cells induces the loss of the basal mitochondrial membrane potential, while melatonin administration enhances the accumulation of ROS species in the mitochondria. These two events stabilize PINK1 in the OMM, inducing the recruitment of the E3 ligase Parkin to this membrane. This system introduces the mitochondria in the autophagosome for its degradation by ubiquitinating multiple OMM substrates, such as MFN2. Besides, melatonin administration diminishes the expression of the main mitochondrial fusion proteins (OPA1 and MFN2) which leads to enhancing the activation of mitophagy response in HCC cells.

Summarizing, melatonin can reduce the innate resistance of Hep3B cells to sorafenib under normoxia by inducing mitophagy (Fig. 44). This cellular response is enhanced by both ROS accumulation and membrane depolarization and is regulated by the main mitochondrial fusion and fission proteins (Fig. 44). Finally, this induction of mitophagy after the coadministration of both drugs leads to enhancing Hep3B cell death through apoptosis (Fig. 44).

3. Effects of melatonin and sorafenib cotreatment under hypoxia in HCC cells.

An inadequate oxygen distribution during the later phases of tumor evolution could lead to enhance tumor progression due to the stimulation of angiogenesis, EMT, metastasis and immune evasion [89]. Besides, this situation usually reduces the sensitiveness to chemotherapy through several cellular mechanisms (MOC-6), such as the induction of drug efflux or the reparation of the DNA damage induced by anticancer drugs [432]. Prolonged sorafenib treatments aggravate this situation since the antiangiogenic effects of this drug in HCC cells leads to hindering the correct distribution of oxygen in the tumor [122]. This reduction in oxygen availability arises the number of HCC cells with acquired resistance to this drug, which eventually leads to the failure of the chemotherapy with this anticancer compound [122]. Accordingly, the combination of sorafenib with a compound that can sensitize advanced HCC cells to sorafenib under hypoxia could be necessary to maintain the cytotoxic activity of this anticancer drug [122].

Melatonin has demonstrated to restrain hypoxia-mediated effects, such as angiogenesis, in HCC cells cultured *in vitro* [16], thus this molecule could restrain the appearance of acquired resistance to sorafenib in HCC tumors under low oxygen concentrations. As expected, the combination of pharmacological concentrations of sorafenib (2.5, 5 and 10 μM) and melatonin (1 and 2 mM) significantly reduced the viability of Hep3B cells cultured for 48 h under normoxia conditions. Otherwise, melatonin was also able to enhance the cytotoxic effects of sorafenib in hypoxia. Indeed, the use of this hormone allowed to cut the minimum dose that is necessary to induce a significant reduction in cell viability levels by half (from 10 μM commonly used in several *in vitro* studies to 5 μM). According to the data, the use of this therapeutic combination in the treatment of HCC could extend the duration of sorafenib treatment by reducing its side effects and presenting a great cost-benefit advantage due to the high cost that present cancer therapies based on this drug [472,473].

HIF-1 α and HIF-2 α are the main cellular sensors of hypoxia since they can detect fluctuations in oxygen microenvironmental levels and induce consequently hypoxia-dependent cellular responses, such as EMT or angiogenesis [137]. It has recently been proposed that the overactivation of these transcriptional factors are directly associated with the loss of cell sensitivity [474]. Moreover, it has been reported that tissues samples from

sorafenib-resistant patients express higher levels of HIF-1 than those that belong to sensitive patients, suggesting that this protein is clearly implied in the loss of sensitiveness to this drug [122]. Therefore, the development of different strategies that can prevent the overexpression of this protein could be useful to increase the sensitiveness to sorafenib. For instance, EF24 has been demonstrated to diminish cell resistance to this drug by inducing the VHL-dependent degradation of HIF-1 α [122]. Otherwise, miR-338-3p has been reported to sensitize both HCC cells *in vitro* and mice xenograft tumors to sorafenib by restraining the expression of HIF-1 α and of its downstream genes [475]. Finally, the targeting of the HIF-1 β subunit by miR-107 is able to indirectly suppress the activity of both HIF-1 and HIF-2, leading to reduce the volume of the tumor and to arrest cell cycle progression [166].

Melatonin has been reported to alter the levels of HIF-1 α expression in several cancer types, such as in renal, hepatic, colorectal and oral squamous carcinoma [476], although the mechanism that underlies these effects is not known. In the present study, melatonin treatment alone under hypoxia was able to reduce HIF-1 α expression in a time-dependent and reversible manner, as well as to diminish HIF-2 α protein levels. Besides, sorafenib single treatment reduced the accumulation of HIF-1 α but was unable to inhibit the HIF-2 α expression under hypoxia. Conversely, combined treatment abolished the expression of HIF-1 α and HIF-2 α . Moreover, sorafenib and melatonin coadministration was also able to decrease sharply the expression of their specific target VEGF under low oxygen concentrations. These data could indicate that the addition of melatonin to sorafenib-treated cells is able to prevent the expression and activation of both oxygen-sensitive HIF subunits under hypoxia. These effects has also been reported after the use of combinations of sorafenib and other compounds, such as 2-methoxyestradiol [195].

Otherwise, the role of HIF-1 α inhibition under hipoxia on the induction of the sorafenib cytotoxic effects by melatonin was analyzed by silencing this transcription factor. The coadministration of these two molecules in combination with the HIF-1 α siRNA induced a slight and synergistic reduction in Hep3B cell viability, although there were not significant differences between silenced and non-silenced cells of each treatment. This unexpected situation could be owing to the activation of a compensatory mechanism that induces the expression of HIF-2 α and its dependent pathways after HIF-1 α knockdown to maintain hypoxia-induced responses in tumor cells [196]. Indeed, HIF-2 α expression increased sharply after the silencing of HIF-1 α under hypoxia in our experimental model,

validating the previous hypothesis. Summarizing, although HIF-1 α seems to contribute to the arising of acquired resistant cells to sorafenib in HCC tumors, the inhibition of this mediator is not enough for preventing the loss of cell sensitivity to this drug due to the activation of a compensatory pathway that involves the stimulation of HIF-2 α . Therefore, the coordinated silencing of the two oxygen-dependent HIF subunits should be necessary to determinate the role of these molecules in the appearance of sorafenib resistant cells.

HIF-1 α expression is tightly regulated at various levels [145]. Therefore, the reduction showed in the steady-state levels of this protein after the addition of melatonin to sorafenib-treated cells could be associated with alterations in its transcription, translation or degradation. Our results demonstrated that melatonin reduced the protein synthesis of HIF-1 α neither affecting to its proteasomal degradation nor decreasing its transcription. Similarly, this hormone also reduces the translation of this transcription factor in prostate cancer without altering its mRNA levels [427]. However, this mechanism seems to be cell-type-dependent and context-dependent, since melatonin prevents the ROS-dependent inactivation of PHDs in glioblastoma and colon cancer cells, which induces hypoxia-dependent degradation of HIF-1 α by the proteasome [477,478]. In this situation, melatonin acts as an antioxidant, since it is able to prevent the inactivation of PHDs through scavenging hypoxia-induced ROS overproduction [477,478]. Oppositely, melatonin works as a prooxidant molecule in our experiment, enhancing the accumulation of ROS and inactivating detoxifying enzymes, thus it is improbable that melatonin limits HIF-1 α degradation through this mechanism in this model.

It has been reported that the PI3K/Akt/mTORC1 pathway is the main mechanism that modulates the translation of HIF-1 α in response to different external stimuli, such as growth factors, oncoproteins and cytokines [171]. Indeed, mTORC1 induces protein synthesis by activating both RP-S6 and eIF-4E, which are necessary for ribosome-dependent translation [145,173]. On the other hand, mTORC2 can indirectly induce the synthesis of the proteins by enhancing the phosphorylation of Akt, which in turn represses the inhibitor of mTORC1 [261]. Moreover, the mTORC1-dependent effector p70S6K could restrain the activation of this pathway by inducing a negative feedback mechanism that represses the activity of the PI3K/Akt pathway by preventing the induction of mTORC2 [145]. In our study, melatonin inhibited the phosphorylation of mTORC1, p70S6K and RP-S6 under hypoxia, leading to induce a clear decrease in the synthesis of HIF-1 α . Similar results were obtained in prostate cancer cells since the downregulation of

mTORC1 and its effector proteins reduces the HIF-1 α protein levels [427]. Moreover, silibinin is also able to target this pathway to abolish HIF-1 α translation in HCC and in cervical cancer cells [173]. On the other hand, melatonin stimulated transiently the phosphorylation of mTORC2 and Akt under hypoxia. The activation of this negative feedback that tries to rescue the expression of mTORC1 has already been reported in HCC cells after the administration of other natural compounds, such as silibinin [173].

With the purpose of validating these results, melatonin was combined in our studies with either rapamycin or LY294002. Rapamycin is a universal mTORC1 inhibitor that can also restrain mTORC2 in a cell-type-dependent and context-dependent manner [173], whereas LY294002 restrains PI3K phosphorylation [479]. As shown in our results, rapamycin-dependent inhibition of mTORC1 phosphorylation restrained the synthesis of HIF-1 α and induced the activation of the negative feedback mechanism by inducing mTORC2 and Akt phosphorylation. Melatonin-induced exactly the same tendency as rapamycin, thus we concluded that this molecule could act as an mTORC1 repressor. Moreover, this indoleamine induced mTORC2 and Akt phosphorylation because of the induction of the negative feedback loop, but independently of PI3K, since the addition of LY294002 failed to abolish completely Akt phosphorylation. Despite melatonin has been reported to modify Akt phosphorylation in different cancer cells, its effects seem to be highly context-dependent since it is able to either induce [480] or restrain its activity [446]. Otherwise, although the effect of melatonin on mTOR complexes in cancer cells has been less studied, it has been shown that this indoleamine can restrain mTORC1 pathway in prostate cancer cells [427]. Finally, it seems that other additional pathways than PI3K/Akt/mTORC1, such as MAPK [145], could be involved in the melatonin-dependent inhibition of HIF-1 α synthesis under low oxygen concentrations since this hormone was able to decrease more sharply the expression of HIF-1 α than rapamycin.

As previously demonstrated, melatonin is able to induce mitophagy response under normoxia to reduce the innate resistance of cancer cells to sorafenib. Therefore, we subsequently analyzed if this effect is also reproducible in hypoxia. The HIF-1 α targets BNIP3 and Nix are the main proteins that induce mitophagy when the oxygen concentration in the microenvironment is low due to its ability to interact with LC3 [330]. Otherwise, p62 is broadly used to measure autophagosome formation and degradation due to its ability to specifically integrate ubiquitinated proteins and organelles into this vesicle [247]. Despite the administration of sorafenib alone diminished significantly hypoxia-induced BNIP3 and

Nix expression, this reduction was only able to delay the activation of this cellular response from 12 to 24 h, as shown by the augment in mitochondrial and lysosomal colocalization and in the expression of LC3-II and p62. Melatonin administration to sorafenib-treated cells abolished synergistically the expression of all the mitophagy- and autophagy-related markers tested in this experiment, as well as the colocalization between mitochondria and lysosomes. Moreover, the concomitant downregulation of BNIP3, Nix and HIF-1 α after melatonin and sorafenib cotreatment and the reduction of BNIP3 protein levels after HIF-1 α silencing suggests that the coadministration of these two molecules is able to reduce mitophagy response by targeting the activity of this transcription factor.

Backing up our results, it has recently been reported that the specific combination of a chemotherapeutical drug with a mitophagy repressor can restrain more effectively the proliferation of cancer cells. For instance, the mitophagy and mitochondrial inhibitor-1 (mdivi-1) is able to promote the cytotoxic effects of cisplatin [481], as well as to reduce the harmful off-target effects of doxorubicin [482]. Besides, the addition of liensinine, an isoquinoline alkaloid that impedes the fusion between autophagosomes and lysosomes, to doxorubicin enhances its capability to induce cell death in breast cancer cells [483]. Finally, the coadministration of sorafenib and Baf A1 sharply decreases breast tumor growth *in vivo*, as well as metastasis occurrence in lung, thymus and neck [484].

As previously claimed, mitophagy can exert divergent roles in the different phases of cancer progression [361]. More in detail, BNIP3 prevents tumorigenesis by alleviating ROS-dependent DNA damage during early stages of tumorigenesis, whereas it promotes cancer cell survival against different stress situations, such as hypoxia or oxidative stress, and reduces sensitivity to chemotherapy in later stages [361]. In our experiment, BNIP3 silencing induced a significant reduction in the viability of Hep3B cells. Moreover, PARP cleavage and Bax expression only increased significantly when the coadministration of the two compounds restrained this cellular response. Therefore, these data suggest that this cellular response sustains HCC growth under hypoxia and prevents the induction of apoptosis cell death. Indeed, the overexpression of BNIP3 has been related to the increment of tumor aggressiveness and to the prevention of cell death in endometrium and prostate cancers [485,486]

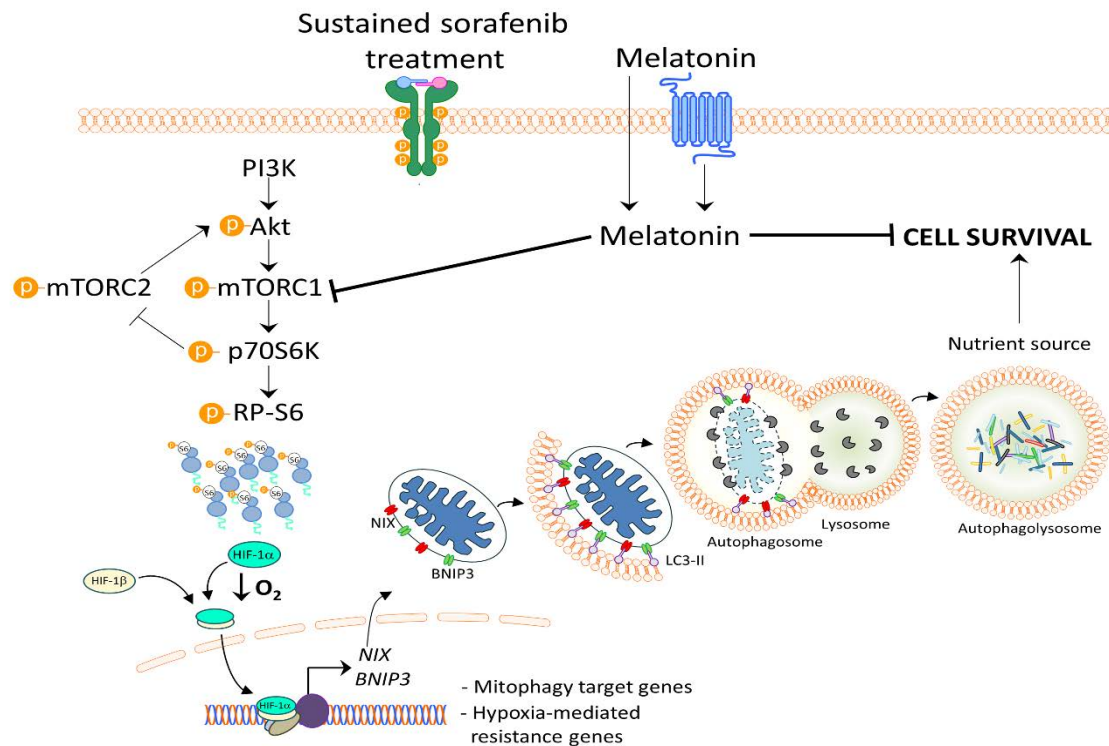
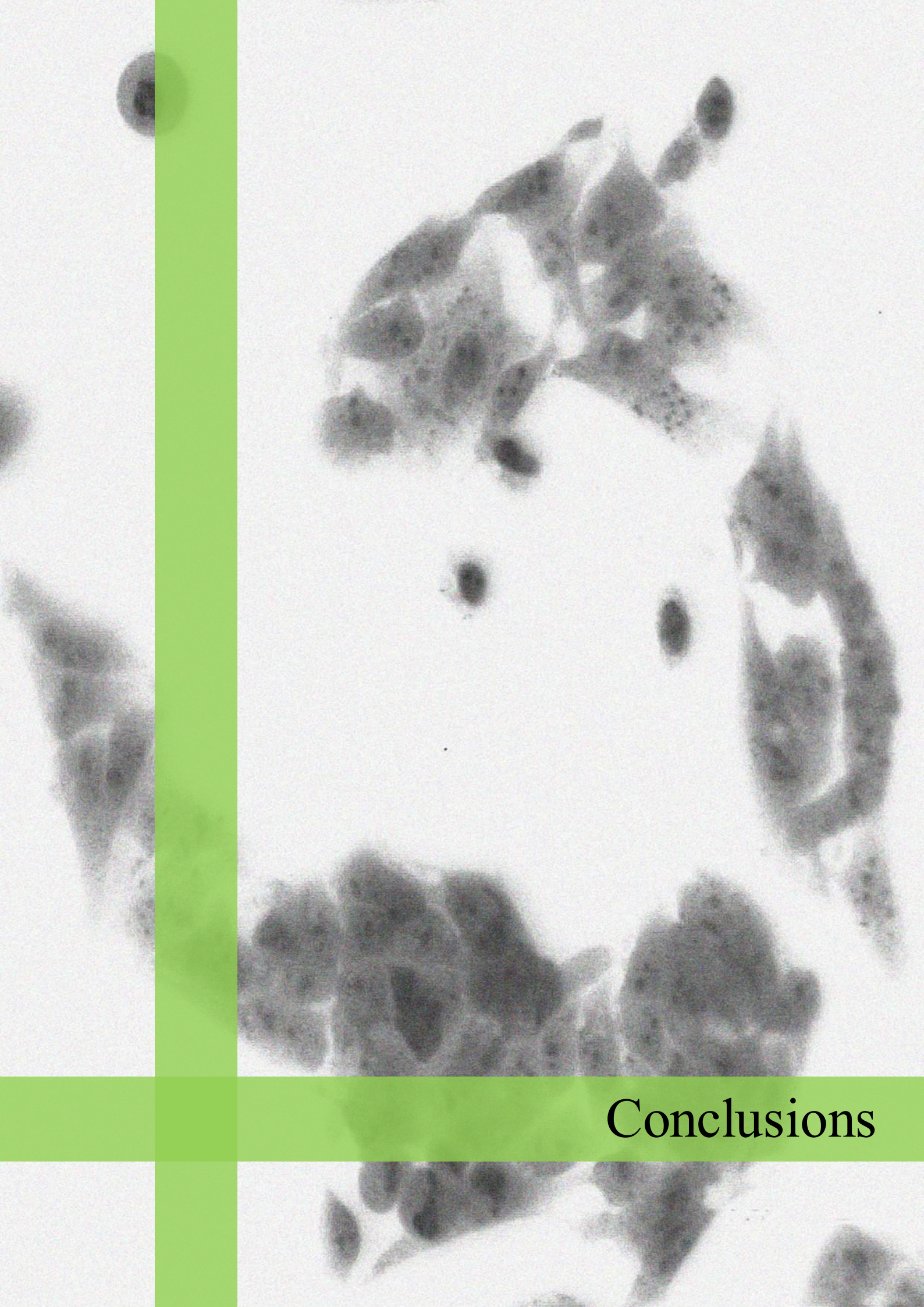


Figure 45: Proposed model of melatonin-dependent inhibition of hypoxia-induced mitophagy in sorafenib-treated cells. Melatonin restrains the synthesis of HIF-1 α by reducing the activation of mTORC1 and its downstream effectors p70S6K and RP-S6. This process leads to the decrease of BNIP3 and Nix transcription, preventing the induction of pro-survival mitophagy and inducing HCC cell death.

Curiously, it seems that the effect which presents mitophagy in Hep3B viability is highly dependent on microenvironmental status because it promotes Hep3B cell death under normoxia, but it favors cell survival under hypoxia. Summarizing, it seems that the determination of the oxygen availability in the milieu of the tumor should be necessary to determinate what role is exerting mitophagy on cancer cell death.

Altogether, our results demonstrate that melatonin is able to enhance the cytotoxic effects of sorafenib under hypoxia by restraining the expression and activity of both oxygen-sensitive HIF subunits (Fig. 45). More in detail, this indoleamine inhibits HIF-1 α protein synthesis through deregulating mTORC1/p70S6K pathway (Fig. 45). On the other hand, the coadministration of these two molecules induce apoptosis and reduced HIF1 α -dependent pro-survival mitophagy. To sum, melatonin seems to reduce acquired resistance to sorafenib in HCC cells under hypoxia.



Conclusions

First conclusion

Melatonin single administration stimulates a complete autophagy response in HCC cells through the induction both the UPR and the JNK pathways, leading ultimately to the disruption of the Beclin1 and Bcl-2 complex. In addition, melatonin-induced autophagy seems to be independent on mTORC1 signaling and to exert a prosurvival role in HCC, since this cellular response protects HCC cells from the cytotoxic actions of melatonin.

Second conclusion

Melatonin is able to stimulate the cytotoxic actions of sorafenib in HCC cells either under normoxia or hypoxia conditions through enhancing intrinsic apoptosis response.

Third conclusion

Melatonin and sorafenib coadministration under normoxia increases the accumulation of ROS in mitochondria, as well as the loss of its basal membrane potential, enhancing the elimination of these damaged organelles through PINK1/Parkin-dependent mitophagy. This cellular response exerts a prodeath behavior in HCC cells under normoxia, which leads to reducing the appearance of sorafenib innate resistant cells.

Fourth conclusion

Melatonin addition to sorafenib-treated cells can transiently reduce mitochondrial fusion in HCC cells under normoxia, which ultimately facilitates the engulfment of mitochondria by autophagosomes. Moreover, this combination can also restrain mitochondrial fission after extended time periods of treatment in order to prevent excessive and continued mitophagy induction in HCC cells.

Fifth conclusion

Melatonin and sorafenib coadministration can synergistically reduce the expression and activity of HIF-1 α in HCC cells under low oxygen concentrations. Moreover, melatonin addition to sorafenib-treated cells can also downregulate HIF-2 α protein levels in this cellular model, which sorafenib administration alone is unable to achieve. On the

other hand, the total inhibition of HIF-1 α expression in HCC cells maintained under hypoxia conditions partly reduces acquired cell resistance to sorafenib. However, these results are not significant because of the activation a compensatory mechanism that induces HIF-2 α -dependent pathways when HIF-1 α expression drops.

Sixth conclusion

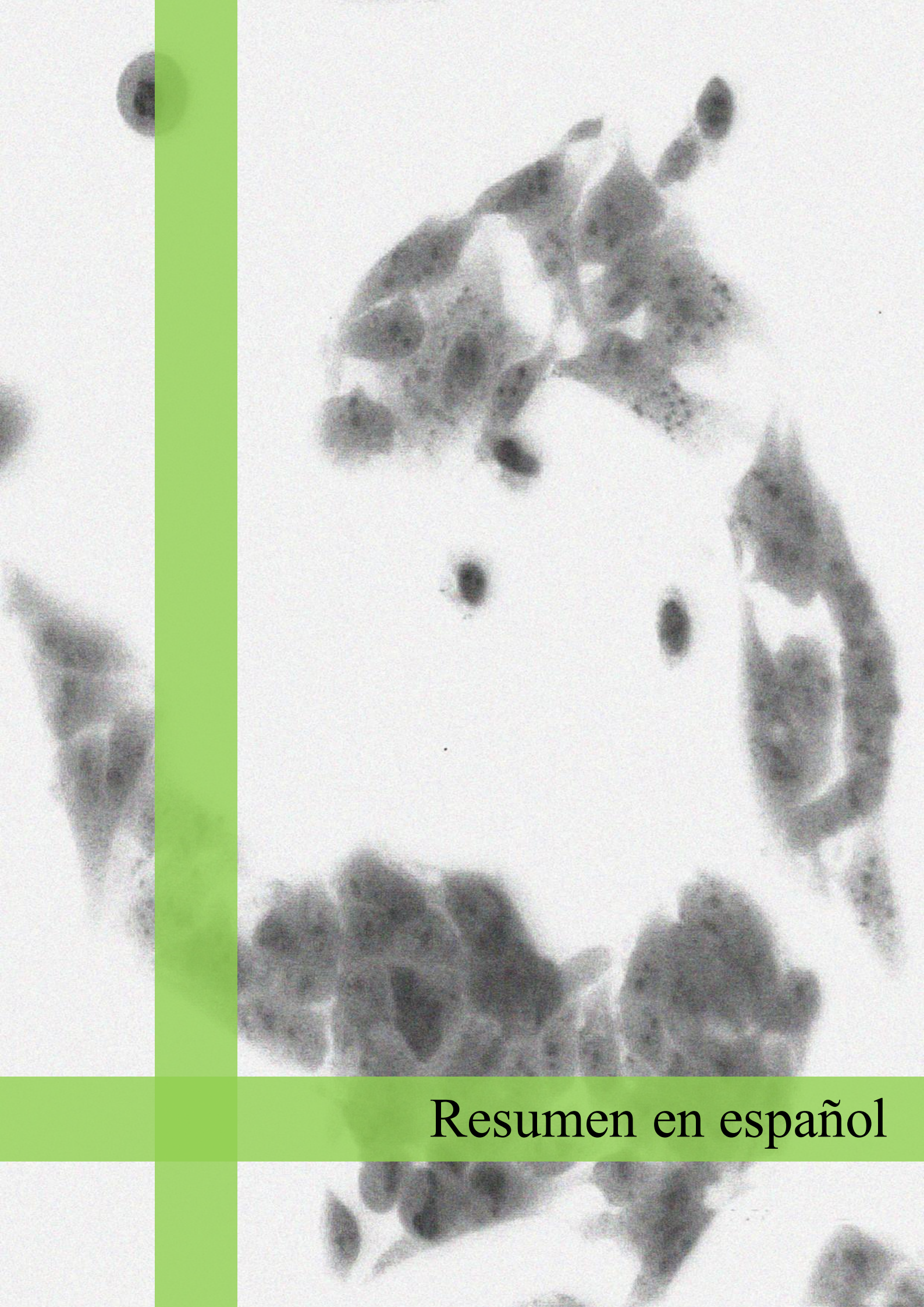
Melatonin reduces HIF-1 α protein synthesis in HCC cells under hypoxia by preventing the activation of mTORC1 and its downstream targets p70S6K and RP-S6.

Seventh conclusion

Melatonin and sorafenib coadministration decreases the hypoxia-induced degradation of damaged mitochondria into autophagosomes through reducing the expression of BNIP3 and Nix. This complete mitophagy response seems to promote the survival of HCC cells under hypoxia, since the restraining of this cellular pathway by combined treatment will reduce acquired resistance to sorafenib.

Final conclusion

Melatonin seems to modulate both nonspecific and specific mitochondrial autophagy in HCC cells, which leads to a reduction of innate and acquired resistance to sorafenib both under basal and low oxygen concentrations. Our findings support the use of this molecule to improve the efficacy of sorafenib in the treatment of advanced HCC patients. Nevertheless, these beneficial effects should be verified in some *in vivo* preclinical models, as well as in clinical trials to analyze its security and to establish optimal doses.



Resumen en español



Universidad de León

Instituto Universitario de Biomedicina (IBIOMED)

Modulación de la autofagia selectiva y no selectiva por melatonina en condiciones de normoxia e hipoxia: Potencial interés en el tratamiento del hepatocarcinoma con sorafenib

Modulation of selective and non-selective autophagy by melatonin in conditions of normoxia and hypoxia: potential interest in the treatment of hepatocarcinoma with sorafenib



Memoria presentada por D. Néstor Prieto Domínguez para la obtención del título de Doctor por parte de la Universidad de León

León, septiembre de 2018

Índice general

<i>Índice de figuras</i>	<i>vii</i>
<i>Índice de tablas</i>	<i>xvii</i>
<i>Índice de abreviaturas</i>	<i>xix</i>
1. Introducción y objetivos	1
2. Revisión de la literatura	5
2.1. Cáncer hepatocelular.....	7
2.2. El sorafenib.....	20
2.3. Hipoxia y microambiente celular en la progresión tumoral. Papel de los HIFs.....	29
2.4. La autofagia.....	38
2.5. Dinámica mitocondrial y mitofagia.....	56
2.6. La apoptosis y su interrelación con la autofagia.....	69
2.7. Melatonina: estructura, síntesis y funciones.....	74
3. Material y métodos	81
3.1. Ámbito de trabajo.....	83
3.2. Cultivo celular, tratamiento y reactivos.....	83
3.3. Determinación de los niveles de viabilidad celular y apoptosis.....	84
3.4. Determinación de los niveles de expresión proteica.....	86
3.5. Técnicas de análisis de ácidos nucleicos.....	89
3.6. Determinación del daño mitocondrial.....	91
3.7. Técnicas de microscopía confocal de barrido laser.....	92
3.8. Silenciamiento génico.....	94
3.9. Análisis estadístico.....	95
4. Resultados	97
4.1. Efecto de la melatonina sobre la autofagia en las células de HCC.....	99
4.2. La melatonina modula la sensibilidad al sorafenib de las células HCC mantenidas en hipoxia.....	105

4.3. La modulación de la sensibilidad al sorafenib de las células de HCC mantenidas en hipoxia.	115
5. <i>Discusión</i>.....	129
5.1. Efectos de la administración de melatonina sobre la respuesta autofágica en las células HCC.	133
5.2. Efectos del cotratamiento de melatonina y sorafenib sobre las células de HCC mantenidas en normoxia.	136
5.3. Efectos del cotratamiento de melatonina y sorafenib sobre las células de HCC mantenidas en hipoxia.....	142
6. <i>Conclusiones</i>	149
7. <i>Resumen en español</i>.....	153
7.1. Introducción.....	159
7.2. Objetivos.....	173
7.3. Material y métodos.....	175
7.4. Resultados y discusión.....	184
7.5. Conclusiones.....	205
8. <i>Referencias</i>.....	207

1. Introducción.

1.1. El cáncer hepatocelular (HCC por sus siglas en inglés).

El HCC es el cáncer hepático más diagnosticado anualmente, estimándose la aparición de 841,000 nuevos casos este 2018 [1]. La incidencia de esta patología es bastante desigual entre las diferentes regiones del mundo, siendo más frecuente en el Sudeste Asiático y en África Subsahariana y menos en América del Norte, Europa y Oceanía (Fig. 1) [1,3]. Dentro de Europa, la zona sur presenta la mayor incidencia de todo el continente (Fig. 1) [2]. De hecho, en 2015 en España se diagnosticaron 4.252 nuevos casos de HCC en varones y 1.610 en mujeres respectivamente [5], lo cual fue bastante más elevado que la media europea [6]. Aunque las técnicas de diagnóstico precoz y de tratamiento del HCC han avanzado considerablemente en los últimos años, la prognosis de este cáncer sigue siendo muy pobre, con una ínfima tasa de supervivencia a 5 años, lo que lo lleva a ser la segunda causa global de muerte relacionada con el cáncer en varones [1,2].

Existen múltiples factores etiológicos que favorecen la aparición del HCC [18]. Entre ellos, el desarrollo de una hepatitis crónica debido al contagio con el virus de la hepatitis B (HBV por sus siglas en inglés) o con el virus de la hepatitis C (HCV por sus siglas en inglés) son los principales factores que inducen la hepatocarcinogénesis [18]. Aunque la vacunación y los nuevos protocolos antivirales están reduciendo progresivamente la aparición de nuevos casos de HCC con origen viral, la incidencia de dicha enfermedad en los países desarrollados sigue aumentando debido a causas no víricas, como el consumo abusivo de alcohol y/o tabaco, la obesidad y la diabetes de tipo II [1]. Diversos estudios han demostrado que el control de la ingesta de dichas sustancias nocivas, así como el consumo abundante de fruta, vegetales de hoja verde, carne blanca, huevos, derivados de soja y café puede impedir la aparición de tumores hepáticos [30–32]. Por otra parte, el HCC presenta mayor incidencia en hombres, en personas de edad avanzada, en los asiáticos y en los nativos americanos [19,42,43].

El diagnóstico temprano de este cáncer es clave para conseguir su total remisión [19]. Sin embargo, existen grandes dificultades debido a que los tumores hepáticos suelen ser asintomáticos o presentar síntomas semejantes a otras enfermedades hepáticas como la cirrosis [9]. Actualmente, las técnicas de imagen, como la ultrasonografía, la tomografía axial computarizada, la resonancia magnética nuclear y la angiografía, son muy usadas en el diagnóstico de pequeños tumores hepáticos debido al bajo riesgo que poseen para el

paciente (Fig. 3) [45–47]. Por otra parte, la mejora de las técnicas de análisis de distintos marcadores diagnósticos, como la α -fetoproteína (AFP), la des- Γ -carboxiprotrombina (DCP), la osteopontina (OPN) o el glipicano-3 (GPC-3), ha acrecentado la detección temprana de pequeñas masas tumorales [53]. No obstante, la presencia de tejido cirrótico alrededor del tumor puede enmascararlo parcialmente, por lo que nuevas técnicas deben de ser desarrolladas para posibilitar la detección de estos tumores [9].

El tratamiento del cáncer hepatocelular es altamente dependiente del estadio en el que se encuentre el tumor, por lo que la correcta categorización de los pacientes es esencial en la toma de decisiones clínicas [61]. Aunque se han desarrollados múltiples escalas para categorizar a los pacientes con HCC, el índice para cáncer de hígado desarrollado en el hospital Clínic de Barcelona (BCLC por sus siglas en inglés) es la que presenta mayor precisión en la estadificación de dicha patología (Fig. 4) [63]. Este sistema divide los pacientes afectados con HCC en 5 categorías diferentes, según el tamaño del tumor y la funcionalidad del tejido circundante, asignando a cada uno de ellos un tratamiento específico (Fig. 4) [62]. Los pacientes que poseen tumores de pequeño tamaño (menores de 3 cm) y función hepática intacta son susceptibles a los tratamientos quirúrgicos, como el trasplante, la resección y la ablación hepática; los cuales pueden lograr la remisión total del cáncer [67]. Sin embargo, aquellos pacientes detectados en estadios avanzados de la progresión tumoral solo son susceptibles a la quimioembolización o radioembolización transarterial y al tratamiento sistémico con sorafenib o lenvatinib [64]. Desgraciadamente, estos tratamientos solo presentan efectos paliativos, pues retrasan pero no impiden el avance del cáncer hepatocelular [69]. Por tanto, el desarrollo de nuevas terapias es fundamental para lograr la remisión del HCC en los estadios tardíos [66].

1.2. El sorafenib.

El sorafenib ha sido el primer fármaco quimioterápico sistémico que demostró tener capacidad para incrementar la supervivencia de los pacientes con dicho tumor en estadios avanzados [78,79]. Dichos resultados fueron confirmados en dos ensayos clínicos independientes de fase III que fueron realizadas en países occidentales (SHARP) y en la región Asia-Pacífico [78,79]. Estos efectos beneficiosos posibilitaron su aprobación por la *American Food and Drug Administration* (FDA) y la *European Medicines Agency* (EMA) para el tratamiento de los estadios avanzados de dicha patología [82]. Este quimioterápico

también ha sido autorizado para su uso en el tratamiento del cáncer renal y del cáncer tiroideo metastático y resistente a la radioterapia [83,84].

El sorafenib es capaz de restringir la proliferación, angiogénesis y progresión del HCC a través de la inhibición de diversas serina/treonina proteín quinasas, así como algunos receptores tirosina quinasa [89,90]. Por ejemplo, esta molécula es capaz de reducir la actividad de las quinasas de proteína activadas por mitógeno (MAPK), concretamente de la quinasa regulada por señales extracelulares 1 (ERK1) y la quinasa c-Jun N-terminal (JNK), a través de la inhibición de cRaf y RafB, lo cual provoca la detención del ciclo celular y la reducción de la malignidad celular (Fig. 5A) [91,93]. Además, este fármaco es capaz de inducir la vía intrínseca de la apoptosis a través de la reducción de la expresión de la proteína de leucemia mieloide-1 (Mcl-1), la cual impide la acción del exterminador celular homólogo de la proteína de linfoma de células B (Bak) (Fig. 5A) [81,90]. Por otra parte, el tratamiento con sorafenib inhibe la actividad tirosina quinasa de los receptores del factor de crecimiento del endotelio vascular 2 y 3 (VEGFR2, VEGFR3) y del factor de crecimiento plaquetario (PDGFR- β), lo cual previene el crecimiento de vasos sanguíneos hacia el tumor [81,89]. Esta reducción en la angiogénesis tumoral promueve la muerte programada de las células tumorales debido a una distribución deficiente de nutrientes y oxígeno en la masa tumoral [81]. Por último, estudios recientes han demostrado que el sorafenib es capaz de inducir la respuesta macroautofágica en las células tumorales (Fig. 6) [81,90]. Esta inducción esta modulada por un gran número de mecanismos intracelulares, entre las que destaca las vías de fosfoinositol 3-quinasa (PI3K)/Akt/complejo 1 de la diana de la rapamicina en mamíferos (mTORC1), de las ceramidas, de la quinasa activada por AMP (AMPK), así como de la respuesta a proteínas desplegadas (UPR) (Fig. 6) [90].

Aunque los tratamientos con sorafenib son inicialmente bien tolerados, no es extraño la aparición de efectos adversos que pueden forzar la reducción de las dosis o la suspensión de su administración [88,99]. Afortunadamente, la mayoría de esos efectos son leves o moderados [88]. Sin duda, las lesiones cutáneas y la diarreas son los efectos adversos más abundantes, pues afectan respectivamente al 90% y al 27,1% de los pacientes en tratamiento con sorafenib [100,102]. Otros efectos nocivos que pueden aparecer tras el tratamiento con sorafenib son la hipertensión, la fatiga o los síndromes cardiacos como la isquemia cardiaca o el infarto de miocardio [98,99]

Además de los efectos adversos anteriormente descritos, otra limitación importante a tener en cuenta durante la administración prolongada de sorafenib es la aparición de

células resistentes que no son capaces de responder al tratamiento con dicho fármacos [89,105]. Estos procesos son responsables de la decepcionante tasa de beneficio obtenida tras la administración de dicho quimioterápico en pacientes con HCC, la cual es del 30% al inicio del tratamiento [105]. Existen principalmente dos tipos diferentes de resistencias al sorafenib [105]:

- La resistencia primaria o innata, que parece debida a la elevada heterogeneidad que presenta los tumores hepáticos, lo cual puede ocasionar que las dianas terapéuticas del sorafenib no se expresen; impidiendo que dicha droga pueda ejercer sus efectos antitumorales (Fig. 7) [105,108].
- La resistencia adquirida, que parece asociada al progresivo bloqueo de la capacidad oncostática del sorafenib a través de la activación de determinados mecanismos celulares como la autofagia, la respuesta a hipoxia o la transición epitelio mesénquima (EMT por sus siglas en inglés) (Fig. 7) [105,108]. A diferencia de la innata, la cual aparece al inicio del tratamiento con el sorafenib, la adquirida suele darse tras la administración prolongada de dicho fármaco [105,108].

Afortunadamente, se están desarrollando progresivamente nuevas estrategias terapéuticas que evitan la desensibilización celular al sorafenib, aumentando de esa forma su eficacia en el tratamiento del HCC [107]. Dichas estrategias incluyen el uso de adyuvantes terapéuticos que impidan la activación de las vías que encubren los efectos antitumorales del sorafenib, así como el uso de terapias de segunda línea que permitan la reducción de la proliferación celular tras la desensibilización, como el regorafenib o el nivolumab [80,107].

1.3. Hipoxia y microambiente celular en la progresión cancerígena, papel de los factores inducibles por hipoxia (HIF).

Durante las fases tardías de la progresión tumoral, no es raro observar áreas en el interior de la masa tumor que demandan más oxígeno del que se les suministra [129,130]. Este fenómeno es, al menos en parte, debido al alto ratio proliferativo que presentan las células tumorales, lo cual lleva al incremento de la distancia existente entre el centro del tumor y la microvasculatura, lo que reduce el suministro de oxígeno y de nutrientes

[129,130]. Las células tumorales situadas en dichas áreas presentan mayor agresividad y menor sensibilidad a la quimioterapia y la radioterapia [128], a través de la activación de múltiples vías de supervivencia, como la angiogénesis, la EMT y la metástasis [131].

Todas estas respuestas están moduladas por los HIFs, un conjunto de proteínas que detectan cambios en la concentración de oxígeno en el microambiente [131]. Estos factores reconocen una región específica de 5 nucleótidos en la secuencia de ADN que se conoce como elemento de respuesta a hipoxia (HRE), la cual se encuentra situada en las regiones promotoras de sus genes diana [138]. Estas proteínas están constituidas por una subunidad α que es dependiente de oxígeno, de la cual se conocen 3 tipos diferentes, HIF-1 α , HIF-2 α y HIF-3 α [137]. Por otra parte, también están formados por una subunidad β que es independiente de la concentración de ese gas en el microambiente, de las cuales también se conocen 3 subunidades diferentes, HIF-1 β /translocador nuclear del receptor de los hidrocarburos arilos (ARNT1), ARNT2 y ARNT3 [137]. Las subunidades α se hidroxilan en normoxia por las prolinas hidroxilasas (PHDs) para ser posteriormente reconocidas por la proteína von Hippel–Lindau (VHL), la cual poliubiquitina a dichas subunidades, lo cual lleva a su degradación en el proteasoma (Fig. 9) [145]. Cuando la concentración de oxígeno se reduce, se produce una situación de hipoxia, siendo las PHDs incapaces de hidroxilar a dichas subunidades, lo cual les permite translocarse al núcleo y heterodimerizarse con una subunidad β (Fig. 9) [146,154]. Esta unión permite unirse a las regiones HRE y activar la transcripción de los genes diana en conjunto con la proteína coactivadora unida a CREB (CBP) y p300 (Fig. 9) [146,154]. Por otra parte, el factor inhibidor de HIFs (FIH) actúa como un segundo regulador de la actividad de estas proteínas en normoxia, impidiendo su unión con CBP y p300 (Fig. 9) [144].

Además de la regulación de la proteína HIF-1 α por parte de las PHDs y de FIH, también existen otros mecanismos que no están regulados por la concentración de oxígeno en el medio (Fig. 10) [145]. Algunos de esos son capaces de modular la traducción de dicho factor, como la vía de PI3K/Akt/mTORC1 y de las MAPK, mientras que otros estimulan la degradación de HIF-1 α por el proteasoma, como p53 (Fig. 10) [145]. Por último, la unión entre estos factores y sus proteínas coactivadoras p300 y CBP se ve estimulada por la ruta de las MAPK (Fig. 10) [174].

1.4. La autofagia.

La autofagia se encarga de regular la homeostasis celular en los organismos eucariotas a través de la degradación de las macromoléculas y orgánulos que se encuentren dañados o que sean disfuncionales para la célula [197,198]. Sin embargo, la activación prolongada de esta vía puede llevar a la inducción de la muerte celular programada (PCD por sus siglas en inglés) debido a la eliminación de componentes vitales para la célula [198]. No obstante, no está claro si es la autofagia la que induce la PCD de tipo II o si es la sobresaturación de esta vía homeostática lo que estimula la aparición de esta respuesta nociva [201].

Hasta la fecha se han descrito tres tipos diferentes de autofagia: la macroautofagia, la mediada por chaperonas (CMA por sus siglas en inglés) y la microautofagia (Fig. 11) [202]. La macroautofagia (que a partir de ahora llamaremos simplemente autofagia) es el mecanismo autofágico más frecuentemente inducido en las células eucarióticas [208]. Éste se caracteriza por la formación de una vesícula de doble membrana, llamada autofagosoma, que contiene el conjunto de macromoléculas y orgánulos a degradar (Fig. 11) [209,210]. Posteriormente, el autofagosoma se fusiona con los lisosomas para formar una vesícula híbrida denominada autolisosoma, donde el contenido autofagosomal será degradado por las enzimas lisosomales (Fig. 11) [209,210]. Finalmente, el resultado de la degradación es liberado al citosol, donde se reutilizará si fuese necesario para formar nuevos componentes celulares [209,210]. La carga contenida en el autofagosoma puede ser introducida selectivamente a través de una serie de proteínas sensoras que detectan orgánulos dañados y los introducen en el autofagosoma [211]. Dependiendo de la carga que selectivamente entre en el autofagosoma podemos distinguir varios tipos de autofagia, como la mitofagia, la pexofagia, la agrefagia o la reticulofagia (Fig. 11) [211].

La maquinaria molecular que permite la formación del autofagosoma y su maduración está constituida por las proteínas reguladoras de la autofagia (Atg) (Fig. 12) [209,210]. En mamíferos, estas proteínas se asocian entre sí para formar 5 complejos que actúan correlativamente en la formación de dichas vacuolas (Fig. 12) [209,210]. El primer complejo, el de la proteína semejante a Unc-51 (ULK1), se encarga de iniciar dicho proceso a través del reclutamiento del resto de ellos (Fig. 12) [216]. Seguidamente, el complejo formado por la proteína de clasificación vacuolar (Vps34)-Beclin1 permite el aislamiento del fragmento de membrana que va a dar origen al autofagosoma, además de que promueve

su nucleación al incrementar la concentración de fosfatidilinositol 3 fosfato (PI3P) en una zona concreta del fagóforo (Fig. 12) [214,223]. Por otro lado, la proteína mAtg9 se encarga de la elongación del fragmento aislado de membrana (Fig. 12) [232]. Por otra parte, la acción correlativa de los complejos semejantes a ubiquitina Atg5-Atg12-Atg16L y la proteína asociada a la cadena ligera de los microtúbulos (LC3) con fosfatidiletanolamina (PE) (LC3-II) estimula la expansión final de la membrana autofagosomal y su cierre hasta formar la vesícula madura (Fig. 12) [240]. Así mismo, LC3-II también se encarga de reconocer selectivamente la carga a introducir en el autofagosoma, puesto que interacciona con la mayoría de las proteínas que insertan orgánulos en dicha vesícula [245]. Finalmente, la familia de los receptores de proteínas de fijación soluble de NSF (SNARE) median la fusión entre el autofagosoma y el lisosoma (Fig. 13) [251].

La respuesta autofágica puede estar modulada por un gran número de factores tanto extracelulares como intracelulares [212]. Estos son capaces de alterar tanto la expresión como la actividad de los principales componentes que intervienen en la formación de las vesículas autofágicas [212,257]. Algunos de estos factores son la falta de nutrientes o energía, la UPR, el estrés oxidativo, la producción de esfingosina 1-fosfato (S1P) y la falta de oxígeno en el medio (Fig. 12) [257].

Diversos estudios han demostrado que la desregulación de la autofagia puede favorecer la progresión de determinadas patologías, como el cáncer, las enfermedades neurodegenerativas, las cardiovasculares o las gastrointestinales (Fig. 14) [290]. En el caso del cáncer, la autofagia parece ejercer un doble papel durante las distintas fases de la progresión tumoral, puesto que esta vía previene la tumorigénesis en las etapas más tempranas, mientras que promueve la supervivencia de las células tumorales y su resistencia a la quimioterapia en las más tardías [287,289]. Por otra parte, la autofagia previene la progresión de las enfermedades neurodegenerativas a través de la eliminación de los acúmulos de proteínas mal plegadas que impiden el funcionamiento normal de las neuronas (Fig. 14) [287,288]. Además, la reducción de los niveles de autofagia en el hígado induce un desequilibrio entre las vías catabólicas y anabólicas, lo cual lleva a la agravación de múltiples desordenes metabólicos, como la obesidad, la esteatosis hepática no alcohólica (NAFLD por sus siglas en inglés) o la diabetes de tipo II (Fig. 14) [289,290]. Por último, la desregulación de los niveles basales de dicha vía en los cardiomiocitos induce la muerte de estas células debido a la acumulación de sustancias dañinas para las mismas, induciendo

algunas cardiopatías, como el infarto de miocardio o la hipertrofia cardiaca (Fig. 14) [287,290].

1.5. Dinámica mitocondrial y mitofagia.

1.5.1. Los procesos de fusión y fisión celular.

Las mitocondrias no son orgánulos quiescentes, sino que su morfología, y distribución cambia constantemente en función de diferentes estímulos externos e internos [303]. Los procesos de fusión y fisión mitocondrial son los principales mecanismos que regulan su dinámica (Fig. 15) [303]. A su vez, dichas respuestas celulares se encuentran estrechamente moduladas por un conjunto de proteínas situadas tanto en la membrana externa (OMM por sus siglas en inglés) como en la interna (IMM por sus siglas en inglés) de la mitocondria (Fig. 15) [303].

La fusión mitocondrial se encuentra regulada por una serie de proteínas asociadas a GTP situadas tanto en la membrana externa como en la interna de dicho orgánulo (Fig. 15) [304]. Estas proteínas son capaces de anclar las membranas de dos mitocondrias vecinas a través de la formación tanto de homodímeros, como de heterodímeros (Fig. 15) [304]. Posteriormente, dichas membranas se aproximan hasta su unión a través de la generación de un cambio conformacional en dichas proteínas que es dependiente de la hidrólisis de una molécula de GTP [304]. El proceso se inicia con la fusión de la OMM por parte de las mitofusina 1 y 2 (MFN1 y MFN2), y continúa tras la fusión de dicha membrana con la fusión de la IMM por parte del factor de atrofia óptica (OPA1) y la cardiolipina (CL) (Fig. 15) [311]. Aunque este proceso está completamente coordinado entre las dos membranas, no se ha esclarecido aún totalmente el mecanismo molecular que permite dicho acoplamiento [305].

Por otra parte, la fisión mitocondrial está mediada principalmente por la proteína relacionada con la dinamina (Drp1), la cual también está asociada a GTP (Fig. 15) [303]. Esta proteína es atraída a las mitocondrias diana debido a que en la OMM de dichos orgánulos se expresan una serie de receptores que presentan alta afinidad por dicha proteína, como el factor de fisión mitocondria (Mff) y las proteínas de dinámica mitocondrial N-terminalmente ancladas de 49 y 51 kDa (MiD49 y MiD51 respectivamente) [305]. Una vez asociada a esos receptores, Drp1 es capaz de oligomerizar y formar una

estructura en forma de anillo rodeando la mitocondria (Fig. 15) [311]. Posteriormente, la hidrólisis de la molécula de GTP unida a Drp1 induce la disminución del diámetro del anillo y la escisión de ambas membranas mitocondriales (Fig. 15) [305]. Estudios recientes han demostrado que la unión de un ramal de retículo endoplasmático alrededor de la mitocondria a través de la interacción de la proteína de fisión mitocondrial 1 (Fis1) con Mff-Drp1 facilita el proceso de ruptura de dicho orgánulo [318,322].

1.5.2. La mitofagia.

La inserción selectiva de las mitocondrias disfuncionales en los autofagosomas para su degradación, o mitofagia, es el principal mecanismo que tiene la célula para mantener la homeostasis mitocondrial tras periodos prolongados de estrés (Figs. 16 y 17) [330,331]. Este proceso normalmente se encuentra precedido por la pérdida del potencial basal de la membrana mitocondrial, así como de la fragmentación de dicho orgánulo [332]. Sorprendentemente, la fusión mitocondrial parece proteger parcialmente a las mitocondrias funcionales, puesto que impide su degradación en el autofagosoma al incrementar su tamaño [332,333]. De hecho, se ha demostrado que la expresión y la actividad de las proteínas que modulan la dinámica mitocondrial se modifica tras la inducción de la mitofagia [332]. Por ejemplo, la proteína de 19 kDa que interactúa con Bcl-2 y E1B (BNIP3) promueve la traslocación de Drp1 a la membrana, así como la desactivación de la proteína OPA1 [316,325], mientras que Parkin poliubiquitina y desactiva a las MFNs [317]. Estos procesos promueven la activación de la fisión mitocondrial, mientras que reducen la agregación de dichos orgánulos [332].

La desregulación de los niveles basales de mitofagia en los diferentes tejidos se ha relacionado con la agravación de diversas patologías como el cáncer, la enfermedad de Parkinson, la atrofia muscular o la diabetes mellitus tipo II (Fig. 17) [347]. Al igual que la autofagia, la mitofagia ejerce una doble función en el cáncer, protegiendo a las células sanas frente a la tumorigénesis en etapas tempranas del desarrollo tumoral, pero induciendo la supervivencia de las células tumorales a través de la reducción del daño oxidativo en fases más tardías (Fig. 17) [361]. Además, la inhibición de la mitofagia induce la acumulación de especies reactivas del oxígeno (ROS por sus siglas en inglés) y del nitrógeno (RNS por sus siglas en inglés) en diferentes patologías, como el Parkinson o la atrofia muscular (Fig. 17) [347]. También la acumulación de lípidos en las mitocondrias dañadas, debido a una

deficiente degradación de las mismas por la autofagia, induce la aparición de resistencia a la insulina (Fig. 17) [347]. Por todo ello, el control molecular de la mitofagia parece fundamental para evitar la progresión de dichos procesos patológicos [347].

Los principales mecanismos que insertan las mitocondrias dañadas en el autofagosoma son el que involucra a la proteína inducida por PTEN (PINK1)/Parkin y a BNIP3/proteína semejante a BNIP3 (BNIP3L/Nix) (Figs. 16 y 17) [330,331]. Otras macromoléculas que pueden también inducir la mitofagia en determinadas situaciones son la proteína contenedora del dominio FUN14 (FUNDC1), proteína 2 de linfoma de células B-L-13 (Bcl-2-L-13), prohibitina-2 (PHB-2), CL y la ceramida C₁₈ (Figs. 16 y 17) [330,331].

La quinasa de serina/treonina PINK1 y la ligasa de tipo E3 Parkin son responsables de la degradación en el autofagosoma de las mitocondrias que presenten alteraciones en su potencial basal de membrana (Figs. 16A y 17) [331]. Esta situación perjudicial es detectada por PINK1, pues esta proteína solo se puede acumular en la OMM de las mitocondrias despolarizadas (Figs. 16A y 17) [331]. Una vez almacenada en dichas estructuras, esta proteína induce la fosforilación de determinadas proteínas, como MFN2 o ubiquitina, atrayendo a Parkin a la mitocondria (Fig. 16A) [331,338]. Por otra parte, la fosforilación por parte de PINK1 del dominio de ubiquitinación de Parkin estimula su actividad ubiquitin ligasa (Fig. 16A) [331]. Una vez localizada en esta membrana, Parkin comienza a ubiquitinar progresivamente a determinadas proteínas, como MFN2, el canal selectivo a aniones dependiente de voltaje (VDAC1), la translocasa de la OMM (TOMM) y la pequeña Rho GTPasa mitocondrial (Miro) [330,331]. Este proceso estimula el reclutamiento a esa estructura de determinados receptores autofágicos, como optineurina (OPTN), p62 y proteína puntual nuclear de 52 kDa (NDP52) (Fig. 16A) [330,331]. Estas proteínas se encargan de asociar las proteína ubiquitinadas en la OMM con LC3-II, insertando de esa manera la mitocondria despolarizada en el autofagosoma (Fig. 16A) [330,331].

A diferencia de la vía Parkin/PINK1, las proteínas BNIP3 y Nix son capaces de introducir directamente las mitocondrias dañadas en los autofagosomas, debido a que poseen un dominio LIR capaz de interactuar con LC3-II en la membrana de dicha vesícula (Figs. 16B y 17) [347]. Además, la afinidad por dicha proteína se ve incrementada cuando se fosforilan determinados residuos de serina localizados cerca del dominio LIR de dichos adaptadores mitofágicos, constituyendo un segundo mecanismo para estimular aún más intensamente la mitofagia en respuesta a situaciones de estrés muy severas (Fig. 16B)

[331,347]. Estas proteínas regulan principalmente la eliminación de las mitocondrias dañadas por la falta de oxígeno, debido a que presentan un dominio HRE en su promotor (Figs. 16B y 17) [348]. Aunque dichas proteínas comparten un alto porcentaje de similitud en su secuencia y presentan una función parecida, se diferencian principalmente en su distribución espacio-temporal [330,331]. De hecho, BNIP3 está más claramente asociado con la modulación del estrés en hígado y musculo, mientras que Nix regula la eliminación de estos orgánulos en determinados procesos fisiológicos, como en la formación de eritrocitos o en la maduración de espermatozoides [330]. Además, los patrones de inducción de estas proteínas en hipoxia también difieren, puesto que BNIP3 se induce más intensamente que Nix en condiciones moderadas de falta de oxígeno [349].

1.6. La apoptosis.

La apoptosis, también llamada PCD de tipo I es, junto con la autofagia y la necroptosis, una de las principales vías por las cuales se eliminan las células dañadas o que no son funcionales [364]. La apoptosis se caracteriza por la ruptura de la cromatina nuclear, la condensación del núcleo, la desorganización del nucléolo, la reducción del tamaño celular y la pérdida de la integridad de la membrana plasmática al alterar la distribución de la fosfatidilserina en esta estructura [365,366]. Todas estas alteraciones morfológicas inducen la liberación del contenido celular en pequeñas vesículas, llamadas cuerpos apoptóticos, que serán posteriormente fagocitados por los macrófagos [366].

Las cisteínil-aspartato proteasas (caspasas) son las enzimas clave en la modulación de la apoptosis (Fig. 18) [366,367]. Se han descrito al menos cuatro diferentes vías de activación de las caspasas en las células humanas, siendo las más importantes la vía intrínseca (o mitocondrial) y la extrínseca (Fig. 18) [366]. En la primera se produce la activación de las caspasas al romperse la OMM y liberarse determinados componentes localizados en el espacio transmembrana de la mitocondria, como el citocromo c (Fig. 18) [369]. Sin embargo, en la segunda la activación de dichas proteínas se produce tras la activación de determinados receptores, como Fas, para formar el complejo inductor de la señal de muerte celular (DISC) (Fig. 18) [364,372].

1.6.1. Interrelación entre la apoptosis y la autofagia.

Los procesos de autofagia y de apoptosis están estrechamente interconectados para desarrollar una respuesta celular equilibrada ante situaciones de estrés, lo cual favorece la homeostasis tisular [374]. Esta regulación es muy compleja, pues existen gran número de mediadores involucrados en la misma [373].

La regulación de la apoptosis por parte de la autofagia comprende principalmente tres procesos diferentes [373]. Por un lado, la mayoría de las proteínas autofágicas presentan dominio 3 de homología a Bcl-2 (BH3) o tienen una función análoga a las de las proteínas con dicho dominio, lo que les permite inducir la apoptosis al secuestrar las proteínas antiapoptóticas [373]. Por otro lado, los autofagosomas pueden ser usados como una plataforma para la activación de la caspasa 8 en ausencia del complejo DISC [373]. Finalmente, la capacidad de la autofagia para modular el metabolismo celular puede llevar a la modificación indirecta de los niveles de la respuesta apoptótica [373].

Además, la regulación de la autofagia por parte de la apoptosis comprende dos procesos diferentes [373]. En primer lugar, la proteína antiapoptótica Bcl-2 puede impedir la formación de autofagosomas al secuestrar a Beclin1 [373]. Esta unión puede ser desplazada por otras proteínas con dominio BH3, como BNIP3 o Nix, lo que llevaría a la inducción de la autofagia [346]. Por otra parte, las caspasas son capaces de inducir la ruptura de un alto número de proteínas implicadas en la formación de los autofagosomas, como Beclin1, Atg5, Vps34, Atg3 o Atg4, para prevenir la activación de esta respuesta celular durante la apoptosis [373]. Los productos obtenidos tras la fractura de las proteínas Beclin1 y Atg5 promueven posteriormente la liberación de citocromo c al citosol [376].

1.7. La melatonina.

La melatonina (N-acetil-5-metoxitriptamina) es una hormona presente en tres grupos de bacterias y en la mayoría de los reinos que conforman el dominio Eukarya, como los hongos, las plantas y los animales. En los mamíferos se sintetiza principalmente en los pinealocitos de la glándula pineal. Esta estructura derivada a partir del diencéfalo, se sitúa entre el colículo superior del mesencéfalo y bajo el tercer ventrículo, justo entre los dos hemisferios cerebrales.

Aunque anteriormente se pensaba que esta glándula era la única fuente sistémica de melatonina, diversos estudios han demostrado que esta molécula se produce también en la mayoría de los tejidos humanos [379,383]. Algunos de los sitios extrapineales donde se produce esta indolamina son la retina, el cristalino, la cóclea, el pulmón, la piel, el intestino, el hígado, el riñón, el páncreas, el timo, el bazo, el tracto reproductivo, las plaquetas, la médula ósea roja y el sistema inmune [377,381]. La producción de melatonina en estos tejidos es incapaz de distribuirse al resto del organismo a través de la sangre y no sigue los ciclos circadianos (salvo la que se produce en la retina) [379,383]. Estos datos sugieren que la melatonina extrapineal presenta principalmente una función antioxidante, reduciendo la sobreproducción de ROS y RNS en los tejidos humanos [379].

La melatonina se sintetiza a partir del aminoácido triptófano a través de una vía celular formada por cuatro reacciones químicas sucesivas. En la primera se produce la transformación de dicho aminoácido en 5-hidroxitriptófano a través de la triptófano 5-hidroxilasa (TPH) (Fig. 19) [384,385]. A continuación, esta molécula se descarboxila a través de la L-aminoácido-aromático descarboxilasa (AAAD), formando la 5-hidroxitriptamina (o serotonina) (Fig. 19) [384,385]. Posteriormente, en N-acetilserotonina a través de la N-acetil transferasa (AANAT) y en melatonina a través de la hidroxindol-O-metiltransferasa (HIOMT) (Fig. 19) [384,385]. Estudios recientes han demostrado que la síntesis de la melatonina podría ser al menos parcialmente mitocondrial, debido a que la AANAT (enzima limitante del proceso), se localiza en el lumen de este orgánulo y necesita usar la coenzima A como cofactor [386].

En los mamíferos la melatonina se degrada por distintas hemoproteínas, como el citocromo P450 (CYP450), la indolamina 2,3-dioxigenasa (IDO), la mieloperoxidasa (MPO) y la eosinofil peroxidasa (EPO) [385]. El CYP450 degrada la melatonina circulante en 6-hidroxi melatonina y en N-acetilserotonina en el hígado y en otros órganos periféricos, como el intestino o la piel [387]. Posteriormente, los derivados de la melatonina son excretados como conjugados de sulfato o del ácido glucurónico [387]. Por otra parte, la IDO degrada este compuesto en N¹-acetil-N²-formil-5-metoxikinuramina (AFMK) en el sistema nervioso, mientras que la MPO y la EPO realizan este proceso en tejidos inflamatorios [387]. Además, la melatonina se puede degradar de forma no enzimática al interactuar con los ROS y los RNS [385,387].

La producción de la melatonina en la glándula pineal se regula bajo condiciones de oscuridad por el núcleo supraquiasmático (SCN) (Fig. 19) [383,384]. Durante la noche,

este núcleo hipotalámico envía una señal a la glándula pineal a través del núcleo paraventricular (PVN), el núcleo intermediolateral de la medula espinal y el ganglio superior cervical (SCG) (Fig. 19) [383,384]. La estimulación de ese ganglio induce la liberación de noradrenalina por parte de las fibras simpáticas que salen de dicha estructura, lo cual estimula la generación de AMP cíclico (cAMP) en el pinealocito, induciendo la expresión de las enzimas AANAT y HIOMT [383,384]. Algunos estudios recientes han demostrado que la dopamina también presenta un papel regulador en la producción de la melatonina en la glándula pineal, pues los receptores D₄ impiden la inducción de la síntesis de dicha molécula por la noradrenalina al unirse e impedir la activación de los receptores adrenérgicos [392].

Los mecanismos de acción que induce la melatonina están mediados en mamíferos por cuatro receptores celulares diferentes, dos transmembranales, uno citoplasmático y uno nuclear [383,388]. Los receptores de membrana MT1 y MT2 pertenecen a la superfamilia de receptores acoplados a proteínas G, siendo los encargados de regular las principales respuestas metabólicas y reproductivas asociadas a los ritmos circadianos de dicha molécula [383]. Por otra parte, la activación del receptor citoplasmático a la melatonina MT3, también llamado reductor de quinonas 2 (NQO2), protege a las células frente al estrés oxidativo [389]. Finalmente, los receptores huérfanos asociados a retinoides en el núcleo, especialmente los subtipos α y γ , actúan incrementando la transcripción de las principales dianas de dicha indolamina [383,390].

La melatonina es capaz de ejercer un alto número de funciones distintas en los mamíferos, siendo las más importantes el control de los ritmos circadianos y estacionales [381]. Por otra parte, diversos estudios han demostrado que esta molécula también presenta efectos hipnóticos, antinociceptivos, antidepresivos, ansiolíticos, anticonvulsiantes, neuroprotectores, antioxidantes, inmunomoduladores y antitumorales [392]. En HCC, esta molécula puede prevenir la proliferación tumoral a través de la inducción de la apoptosis, así como evitar la angiogénesis y la metástasis de dicho cáncer [16,17,406–408]. Todos estos datos parecen indicar que la melatonina podría ser usada como adyuvante para tratar dicha patología.

2. Objetivos.

El HCC es la quinta enfermedad maligna más prevalente globalmente, así como la segunda causa de muerte relacionada con el cáncer más frecuente en hombres. El pronóstico de esta enfermedad es muy pobre debido a la dificultad para diagnosticar esta enfermedad en estadios tempranos, así como a la falta de tratamientos curativos que tengan efecto en sus etapas tardías. Por lo tanto, el desarrollo de nuevas estrategias terapéuticas es fundamental para conseguir mejorar la supervivencia de los pacientes con HCC en etapas avanzadas.

El sorafenib fue el primer fármaco quimioterápico aprobado para el tratamiento de los estadios avanzados de dicho cáncer. Dicha molécula es capaz de reducir la proliferación y angiogénesis de células tumorales, así como de promover la apoptosis, al restringir la actividad de múltiples receptor tirosina y serina/treonina proteína quinasas. Sin embargo, la administración continuada de sorafenib normalmente reduce la disponibilidad de oxígeno en el interior de la masa tumoral debido a las propiedades antiangiogénicas que presenta este fármaco, lo que en última instancia parece estimular la aparición de células resistentes en el tumor. Además, muchos tumores hepáticos no son sensibles a dicho fármaco debido a la alta heterogeneidad que presenta este tipo de cáncer. Por lo cual, nuevas estrategias deben de ser desarrolladas para prevenir la aparición de células tumorales hepáticas que presenten insensibilidad a dicho fármaco. Recientemente han aparecido nuevos fármacos que permiten abordar esta situación, como el regorafenib o el nivolumab, pues pueden seguir reduciendo la viabilidad celular tras el fracaso del tratamiento con sorafenib.

Uno de los principales mecanismos que modulan la aparición de células resistentes es la alteración del equilibrio entre los mecanismos de supervivencia y muerte celular. Aunque tanto la autofagia no específica como la específica pueden modular estos procesos en HCC, esta regulación es dependiente de múltiples factores externos e internos. Por ejemplo, estas vías obstaculizan la tumorigénesis en las etapas más tempranas de la progresión tumoral, mientras que protegen a los tumores en estadios más avanzados frente a la quimioterapia y a la radioterapia. Por otra parte, dichas vías se encuentran estrechamente conectadas con la apoptosis, modulando la respuesta celular en función de los estímulos que lleguen a la célula tumoral. Por lo tanto, el ajuste de la respuesta

autofágica en HCC podría controlar la sensibilidad de las células tumorales a la quimioterapia.

La melatonina juega un papel clave en los mamíferos para ajustar los ritmos circadianos y estacionales a las fluctuaciones de luz y oscuridad. Esta indolamina también protege localmente a diversos órganos y tejidos frente a la inflamación, el daño oxidativo y la tumorigénesis. De hecho, diversos estudios han demostrado los efectos antiproliferativos, antiangiogénicos y antimetastásicos de la melatonina en diversos tumores humanos, así como su capacidad para estimular los efectos citotóxicos de otros quimioterápicos, como la doxorubicina o la clofarabina. Estos datos avalan su uso como adyuvante en la terapia cancerígena.

Por lo tanto, el objetivo principal de esta tesis doctoral fue el análisis de la capacidad de la melatonina para aumentar el efecto citotóxico de sorafenib, así como para reducir la aparición de resistencia innata y adquirida a este fármaco en tres líneas diferentes de células de HCC mantenidas bajo normoxia o hipoxia, a través de la modulación de las respuestas autofágicas y la apoptóticas.

Además, se propusieron los siguientes objetivos específicos:

- Determinar si la melatonina es capaz de modular la respuesta autofágica en la línea celular HepG2, así como si esta contribuye a su capacidad para reducir la viabilidad celular de las células de HCC en cultivo.
- Analizar la capacidad de la melatonina para promover los efectos citotóxicos del sorafenib en normoxia a través de la inducción de la mitofagia en la línea celular Hep3B bajo normoxia, así como el mecanismo subyacente implicado en ese proceso.
- Determinar si la melatonina es capaz de estimular los efectos oncostáticos del sorafenib en las células Hep3B mantenidas en hipoxia a través de la reducción de la expresión y actividad de los HIF.
- Estudiar el mecanismo molecular a través del cual la melatonina reduce los niveles de HIF-1 α en la línea celular Hep3B en hipoxia.
- Analizar si la coadministración de melatonina y sorafenib es capaz de modular la mitofagia en las células Hep3B mantenidas en hipoxia, así como el papel que ejerce dicha respuesta celular sobre la viabilidad de dichas células.

3. Material y métodos.

3.1. *Ámbito de trabajo.*

El trabajo experimental de la presente Tesis Doctoral se realizó en las instalaciones del Instituto Universitario de Biomedicina (IBIOMED) de la Universidad de León. Por su parte, los experimentos de microscopía confocal se realizaron en el Servicio de Microscopia de la Universidad de León y en el Departamento de Muerte y Proliferación Celular del Instituto de Investigaciones Biomédicas de Barcelona (IIB) y del Consejo Superior de Investigaciones Científicas (CSIC) de Barcelona.

3.2. *Cultivo celular, tratamientos y reactivos.*

3.2.1. *Cultivo celular.*

Durante el procedimiento experimental se usaron tres líneas celulares diferentes derivadas de HCC humano, Hep3B, HepG2 y Huh7, las cuales se obtuvieron de la Colección Americana de Cultivos tipo (ATCC) (Manassas, VA, EE.UU.). Para realizar el cultivo en monocapa de dichas líneas se usó medio de Eagle modificado por Dulbecco (DMEM por sus siglas en inglés) (Sigma-Aldrich, San Luis, MO, EE.UU.) suplementado con 10% de suero fetal bovino (FBS por sus siglas en inglés) y 100 U/ml de penicilina/estreptomicina (Gibco, Grand Island, NY, EE.UU.). Las células se mantuvieron bajo condiciones controladas de temperatura (37 °C) y de humedad (95%). Cuando la confluencia de las tres líneas superó el 75%, estas fueron subcultivadas con tripsina al 0,05% (Life Technologies, Carlsbad, CA, EE.UU.), sembrando para su mantenimiento $2 \cdot 10^6$ células de cada una en *flasks* T75 (BD Falcon, Franklin Lakes, NJ, USA).

3.2.2. *Tratamientos celulares y reactivos usados.*

Para realizar los distintos tratamientos, las células se sembraron a una densidad de $2.5 \cdot 10^5$ células por pocillo en placas de cultivo de 9,6 cm² de área. Transcurridas 24 h desde ese proceso, se reemplazó el medio contenido en los pocillos por DMEM fresco, el cual contenía diferentes concentraciones de melatonina (0,1; 0,5; 1 y 2, mM) (Sigma-Aldrich) y/o sorafenib (0,01; 0,05; 0,1; 1; 2,5; 5; 10 y 50 μM) (Santa Cruz Biotechnology,

Dallas, TX, EE.UU.). Dichos compuestos iban disueltos en dimetilsulfoxido (DMSO) (Sigma-Aldrich) con el fin aumentar su solubilidad en solventes acuosos. Para inducir la respuesta hipóxica se utilizó CoCl_2 100 μM (Panreac AppliChem, Barcelona, España). Por otra parte, los inhibidores de la acidificación lisosómica bafilomicina A1 (Baf A1) (100 nM y 5 μM) (Tocris Bioscience, Bristol, Reino Unido) y cloroquina (CQ) (50 μM) (Sigma-Aldrich) se añadieron 3 h antes del final de ciertos experimentos para determinar la integridad del flujo autofágico. Así mismo, también se usaron en determinados experimentos: SP600125, como inhibidor de JNK, a una concentración 10 μM ; LY294002, como represor de PI3K, a 50 μM ; cicloheximida (CHX), como represor de la síntesis proteica, a 100 μM ; DMOG, que inhibe la actividad de las PHD, a 1 mM; MG132, que inhibe la degradación proteasomal, a 10 μM (Tocris Bioscience); y rapamicina, como represor de mTORC1, a 20 nM (VWR, Radnor, PA, EE. UU.).

3.3. Ensayos de viabilidad celular y apoptosis.

3.3.1. Ensayo MTT.

El ensayo de bromuro de 3-(4,5-dimetiltiazol-2-il)-2,5-difeniltetrazolio (MTT), se utilizó para comparar el efecto de la administración de melatonina y/o sorafenib sobre la viabilidad celular [410]. Para realizar dicha técnica, se sembraron las células Hep3B, HepG2 and Huh7 en placas de 96 pocillos a una densidad de 5.000 células/pocillo y se trataron con las concentraciones anteriormente descritas de melatonina y/o sorafenib. Transcurridas 48 horas, el medio de tratamiento se desechó y se reemplazó por DMEM sin FBS con el reactivo MTT (Sigma-Aldrich) disuelto a una concentración 0,5 mg/ml, incubándose las células con este compuesto durante 3 h a 37 °C. Una vez transcurrido ese tiempo, se eliminó el medio libre de suero y los precipitados de color violeta fueron disueltos en DMSO, analizándose la densidad óptica de cada pocillo a 560 nm con un lector de placas (SynergyTM HT Multi-Mode Microplate Reader; BioTek Instruments, Inc.; Winooski, VT, EE.UU.).

3.3.2. Ensayo Anexina V-yoduro de propidio.

Esta técnica nos permitió determinar el porcentaje de células que estaban sufriendo PCD de tipo I en respuesta del tratamiento con melatonina y/o sorafenib [411]. Para realizar esta técnica se utilizó el kit *Alexa Fluor 448 annexin V/Dead apoptosis* (Invitrogen, Carlsbad, CA, EE.UU.), siguiendo las instrucciones del fabricante. Para ello, se sembraron las células Hep3B a una densidad de $2,5 \cdot 10^5$ células por pocillo en placas de 6 pocillos y se trataron con melatonina a una concentración de 1 mM y/o sorafenib a 2,5 μ M durante 48 horas. Transcurrido ese periodo, las células fueron tripsinizadas y centrifugadas, resuspendiéndose los pellets en 100 μ l del tampón 1x de unión a anexina con 5 μ l de anexina V y 1 μ l de yoduro de propidio. Estas muestras se incubaron durante 15 minutos a temperatura ambiente y en oscuridad. Una vez transcurrido ese tiempo, se ajustó el volumen final a 500 μ l y se pasaron 10,000 células de cada muestra por el citómetro de flujo SCAN (Becton-Dickinson, San José, CA, EE.UU.) El porcentaje de muerte celular presente en cada muestra fue analizado con el programa *Cell Quest* (Becton-Dickinson).

3.4. Western blot.

La técnica de Western blot se utilizó para detectar variaciones en la expresión de determinadas proteínas involucradas en la apoptosis, autofagia, hipoxia, mitofagia y dinámica mitocondrial entre los distintos grupos experimentales [413]. Una vez transcurrido el tiempo de tratamiento, las células Hep3B y HepG2 se separaron de la superficie de la placa de cultivo con ayuda de un buffer de homogenización que contenía 0,25 mM de sacarosa, 10 mM de Tris, 1 mM de ácido etilendiaminotetraacético (EDTA) e inhibidores comerciales de las proteasas y las fosfatasas (Roche Diagnostics, Basilea, Suiza). Posteriormente, las muestras se sometieron a un protocolo de sonicación de 2 pulsos de 20 s cada uno a amplitud 60% en un procesador ultrasónico compacto (Hielscher-Ultrasound Technology, Teltow, Alemania). La cuantificación proteica de las muestras se realizó con el reactivo de Bradford (Bio-Rad, Hercules, CA, EE.UU.) siguiendo las instrucciones del fabricante. Cantidades iguales de proteína se desnaturalizaron al mezclarse con el buffer de Laemmli y al mantenerse a 100 °C durante 5 minutos.

Las diferentes proteínas contenidas en las muestras se separaron en geles de poliacrilamida en condiciones desnaturalizantes con dodecilsulfato sódico (SDS-PAGE por

sus siglas en inglés) y se transfirieron a una membrana de fluoruro de polivinilideno (PVDF) (Bio-Rad), usando para ello el sistema de transferencia *Trans-Blot® Turbo™* (Bio-Rad) según las instrucciones del fabricante. Posteriormente, las membranas se bloquearon durante 1 h a temperatura ambiente con leche desnatada disuelta al 5% en PBS suplementado con Tween 20 al 0,05% (PBS-T) y se incubaron a 4 °C durante toda la noche con los anticuerpos primarios recogidos en la tabla 1. Así mismo, se usó un anticuerpo monoclonal contra la proteína constitutiva β -actina conjugado con la peroxidasa de rábano picante (HRP por sus siglas en inglés) a una concentración 1:50.000 (A3854, Sigma-Aldrich) como control de carga. Una vez transcurrido el tiempo de incubación con el anticuerpo primario, las membranas se lavaron tres veces con PBS-T y se incubaron durante 1 hora a temperatura ambiente con un secundario con capacidad para detectar anticuerpos procedentes de conejo (1:20.000, 31460, Thermo Fisher Scientific) o de ratón (1:5.000, P0260, Dako, Glostrup, Alemania). Las proteínas fueron detectadas con la ayuda del sustrato lumínico para Western blot *Pierce enhanced chemiluminescence (ECL)* (Thermo Fisher Scientific), siendo la densidad de cada banda medida con el programa *ImageJ* (National Institute of Mental Health, Bethesda, MD, EE.UU.).

3.5. Técnicas de análisis de ácidos nucleicos.

3.5.1. Reacción en cadena de la polimerasa cuantitativa con transcripción reversa (RT-qPCR por sus siglas en inglés).

La técnica de RT-qPCR fue utilizada para comparar la transcripción génica de determinados genes entre los diferentes grupos experimentales, identificando de ese modo determinados patrones en la expresión génica [414]. Tras realizar los tratamientos con melatonina y/o sorafenib en hipoxia o normoxia, el reactivo TRIzol® (Applied Biosystems, Calsbad, CA, EE.UU.) se utilizó para aislar el contenido en ARN de las células. La concentración de dicho ácido nucleico presente en cada una de las muestras se midió por espectrofotometría con el Nanodrop 1000 (Thermo Fisher Scientific) y el ADN residual se eliminó con el kit *RQ1 RNase-free DNase* (Promega, Madison, WI, EE.UU.). Cantidades iguales de ARN se retrotranscribieron con el kit *High Capacity cDNA reverse transcription* (Applied Biosystems). El análisis de RT-qPCR se realizó utilizando el kit *SYBR Green Probe master* (Invitrogen) con los primers listados en la tabla 2. El gen de la β -actina se usó como control endógeno. Por otra parte, la RT-qPCR de los genes *Atg5* y *HIF-1 α* se

realizó con el kit *FastStart TaqMan™ Probe Master* (Roche Diagnostics GmbH, Mannheim, Alemania). Los primers usados para detectar los genes *HIF1A* (NM001243084.1 and Hs00153153_m1) y *ATG5* (NM_001286106.1 and Hs00169468_m1) se adquirieron en *Thermo Fisher Scientific*. El gen *GADPH* (NM_002046.3 and 4326317E) se usó en este caso como control de carga. Las variaciones de la expresión génica entre los distintos grupos experimentales se midieron a través del método $2^{-\Delta\Delta CT}$, el cual fue descrito por Livak and Schmittgen [415].

3.5.2. Medida del contenido mitocondrial de ADN por reacción en cadena de la polimerasa cuantitativa (qPCR por sus siglas en inglés).

El análisis de las variaciones en el contenido de ADN mitocondrial (mtDNA por sus siglas en inglés) con respecto a los niveles de ADN nuclear (ncDNA por sus siglas en inglés) a través de la técnica de qPCR permitió monitorizar variaciones en el número de mitocondrias sin tener que purificar su contenido desde el lisado celular [416]. Tras los tratamientos, se aisló el contenido total de ADN desde el lisado celular con 250 μ l de una solución 25:24:1 de fenol, cloroformo y alcohol isoamílico respectivamente (Sigma-Aldrich). Posteriormente, se produjo la precipitación de dicho ácido nucleico con alcohol absoluto (Merck Millipore, Burlington, MA, EE.UU.) y una disolución 0,3 M de acetato de sodio (Merck Millipore). La concentración total de ADN en cada muestra se midió por espectrofotometría con el Nanodrop 1000 (Thermo Fisher Scientific). La qPCR se realizó con el kit *SYBR Green Master Mix* (Invitrogen) y con los primers enumerados en la tabla 3. Al igual que en el caso de la RT-qPCR, las variaciones en el contenido de DNA mitocondrial se midieron a través del método $2^{-\Delta\Delta CT}$ [415].

3.6. Determinación del daño mitocondrial.

3.6.1. Medida de la producción de ROS.

La sonda fluorescente DCF-DA se usó para analizar los niveles de estrés oxidativo de las células tras los tratamientos con sorafenib y/o melatonina tanto en normoxia, como en hipoxia. Para ello, las células Hep3B se sembraron a una densidad de 5.000 células por pocillo en placas de 96 pocillos y se trataron con los compuestos anteriormente descritos

individualmente o en conjunto. Justo después de este proceso, las células se trataron con DCF-DA a una concentración de 20 μ M (Sigma-Aldrich) y con Hepes a 15 mM (Sigma-Aldrich). La fluorescencia se midió inmediatamente con un lector de placas (Biotek Instruments Inc.) a 1, 3, 6 h. Para realizar dicho proceso se utilizó 485 nm como la longitud de onda de excitación y 520 nm como la de emisión. Además de los compuestos anteriormente mencionados, también se utilizaron los compuestos N-acetil cisteína (NAC) a una concentración 5 mM (Sigma-Aldrich) como captador de ROS, y peróxido de hidrógeno (Merck Millipore) como control positivo de la generación de estas especies dañinas.

3.6.2. Medida del potencial de la membrana mitocondrial.

El yoduro de 5,5',6,6'-tetracloro-1,1',3,3'-tetraetil-benzimidazolilcarbocianina (JC-1), una sonda fluorescente catiónica que se acumula únicamente en las mitocondrias no dañadas, se utilizó para medir los cambios observados en el potencial de membrana de dicho orgánulo tras la administración de melatonina y/o sorafenib [418]. Para realizar este experimento, se sembraron 60.000 células por pocillo en las placas de 24 pocillos y fueron tratadas con ambos compuestos individualmente o combinadamente durante 1, 3 y 6 h. El kit *Mitochondrial membrane potential assay* (Cayman Chemical, Ann Arbor, MI, EE.UU.) se usó para realizar este experimento según las recomendaciones del fabricante. Tras los tratamientos, las células se incubaron con el colorante JC-1 disuelto en medio fresco durante 20 minutos. La fluorescencia emitida por este compuesto se midió con ayuda de un lector de placas (Biotek Instruments Inc.). Para detectar la fluorescencia basal verde de dicho compuesto se utilizó 485 nm como longitud de onda de excitación y 535 como longitud de onda de emisión, mientras que para detectar la fluorescencia roja de dicho compuesto, la cual solo aparece cuando se agrega en las mitocondrias no dañadas [418], se usaron 550 y 600 nm respectivamente. El cociente entre los valores obtenidos de fluorescencia roja y verde se utilizó para comparar la cantidad de mitocondrias que presentaban niveles basales de potencial de membrana entre los distintos grupos.

3.7. Técnicas de microscopia confocal de barrido laser.

3.7.1. Tinción con naranja de acridina.

El colorante fluorescente naranja de acridina, el cual puede cambiar el color de la fluorescencia emitida de verde a roja cuando se almacena en las vesículas ácidas de la célula, se utilizó para analizar las variaciones temporales en la cantidad y tamaño de los autofagosomas tras la administración de melatonina [419]. Para realizar este experimento, se sembraron 10.000 células por pocillo en una placa de 24 pocillos y se trataron con melatonina a una concentración 1 mM durante 4, 8, 12, 24 y 48 horas. Una vez tratadas, las células se incubaron durante 15 minutos, a temperatura ambiente y en oscuridad con el colorante naranja de acridina a una concentración de 5 µg/ml. Posteriormente, las muestras se lavaron 2 veces con PBS para eliminar el exceso de colorante y se observaron con ayuda del microscopio de fluorescencia de barrido laser Leica SPE (Leica Microsystems, Wetzlar, Alemania). Las áreas de color rojo y verde se cuantificaron con el programa *ImageJ* (National Institute of Mental Health), calculándose el ratio de intensidad de fluorescencia entre las áreas rojas y verdes (R/GFIR por sus siglas en inglés) con el objetivo monitorear cuantitativamente las variaciones temporales en el contenido celular de vesículas ácidas [419].

3.7.2. Colocalización entre LAMP2 y Tom20.

El análisis de la colocalización entre el marcador lisosomal LAMP2 y el mitocondrial Tom20 permitió determinar el conjunto de mitocondrias que están siendo introducidas en los lisosomas para su degradación en cada uno de los grupos experimentales [420]. Para realizar este experimento, se sembraron 10.000 células por pocillo en una placa de 24 pocillos con cubreobjetos de cristal y se trataron con las concentraciones anteriormente indicadas de CoCl₂, sorafenib y/o melatonina durante 6, 12 y 24 h. Una vez tratadas, las células se fijaron con paraformaldehído al 4% durante 15 minutos (Thermo Fisher Scientific) y se lavaron dos veces con PBS. A continuación, las células se permeabilizaron con 0,2% de saponina (Sigma-Aldrich) y 1% de albumina sérica bovina libre de ácidos grasos (FFA-BSA por sus siglas en inglés) (Sigma-Aldrich) disueltas en PBS durante 15 minutos a temperatura ambiente. Posteriormente, las células se lavaron de nuevo con PBS y se incubaron durante toda la noche a 4 °C con el anticuerpo monoclonal

obtenido en ratón contra la proteína LAMP2 (ab25631, Abcam) y con el anticuerpo policlonal obtenido en conejo contra la proteína Tom20 (sc-11415, Santa Cruz Biotechnology). Estos anticuerpos se disolvieron en PBS a una concentración 1:300 en PBS con un 1% de FFA-BSA. Tras lavar de nuevo las membranas dos veces con PBS, las células se incubaron durante 1 h a temperatura ambiente con el anticuerpo secundario que detecta anticuerpos de ratón y está conjugado con el fluorocromo Alexa-488 (1:1.000, Z25002, Molecular Probes, Eugene, OR, EE.UU.), así como con otro secundario que detecta anticuerpos de conejo y está conjugado con Alexa-647 (1:500, Z25308, Molecular Probes). Posteriormente, los cubreobjetos de cristal se lavaron de nuevo 2 veces con PBS y se montaron sobre portaobjetos de cristal usando para ello el medio comercial *FluoroshieldTM medium* con 4',6-diamino-2-fenilindol (DAPI) (Sigma-Aldrich). Los cubreobjetos se visualizaron en un microscopio confocal de barrido laser Zeiss LSM 800 (Zeiss AG, Jena, Alemania), y se analizaron con el programa *ZEN software* (Zeiss AG). Para determinar cuantitativamente el grado de superposición entre ambos fluorocromos en cada grupo experimental se usó el programa *ImageJ* (National Institute of Mental Health) con el plugin *Colocalization Colormap* (Academia Polaca de Ciencias, Varsovia, Polonia).

3.8. Silenciamiento génico.

La inhibición de la expresión proteica con ARN pequeño de interferencia (siRNA, por sus siglas en inglés) permitió determinar la repercusión que presenta dicha proteína sobre la viabilidad celular, la apoptosis y la autofagia [421,422]. Para realizar esta técnica, los siRNA comerciales contra las proteínas HIF-1 α (sc-35561), BNIP3 (sc-37451), Parkin (sc-42158), Atg5 (sc-41445), así como el usado como control negativo (sc-37007) (todos ellos de Santa Cruz Biotechnology) se introdujeron en las células Hep3B y HepG2 usando el reactivo *Lipofectamine[®] RNAiMAX* (Thermo Fisher Scientific). Transcurridas 5 horas desde la transfección, el medio celular se sustituyó por DMEM fresco con suero y antibióticos. 16 h después, las células se trataron con melatonina y/o sorafenib, determinando su viabilidad y los niveles de expresión proteica a través de las técnicas MTT y Western blot respectivamente.

3.9. Análisis estadístico.

Los resultados obtenidos en los distintos experimentos se expresaron como los valores medios \pm desviación estándar de al menos tres experimentos diferentes. Los resultados se analizaron con el programa estadístico *GraphPad Prism 6* (*GraphPad Software*, San Diego, CA, EE.UU.) La prueba de Kolmogorov-Smirnov se utilizó para comprobar la normalidad de los datos, mientras que el análisis de varianza (ANOVA) seguido de la prueba de rango post-hoc de Bonferroni permitió determinar la presencia de diferencias significativas entre los grupos experimentales. Se consideró como significativo cuando el valor p fue menor de 0,05.

4. Resultados y discusión.

Aunque se han testado múltiples quimioterápicos para el tratamiento del HCC, la mayoría de ellos han fracasado en pruebas clínicas de fase III, debido a que presentaban una alta toxicidad hepática o una baja potencialidad antitumoral [430]. Hasta muy recientemente, el sorafenib era el único quimioterápico sistémico que había demostrado tener capacidad para reducir la progresión del HCC avanzado y de incrementar la supervivencia de los pacientes con dicha patología [78,79], siendo aprobado por la FDA y la EMA para su uso en el tratamiento de tumores hepáticos avanzados [82]. Sin embargo, los tratamientos sostenidos con este fármaco no producen efectos satisfactorios, debido a la aparición de efectos adversos severos o a la pérdida progresiva de sensibilidad celular a este fármaco [108]. Además, existe una resistencia innata al sorafenib debido a la alta heterogeneidad genética que presentan las células de este tumor, lo que lleva a que algunas de las dianas directas del sorafenib no se expresen en dichas células, siendo esta droga ineficaz en esas células [105,108]. Como resultado de estas situaciones, la administración del sorafenib muchas veces tiene que ser suspendida [431].

La desensibilización de las células hepáticas a la quimioterapia esta mediada por un grupo de vías celulares que se conocen como mecanismos de quimiorresistencia (MOC por sus siglas en inglés) [432]. Dichos procesos incluyen: la reducción de la captación celular de fármacos o el incremento de su exportación (MOC-1), la inactividad de sus procesos activadores (MOC-2), la subexpresión de sus dianas moleculares (MOC-3), la reparación de los daños que inducen dichos fármacos en la célula (MOC-4), la alteración del equilibrio entre los mecanismos de muerte y supervivencia celular (MOC-5), la perturbación del microambiente celular (MOC-6) y la transición entre diferentes fenotipos celulares (MOC-7) [432]. Las células resistentes al tratamiento con sorafenib presentan también alteraciones en estos mecanismos. Por ejemplo, la reducción de los niveles de la octapeptidil aminopeptidasa 1 (OCT1), la cual está encargada de la captación celular de sorafenib (MOC-1), se ha relacionado recientemente con el aumento de la resistencia a dicho quimioterápico [433,434]. Así mismo, la sobreactivación de sistemas de compensación celular, como la vía PI3K/Akt/mTOR, o la inducción de determinados procesos que estimulan la supervivencia celular, como la autofagia, son capaces de enmascarar los efectos citotóxicos del sorafenib (MOC-5) [90,114]. Además, la EMT (MOC-7) y el microambiente celular que rodea al HCC (MOC-6), incluyendo el estado de inflamación

hepática, la reactivación viral, el estrés oxidativo o la hipoxia también influyen en la pérdida de la sensibilidad celular al sorafenib [108,119,122].

En la actualidad se están desarrollando múltiples estrategias terapéuticas para lograr superar la resistencia al sorafenib [105]. Por un lado, se están investigando nuevos fármacos, como el nivolumab o el regorafenib, que permiten continuar reduciendo la proliferación cuando el tratamiento con sorafenib ya no tiene efecto citotóxico sobre el HCC [105,107]. Por otro lado, la combinación de distintos compuestos con el sorafenib puede extender la supervivencia de los pacientes con HCC avanzado al sensibilizar a las células frente a dicha molécula. De hecho, este efecto ya ha sido visto *in vitro* con determinados quimioterápicos, como el celecoxib o la fluvastatina [435,436], así como con determinados compuestos naturales, como la curcumina o la silibinina [437,438]. Así mismo, se ha comprobado en una prueba clínica de fase II que el 5-fluorouracilo es capaz de inducir los efectos oncostáticos de dicha droga [439]. Sin embargo, la molécula perfecta que evite la aparición de células resistentes al sorafenib no ha sido todavía encontrada.

Diversos estudios han demostrado que la melatonina puede ejercer un gran número de efectos beneficiosos en las enfermedades hepáticas no relacionadas con el cáncer, como el fallo hepático fulminante o la NAFLD [440–442]. Así mismo, esta indolamina también presenta múltiples efectos antitumorales en el HCC. Por ejemplo, esta molécula es capaz de reducir la proliferación celular a través de la estimulación de las vías intrínseca y extrínseca de la apoptosis [407]. Estos efectos antiproliferativos están altamente relacionados con su capacidad para modular las vías MAPK y PI3K/Akt [443,444]. Por otra parte, estudios recientes han demostrado la capacidad de dicha hormona para prevenir la migración de los hepatocitos tumorales al reducir la actividad y expresión de la metaloproteinasas 9 (MMP9) [17]. Además, la melatonina es capaz de reducir la angiogénesis tumoral al reducir la expresión e impedir la liberación de VEGF en hipoxia [16]. Estos efectos anticancerígenos también han sido demostrados en modelos *in vivo* de HCC [408]. Todos estos datos motivan el uso de la melatonina como adyuvante en la terapia del HCC.

Como se dijo previamente, la falta de equilibrio entre las respuestas celulares de muerte y las de supervivencia, como la autofagia inespecífica o la mitofagia, pueden llevar a incrementar la resistencia a la quimioterapia (MOC-5) [198,432]. La autofagia inespecífica o específica presenta un comportamiento dual en las células tumorales, pues pueden promover o reducir la supervivencia de las células tumorales en diferentes fases de

la progresión tumoral [287,289]. Así mismo, estas vías pueden proteger a las células cancerígenas frente a los efectos citotóxicos de la quimioterapia y la radioterapia, promoviendo la progresión y la invasión tumoral [287]. Con lo cual, el desarrollo de compuestos que puedan modificar esta respuesta celular parece ser una estrategia prometedora, pero compleja, para reducir la progresión del cáncer hepático [287]. Consecuentemente con lo anteriormente dicho, en esta tesis doctoral se analizará la capacidad de la melatonina para estimular los efectos citotóxicos del sorafenib en normoxia e hipoxia a través de la modulación de las respuestas autofágica y mitofágica en condiciones basales de oxígeno.

4.1. Efecto de la melatonina sobre la respuesta autofágica en las células de HCC.

4.1.1. La melatonina induce una respuesta autofágica transitoria y completa en las células de HCC.

En primer lugar, se analizó la capacidad de la melatonina para inducir la respuesta autofágica no específica en las células HCC en nuestros experimentos a través del análisis de los principales marcadores de esa vía. Como se observa en las Figs. 20A y 20B, la adición de melatonina a las células de HCC fue capaz de estimular gradualmente la expresión y lipidación de LC3 hasta llegar a un máximo entre las 8 y las 12 h desde el inicio del tratamiento. Posteriormente, la lipidación de esta proteína fue reduciéndose progresivamente hasta el punto final del experimento. Así mismo, la transcripción de otros marcadores de dicha vía celular, como Beclin1 o Atg3 también sigue una tendencia similar a la que presentaba LC3 (Fig. 20B). El incremento observado en la expresión de dichas proteínas debido a la administración de melatonina se correlacionó con el aumento en la formación de vesículas autofágicas en las células HepG2 transcurridas 4, 8 y 12 h desde la administración de melatonina (Fig. 21). Al igual que la expresión de los marcadores autofágicos, la formación de vesículas autofágicas disminuyó claramente cuando transcurrieron 24 y 48 h de tratamiento, empezando a aparecer características apoptóticas en las células tratadas con dicha molécula (Fig. 21). Resumiendo, estos datos parecen sugerir que la melatonina es capaz de estimular la formación de una respuesta autofágica transitoria en las células HepG2. Estos efectos también se han observado *in vitro* en patologías tanto tumorales como no tumorales [447,448], así como en un modelo *in vivo* de células derivadas de hepatoma [449]. Sin embargo, diversos estudios han indicado que

la melatonina podría ser capaz de inducir la respuesta contraria, reduciendo la respuesta autofágica en un modelo de insuficiencia hepática fulminante o en neuronas de rata tratadas con morfina [450,451]. Estos datos aseveran que la modulación de la respuesta autofágica por parte de la melatonina es dependiente del contexto celular. Esta respuesta cambiante también se ha observado con otras moléculas, como la quercetina o la silibinina [198].

Aunque la sobreexpresión de los marcadores autofágicos suele estar relacionada con la inducción de la degradación del contenido autofagosomal, también se puede asociar con la acumulación de autofagosomas defectivos que son incapaces de unirse con los lisosomas [247]. Con el propósito de discernir entre estas dos situaciones, la integridad del flujo autofágico fue analizada utilizando los inhibidores de la acidificación endosomal CQ y Baf A1 [247]. La melatonina promovió la acumulación de LC3-II incluso en presencia de dichos inhibidores, lo cual parece indicar que dicha hormona es capaz de inducir una respuesta autofágica completa (Fig. 20C). Así mismo, la reducción observada en los niveles de p62 tras el pico máximo de expresión de LC3-II (Fig. 20A), así como la disminución en los niveles de autofagosomas a 24 y 48 h (Fig. 21) también sugieren que la melatonina es capaz de inducir la degradación del contenido autofagosomal en los lisosomas. La capacidad de esta hormona para mantener la integridad del flujo autofágico se ha estudiado también en otras patologías, como en la cardiomiopatía diabética [452]. En esta enfermedad, la melatonina induce la degradación del contenido autofagosomal preveniendo la disfunción mitocondrial en los cardiomiocitos [452]. Así mismo, otras moléculas naturales con efectos antioxidantes, como la baicaleína o la quercetina, son capaces de inducir una respuesta autofágica completa [198].

4.1.2. La inducción de la autofagia por la melatonina es dependiente de la vía de JNK, pero no de la de mTORC1.

La serina/treonina proteína quinasa mTORC1 es capaz de inhibir la inducción de la respuesta autofágica en presencia de nutrientes, oxígeno, factores de crecimiento u hormonas en el microambiente celular [261]. Debido a esto, analizamos si la melatonina era capaz de modular temporalmente la respuesta autofágica a través de la alteración de los niveles de esta quinasa. Sorprendentemente, la melatonina fue incapaz de inhibir la fosforilación de esta quinasa a tiempos cortos y largos, induciendo incluso su activación transcurridas 2, 4 y 8 horas de tratamiento (Figs. 22A y 22B). De forma simultánea, se

produjo el aumento de los niveles de Beclin1 como respuesta a la administración de dicha molécula. Estos resultados parecen indicar que la inducción de la autofagia a través de la melatonina es independiente de la fosforilación de mTORC1 en este modelo celular, con lo que la modulación de esta respuesta autofágica debería ocurrir a través de otra vía. Esta situación inesperada ha sido también encontrada en un modelo de isquemia cerebral, en el cual la adición de melatonina no fue capaz de alterar la fosforilación de mTORC1 [453]. Sin embargo, otros estudios han demostrado que la melatonina es capaz de inducir la autofagia a través de la reducción de la actividad de esta quinasa en modelos *in vivo* de cáncer hepático y en modelos *in vitro* de distrofia corneal glanular de tipo II [448,449]. Estos datos indican que la capacidad de la melatonina para inducir la respuesta autofágica a través de la inhibición de mTORC1 parece ser altamente dependiente del contexto celular.

Por otra parte, la respuesta autofágica puede ser modulada en las células humanas en respuesta a diferentes estímulos tanto extracelulares como intracelulares, como la inducción de la UPR a través de la activación de JNK [285]. De hecho, esta proteína es capaz de fosforilar a Bcl-2, desplazando de ese modo su unión con la proteína Beclin1 [271,285]. En nuestros experimentos la administración de melatonina a las células de HCC fue capaz de inducir la fosforilación de JNK y la expresión de grp78 (Fig. 22C), la principal chaperona implicada en la superación del estrés de retículo [285]. Estas variaciones ocurrieron de forma simultánea al incremento de la expresión de Beclin1 tras la administración de la hormona (Fig. 22A y 22B), lo que sugiere que la melatonina puede inducir la respuesta autofágica a través de la proteína JNK. De hecho, la inhibición de dicha proteína por el inhibidor químico SP600125 indujo una reducción en la expresión de LC3-II, corroborando nuestra hipótesis previa. Otros estudios han demostrado que esta molécula también puede inducir la expresión de JNK en el cáncer gástrico [454]. Además, los autores de ese artículo sugieren que la activación de esta vía podría ser responsable de la inducción de la respuesta autofágica en las células tumorales [454].

4.1.3. La autofagia inducida por la melatonina protege a las células tumorales frente a la muerte celular.

Como se comentó anteriormente, la autofagia puede promover o prevenir la supervivencia de las células tumorales en función de distintos factores, como la fase de la progresión en la que se encuentren [287,289]. Con lo cual, es esencial determinar la

contribución que presenta esta vía sobre los efectos citotóxicos que presenta la melatonina sobre las células de cáncer hepático. La inhibición de la expresión de Atg5 con un siRNA comercial indujo una supresión clara de los niveles de la respuesta autofágica en las células HepG2 a través de la inhibición de la lipidación de LC3-II y de la degradación de p62 en presencia o no de melatonina a 2 mM (Fig. 23B). La inhibición de dicha vía en las células de HCC aumentó de forma significativa los efectos citotóxicos de la melatonina a través de la estimulación de la respuesta apoptótica (Fig. 24). Estos datos sugieren que la autofagia presenta una función claramente protectora en las células HepG2 frente a los efectos citotóxicos de la melatonina. Esta capacidad de la autofagia se ha visto también en un modelo *in vivo* de hepatoma [449]. Por otra parte, se ha visto efectos análogos en cáncer gástrico y prostático tratados respectivamente con quercetina y silibinina [455,456].

En función de los datos anteriormente presentados podemos concluir que la melatonina parece ser capaz de estimular la respuesta autofágica protectora en las células HepG2 a través de la activación de la fosforilación de JNK (Fig. 43). Por lo cual, la inhibición de esta vía podría estimular los efectos oncostáticos de esta molécula en el cáncer hepático.

4.2. La melatonina es capaz de modular los efectos citotóxicos del sorafenib en las células de HCC mantenidas en normoxia.

4.2.1. La melatonina estimula la capacidad citotóxica del sorafenib en las células HCC mantenidas en normoxia.

Tras analizar la capacidad de la administración de melatonina sobre la respuesta autofágica en las células de HCC, se decidió analizar su capacidad para estimular los efectos citotóxicos del sorafenib en normoxia. Nuestros resultados demostraron que la respuesta a la administración individual o conjunta de melatonina y sorafenib variaba entre las tres líneas de HCC testadas, Hep3B, HepG2 y Huh7; debido a la alta heterogeneidad genética que presentan entre ellas [105]. Las células HepG2 y Huh7 presentaban alta sensibilidad a los tratamientos individuales con sorafenib y con melatonina, mientras que solo las dosis más altas de dichos compuestos fueron capaces de reducir significativamente la viabilidad de las células Hep3B transcurridas 48 h desde el inicio del tratamiento (Fig. 25). Estos datos sugieren que existe una resistencia innata a la administración de dichas

moléculas en las células Hep3B, pero ni en las Huh7, ni en las HepG2. Otros estudios también han demostrado esta resistencia innata al sorafenib en las líneas Hep3B [457,458]. Sin embargo, el efecto contrario ha sido observado tras la administración de paclitaxel, pues las células HepG2 presentan una mayor resistencia innata al tratamiento con dicho fármaco que las Hep3B [459]. Estos datos indican que las células de cáncer hepático no presentan la misma sensibilidad a diferentes agentes quimioterápicos, debido principalmente a que el conjunto de proteínas que expresa cada línea celular es totalmente distinto.

Tras comprobar el efecto que presentaba la administración individual de dichas moléculas sobre la viabilidad celular, se analizó la capacidad de la melatonina para estimular los efectos citotóxicos del sorafenib. Como se puede observar en la Fig. 26, la coadministración de dichos compuestos redujo de manera sinérgica la viabilidad de las células de HCC tras 48 h de tratamiento. De entre las tres líneas experimentales, las células Hep3B fueron las que presentaron una menor respuesta a la administración de dicha combinación (Fig. 26). Otros estudios han demostrado recientemente la existencia de este efecto aditivo tras la coadministración de melatonina y sorafenib en la línea celular Huh7 [460]. Así mismo, esta indolamina es capaz de estimular los efectos citotóxicos de otras drogas, como la doxorubicina, la clofarabina o el 5-fluorouracilo [404,405,446]. De forma similar a la melatonina, la administración del flavonoide quercetina también induce una reducción significativa en la viabilidad de las células de glioblastoma multiforme y de astrocitoma anaplásico tratadas con sorafenib [461]. Con el fin de analizar las vías celulares que participan en la desensibilización de las células de HCC al sorafenib, se seleccionaron las células Hep3B y las concentraciones 1 mM de melatonina y 2,5 μ M de sorafenib, las cuales no inducen ningún efecto significativo sobre la viabilidad celular (Fig. 25), para realizar el resto de experimentos.

4.2.2. La coadministración de sorafenib y melatonina induce la activación de la apoptosis en las células Hep3B.

La apoptosis es la principal vía celular a través de la cual se induce la PCD de las células tumorales tras la administración de la mayoría de los fármacos quimioterápicos [365]. Por lo cual, no es extraño que los niveles de esta respuesta celular se encuentren reducidos en las células tumorales que presenten resistencia a la quimioterapia [432].

Además, la estimulación de la apoptosis por la melatonina parece ser capaz de reducir la resistencia celular a la doxorubicina [404]. Todos estos datos sugieren que esta vía celular podría estar detrás de la capacidad de la melatonina para estimular los efectos citotóxicos del sorafenib en normoxia. Como se muestra en la Fig. 27A, la coadministración de ambas moléculas fue capaz de inducir la expresión de Bax y la escisión de PARP transcurridas 24 y 48 h desde el inicio del tratamiento, mientras que el tratamiento individual con sorafenib fue incapaz de estimular este fenotipo. De forma similar, la fracción de células muertas por apoptosis a las 48 h sólo se vio incrementada de forma significativa tras la coadministración de melatonina y sorafenib, pero no tras el tratamiento individual con dichas moléculas (Figs. 27A y 27B). Estos datos concuerdan con los obtenidos tras la administración conjunta de quercetina y sorafenib en las células de glioblastoma multiforme y de astrocitoma anaplásico [461], lo cual nos sugiere que la melatonina reduce parcialmente la resistencia innata al sorafenib en las células Hep3B a través de la inducción de la apoptosis.

4.2.3. La coadministración de melatonina y sorafenib induce la degradación mitocondrial a través de la mitofagia en las células Hep3B.

Estudios recientes han demostrado que el sorafenib es capaz de inducir la autofagia en las células Huh7, pero no en las Hep3B [458]. Estos datos nos sugieren que la falta de esta respuesta celular, la cual puede reducir la viabilidad de las células tumorales a través de la PCD de tipo II [365], podría ser responsable de la baja sensibilidad que presentan estas células a dicho fármaco. Al igual que la autofagia no específica, la inducción de la respuesta mitofágica en las células tumorales se ha relacionado con la reducción de la proliferación y de la progresión tumoral [347]. Ciertamente, la desregulación de la expresión de Parkin se ha asociado con la reducción de la hepatocarcinogénesis, indicando que esta molécula actuaría como una proteína supresora de tumores en el hígado [347]. Nuestros resultados demostraron que la coadministración de melatonina y de sorafenib era capaz de estimular transitoriamente la expresión de este mediador transcurridas 3 y 6 horas desde el inicio del experimento, mientras que la administración individual de dicho quimioterápico no fue capaz de inducir la expresión de dicho compuesto (Fig. 31A). Este aumento fue concomitante con el de la proteína PINK1 (Fig. 31A), la cual recluta Parkin a las mitocondrias dañadas para inducir su degradación [331]. De forma análoga, los niveles de la forma lipidada de LC3 también aumentaron de forma transitoria transcurridas 6 y 12

h tras la coadministración de melatonina y sorafenib, pero no tras la administración individual de dicho quimioterápico (Fig. 31B), lo cual sugiere que el fin de la sobreestimulación de la vía PINK1/Parkin es la inducción de la mitofagia y no de la degradación mitocondrial por el sistema ubiquitina/proteasoma. El incremento de la colocalización entre las mitocondrias y los lisosomas transcurridas 6 y 12 h desde la coadministración de ambas moléculas, pero no tras la administración individual de sorafenib y de melatonina, así como su reducción pasadas 48 h corroboró la degradación de las mitocondrias a través de la mitofagia (Fig. 30). Todos estos datos parecen indicar que la adición de la melatonina a las células tratadas con sorafenib estimula la activación de la mitofagia dependiente de PINK1 y de Parkin.

Con el fin de comprobar la degradación de las mitocondrias en los lisosomas, se analizaron las variaciones en el número de copias de mtDNA con respecto al contenido en ncDNA. Como queda recogido en la Fig. 30B, la administración individual de melatonina y sorafenib no fue capaz de modificar los niveles mitocondriales, mientras que el tratamiento conjunto con ambas moléculas permitió reducir el contenido en mtDNA transcurridas 12 y 24 h desde el inicio del experimento. Así mismo, los niveles de la proteína de choque térmico de 60 kDa (HSP60), la cual está encargada de mantener el plegamiento correcto de las proteínas mitocondriales [424], también experimentaron una reducción significativa transcurridas 12 y 24 h desde la coadministración de sorafenib y melatonina (Fig. 30B). Estos datos demuestran que la adición simultánea de estas dos moléculas estimula la degradación de las mitocondrias en los autofagosomas a través de las proteínas PINK1 y Parkin. Otros estudios han demostrado que la administración de melatonina individualmente o en combinación con la rapamicina puede inducir la mitofagia en las células de cáncer de cabeza y cuello [462]. Sin embargo, esta respuesta celular parece ser defectiva, debido a que no se vio acompañada de una disminución en el contenido de mtDNA [462]. De forma similar a la autofagia, la inducción de la mitofagia por parte de esa indolamina parece ser altamente dependiente del contexto celular [463].

La regulación de la forma, localización, tamaño y degradación de las mitocondrias en las células es fundamental para mantener la homeostasis de dichos orgánulos [303]. Por ejemplo, las variaciones entre los procesos de fusión y fisión mitocondrial pueden modular de forma transitoria el alcance de la respuesta mitofágica [332]. De hecho, la fusión mitocondrial incrementa el tamaño de los orgánulos, previniendo su incorporación en los autofagosomas por motivos estéricos [330]. Por otra parte, la fisión mitocondrial induce la

fragmentación de las mitocondrias dañadas, lo cual promueve su degradación en los autofagosomas [332]. Con lo cual, la regulación de dichos procesos de forma externa podría afectar a la activación de la respuesta mitofágica en las células tumorales [332].

La fusión mitocondrial esta modulada principalmente por las proteínas MFN1 y MFN2 en la OMM y por OPA1 en la IMM [303,304]. La proteína MFN2 está implicada en la inducción de la mitofagia, ya que la fosforilación de esta molécula por parte de PINK1 induce la traslocación de Parkin a la OMM [338]. Así mismo, esta proteína sirve como sustrato de la proteína Parkin, lo cual induce su ubiquitinación y la inhibición de la fusión mitocondrial durante la mitofagia [332]. Como se puede observar en la Fig. 30A, la coadministración de melatonina y sorafenib en las células Hep3B indujo una progresiva reducción de la expresión de MFN2 transcurridas 6 h desde el inicio del experimento, restaurándose los niveles basales de dicha proteína a las 12 h. Esta disminución fue concomitante con el aumento transitorio de los niveles de Parkin (Fig. 29A). Estudios recientes han relacionado la sobreexpresión de dicha proteína a tiempos tardíos con la estimulación de la apoptosis [464]. Estos datos parecen indicar que la sobreestimulación de dicha proteína tras periodos prolongados de tratamiento combinado con sorafenib y melatonina podría estar implicado con la inducción de la vía apoptótica en las células Hep3B.

Por otra parte, se ha demostrado que durante la mitofagia se produce la escisión de la proteína OPA1, lo cual lleva a la reducción de la fusión de la IMM durante ese proceso [316]. De forma similar a MFN2, la proteína OPA1 experimentó una reducción transitoria de su expresión transcurridas 3 y 6 h desde la coadministración de melatonina y de sorafenib, restaurandose los niveles basales de dicha proteína a 12h (Fig. 30A). Esta disminución temporal se asoció con el incremento de los niveles de Parkin tras el cotratamiento (Fig. 29A). Por otro lado, estudios recientes han descrito un aumento de la expresión de esta proteína tras la sobreexpresión de Parkin a través de la vía del factor nuclear potenciador de las cadenas κ de los células B activadas (NF- κ B) [465]. Este proceso podría explicar la restauración de los niveles de OPA1 tras la sobreexpresión de Parkin.

La fusión mitocondrial está principalmente modulada por las proteínas Drp1, Fis1, Mff, MiD49 y MiD51 [305]. La sobreexpresión de la proteína Fis1 se encuentra muy relacionada con la inducción de la mitofagia dependiente de Parkin en las células madre de la leucemia mieloide aguda (AML por sus siglas en inglés) [466]. Inesperadamente, en nuestro trabajo los niveles de Fis1 disminuyeron de forma notable transcurridas 6 h desde

la coadministración de melatonina y de sorafenib, mientras que la expresión de esta proteína aumentó tras el tratamiento con sorafenib (Fig. 30A). Esta extraña reducción podría explicar la restauración de los niveles basales de mitofagia tras 24 h desde el inicio del experimento. Por otra parte, la supresión de la expresión de la proteína Fis1 se ha relacionado recientemente con la detención del ciclo celular y con la reducción de la viabilidad celular [466]. Por lo tanto, la reducción de los niveles de esta proteína tras la coadministración de sorafenib y de melatonina podría parcialmente reducir la resistencia innata a dicha droga en las células de HCC.

4.2.4. La mitofagia inducida por la coadministración de melatonina y de sorafenib induce la despolarización mitocondrial y la acumulación de ROS en las células Hep3B.

La mitofagia es la principal vía encargada de mantener la homeostasis mitocondrial frente a diversas situaciones dañinas como la acumulación de ROS o a la falta de nutrientes en el medio [329]. La capacidad prooxidante que presentan las concentraciones farmacológicas de la melatonina sobre células tumorales y no tumorales podría ser parcialmente responsable de la inducción de la respuesta mitofágica tras el tratamiento combinado [425]. Como se puede observar en la Fig. 31A, la administración de melatonina individualmente o en combinación con el sorafenib estimuló la formación de ROS en las células Hep3B. Por otra parte, este fenotipo no fue inducido en las células tratadas únicamente con sorafenib (Fig. 31A). Diversos estudios han demostrado la capacidad de dicha indolamina para inducir la formación de ROS en determinados tipos de cáncer, como en el HCC o en distintos tipos de leucemias [467,468]. Por otra parte, aunque se ha detectado que el sorafenib es capaz de inducir la producción de ROS en determinadas líneas celulares hepáticas [469], lo cierto es que este proceso parece ser muy dependiente del contexto en el cual se encuentren dichas células.

Múltiples estudios han demostrado la existencia de una relación directa entre la pérdida del potencial basal de la membrana mitocondrial y la inducción de la mitofagia a través de la vía de PINK1/Parkin [331]. Debido a esto, no es extraño pensar que la inducción de la despolarización de la membrana mitocondrial podría ser parcialmente responsable de la inducción de la mitofagia en las células cotratadas con melatonina y sorafenib. Como se puede ver en la Fig. 31B, la adición del fármaco quimioterapéutico a las células Hep3B en cultivo fue capaz de reducir el número de mitocondrias que

conservaban el potencial de membrana intacto, mientras que la adición de melatonina no fue capaz de inducir este fenotipo. La adición conjunta de ambos compuestos fue también capaz de inducir la pérdida de dicho potencial de membrana, lo que conjuntamente con la sobreestimulación de ROS, lleva a la inducción de la mitofagia en las células de HCC (Fig. 31). Dicho fenotipo también ha sido observado tras la combinación de la melatonina con 5-fluorouracilo, doxorubicina y cisplatino [470]. Estos datos parecen indicar que la activación coordinada de dichas repuestas mitocondriales es la responsable de inducir la mitofagia en las células Hep3B en respuesta a la coadministración de melatonina y sorafenib.

4.2.5. La mitofagia inducida por la coadministración de melatonina y sorafenib potencia la muerte de las células Hep3B.

La mitofagia presenta un doble comportamiento en las células tumorales, pues puede estimular o prevenir la progresión tumoral en función de determinados factores intracelulares y extracelulares [361]. Por eso, es esencial definir el rol que presenta la respuesta mitofágica inducida por melatonina y sorafenib sobre la viabilidad de las células Hep3B en normoxia a través de la supresión de la expresión de Parkin. Esta proteína funciona como una proteína supresora de tumores, pues es capaz de impedir la formación espontánea de tumores en diversos tejidos humanos [347]. Así mismo, la expresión de este factor se encuentra disminuida en más del 50% de los tumores hepáticos primarios [471]. Estos datos parecen indicar que la pérdida de la expresión de este factor potencia la progresión tumoral y la tumorigénesis. Como se puede ver en la Fig. 32A, la viabilidad celular se incrementó tras la inhibición de Parkin en nuestros experimentos cuando ambos compuestos fueron coadministrados, pero no tras el tratamiento individual con cada uno de ellos. Además, este silenciamiento evitó la inducción de la PCD de tipo I en las células Hep3B tratadas con melatonina y sorafenib (Fig. 32B). Estos datos sugieren que la mitofagia inducida tras la administración de melatonina en las células tratadas con sorafenib estimula la capacidad citotóxica de dicho fármaco en el HCC, reduciendo su sensibilidad innata a dicho quimioterapéutico.

Resumiendo, la melatonina parece ser capaz de reducir la resistencia innata de las células Hep3B al sorafenib en normoxia a través de la inducción de la mitofagia (Fig. 44). Esta respuesta celular se estimula en dichas células tras la acumulación de ROS y la pérdida

de la polaridad basal de la membrana mitocondrial y se encuentra regulada por los procesos de dinámica mitocondrial (Fig. 44). Finalmente, la inducción de la mitofagia tras el tratamiento combinado lleva a la estimulación de la muerte de las células Hep3B a través de la apoptosis (Fig. 44).

4.3. La melatonina es capaz de modular los efectos citotóxicos del sorafenib en las células de HCC mantenidas en hipoxia.

4.3.1. La melatonina estimula la capacidad citotóxica del sorafenib en las células HCC mantenidas en hipoxia.

Una inadecuada distribución de oxígeno en los tumores hepáticos avanzados estimula su progresión a través de la inducción de distintas vías procarcinogénicas, como la angiogénesis, la EMT y la metástasis [89]. Esta situación puede incluso llevar a la aparición de células resistentes a la quimioterapia a través de la activación de diversos mecanismos celulares (MOC-6) que pueden inducir el eflujo de los fármacos quimioterápicos o la reparación de los efectos nocivos que presentan estas moléculas sobre el ADN [432]. Recientemente, se ha observado que los efectos antiangiogénicos que presenta el sorafenib podrían agravar esta situación al impedir la correcta distribución de oxígeno en el tumor [122]. Esta reducción incrementa la aparición de células tumorales insensibles a dicho fármaco y la disminución de la efectividad antitumoral del mismo [122]. Por todo ello, la adición de un compuesto que pueda sensibilizar a las células de HCC al sorafenib podría constituir una buena estrategia para poder mantener sus efectos terapéuticos [122].

Diversos estudios han demostrado que la melatonina es capaz de modular las respuestas mediadas por hipoxia, como la angiogénesis, en las células hepáticas cancerígenas [16]. Así, potencialmente la adición de esta molécula a la terapia con sorafenib podría ser capaz de reducir la aparición de resistencias adquiridas en hipoxia. Como se esperaba, en nuestros experimentos todas las concentraciones testadas de sorafenib (2,5; 5 y 10 μM) y de melatonina (1 y 2 mM) fueron capaces de reducir individualmente y de forma significativa la viabilidad de las células Hep3B mantenidas durante 48 h en normoxia (Fig. 33). Sin embargo, solo la concentración más elevada de sorafenib fue capaz de inducir dicho fenotipo en hipoxia (Fig. 33). Por su parte, la

melatonina fue capaz de estimular los efectos citotóxicos del sorafenib en hipoxia, permitiendo incluso reducir la dosis mínima necesaria para inducir efectos significativos en la viabilidad celular a la mitad (Fig. 33). En resumen, nuestros resultados sugieren que el uso de esta combinación terapéutica en el tratamiento de los tumores hepáticos podría extender la duración del tratamiento con sorafenib y reducir sus efectos secundarios [472,473]. Con el fin de analizar de forma más profunda los mecanismos moleculares que modulan la sensibilización de las células de HCC al sorafenib tras la administración de melatonina en hipoxia, se seleccionaron las concentraciones 2 mM de melatonina y 5 μ M de sorafenib para realizar el resto de los experimentos.

4.3.2. La coadministración de melatonina y de sorafenib modula la expresión y la actividad de HIF-1 α y HIF-2 α , lo cual reduce la viabilidad de las células Hep3B.

HIF-1 α and HIF-2 α son los principales sensores celulares que detectan fluctuaciones en los niveles de oxígeno del microambiente celular, e inducen en consecuencia diferentes respuestas celulares como la EMT o la angiogénesis [137]. Diversos estudios han relacionado los niveles altos de estos factores con el incremento de la agresividad de las células tumorales, así como con la reducción de su sensibilidad a distintos quimioterápicos [474]. De hecho, las células tumorales primarias provenientes de pacientes con resistencia al sorafenib presentaban niveles más altos de HIF-1 que las provenientes de pacientes con sensibilidad a dicho fármaco [122]. Con lo cual, la adición de moléculas que puedan inhibir la expresión de dicha proteína en las células de cáncer hepático podría ser una buena estrategia para reducir la resistencia celular al sorafenib. Por ejemplo, el análogo de la curcumina EF24 es capaz de reducir la resistencia al sorafenib a través de la inducción de la degradación de HIF-1 α dependiente de VHL [122]. Por otra parte, el siRNA miR-338-3p también fue capaz de incrementar la sensibilidad celular al sorafenib a través de la inhibición de la expresión de HIF-1 α y de sus genes relacionados [475]. Finalmente, la inhibición de HIF-1 β con el siRNA miR-107 induce la reducción del volumen tumoral y la parada del ciclo celular en cáncer de colon [166].

Diversos estudios han demostrado que la melatonina es capaz de modular los niveles de HIF-1 α en cáncer renal, hepático, colorrectal y oral de células escamosas [476], aunque el mecanismo a través del cual induce estos efectos no está totalmente aclarado. De forma análoga, en nuestro trabajo el tratamiento individual con melatonina en las células

Hep3B mantenidas en hipoxia fue capaz de reducir la expresión de HIF-1 α y de HIF-2 α , mientras que el sorafenib solo disminuyó los niveles proteicos de HIF-1 α , pero no los de HIF-2 α (Fig. 34A). Además, la inhibición de HIF-1 α por parte de la melatonina en hipoxia fue reversible, pues la expresión de HIF-1 α volvía de nuevo a los niveles basales tras la eliminación de dicho compuesto (Fig. 34B). El tratamiento combinado con sorafenib y melatonina en hipoxia fue capaz de suprimir casi totalmente la expresión de HIF-1 α y HIF-2 α (Fig. 34A). La coadministración de melatonina y de sorafenib también redujo la expresión de alguna de las dianas específicas de dichos factores como VEGF (Fig. 34A). Estos datos indican que la adición de melatonina a las células tratadas con oxígeno fue capaz de suprimir la expresión y la activación de HIF-1 α y HIF-2 α en las células Hep3B mantenidas en hipoxia. Efectos similares también se han detectado por otros investigadores tras la coadministración de sorafenib con compuestos naturales como el 2-metoxiestadiol [195].

Una vez determinado el efecto que poseen el sorafenib y la melatonina sobre la expresión de HIF-1 α , se decidió estudiar el papel que tenía la inhibición de dicha proteína sobre la reducción de la resistencia adquirida a sorafenib en las células Hep3B mantenidas en hipoxia a través de la adición de un siRNA comercial. Como se puede observar en la Fig. 35, el silenciamiento de dicho factor de transcripción en las células tratadas con melatonina y/o sorafenib en hipoxia fue capaz de reducir tanto la expresión como la actividad de HIF-1 α . Sin embargo, no se observaron diferencias significativas en la viabilidad celular entre las células silenciadas y las no silenciadas (Fig. 35C). Esta inesperada situación podría deberse a la activación de un mecanismo compensatorio que induzca la expresión de HIF-2 α y de sus vías relacionadas cuando la expresión de HIF-1 α decae, manteniendo de esa forma la respuesta a la falta de oxígeno en las células tumorales [196]. De hecho, las células silenciadas presentaban niveles anormalmente altos de HIF-2 α (Fig. 35A), lo cual soportaría esa hipótesis. En resumen, aunque la proteína HIF-1 α parece contribuir en la aparición de células resistentes al sorafenib, la inhibición de este mediador no parece ser suficiente para sensibilizar a las células tumorales, debido a la activación de un sistema de compensación. En consecuencia, el silenciamiento coordinado de ambas subunidades es necesario para determinar su papel en la desensibilización celular al sorafenib.

4.3.3. La melatonina estimula la síntesis proteica de HIF-1 α , pero no es capaz de modificar ni su transcripción ni su degradación.

La expresión de HIF-1 α se encuentra estrechamente regulada a diferentes niveles [145], con lo que la reducción observada tras la administración de melatonina a las células tratadas con sorafenib puede deberse a modificaciones en los procesos de transcripción, traducción o degradación. Como queda puesto de manifiesto en la Fig. 36A los niveles de mRNA de la proteína HIF-1 α en hipoxia no sufrieron variaciones significativas tras la administración de melatonina. Por otra parte, la inhibición de los dos principales sistemas que participan en la degradación de HIF-1 α (las PHDs y el sistema ubiquitin-proteasoma) no impidió que dicha indolamina continuara reduciendo los niveles proteicos de dicha proteína (Fig. 37A). En contraste, los efectos inhibitorios de dicha molécula sobre HIF-1 α fueron análogos a los obtenidos con la CHX, la cual reprime la síntesis proteica (Fig. 37B). En consecuencia, nuestros resultados demuestran que la melatonina es capaz de reducir la síntesis de HIF-1 α sin afectar ni a su degradación proteasomal ni a su transcripción en las células de cáncer hepático mantenidas en hipoxia. Tal como indican otros autores esta hormona también fue capaz de ejercer efectos similares en el cáncer de próstata [427]. No obstante, otros investigadores han descrito que la melatonina puede promover la degradación de HIF-1 α a través de la prevención de la inactivación de las PHDs por la sobreproducción de ROS en células de glioblastoma y de cáncer de colon [477,478]. Estos datos parecen indicar que el mecanismo de inhibición de los niveles de HIF-1 α por parte de la melatonina es altamente dependiente del contexto y del tipo celular, así como del papel que presenta dicha molécula sobre la regulación de la producción de ROS. En los casos anteriormente descritos, esta hormona presenta efectos antioxidantes, ya que es capaz de prevenir la inactivación de las PHDs a través de la reducción de los niveles de ROS [477,478]. Sin embargo, la melatonina presenta efectos prooxidantes en nuestro modelo experimental (Fig. 36B), por lo que es bastante improbable que inhiba los niveles proteicos de HIF-1 a través del mecanismo anteriormente descrito.

4.3.4. La melatonina restringe la síntesis proteica de HIF-1 α al desregular la vía de mTORC1/p70S6K.

Diversos estudios han descrito a la vía PI3K/Akt/mTORC1 como al principal mecanismo que modula la traducción de HIF-1 α en respuesta a determinados estímulos

extracelulares, como la presencia de factores de crecimiento, hormonas y citoquinas en el medio [171]. De hecho, mTORC1 es capaz de estimular la síntesis proteica a través de la activación de dos proteínas esenciales para la activación de la traducción ribosomal, el factor iniciador de la traducción eucariótica 4E (eIF-4E) y la proteína ribosomal S6 (RP-S6) [145,173]. Por contra, el complejo 2 de mTOR (mTORC2) es capaz de inducir de forma indirecta la síntesis proteica a través de la fosforilación de la proteína Akt, la cual reprime al inhibidor de mTORC1 [261]. Estudios recientes han detectado la presencia de un sistema de retroalimentación negativo que previene la sobreestimulación de mTORC1 a través de la represión de mTORC2 y de PI3K/Akt [145]. En nuestros experimentos la incubación de las células Hep3B mantenidas en hipoxia con melatonina impidió la fosforilación de mTORC1, así como la de la quinasa β -1 de RP-S6 (p70S6K) y de la propia RP-S6 (Fig. 38A). Esta reducción fue concomitante con la disminución de los niveles proteicos de HIF-1 α (Fig. 38A). Se ha descrito que la administración de silibinina a las células de HCC y de cáncer de cérvix parece inducir la restricción de la traducción de HIF-1 a través de la inhibición de mTORC1 de forma similar a la melatonina [173]. Por otra parte, la administración de melatonina en hipoxia también aumentó de forma transitoria la expresión de mTORC2 y de Akt. Así mismo, la incubación de las células de HCC con silibinina llevó a la activación de esta vía de retroalimentación de forma análoga a la melatonina [173].

Posteriormente, se combinó la melatonina con rapamicina o con LY2940002 con el objetivo de analizar si la inhibición de la vía de mTORC1 por parte de dicha indolamina era capaz de restringir la síntesis proteica de HIF-1 α . La rapamicina es un inhibidor universal de mTORC1 que también puede restringir la expresión de mTORC2 en determinados contextos celulares [173], mientras que LY294002 suprime la fosforilación de PI3K [479]. Como se puede observar en la Fig. 38B, la inhibición de la fosforilación de mTORC1 por parte de la rapamicina restringió la síntesis de HIF-1 α e indujo la activación del mecanismo de retroalimentación formado por mTORC2 y Akt. Este efecto fue análogo al que observamos tras la administración de melatonina, lo que sugiere que esta molécula actúa como un represor de mTORC1 y a través de esta vía reduce la transcripción de HIF-1 α (Fig. 38B). Por otra parte, la coadministración de melatonina y LY294002 no fue capaz de restringir de forma total la fosforilación de Akt (Fig. 38C). Esto sugiere que dicha indolamina fosforila y activa dicha proteína a través del sistema de retroalimentación que involucra a mTORC2 y no a través de PI3K (Fig. 38C). Aunque diversos estudios han demostrado la capacidad de la melatonina para regular la fosforilación de Akt, estos

parecen ser altamente dependientes del contexto celular, pues esta molécula es capaz de inducir [480] o inhibir la actividad de esta proteína [446]. Por otra parte, aunque la capacidad de la melatonina para modular la actividad de mTORC1 haya sido menos estudiada que la de Akt, se ha demostrado que dicha indolamina puede inhibir la actividad de dicha proteína en cáncer de próstata [427]. Finalmente, los efectos inhibitorios que ejerció la melatonina sobre los niveles proteicos de HIF-1 α fueron más pronunciados que los de la rapamicina, lo cual sugiere que dicho proceso no solo está mediado por la vía PI3K/Akt/mTORC1, sino que otros mecanismos celulares, como la vía de las MAPK, también deben de encontrarse potencialmente involucrados en este proceso [145].

4.3.5. La coadministración de melatonina y de sorafenib inhibe la mitofagia inducida por la hipoxia, lo cual lleva a la reducción de la viabilidad celular.

Como se demostró anteriormente, la melatonina es capaz de inducir la respuesta mitofágica en normoxia con el objetivo de reducir la resistencia innata de las células hepáticas cancerígenas al sorafenib. Con lo cual, se analizó si dicha molécula ejercía un efecto similar cuando dichas células se encuentran en hipoxia. Las principales proteínas encargadas de introducir las mitocondrias dañadas por la falta de oxígeno dentro de los autofagosomas son BNIP3 y Nix [348]. Estas proteínas se encuentran directamente reguladas por HIF-1 α y son capaces de interactuar directamente con LC3 a través de su dominio LC3. En la presente Tesis Doctoral la administración de sorafenib en las células de HCC mantenidas en hipoxia fue capaz de reducir la expresión tanto de BNIP3 como de Nix (Fig. 39A). Sin embargo, esta reducción solo indujo un retraso en la activación de dicha vía celular desde las 12 a las 24 h, como se pudo ver por el aumento de la colocalización entre las mitocondrias y los lisosomas, así como en la expresión de LC3-II y p62 transcurridas 24 h desde la administración de dicho fármaco (Figs. 40 y 41A). Por su parte, la adición de melatonina a las células tratadas con sorafenib no solo fue capaz de inhibir de forma clara la expresión de todos los marcadores testados en este experimento (Figs. 39A y 41A), sino que también redujo la interacción entre las mitocondrias y los lisosomas a todas las horas testadas (Fig. 40). Por otra parte, la reducción simultánea de los niveles proteicos de BNIP3, Nix y HIF-1 α tras el tratamiento conjunto con melatonina y sorafenib, así como la reducción de la expresión de BNIP3 tras el silenciamiento de dicho factor de

sugiere que la reducción de la mitofagia en las células de HCC en cultivo es debido a la reducción de la actividad de HIF-1 α debido al cotratamiento con melatonina y sorafenib.

Diversos estudios han demostrado que los inhibidores de la mitofagia pueden estimular los efectos citotóxicos de determinados fármacos, así como reducir la aparición de efectos adversos a la quimioterapia. Por ejemplo, la adición del inhibidor mitocondrial y de la mitofagia-1 (mdivi-1) es capaz de promover los efectos citotóxicos del cisplatino [481], así como de reducir los efectos nocivos sobre las células cardiacas de la doxorubicina [482]. Por otra parte, la liensinina, un alcaloide isoquinolina que impide la fusión entre los autofagosomas y los lisosomas, estimula la muerte celular de las células de cáncer de mama por parte de la doxorubicina [483]. Finalmente, la coadministración de sorafenib y Baf A1 reduce de forma clara el crecimiento de los tumores de mama en un estudio *in vivo*, así como la aparición de tumores secundarios en pulmón, cuello y timo [484].

La mitofagia presenta efectos totalmente opuestos entre las distintas fases de la progresión tumoral [361]. De forma más detallada, la proteína BNIP3 previene la tumorigénesis al aliviar el daño oxidativo durante las etapas tempranas de la tumorigénesis, mientras que en estadios avanzados protege a las células tumorales frente a situaciones de estrés y reduce su sensibilidad a la quimioterapia [361]. Como se puede ver en la Fig. 39B, el silenciamiento de la proteína BNIP3 indujo una reducción significativa de la viabilidad de las células Hep3B mantenidas en hipoxia. Así mismo, la restricción de la respuesta mitofagia tras la coadministración de melatonina y sorafenib estimuló de forma significativa la apoptosis, ya que indujo la escisión de PARP y la expresión de Bax en dichas células. Estos datos sugieren que la respuesta mitofágica inducida por la hipoxia es capaz de mantener el crecimiento de las células de HCC y de prevenir la inducción de apoptosis. De hecho, la sobreexpresión de BNIP3 se ha relacionado con el incremento de la agresividad tumoral y con la prevención de la muerte celular en el endometrio y en el cáncer de próstata [485,486].

Al comparar los resultados obtenidos por nosotros en hipoxia y en normoxia podemos observar que el papel que presenta la respuesta mitofagia en las células Hep3B es dependiente de la concentración de oxígeno presente en el microambiente. Esto es debido a que esta respuesta celular promueve la muerte de dichas células en normoxia, pero estimula su supervivencia en hipoxia. Con lo cual, la determinación de los niveles de

oxígeno disponibles en el microambiente tumoral ha de ser necesario para determinar el rol que presenta dicha molécula en la supervivencia celular.

Resumiendo, nuestros resultados han demostrado que la melatonina es capaz de estimular los efectos citotóxicos del sorafenib en hipoxia a través de la supresión de la expresión y la actividad de HIF-1 α y HIF-2 α (Fig. 45). Más detalladamente, esta indolamina es capaz de inhibir la síntesis proteica de HIF-1 α a través de la desregulación de la vía de mTORC1/p70S6K (Fig. 45). Por otra parte, la coadministración de esas moléculas induce la apoptosis a través de la represión de la respuesta mitofagia inducida por HIF-1 α (Fig. 45). Como conclusión, la melatonina parece ser capaz de reducir la resistencia adquirida al sorafenib de las células de HCC mantenidas en hipoxia.

5. Conclusiones.

Conclusión primera

La melatonina es capaz de inducir la autofagia en las células de HCC en cultivo a través de la activación de la UPR y de la vía de JNK, lo cual promueve en última instancia la disrupción del complejo formado entre Beclin1 y Bcl-2. Así mismo, mTORC1 parece no tener influencia en la inducción de esa respuesta celular. Por otra parte, dicha respuesta autofágica presenta una función protectora en las células de HCC, ya que previene los efectos citotóxicos de la melatonina.

Conclusión segunda

La melatonina es capaz de estimular la capacidad citotóxica del sorafenib en las células de HCC mantenidas en normoxia o hipoxia a través de la inducción de la vía intrínseca de la apoptosis.

Conclusión tercera

La coadministración de melatonina y sorafenib en normoxia estimula la sobreproducción de ROS en las mitocondrias, así como la pérdida del potencial de membrana basal de estos orgánulos. Estos dos procesos inducen la eliminación de las mitocondrias dañadas a través de la mitofagia dependiente de PINK1 y Parkin. Dicha respuesta parece promover la muerte de las células HCC en normoxia e induce la resistencia innata del tumor al sorafenib.

Conclusión cuarta

La coadministración de sorafenib y melatonina reduce transitoriamente la fusión mitocondrial en las células de HCC mantenidas en normoxia, lo que facilita la introducción de las mitocondrias dañadas en los autofagosomas. Así mismo, esta combinación terapéutica también es capaz de limitar la inducción de la fisión mitocondrial tras periodos de tratamiento prolongados con el fin de evitar que la respuesta mitofágica se active de forma continuada.

Conclusión quinta

La coadministración de melatonina y sorafenib reduce sinérgicamente la expresión y la actividad de HIF-1 α en células de HCC mantenidas en hipoxia. Además, la adición de melatonina a las células tratadas con sorafenib también es capaz de inhibir los niveles altos de expresión de la proteína HIF-2 α en este modelo celular, algo que no ocurre tras la administración única de sorafenib. Por otro lado, la restricción de la expresión de HIF-1 α en dicho modelo experimental induce una reducción parcial de la resistencia de esas células al sorafenib. No obstante, estos resultados no son suficientemente significativos debido a que se enmascara la falta de HIF-1 α a través de la inducción de las vías dependientes de HIF-2 α .

Conclusión sexta

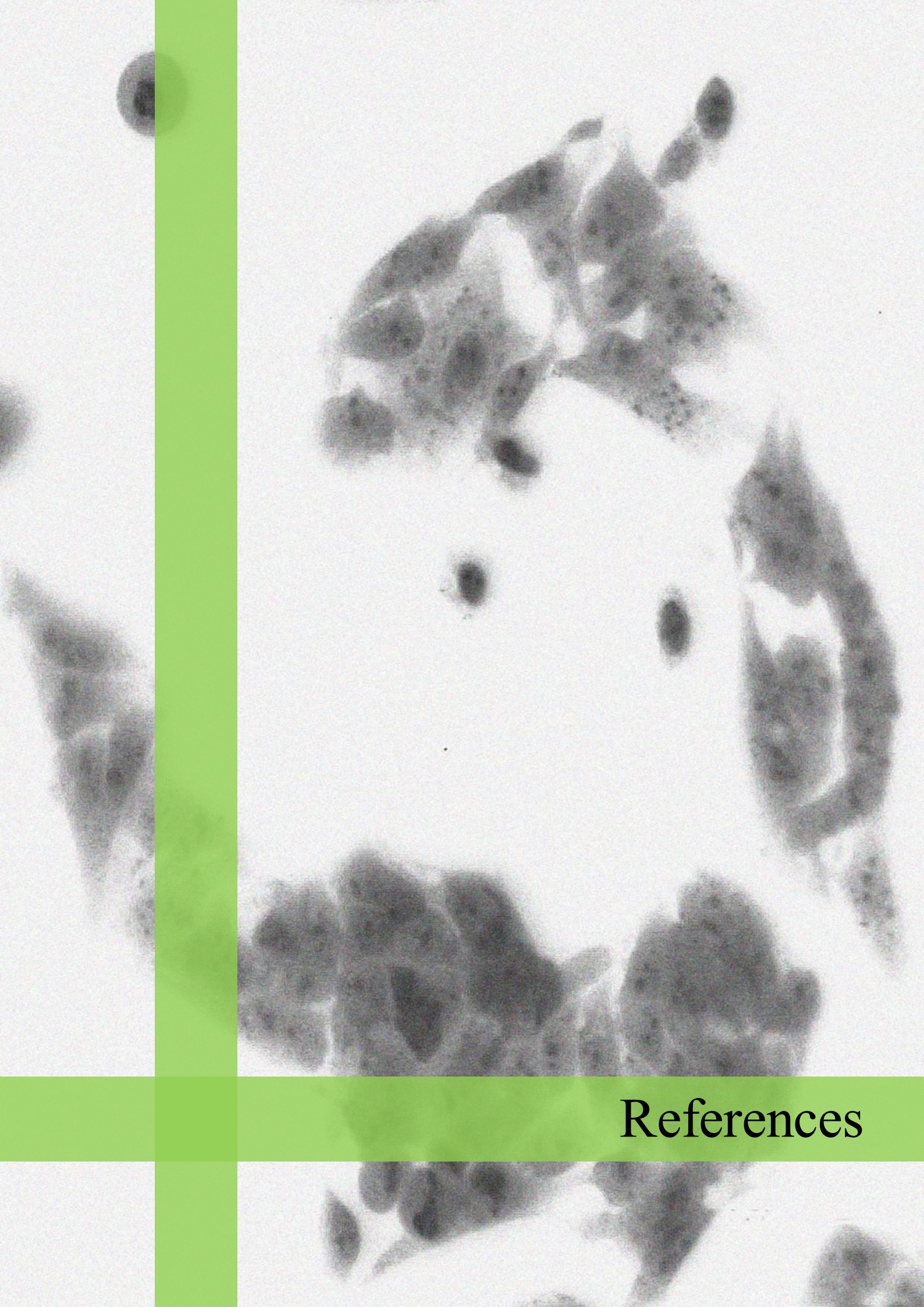
La melatonina reduce la síntesis de HIF-1 α en las células de HCC en hipoxia al prevenir la activación de la vía de mTORC1/p70S6K/RP-S6.

Conclusión séptima

La coadministración de melatonina y sorafenib reduce la mitofagia inducida por la falta de oxígeno a través de la prevención de la expresión de BNIP3 y Nix. Esta respuesta celular promueve la supervivencia de las células de HCC bajo hipoxia, con lo que su restricción por el tratamiento conjunto sensibilizará a las células al sorafenib.

Conclusión final

La melatonina es capaz de modular tanto la autofagia específica como la inespecífica en las células de HCC, reduciendo tanto la resistencia innata como la adquirida al sorafenib en normoxia e hipoxia. Estos datos respaldan el uso de la melatonina para mejorar la eficacia de sorafenib en el tratamiento de los pacientes con HCC en estadios avanzados. Sin embargo, estos efectos beneficiosos deberían verificarse tanto en estudios preclínicos como en clínicos para analizar su seguridad y su uso óptimo. Estos ensayos serán los que finalmente permitan el uso de esta combinación en el tratamiento de dichos pacientes.



References

1. Bray F, Ferlay J, Soerjomataram I, Siegel RL, Torre LA, Jemal A. Global cancer statistics 2018: GLOBOCAN estimates of incidence and mortality worldwide for 36 cancers in 185 countries. *CA Cancer J Clin.* 2018;In press.
2. Wan HG, Xu H, Gu YM, Wang H, Xu W, Zu MH. Comparison osteopontin vs AFP for the diagnosis of HCC: A meta-analysis. *Clin. Res. Hepatol. Gastroenterol.* 2014;38(6):706–14.
3. Ferlay J, Soerjomataram I, Dikshit R, Eser S, Mathers C, Rebelo M, et al. Cancer incidence and mortality worldwide: sources, methods and major patterns in GLOBOCAN 2012. *Int. J. Cancer.* 2015;136(5):E359-86.
4. Siegel RL, Miller KD, Jemal A. Cancer statistics, 2015. *CA Cancer J Clin.* 2015;65(1):5–29.
5. Galceran J, Ameijide A, Carulla M, Mateos A, Quirós JR, Rojas D, et al. Cancer incidence in Spain, 2015. *Clin. Transl. Oncol.* 2017;19(7):799–825.
6. Lepage C, Capocaccia R, Hackl M, Lemmens V, Molina E, Pierannunzio D, et al. Survival in patients with primary liver cancer, gallbladder and extrahepatic biliary tract cancer and pancreatic cancer in Europe 1999 – 2007: Results of EURO CARE-5. *Eur. J. Cancer.* 2015;51(15):2169–78.
7. Sia D, Villanueva A, Friedman SL, Llovet JM. Liver cancer cell of origin, molecular class, and effects on patient prognosis. *Gastroenterology.* 2017;152(4):745–61.
8. Hirohashi S, Blum HE, Ishak KG, Deugnier Y, Kojiro M, Laurent Puig P, et al. Tumours of the liver and intrahepatic bile ducts. In: Hamilton SR, Aaltonen LA, editors. *Pathology and genetics of tumours of the digestive system.* Lyon: International Agency for Research on Cancer (IARC); 2000. p. 157–202.
9. Janevska D, Chaloska-Ivanova V, Janevski V. Hepatocellular carcinoma: Risk factors, diagnosis and treatment. *Open access Maced. J. Med. Sci.* 2015;3(4):732–6.
10. Mu X, Español-Suñer R, Mederacke I, Affò S, Manco R, Sempoux C, et al. Hepatocellular carcinoma originates from hepatocytes and not from the progenitor/biliary compartment. *J. Clin. Invest.* 2015;125(10):3891–903.
11. Mokkapatil S, Niopek K, Huang L, Cunniff KJ, Ruteshouser EC, DeCaestecker M, et al. β -catenin activation in a novel liver progenitor cell type is sufficient to cause hepatocellular carcinoma and hepatoblastoma. *Cancer Res.* 2014;74(16):4515–25.

12. Lee JS, Heo J, Libbrecht L, Chu IS, Kaposi-Novak P, Calvisi DF, et al. A novel prognostic subtype of human hepatocellular carcinoma derived from hepatic progenitor cells. *Nat. Med.* 2006;12(4):410–6.
13. Marquardt JU, Andersen JB, Thorgeirsson SS. Functional and genetic deconstruction of the cellular origin in liver cancer. *Nat. Rev. Cancer.* 2015;15(11):653–67.
14. Feitelson MA, Sun B, Satiroglu Tufan NL, Liu J, Pan J, Lian Z. Genetic mechanisms of hepatocarcinogenesis. *Oncogene.* 2002;21(16):2593–604.
15. Pivonello C, De Martino MC, Negri M, Cuomo G, Cariati F, Izzo F, et al. The GH-IGF-SST system in hepatocellular carcinoma: Biological and molecular pathogenetic mechanisms and therapeutic targets. *Infect. Agent. Cancer.* 2014;9:27.
16. Carbajo-Pescador S, Ordoñez R, Benet M, Jover R, García-Palomo A, Mauriz JL, et al. Inhibition of VEGF expression through blockade of Hif1 α and STAT3 signalling mediates the anti-angiogenic effect of melatonin in HepG2 liver cancer cells. *Br. J. Cancer.* 2013;109(1):83–91.
17. Ordoñez R, Carbajo-Pescador S, Prieto-Dominguez N, García-Palomo A, González-Gallego J, Mauriz JL, et al. Inhibition of matrix metalloproteinase-9 and nuclear factor kappa B contribute to melatonin prevention of motility and invasiveness in HepG2 liver cancer cells. *J. Pineal Res.* 2014;56(1):20–30.
18. Trad D, Bibani N, Sabbah M, Elloumi H, Gargouri D, Ouakaa A, et al. Known, new and emerging risk factors of hepatocellular carcinoma. *Presse Med.* 2017;46(11):1000–7.
19. Balogh J, Victor III D, Asham EH, Burroghs SG, Boktour M, Saharia A, et al. Hepatocellular carcinoma : a review. *J Hepatocell Carcinoma.* 2016;3:41–53.
20. Raimondo G, Caccamo G, Filomia R, Pollicino T. Occult HBV infection. *Semin. Immunopathol.* 2013;35(1):39–52.
21. Kao JH. Hepatitis B vaccination and prevention of hepatocellular carcinoma. *Best Pract. Res. Clin. Gastroenterol.* 2015;29(6):907–17.
22. Hosaka T, Suzuki F, Kobayashi M, Seko Y, Kawamura Y, Sezaki H, et al. Long-term entecavir treatment reduces hepatocellular carcinoma incidence in patients with hepatitis B virus infection. *Hepatology.* 2013;58(1):98–107.

23. Choi J, Corder NLB, Koduru B, Wang Y. Oxidative stress and hepatic Nox proteins in chronic hepatitis C and hepatocellular carcinoma. *Free Radic. Biol. Med.* 2014;72:267–84.
24. Sheikh MY, Choi J, Qadri I, Friedman JE, Sanyal AJ. Hepatitis C virus infection: Molecular pathways to metabolic syndrome. *Hepatology.* 2008;47(6):2127–33.
25. Morgan RL, Baack B, Smith BD, Yartel A, Pitasi M, Falck-Ytter Y. Eradication of hepatitis C virus infection and the development of Hepatocellular Carcinoma. *Ann. Intern. Med.* 2013;158(5 Pt 1):329–37.
26. Abbas Z, Abbas M, Abbas S, Shazi L. Hepatitis D and hepatocellular carcinoma. *World J. Hepatol.* 2015;7(5):777–86.
27. Jewell J, Sheron N. Trends in European liver death rates: Implications for alcohol policy. *Clin. Med.* 2010;10(3):259–63.
28. Galati G, Dell'Unto C, Vespasiani-Gentilucci U, De Vincentis A, Gallo P, Guidi A, et al. Hepatocellular carcinoma in alcoholic liver disease: Current management and recent advances. *Rev. Recent Clin. Trials.* 2016;11(3):238–52.
29. Pisonero-Vaquero S, González-Gallego J, Sánchez-Campos S, García-Mediavilla MV. Flavonoids and related compounds in non-alcoholic fatty liver disease therapy. *Curr. Med. Chem.* 2015;22(25):2991–3012.
30. Sharp GB, Lagarde F, Mizuno T, Sauvaget C, Fukuhara T, Allen N, et al. Relationship of hepatocellular carcinoma to soya food consumption: A cohort-based, case-control study in Japan. *Int. J. Cancer.* 2005;115(2):290–5.
31. Petrick JL, Freedman ND, Graubard BI, Sahasrabudhe V V., Lai GY, Alavanja MC, et al. Coffee consumption and risk of hepatocellular carcinoma and intrahepatic cholangiocarcinoma by sex: The liver cancer pooling project. *Cancer Epidemiol. Biomarkers Prev.* 2015;24(9):1398–406.
32. Talamini R, Polesel J, Montella M, Dal Maso L, Crispo A, Tommasi LG, et al. Food groups and risk of hepatocellular carcinoma: A multicenter case-control study in Italy. *Int. J. Cancer.* 2006;119(12):2916–21.
33. Kumar P, Mahato DK, Kamle M, Mohanta TK, Kang SG. Aflatoxins: A global concern for food safety, human health and their management. *Front. Microbiol.* 2017;7:2170.

34. Kucukcakan B, Hayrulai-Musliu Z. Challenging role of dietary aflatoxin B₁ exposure and hepatitis B infection on risk of hepatocellular carcinoma. Open access Maced. J. Med. Sci. 2015;3(2):363–9.
35. Chu YJ, Yang HI, Wu HC, Liu J, Wang LY, Lee MH, et al. Aflatoxin B₁ exposure increases the risk of cirrhosis and hepatocellular carcinoma in chronic hepatitis B virus carriers. Int J Cancer. 2017;141(4):711–20.
36. Qi LN, Bai T, Chen ZS, Wu FX, Chen YY, Xiang B De, et al. The p53 mutation spectrum in hepatocellular carcinoma from Guangxi, China: Role of chronic hepatitis B virus infection and aflatoxin B₁ exposure. Liver Int. 2015;35(3):999–1009.
37. Jiao J, Niu W, Wang Y, Baggerly KA, Ye Y, Wu X, et al. Prevalence of aflatoxin-associated *TP53R249S* mutation in hepatocellular carcinoma in hispanics in South Texas. Cancer Prev. Res. 2018;11(2):103–12.
38. VoPham T, Bertrand KA, Hart JE, Laden F, Brooks MM, Yuan J-M, et al. Pesticide exposure and liver cancer: A review. Cancer Causes Control. 2017;28(3):177–90.
39. Waluga M, Kukla M, Zorniak M, Bacik A, Kotulski R. From the stomach to other organs: *Helicobacter pylori* and the liver. World J. Hepatol. 2015;7(18):2136–46.
40. Ito K, Nakamura M, Toda G, Negishi M, Torii A, Ohno T. Potential role of *Helicobacter pylori* in hepatocarcinogenesis. Int. J. Mol. Med. 2004;13(2):221–7.
41. Zhang Y, Fan XG, Chen R, Xiao ZQ, Feng XP, Tian XF, et al. Comparative proteome analysis of untreated and *Helicobacter pylori*-treated HepG2. World J. Gastroenterol. 2005;11(22):3485–9.
42. Yang D, Hanna DL, Usher J, LoCoco J, Chaudhari P, Lenz HJ, et al. Impact of sex on the survival of patients with hepatocellular carcinoma: A surveillance, epidemiology, and end results analysis. Cancer. 2014;120(23):3707–16.
43. Lee HW, Ahn SH. Prediction models of hepatocellular carcinoma development in chronic hepatitis B patients. World J. Gastroenterol. 2016;22(37):8314–21.
44. Attwa MH, El-Etreby SA. Guide for diagnosis and treatment of hepatocellular carcinoma. World J. Hepatol. 2015;7(12):1632–51.

45. Goshima S. Use of imaging techniques to screen hepatocellular carcinoma. In: Carr BI, editor. *Hepatocellular Carcinoma*. 3rd ed. Basel: Springer International Publishing; 2016. p. 355–65.
46. Gomaa AI, Khan SA, Leen ELS, Waked I, Taylor-Robinson SD. Diagnosis of hepatocellular carcinoma. *World J. Gastroenterol.* 2009;15(11):1301–14.
47. Bialecki ES, Di Bisceglie AM. Diagnosis of hepatocellular carcinoma. *HPB.* 2005;7(1):26–34.
48. Memon WA, Haider Z, Beg MA, Idris M, Ul-Haq T, Akhtar W, et al. Diagnosis of hepatoma using grayscale and Doppler ultrasound in patients with chronic liver disease. *Int. J. Gen. Med.* 2011;4:751–4.
49. Daniele B, Bencivenga A, Megna AS, Tinessa V. α -fetoprotein and ultrasonography screening for hepatocellular carcinoma. *Gastroenterology.* 2004;127(5 Suppl 1):S108–12.
50. Ayuso C, Rimola J, García-Criado A. Imaging of HCC. *Abdom. Imaging.* 2012;37(2):215–30.
51. Bertino G, Ardiri A, Malaguarnera M, Malaguarnera G, Bertino N, Calvagno GS. Hepatocellular carcinoma serum markers. *Semin. Oncol.* 2012;39(4):410–33.
52. Shu H, Li W, Shang S, Qin X, Zhang S, Liu Y. Diagnosis of AFP-negative early-stage hepatocellular carcinoma using Fuc-PON1. *Discov. Med.* 2017;23(126):163–8.
53. Hung CH, Hu TH, Lu SN, Kuo FY, Chen CH, Wang JH, et al. Circulating microRNAs as biomarkers for diagnosis of early hepatocellular carcinoma associated with hepatitis B virus. *Int. J. Cancer.* 2016;138(3):714–20.
54. Li D, Satomura S. Biomarkers for hepatocellular carcinoma (HCC): An update. In: Scatena R, editor. *Advances in experimental medicine and biology*. Basel: Springer International Publishing; 2015. p. 179–93.
55. Nakagawa T, Takeishi S, Kameyama A, Yagi H, Yoshioka T, Moriwaki K, et al. Glycomic analyses of glycoproteins in bile and serum during rat hepatocarcinogenesis. *J. Proteome Res.* 2010;9(10):4888–96.

56. Fujikawa T, Shihara H, Yamamoto K. Significance of des-gamma-carboxy prothrombin production in hepatocellular carcinoma. *Acta Med. Okayama.* 2009;63(6):299–304.
57. Shang S, Plymoth A, Ge S, Feng Z, Rosen HR, Sangrajang S, et al. Identification of osteopontin as a novel marker for early hepatocellular carcinoma. *Hepatology.* 2012;55(2):483–90.
58. Wang L, Yao M, Pan LH, Qian Q, Yao DF. Glypican-3 is a biomarker and a therapeutic target of hepatocellular carcinoma. *Hepatobiliary Pancreat. Dis. Int.* 2015;14(4):361–6.
59. Li J, Gao JZ, Du JL, Xin WL. Prognostic and clinicopathological significance of glypican-3 overexpression in hepatocellular carcinoma: A meta-analysis. *World J. Gastroenterol.* 2014;20(20):6336–44.
60. Rockey DC, Caldwell SH, Goodman ZD, Nelson RC, Smith AD. Liver biopsy. *Hepatology.* 2009;49(3):1017–44.
61. Subramaniam S, Kelley RK, Venook AP. A review of hepatocellular carcinoma (HCC) staging systems. *Chinese Clin. Oncol.* 2013;2(4):33.
62. Maida M, Orlando E, Cammà C, Cabibbo G. Staging systems of hepatocellular carcinoma: A review of literature. *World J. Gastroenterol.* 2014;20(15):4141–50.
63. Kim BK, Kim SU, Park JY, Kim DY, Ahn SH, Park MS, et al. Applicability of BCLC stage for prognostic stratification in comparison with other staging systems: Single centre experience from long-term clinical outcomes of 1717 treatment-naïve patients with hepatocellular carcinoma. *Liver Int.* 2012;32(7):1120–7.
64. Forner A, Llovet JM, Bruix J. Hepatocellular carcinoma. *Lancet.* 2012;379(9822):1245–55.
65. Avila MA, Berasain C, Sangro B, Prieto J. New therapies for hepatocellular carcinoma. *Oncogene.* 2006;25(27):3866–84.
66. Mauer K, O’Kelley R, Podda N, Flanagan S, Gadani S. New treatment modalities for hepatocellular cancer. *Curr. Gastroenterol. Rep.* 2015;17(5):442.
67. Rodríguez De Lope C, Tremosini S, Forner A, Reig M, Bruix J. Management of HCC. *J. Hepatol.* 2012;56(Suppl. 1):S75–87.

68. Raza A, Sood GK. Hepatocellular carcinoma review: Current treatment, and evidence-based medicine. *World J. Gastroenterol.* 2014;20(15):4115–27.
69. Schlachterman A, Craft WW, Hilgenfeldt E, Mitra A, Cabrera R. Current and future treatments for hepatocellular carcinoma. *World J. Gastroenterol.* 2015;21(28):8478–91.
70. Mazzaferro V, Bhoori S, Sposito C, Bongini M, Langer M, Miceli R, et al. Milan criteria in liver transplantation for hepatocellular carcinoma: An evidence-based analysis of 15 years of experience. *Liver Transplant.* 2011;17(Suppl. 2):S44–57.
71. Mazzaferro V. Results of liver transplantation: with or without Milan criteria? *Liver Transplant.* 2007;13(11 Suppl. 2):S44–7.
72. Cucchetti A, Piscaglia F, Caturelli E, Benvegnù L, Vivarelli M, Ercolani G, et al. Comparison of recurrence of hepatocellular carcinoma after resection in patients with cirrhosis to its occurrence in a surveilled cirrhotic population. *Ann. Surg. Oncol.* 2009;16(2):413–22.
73. Kim YS, Lim HK, Rhim H, Lee MW. Ablation of hepatocellular carcinoma. *Best Pract. Res. Clin. Gastroenterol.* 2014;28(5):897–908.
74. Kong WT, Zhang WW, Qiu YD, Zhou T, Qiu JL, Zhang W, et al. Major complications after radiofrequency ablation for liver tumors: Analysis of 255 patients. *World J. Gastroenterol.* 2009;15(21):2651–6.
75. Imai N, Ishigami M, Ishizu Y, Kuzuya T, Honda T, Hayashi K, et al. Transarterial chemoembolization for hepatocellular carcinoma: A review of techniques. *World J. Hepatol.* 2014;6(12):844–50.
76. Zeeneldin AA, Salem SE, Tabashy RH, Ibrahim AA, Alieldin NH. Transarterial chemoembolization for the treatment of hepatocellular carcinoma: A single center experience including 221 patients. *J. Egypt. Natl. Canc. Inst.* 2013;25(3):143–50.
77. Sangro B, Carpanese L, Cianni R, Golfieri R, Gasparini D, Ezziddin S, et al. Survival after yttrium-90 resin microsphere radioembolization of hepatocellular carcinoma across Barcelona clinic liver cancer stages: A European evaluation. *Hepatology.* 2011;54(3):868–78.
78. Llovet JM, Ricci S, Mazzaferro V, Hilgard P, Gane E, Blanc JF, et al. Sorafenib in advanced hepatocellular carcinoma. *N. Engl. J. Med.* 2008;359(4):378–90.

79. Cheng AL, Kang YK, Chen Z, Tsao CJ, Qin S, Kim JS, et al. Efficacy and safety of sorafenib in patients in the Asia-Pacific region with advanced hepatocellular carcinoma: A phase III randomised, double-blind, placebo-controlled trial. *Lancet Oncol.* 2009;10(1):25–34.
80. Kudo M. Systemic therapy for hepatocellular carcinoma: 2017 update. *Oncology.* 2017;93(Suppl. 1):135–46.
81. Gauthier A, Ho M. Role of sorafenib in the treatment of advanced hepatocellular carcinoma: An update. *Hepatol. Res.* 2013;43(2):147–54.
82. Kaplan DE, Mehta R, D’Addeo K, Valderrama A, Taddei TH. Sorafenib prescribed by gastroenterologists and hepatologists for hepatocellular carcinoma. *Med.* 2018;97(4):e9757.
83. Fishman MN, Tomshine J, Fulp WJ, Foreman PK. A systematic review of the efficacy and safety experience reported for sorafenib in advanced renal cell carcinoma (RCC) in the post-approval setting. *PLoS One.* 2015;10(4):e0120877.
84. Thomas L, Lai SY, Dong W, Feng L, Dadu R, Regone RM, et al. Sorafenib in metastatic thyroid cancer: A systematic review. *Oncologist.* 2014;19(3):251–8.
85. Steinbild S, Mross K, Frost A, Morant R, Gillessen S, Dittrich C, et al. A clinical phase II study with sorafenib in patients with progressive hormone-refractory prostate cancer: A study of the CESAR Central European Society for Anticancer Drug Research-EWIV. *Br. J. Cancer.* 2007;97(11):1480–5.
86. Janjigian YY, Vakiani E, Ku GY, Herrera JM, Tang LH, Bouvier N, et al. Phase II trial of sorafenib in patients with chemotherapy refractory metastatic esophageal and gastroesophageal (GE) junction cancer. *PLoS One.* 2015;10(8):e0134731.
87. Llovet JM, Peña CEA, Lathia CD, Shan M, Meinhardt G, Bruix J. Plasma biomarkers as predictors of outcome in patients with advanced hepatocellular carcinoma. *Clin. Cancer Res.* 2012;18(8):2290–300.
88. Lencioni R, Kudo M, Ye SL, Bronowicki JP, Chen XP, Dagher L, et al. GIDEON (Global Investigation of therapeutic DEcisions in hepatocellular carcinoma and Of its treatment with sorafeNib): Second interim analysis. *Int. J. Clin. Pract.* 2014;68(5):609–17.

89. Chen J, Jin R, Zhao J, Liu J, Ying H, Yan H, et al. Potential molecular, cellular and microenvironmental mechanism of sorafenib resistance in hepatocellular carcinoma. *Cancer Lett.* 2015;367(1):1–11.
90. Prieto-Domínguez N, Ordóñez R, Fernández A, García-Palomo A, Muntané J, González-Gallego J, et al. Modulation of autophagy by sorafenib: Effects on treatment response. *Front. Pharmacol.* 2016;7:151.
91. Ezzoukhry Z, Louandre C, Trécherel E, Godin C, Chauffert B, Dupont S, et al. EGFR activation is a potential determinant of primary resistance of hepatocellular carcinoma cells to sorafenib. *Int. J. Cancer.* 2012;131(12):2961–9.
92. Liu L, Cao Y, Chen C, Zhang X, McNabola A, Wilkie D, et al. Sorafenib blocks the RAF/MEK/ERK pathway, inhibits tumor angiogenesis, and induces tumor cell apoptosis in hepatocellular carcinoma model PLC/PRF/5. *Cancer Res.* 2006;66(24):11851–8.
93. Ou DL, Shen YC, Yu SL, Chen KF, Yeh PY, Fan HH, et al. Induction of DNA damage-inducible gene GADD45 β contributes to sorafenib-induced apoptosis in hepatocellular carcinoma cells. *Cancer Res.* 2010;70(22):9309–18.
94. Higgs MR, Lerat H, Pawlowsky JM. Downregulation of GADD45 β expression by hepatitis C virus leads to defective cell cycle arrest. *Cancer Res.* 2010;70(12):4901–11.
95. Gillissen B, Richter A, Richter A, Preissner R, Schulze-Osthoff K, Essmann F, et al. Bax/Bak-independent mitochondrial depolarization and reactive oxygen species induction by sorafenib overcome resistance to apoptosis in renal cell carcinoma. *J. Biol. Chem.* 2017;292(16):6478–92.
96. Chen KF, Tai WT, Liu TH, Huang HP, Lin YC, Shiau CW, et al. Sorafenib overcomes TRAIL resistance of hepatocellular carcinoma cells through the inhibition of STAT3. *Clin. Cancer Res.* 2010;16(21):5189–99.
97. Wilhelm SM, Carter C, Tang L, Wilkie D, McNabola A, Rong H, et al. BAY 43-9006 exhibits broad spectrum oral antitumor activity and targets the RAF/MEK/ERK pathway and receptor tyrosine kinases involved in tumor progression and angiogenesis. *Cancer Res.* 2004;64(19):7099–109.

98. Woo HY, Heo J. Sorafenib in liver cancer. *Expert Opin. Pharmacother.* 2012;13(7):1059–67.
99. Di Marco V, De Vita F, Koskinas J, Semela D, Toniutto P, Verslype C. Sorafenib: From literature to clinical practice. *Ann. Oncol.* 2013;24(Suppl. 2):ii30-7.
100. Ara M, Pastushenko E. Antiangiogenic agents and the skin: Cutaneous adverse effects of sorafenib, sunitinib, and bevacizumab. *Actas Dermosifiliogr.* 2014;105(10):900–12.
101. Zhang L, Zhou Q, Ma L, Wu Z, Wang Y. Meta-analysis of dermatological toxicities associated with sorafenib. *Clin. Exp. Dermatol.* 2011;36(4):344–50.
102. Kudo M, Lencioni R, Marrero JA, Venook AP, Bronowicki JP, Chen XP, et al. Regional differences in sorafenib-treated patients with hepatocellular carcinoma: GIDEON observational study. *Liver Int.* 2016;36(8):1196–205.
103. Keating GM. Sorafenib: A review in hepatocellular carcinoma. *Targ. Oncol.* 2017;12(2):243–53.
104. Stasi R, Abriani L, Beccaglia P, Terzoli E, Amadori S. Cancer-related fatigue: Evolving concepts in evaluation and treatment. *Cancer.* 2003;98(9):1786–801.
105. Zhai B, Sun XY. Mechanisms of resistance to sorafenib and the corresponding strategies in hepatocellular carcinoma. *World J. Hepatol.* 2013;5(7):345–52.
106. Sun T, Liu H, Ming L. Multiple roles of autophagy in the sorafenib resistance of hepatocellular carcinoma. *Cell. Physiol. Biochem.* 2017;44(2):716–27.
107. Niu L, Liu L, Yang S, Ren J, Lai PBS, Chen GG. New insights into sorafenib resistance in hepatocellular carcinoma: Responsible mechanisms and promising strategies. *Biochim. Biophys. Acta - Rev. Cancer.* 2017;1868(2):564–70.
108. Zhu YJ, Zheng B, Wang HY, Chen L. New knowledge of the mechanisms of sorafenib resistance in liver cancer. *Acta Pharmacol. Sin.* 2017;38(5):614–22.
109. Blivet-Van Eggelpoël MJ, Chettouh H, Fartoux L, Aoudjehane L, Barbu V, Rey C, et al. Epidermal growth factor receptor and HER-3 restrict cell response to sorafenib in hepatocellular carcinoma cells. *J. Hepatol.* 2012;57(1):108–15.
110. Hagiwara S, Kudo M, Nagai T, Inoue T, Ueshima K, Nishida N, et al. Activation of JNK and high expression level of CD133 predict a poor response to sorafenib in hepatocellular carcinoma. *Br. J. Cancer.* 2012;106(12):1997–2003.

111. Zhang Z, Zhou X, Shen H, Wang D, Wang Y. Phosphorylated ERK is a potential predictor of sensitivity to sorafenib when treating hepatocellular carcinoma: Evidence from an *in vitro* study. *BMC Med.* 2009;7:41.
112. Jin W, Chen L, Cai X, Zhang Y, Zhang J, Ma D, et al. Long non-coding RNA TUC338 is functionally involved in sorafenib-sensitized hepatocarcinoma cells by targeting RASAL1. *Oncol. Rep.* 2017;37(1):273–80.
113. Vaira V, Roncalli M, Carnaghi C, Faversani A, Maggioni M, Augello C, et al. MicroRNA-425-3p predicts response to sorafenib therapy in patients with hepatocellular carcinoma. *Liver Int.* 2015;35(3):1077–86.
114. Yi H, Ye X, Long B, Ye T, Zhang L, Yan F, et al. Inhibition of the Akt/mTOR pathway augments the anticancer effects of sorafenib in thyroid cancer. *Cancer Biother. Radiopharm.* 2017;32(5):176–83.
115. Chen KF, Chen HL, Tai WT, Feng WC, Hsu CH, Chen PJ, et al. Activation of phosphatidylinositol 3-kinase/Akt signaling pathway mediates acquired resistance to sorafenib in hepatocellular carcinoma cells. *J. Pharmacol. Exp. Ther.* 2011;337(1):155–61.
116. Chai H, Luo AZ, Weerasinghe P, Brown RE. Sorafenib downregulates ERK/Akt and STAT3 survival pathways and induces apoptosis in a human neuroblastoma cell line. *Int. J. Clin. Exp. Pathol.* 2010;3(4):408–15.
117. Tai WT, Cheng AL, Shiau CW, Liu CY, Ko CH, Lin MW, et al. Dovitinib induces apoptosis and overcomes sorafenib resistance in hepatocellular carcinoma through SHP-1-mediated inhibition of STAT3. *Mol. Cancer Ther.* 2012;11(2):452–63.
118. Sakurai T, Yada N, Hagiwara S, Arizumi T, Minaga K, Kamata K, et al. Gankyrin induces STAT3 activation in tumor microenvironment and sorafenib resistance in hepatocellular carcinoma. *Cancer Sci.* 2017;108(10):1996–2003.
119. van Malenstein H, Dekervel J, Verslype C, Van Cutsem E, Windmolders P, Nevens F, et al. Long-term exposure to sorafenib of liver cancer cells induces resistance with epithelial-to-mesenchymal transition, increased invasion and risk of rebound growth. *Cancer Lett.* 2013;329(1):74–83.

120. Shimizu S, Takehara T, Hikita H, Kodama T, Tsunematsu H, Miyagi T, et al. Inhibition of autophagy potentiates the antitumor effect of the multikinase inhibitor sorafenib in hepatocellular carcinoma. *Int. J. cancer.* 2012;131(3):548–57.
121. Jiao M, Nan KJ. Activation of PI3 kinase/Akt/HIF-1 α pathway contributes to hypoxia-induced epithelial-mesenchymal transition and chemoresistance in hepatocellular carcinoma. *Int. J. Oncol.* 2012;40(2):461–8.
122. Liang Y, Zheng T, Song R, Wang J, Yin D, Wang L, et al. Hypoxia-mediated sorafenib resistance can be overcome by EF24 through Von Hippel-Lindau tumor suppressor-dependent HIF-1 α inhibition in hepatocellular carcinoma. *Hepatology.* 2013;57(5):1847–57.
123. Wörns MA, Galle PR. Hepatocellular carcinoma in 2017: Two large steps forward, one small step back. *Nat. Rev. Gastroenterol. Hepatol.* 2018;15(2):74–6.
124. Bruix J, Qin S, Merle P, Granito A, Huang YH, Bodoky G, et al. Regorafenib for patients with hepatocellular carcinoma who progressed on sorafenib treatment (RESORCE): A randomised, double-blind, placebo-controlled, phase 3 trial. *Lancet.* 2017;389(10064):56–66.
125. Kyrochristos ID, Ziogas DE, Roukos DH. Regorafenib: A newly approved drug for advanced hepatocellular carcinoma. *Futur. Oncol.* 2017;13(19):1665–8.
126. El-Khoueiry AB, Sangro B, Yau T, Crocenzi TS, Kudo M, Hsu C, et al. Nivolumab in patients with advanced hepatocellular carcinoma (CheckMate 040): An open-label, non-comparative, phase 1/2 dose escalation and expansion trial. *Lancet.* 2017;389(10088):2492–502.
127. Food and Drug Administration (FDA). Highlights of prescribing information for Opvido. 2018.
128. Peerlings J, Van De Voorde L, Mitea C, Larue R, Yaromina A, Sandeleanu S, et al. Hypoxia and hypoxia response-associated molecular markers in esophageal cancer: A systematic review. *Methods.* 2017;130:51–62.
129. Sormendi S, Wielockx B. Hypoxia pathway proteins as central mediators of metabolism in the tumor cells and their microenvironment. *Front. Immunol.* 2018;9:40.
130. Eales KL, Hollinshead KER, Tennant DA. Hypoxia and metabolic adaptation of cancer cells. *Oncogenesis.* 2016;5:e190.

131. Semenza GL. Oxygen sensing, hypoxia-inducible factors, and disease pathophysiology. *Annu. Rev. Pathol. Mech. Dis.* 2014;9(1):47–71.
132. Semenza GL. HIF-1 mediates metabolic responses to intratumoral hypoxia and oncogenic mutations. *J. Clin. Invest.* 2013;123(9):3664–71.
133. Pescador N, Villar D, Cifuentes D, Garcia-Rocha M, Ortiz-Barahona A, Vazquez S, et al. Hypoxia promotes glycogen accumulation through hypoxia inducible factor (HIF)-mediated induction of glycogen synthase 1. *PLoS One.* 2010;5(3):e9644.
134. Schito L, Semenza GL. Hypoxia-inducible factors: Master regulators of cancer progression. *Trends Cancer.* 2016;2(12):758–70.
135. Carmeliet P, Jain RK. Principles and mechanisms of vessel normalization for cancer and other angiogenic diseases. *Nat. Rev. Drug Discov.* 2011;10(6):417–27.
136. Chang J, Erler J. Hypoxia-mediated metastasis. In: Koumenis C, Hammond E, Giaccia A, editors. *Tumor Microenvironment and Cellular Stress.* New York: Springer Science + Business Media; 2014. p. 55–81.
137. Chen C, Lou T. Hypoxia inducible factors in hepatocellular carcinoma. *Oncotarget.* 2017;8(28):46691–703.
138. Sokkar P, Sathis V, Ramachandran M. Computational modeling on the recognition of the HRE motif by HIF-1: Molecular docking and molecular dynamics studies. *J. Mol. Model.* 2012;18(5):1691–700.
139. Kietzmann T, Mennerich D, Dimova EY. Hypoxia-inducible factors (HIFs) and phosphorylation: impact on stability, localization, and transactivity. *Front. Cell Dev. Biol.* 2016;4:11.
140. Heikkilä M, Pasanen A, Kivirikko KI, Myllyharju J. Roles of the human hypoxia-inducible factor (HIF)-3 α variants in the hypoxia response. *Cell. Mol. Life Sci.* 2011;68(23):3885–901.
141. Maynard MA, Evans AJ, Hosomi T, Hara S, Jewett MAS, Ohh M. Human HIF-3 α 4 is a dominant-negative regulator of HIF-1 and is down-regulated in renal cell carcinoma. *FASEB J.* 2005;19(11):1396–406.

142. Zimna A, Kurpisz M. Hypoxia-inducible factor-1 in physiological and pathophysiological angiogenesis: Applications and therapies. *Biomed Res. Int.* 2015;2015:549412.
143. Bersten DC, Sullivan AE, Peet DJ, Whitelaw ML. bHLH-PAS proteins in cancer. *Nat. Rev. Cancer.* 2013;13(12):827–41.
144. Nordgren IK, Tavassoli A. Targeting tumour angiogenesis with small molecule inhibitors of hypoxia inducible factor. *Chem. Soc. Rev.* 2011;40(8):4307–17.
145. Masoud GN, Li W. HIF-1 α pathway: Role, regulation and intervention for cancer therapy. *Acta Pharm. Sin. B.* 2015;5(5):378–89.
146. Wigerup C, Pålman S, Bexell D. Therapeutic targeting of hypoxia and hypoxia-inducible factors in cancer. *Pharmacol. Ther.* 2016;164:152–69.
147. Cokol M, Nair R, Rost B. Finding nuclear localization signals. *EMBO Rep.* 2000;1(5):411–5.
148. Koh MY, Powis G. HAF : The new player in oxygen-independent HIF-1 α degradation. *Cell cycle.* 2009;8(9):1359–66.
149. Myllyharju J. Prolyl 4-hydroxylases, master regulators of the hypoxia response. *Acta Physiol.* 2013;208(2):148–65.
150. Bishop T, Gallagher D, Pascual A, Lygate CA, de Bono JP, Nicholls LG, et al. Abnormal sympathoadrenal development and systemic hypotension in PHD3^{-/-} mice. *Mol. Cell. Biol.* 2008;28(10):3386–400.
151. Berra E, Benizri E, Ginouvès A, Volmat V, Roux D, Pouyssegur J. HIF prolyl-hydroxylase 2 is the key oxygen sensor setting low steady-state levels of HIF-1 α in normoxia. *EMBO J.* 2003;22(16):4082–90.
152. Wong BW, Kuchnio A, Bruning U, Carmeliet P. Emerging novel functions of the oxygen-sensing prolyl hydroxylase domain enzymes. *Trends Biochem. Sci.* 2013;38(1):3–11.
153. Li M, Kim WY. Two sides to every story: The HIF-dependent and HIF-independent functions of pVHL. *J. Cell. Mol. Med.* 2011;15(2):187–95.
154. Schofield CJ, Ratcliffe PJ. Oxygen sensing by HIF hydroxylases. *Nat. Rev. Mol. Cell Biol.* 2004;5(5):343–54.

155. Khan MN, Bhattacharyya T, Andrikopoulos P, Esteban MA, Barod R, Connor T, et al. Factor inhibiting HIF (FIH-1) promotes renal cancer cell survival by protecting cells from HIF-1 α -mediated apoptosis. *Br. J. Cancer*. 2011;104(7):1151–9.
156. Cheng J, Kang X, Zhang S, Yeh ETH. SUMO-specific protease 1 is essential for stabilization of HIF1 α during hypoxia. *Cell*. 2007;131(3):584–95.
157. Kang X, Li J, Zou Y, Yi J, Zhang H, Cao M, et al. PIASy stimulates HIF1 SUMOylation and negatively regulates HIF1 α activity in response to hypoxia. *Oncogene*. 2010;29(41):5568–78.
158. Zhou F, Dai A, Jiang Y, Tan X, Zhang X. SENP-1 enhances hypoxia-induced proliferation of rat pulmonary artery smooth muscle cells by regulating hypoxia-inducible factor-1 α . *Mol. Med. Rep.* 2016;13(4):3482–90.
159. Carbia-Nagashima A, Gerez J, Perez-Castro C, Paez-Pereda M, Silberstein S, Stalla GK, et al. RSUME, a small RWD-containing protein, enhances SUMO conjugation and stabilizes HIF-1 α during hypoxia. *Cell*. 2007;131(2):309–23.
160. Lee SH, Jee JG, Bae JS, Liu KH, Lee YM. A group of novel HIF-1 α inhibitors, glyceollins, blocks HIF-1 α synthesis and decreases its stability via inhibition of the PI3K/AKT/mTOR pathway and Hsp90 binding. *J. Cell. Physiol.* 2015;230(4):853–62.
161. Liu YV., Baek JH, Zhang H, Diez R, Cole RN, Semenza GL. RACK1 competes with HSP90 for binding to HIF-1 α and is required for O₂-independent and HSP90 inhibitor-induced degradation of HIF-1 α . *Mol. Cell*. 2007;25(2):207–17.
162. Zhang D, Li J, Costa M, Gao J, Huang C. JNK1 mediates degradation HIF-1 α by a VHL-independent mechanism that involves the chaperones Hsp90/Hsp70. *Cancer Res.* 2010;70(2):813–23.
163. Ravi R, Mookerjee B, Bhujwalla ZM, Sutter CH, Artemov D, Zeng Q, et al. Regulation of tumor angiogenesis by p53-induced degradation of hypoxia-inducible factor 1 α . *Genes Dev.* 2000;14(1):34–44.
164. Sermeus A, Michiels C. Reciprocal influence of the p53 and the hypoxic pathways. *Cell Death Dis.* 2011;2:e164.
165. Zhou CH, Zhang XP, Liu F, Wang W. Modeling the interplay between the HIF-1 and p53 pathways in hypoxia. *Sci. Rep.* 2015;5:13834.

166. Yamakuchi M, Lotterman CD, Bao C, Hruban RH, Karim B, Mendell JT, et al. p53-induced microRNA-107 inhibits HIF-1 and tumor angiogenesis. *Proc. Natl. Acad. Sci.* 2010;107(14):6334–9.
167. LaRusch GA, Jackson MW, Dunbar JD, Warren RS, Donner DB, Mayo LD. Nutlin3 blocks vascular endothelial growth factor induction by preventing the interaction between hypoxia inducible factor 1 α and Hdm2. *Cancer Res.* 2007;67(2):450–4.
168. Rempe DA, Lelli KM, Vangeison G, Johnson RS, Federoff HJ. In cultured astrocytes, p53 and MDM2 do not alter hypoxia-inducible factor-1 α function regardless of the presence of DNA damage. *J. Biol. Chem.* 2007;282(22):16187–201.
169. Keith B, Johnson RS, Simon MC. HIF1 α and HIF2 α : Sibling rivalry in hypoxic tumour growth and progression. *Nat. Rev. Cancer.* 2012;12(1):9–22.
170. Bell EL, Guarente L. The SirT3 divining rod points to oxidative stress. *Mol. Cell.* 2011;42(5):561–8.
171. Liu LP, Ho RLK, Chen GG, Lai PBS. Sorafenib inhibits hypoxia-inducible factor-1 α synthesis: Implications for antiangiogenic activity in hepatocellular carcinoma. *Clin. cancer Res.* 2012;18(20):5662–71.
172. Sun HL, Liu YN, Huang YT, Pan SL, Huang DY, Guh JH, et al. YC-1 inhibits HIF-1 expression in prostate cancer cells: Contribution of Akt/NF- κ B signaling to HIF-1 α accumulation during hypoxia. *Oncogene.* 2007;26(27):3941–51.
173. García-Maceira P, Mateo J. Silibinin inhibits hypoxia-inducible factor-1 α and mTOR/p70S6K/4E-BP1 signalling pathway in human cervical and hepatoma cancer cells: Implications for anticancer therapy. *Oncogene.* 2009;28(3):313–24.
174. Sang N, Stiehl DP, Bohensky J, Leshchinsky I, Srinivas V, Caro J. MAPK signaling up-regulates the activity of hypoxia-inducible factors by its effects on p300. *J Biol Chem.* 2003;278(16):14013–14019.
175. Toschi A, Lee E, Gadi N, Ohh M, Foster DA. Differential dependence of hypoxia-inducible factors 1 α and 2 α on mTORC1 and mTORC2. *J. Biol. Chem.* 2008;283(50):34495–9.
176. Rodríguez-Jiménez FJ, Moreno-Manzano V. Modulation of hypoxia-inducible factors (HIF) from an integrative pharmacological perspective. *Cell. Mol. Life Sci.* 2012;69(4):519–34.

177. Nguyen MP, Lee S, Lee YM. Epigenetic regulation of hypoxia inducible factor in diseases and therapeutics. *Arch. Pharm. Res.* 2013;36(3):252–63.
178. Koslowski M, Luxemburger U, Türeci Ö, Sahin U. Tumor-associated CpG demethylation augments hypoxia-induced effects by positive autoregulation of HIF-1 α . *Oncogene.* 2011;30(7):876–82.
179. Walczak-Drzewiecka A, Ratajewski M, Pułaski Ł, Dastych J. DNA methylation-dependent suppression of *HIF1A* in an immature hematopoietic cell line HMC-1. *Biochem. Biophys. Res. Commun.* 2010;391(1):1028–32.
180. Taguchi A, Yanagisawa K, Tanaka M, Cao K, Matsuyama Y, Goto H, et al. Identification of hypoxia-inducible factor-1 α as a novel target for *miR-17-92* microRNA cluster. *Cancer Res.* 2008;68(14):5540–5.
181. Song T, Zhang X, Wang C, Wu Y, Cai W, Gao J, et al. MiR-138 suppresses expression of hypoxia-inducible factor 1 α (HIF-1 α) in clear cell renal cell carcinoma 786-O cells. *Asian Pac J Cancer Prev.* 2011;12(5):1307–11.
182. Yamakuchi M, Yagi S, Ito T, Lowenstein CJ. MicroRNA-22 regulates hypoxia signaling in colon cancer cells. *PLoS One.* 2011;6(5):e20291.
183. Kang SG, Lee WH, Lee YH, Lee YS, Kim SG. Hypoxia-inducible factor-1 α inhibition by a pyrrolopyrazine metabolite of oltipraz as a consequence of microRNAs 199a-5p and 20a induction. *Carcinogenesis.* 2012;33(3):661–9.
184. Ho JJD, Metcalf JL, Yan MS, Turgeon PJ, Wang JJ, Chalsev M, et al. Functional importance of Dicer protein in the adaptive cellular response to hypoxia. *J. Biol. Chem.* 2012;287(34):29003–20.
185. Demaria M, Misale S, Giorgi C, Miano V, Camporeale A, Campisi J, et al. STAT3 can serve as a hit in the process of malignant transformation of primary cells. *Cell Death Differ.* 2012;19(8):1390–7.
186. Zhao J, Du F, Shen G, Zheng F, Xu B. The role of hypoxia-inducible factor-2 in digestive system cancers. *Cell Death Dis.* 2015;6:e1600.
187. Thoma C. Kidney cancer: HIF-2 α a new target in RCC. *Nat. Rev. Urol.* 2016;13(11):627.

188. Yuan P, Cao W, Zang Q, Li G, Guo X, Fan J. The HIF-2 α -MALAT1-miR-216b axis regulates multi-drug resistance of hepatocellular carcinoma cells via modulating autophagy. *Biochem. Biophys. Res. Commun.* 2016;478(3):1067–73.
189. Wang M, Chen MY, Guo XJ, Jiang JX. Expression and significance of HIF-1 α and HIF-2 α in pancreatic cancer. *J. Huazhong Univ. Sci. Technol. - Med. Sci.* 2015;35(6):874–9.
190. Patel SA, Simon MC. Biology of hypoxia-inducible factor-2 α in development and disease. *Cell Death Differ.* 2008;15(4):628–34.
191. Fraisl P, Mazzone M, Schmidt T, Carmeliet P. Regulation of angiogenesis by oxygen and metabolism. *Dev. Cell.* 2009;16(2):167–79.
192. Raval RR, Lau KW, Tran MGB, Sowter HM, Mandriota SJ, Li JL, et al. Contrasting properties of hypoxia-inducible factor 1 (HIF-1) and HIF-2 in Von Hippel-Lindau-associated renal cell carcinoma. *Mol. Cell. Biol.* 2005;25(13):5675–86.
193. Imamura T, Kikuchi H, Herraiz MT, Park DY, Mino-Kenduson M, Lynch MP, et al. HIF-1 α and HIF-2 α have divergent roles in colon cancer. *Int. J. Cancer.* 2009;124(4):763–71.
194. Branco-Price C, Zhang N, Schnelle M, Evans C, Katschinski DM, Liao D, et al. Endothelial cell HIF-1 α and HIF-2 α differentially regulate metastatic success. *Cancer Cell.* 2012;21(1):52–65.
195. Ma L, Li G, Zhu H, Dong X, Zhao D, Jiang X, et al. 2-Methoxyestradiol synergizes with sorafenib to suppress hepatocellular carcinoma by simultaneously dysregulating hypoxia-inducible factor-1 and -2. *Cancer Lett.* 2014;355(1):96–105.
196. Zhao D, Zhai B, He C, Tan G, Jiang X, Pan S, et al. Upregulation of HIF-2 α induced by sorafenib contributes to the resistance by activating the TGF- α /EGFR pathway in hepatocellular carcinoma cells. *Cell. Signal.* 2014;26(5):1030–9.
197. Vallejo D, Crespo I, San-Miguel B, Alvarez M, Prieto J, Tuñón MJ, et al. Autophagic response in the Rabbit Hemorrhagic Disease, an animal model of virally-induced fulminant hepatic failure. *Vet. Res.* 2014;45:15.
198. Prieto-Domínguez N, García-Mediavilla M V, Sánchez-Campos S, Mauriz JL, González-Gallego J. Autophagy as a molecular target of flavonoids underlying their protective effects in human disease. *Curr. Med. Chem.* 2017;25(7):814–38.

199. King JS. Autophagy across the eukaryotes. *Autophagy*. 2012;8(7):1159–62.
200. Shimizu S, Yoshida T, Tsujioka M, Arakawa S. Autophagic cell death and cancer. *Int. J. Mol. Sci.* 2014;15(2):3145–53.
201. Tsujimoto Y, Shimizu S. Another way to die: Autophagic programmed cell death. *Cell Death Differ.* 2005;12(Suppl. 2):1528–34.
202. Boya P, Reggiori F, Codogno P. Emerging regulation and functions of autophagy. *Nat. Cell Biol.* 2013;15(7):713–20.
203. Martinet W, Agostinis P, Vanhooecke B, Dewaele M, De Meyer GR. Autophagy in disease: A double-edged sword with therapeutic potential. *Clin. Sci.* 2009;116(9):697–712.
204. Li WW, Li J, Bao JK. Microautophagy: Lesser-known self-eating. *Cell. Mol. Life Sci.* 2012;69(7):1125–36.
205. Cuervo AM, Wong E. Chaperone-mediated autophagy: Roles in disease and aging. *Cell Res.* 2014;24(1):92–104.
206. Koga H, Martinez-Vicente M, Macian F, Verkhusha VV, Cuervo AM. A photoconvertible fluorescent reporter to track chaperone-mediated autophagy. *Nat. Commun.* 2011;2:386.
207. Kaushik S, Cuervo AM. Chaperone-mediated autophagy: A unique way to enter the lysosome world. *Trends Cell Biol.* 2012;22(8):407–17.
208. Levine B, Kroemer G. Autophagy in the pathogenesis of disease. *Cell.* 2008;132(1):27–42.
209. Tanida I. Autophagy basics. *Microbiol. Immunol.* 2011;55(1):1–11.
210. Tanida I. Autophagosome formation and molecular mechanism of autophagy. *Antioxid. Redox Signal.* 2011;14(11):2201–14.
211. Stolz A, Ernst A, Dikic I. Cargo recognition and trafficking in selective autophagy. *Nat. Cell Biol.* 2014;16(6):495–501.
212. Kroemer G, Mariño G, Levine B. Autophagy and the integrated stress response. *Mol. Cell.* 2010;40(2):280–93.

213. Feng Y, He D, Yao Z, Klionsky DJ. The machinery of macroautophagy. *Cell Res.* 2014;24(1):24–41.
214. Lamb CA, Yoshimori T, Tooze SA. The autophagosome: Origins unknown, biogenesis complex. *Nat. Rev. Mol. Cell Biol.* 2013;14(12):759–74.
215. Kim J, Kundu M, Viollet B, Guan KL. AMPK and mTOR regulate autophagy through direct phosphorylation of Ulk1. *Nat. Cell Biol.* 2011;13(2):132–41.
216. Mizushima N. The role of the Atg1/ULK1 complex in autophagy regulation. *Curr. Opin. Cell Biol.* 2010;22(2):132–9.
217. Young AR, Chan EY, Hu XW, Kochl R, Crawshaw SG, High S, et al. Starvation and ULK1-dependent cycling of mammalian Atg9 between the TGN and endosomes. *J. Cell Sci.* 2006;119(18):3888–900.
218. Lin SY, Li TY, Liu Q, Zhang C, Li X, Chen Y, et al. GSK3-TIP60-ULK1 signaling pathway links growth factor deprivation to autophagy. *Science.* 2012;336(6080):477–81.
219. Wong PM, Puente C, Ganley IG, Jiang X. The ULK1 complex. *Autophagy.* 2013;9(2):124–37.
220. Cianfanelli V, De Zio D, Di Bartolomeo S, Nazio F, Strappazzon F, Cecconi F. Ambra1 at a glance. *J. Cell Sci.* 2015;128(11):2003–8.
221. Nazio F, Strappazzon F, Antonioli M, Bielli P, Cianfanelli V, Bordi M, et al. mTOR inhibits autophagy by controlling ULK1 ubiquitylation, self-association and function through AMBRA1 and TRAF6. *Nat. Cell Biol.* 2013;15(4):406–16.
222. Cianfanelli V, Cecconi F. AMBRA1: When autophagy meets cell proliferation. *Autophagy.* 2015;11(9):1705–7.
223. Krols M, van Isterdael G, Asselbergh B, Kremer A, Lippens S, Timmerman V, et al. Mitochondria-associated membranes as hubs for neurodegeneration. *Acta Neuropathol.* 2016;131(4):505–23.
224. Funderburk SF, Wang QJ, Yue Z. The Beclin 1-VPS34 complex-at the crossroads of autophagy and beyond. *Trends Cell Biol.* 2010;20(6):355–62.
225. Kang R, Zeh HJ, Lotze MT, Tang D. The Beclin 1 network regulates autophagy and apoptosis. *Cell Death Differ.* 2011;18(4):571–80.

226. Itakura E, Mizushima N. Atg14 and UVRAG: Mutually exclusive subunits of mammalian Beclin 1-PI3K complexes. *Autophagy*. 2009;5(4):534–6.
227. Itakura E, Kishi C, Inoue K, Mizushima N. Beclin 1 forms two distinct phosphatidylinositol 3-kinase complexes with mammalian Atg14 and UVRAG. *Mol. Biol. Cell*. 2008;19(12):5360–72.
228. Ahmad ST, Lee JA. Molecular mechanisms underlying the role of autophagy in neurodegenerative diseases. In: Hayat MA, editor. *Autophagy: Cancer, other pathologies, inflammation, immunity, infection, and aging* London: Elsevier Inc.; 2014. p. 45–59.
229. Takahashi Y, Meyerkord CL, Wang HG. Bif-1/Endophilin B1: A candidate for crescent driving force in autophagy. *Cell Death Differ*. 2009;16(7):947–55.
230. Vaccaro MI, Ropolo A, Grasso D, Iovanna JL. A novel mammalian trans-membrane protein reveals an alternative initiation pathway for autophagy. *Autophagy*. 2008;4(3):388–90.
231. He C, Levine B. The Beclin 1 interactome. *Curr. Opin. Cell Biol*. 2010;22(2):140–9.
232. Orsi A, Polson HE, Tooze SA. Membrane trafficking events that partake in autophagy. *Curr. Opin. Cell Biol*. 2010;22(2):150–6.
233. Zhou C, Ma K, Gao R, Mu C, Chen L, Liu Q, et al. Regulation of mATG9 trafficking by Src- and ULK1-mediated phosphorylation in basal and starvation-induced autophagy. *Cell Res*. 2017;27(2):184–201.
234. Longatti A, Tooze SA. Recycling endosomes contribute to autophagosome formation. *Autophagy*. 2012;8(11):1682–3.
235. Knævelsrud H, Carlsson SR, Simonsen A. SNX18 tubulates recycling endosomes for autophagosome biogenesis. *Autophagy*. 2013;9(10):1639–41.
236. Proikas-Cezanne T, Takacs Z, Donnes P, Kohlbacher O. WIPI proteins: Essential PtdIns3P effectors at the nascent autophagosome. *J. Cell Sci*. 2015;128(2):207–17.
237. Mauthe M, Jacob A, Freiburger S, Hentschel K, Stierhof YD, Codogno P, et al. Resveratrol-mediated autophagy requires WIPI-1-regulated LC3 lipidation in the absence of induced phagophore formation. *Autophagy*. 2011;7(12):1448–61.

238. van der Vos KE, Eliasson P, Proikas-Cezanne T, Vervoort SJ, Van Boxtel R, Putker M, et al. Modulation of glutamine metabolism by the PI(3)K-PKB-FOXO network regulates autophagy. *Nat. Cell Biol.* 2012;14(8):829–37.
239. Dooley HC, Razi M, Polson HEJ, Girardin SE, Wilson MI, Tooze SA. WIPI2 links LC3 conjugation with PI3P, autophagosome formation, and pathogen clearance by recruiting Atg12-5-16L1. *Mol. Cell.* 2014;55(2):238–52.
240. Shpilka T, Mizushima N, Elazar Z. Ubiquitin-like proteins and autophagy at a glance. *J. Cell Sci.* 2012;125(10):2343–8.
241. Otomo C, Metlagel Z, Takaesu G, Otomo T. Structure of the human ATG12~ATG5 conjugate required for LC3 lipidation in autophagy. *Nat. Struct. Mol. Biol.* 2013;20(1):59–66.
242. Mizushima N, Kuma A, Kobayashi Y, Yamamoto A, Matsubae M, Takao T, et al. Mouse Apg16L, a novel WD-repeat protein, targets to the autophagic isolation membrane with the Apg12-Apg5 conjugate. *J. Cell Sci.* 2003;116(9):1679–88.
243. Radoshevich L, Murrow L, Chen N, Fernandez E, Roy S, Fung C, et al. ATG12 conjugation to ATG3 regulates mitochondrial homeostasis and cell death. *Cell.* 2010;142(4):590–600.
244. Weidberg H, Shvets E, Shpilka T, Shimron F, Shinder V, Elazar Z. LC3 and GATE-16/GABARAP subfamilies are both essential yet act differently in autophagosome biogenesis. *EMBO J.* 2010;29(11):1792–802.
245. Lee YK, Lee JA. Role of the mammalian ATG8/LC3 family in autophagy: Differential and compensatory roles in the spatiotemporal regulation of autophagy. *BMB Rep.* 2016;49(8):424–30.
246. Huang R, Xu Y, Wan W, Shou X, Qian J, You Z, et al. Deacetylation of nuclear LC3 drives autophagy initiation under starvation. *Mol. Cell.* 2015;57(3):456–67.
247. Mizushima N, Yoshimori T, Levine B. Methods in mammalian autophagy research. *Cell.* 2010;140(3):313–26.
248. Xie Z, Nair U, Klionsky DJ. Atg8 controls phagophore expansion during autophagosome formation. *Mol. Biol. Cell.* 2008;19(8):3290–8.

249. Tamura N, Nishimura T, Sakamaki Y, Koyama-Honda I, Yamamoto H, Mizushima N. Differential requirement for ATG2A domains for localization to autophagic membranes and lipid droplets. *FEBS Lett.* 2017;591(23):3819–30.
250. Yu L, McPhee CK, Zheng L, Mardones GA, Rong Y, Peng J, et al. Termination of autophagy and reformation of lysosomes regulated by mTOR. *Nature.* 2010;465(7300):942–6.
251. Yu S, Melia TJ. The coordination of membrane fission and fusion at the end of autophagosome maturation. *Curr. Opin. Cell Biol.* 2017;47:92–8.
252. Hubert V, Peschel A, Langer B, Gröger M, Rees A, Kain R. LAMP-2 is required for incorporating syntaxin-17 into autophagosomes and for their fusion with lysosomes. *Biol. Open.* 2016;5(10):1516–29.
253. Glick D, Barth S, Macleod KF. Autophagy: Cellular and molecular mechanisms. *J. Pathol.* 2010;221(1):3–12.
254. Pankiv S, Alemu EA, Brech A, Bruun JA, Lamark T, Overvatn A, et al. FYCO1 is a Rab7 effector that binds to LC3 and PI3P to mediate microtubule plus end-directed vesicle transport. *J. Cell Biol.* 2010;188(2):253–69.
255. Wijdeven RH, Janssen H, Nahidiazar L, Janssen L, Jalink K, Berlin I, et al. Cholesterol and ORP1L-mediated ER contact sites control autophagosome transport and fusion with the endocytic pathway. *Nat. Commun.* 2016;7:11808.
256. Kim YM, Jung CH, Seo M, Kim EK, Park JM, Bae SS, et al. mTORC1 phosphorylates UVRAG to negatively regulate autophagosome and endosome maturation. *Mol. Cell.* 2015;57(2):207–18.
257. He C, Klionsky DJ. Regulation mechanisms and signaling pathways of autophagy. *Annu. Rev. Genet.* 2009;43:67–93.
258. Neufeld TP. TOR-dependent control of autophagy: biting the hand that feeds. *Curr. Opin. Cell Biol.* 2010;22(2):157–68.
259. Ramírez-Peinado S, León-Annicchiarico CL, Galindo-Moreno J, Iurlaro R, Caro-Maldonado A, Prehn JHM, et al. Glucose-starved cells do not engage in prosurvival autophagy. *J. Biol. Chem.* 2013;288(42):30387–98.

260. Rabanal-Ruiz Y, Otten EG, Korolchuk VI. mTORC1 as the main gateway to autophagy. *Essays Biochem.* 2017;61(6):565–84.
261. Kim YC, Guan KL. mTOR: A pharmacologic target for autophagy regulation. *J. Clin. Invest.* 2015;125(1):25–32.
262. Arias E, Koga H, Diaz A, Mocholi E, Patel B, Cuervo AM. Lysosomal mTORC2/PHLPP1/Akt regulate chaperone-mediated autophagy. *Mol. Cell.* 2015;59(2):270–84.
263. Sarkar S. Regulation of autophagy by mTOR-dependent and mTOR-independent pathways: autophagy dysfunction in neurodegenerative diseases and therapeutic application of autophagy enhancers. *Biochem. Soc. Trans.* 2013;41(5):1103–30.
264. Carling D, Viollet B. Beyond energy homeostasis: The expanding role of AMP-activated protein kinase in regulating metabolism. *Cell Metab.* 2015;21(6):799–804.
265. Shaw RJ. LKB1 and AMP-activated protein kinase control of mTOR signalling and growth. *Acta Physiol.* 2009;196(1):65–80.
266. Ha J, Guan KL, Kim J. AMPK and autophagy in glucose/glycogen metabolism. *Mol. Aspects Med.* 2015;46:46–62.
267. McEwan DG, Dikic I. The three musketeers of autophagy: Phosphorylation, ubiquitylation and acetylation. *Trends Cell Biol.* 2011;21(4):195–201.
268. Fang Y, Tan J, Zhang Q. Signaling pathways and mechanisms of hypoxia-induced autophagy in the animal cells. *Cell Biol. Int.* 2015;39(8):891–8.
269. Shi RY, Zhu SH, Li V, Gibson SB, Xu XS, Kong JM. BNIP3 interacting with LC3 triggers excessive mitophagy in delayed neuronal death in stroke. *CNS Neurosci. Ther.* 2014;20(12):1045–55.
270. Bellot G, Garcia-Medina R, Gounon P, Chiche J, Roux D, Pouyssegur J, et al. Hypoxia-induced autophagy is mediated through hypoxia-inducible factor induction of BNIP3 and BNIP3L via their BH3 domains. *Mol. Cell. Biol.* 2009;29(10):2570–81.
271. Chen JL, Lin HH, Kim KJ, Lin A, Forman HJ, Ann DK. Novel roles for protein kinase C δ -dependent signaling pathways in acute hypoxic stress-induced autophagy. *J. Biol. Chem.* 2008;283(49):34432–44.

272. Deyoung MP, Horak P, Sofer A, SgROI D, Ellisen LW. Hypoxia regulates TSC1/2–mTOR signaling and tumor suppression through REDD1-mediated 14–3–3 shuttling. *Genes Dev.* 2008;22(2):239–51.
273. Jiang W, Ogretmen B. Autophagy paradox and ceramide. *Biochim. Biophys. Acta.* 2014;1841(5):783–92.
274. Young MM, Kester M, Wang HG. Sphingolipids: Regulators of crosstalk between apoptosis and autophagy. *J. Lipid Res.* 2013;54(1):5–19.
275. Taniguchi M, Kitatani K, Kondo T, Hashimoto-Nishimura M, Asano S, Hayashi A, et al. Regulation of autophagy and its associated cell death by “sphingolipid rheostat”: Reciprocal role of ceramide and sphingosine 1-phosphate in the mammalian target of rapamycin pathway. *J. Biol. Chem.* 2012;287(47):39898–910.
276. Guenther GG, Peralta ER, Rosales KR, Wong SY, Siskind LJ, Edinger AL. Ceramide starves cells to death by downregulating nutrient transporter proteins. *Proc. Natl. Acad. Sci.* 2008;105(45):17402–7.
277. Pattingre S, Bauvy C, Carpentier S, Levade T, Levine B, Codogno P. Role of JNK1-dependent Bcl-2 phosphorylation in ceramide-induced macroautophagy. *J. Biol. Chem.* 2009;284(5):2719–28.
278. Sun T, Li D, Wang L, Xia L, Ma J, Guan Z, et al. c-Jun NH2-terminal kinase activation is essential for up-regulation of LC3 during ceramide-induced autophagy in human nasopharyngeal carcinoma cells. *J. Transl. Med.* 2011;9:161.
279. Copetti T, Bertoli C, Dalla E, Demarchi F, Schneider C. p65/RelA modulates *BECN1* transcription and autophagy. *Mol. Cell. Biol.* 2009;29(10):2594–608.
280. Navarro-Yepes J, Burns M, Anandhan A, Khalimonchuk O, del Razo LM, Quintanilla-Vega B, et al. Oxidative stress, redox signaling, and autophagy: Cell death *versus* survival. *Antioxid. Redox Signal.* 2014;21(1):66–85.
281. Scherz-Shouval R, Shvets E, Fass E, Shorer H, Gil L, Elazar Z. Reactive oxygen species are essential for autophagy and specifically regulate the activity of Atg4. *EMBO J.* 2007;26(7):1749–60.
282. Zmijewski JW, Banerjee S, Bae H, Friggeri A, Lazarowski ER, Abraham E. Exposure to hydrogen peroxide induces oxidation and activation of AMP-activated protein kinase. *J. Biol. Chem.* 2010;285(43):33154–64.

283. Senft D, Ronai ZA. UPR, autophagy, and mitochondria crosstalk underlies the ER stress response. *Trends Biochem. Sci.* 2015;40(3):141–8.
284. B'Chir W, Maurin AC, Carraro V, Averous J, Jousse C, Muranishi Y, et al. The eIF2 α /ATF4 pathway is essential for stress-induced autophagy gene expression. *Nucleic Acids Res.* 2013;41(16):7683–99.
285. Cheng X, Liu H, Jiang CC, Fang L, Chen C, Zhang XD, et al. Connecting endoplasmic reticulum stress to autophagy through IRE1/JNK/Beclin-1 in breast cancer cells. *Int. J. Mol. Med.* 2014;34(3):772–81.
286. Høyer-Hansen M, Jäättelä M. Connecting endoplasmic reticulum stress to autophagy by unfolded protein response and calcium. *Cell Death Differ.* 2007;14(9):1576–82.
287. Cheng Y, Ren X, Hait WN, Yang JM. Therapeutic targeting of autophagy in disease: Biology and pharmacology. *Pharmacol. Rev.* 2013;65(4):1162–97.
288. Schneider JL, Cuervo AM. Autophagy and human disease: Emerging themes. *Curr. Opin. Genet. Dev.* 2014;26:16–23.
289. Rubinsztein DC, Codogno P, Levine B. Autophagy modulation as a potential therapeutic target for liver diseases. *Nat. Rev. Drug Discov.* 2012;11(9):709–30.
290. Choi AMK, Ryter SW, Levine B. Autophagy in human health and disease. *N. Engl. J. Med.* 2013;368(7):651–62.
291. Komatsu M, Waguri S, Chiba T, Murata S, Iwata JI, Tanida I, et al. Loss of autophagy in the central nervous system causes neurodegeneration in mice. *Nature.* 2006;441(7095):880–4.
292. Yang L, Li P, Fu S, Calay ES, Hotamisligil GS. Defective hepatic autophagy in obesity promotes ER stress and causes insulin resistance. *Cell Metab.* 2010;11(6):467–78.
293. He C, Bassik MC, Moresi V, Sun K, Wei Y, Zou Z, et al. Exercise-induced BCL2-regulated autophagy is required for muscle glucose homeostasis. *Nature.* 2012;481(7382):511–55.
294. Numan MS, Amiable N, Brown JP, Michou L. Paget's disease of bone: An osteoimmunological disorder? *Drug Des. Devel. Ther.* 2015;9:4695–707.

295. Jimenez RE, Kubli DA, Gustafsson ÅB. Autophagy and mitophagy in the myocardium: Therapeutic potential and concerns. *Br. J. Pharmacol.* 2014;171(8):1907–16.
296. Ryter SW, Choi AMK. Autophagy in the lung. *Proc. Am. Thorac. Soc.* 2010;7(1):13–21.
297. Zeki AA, Yeganeh B, Kenyon NJ, Post M, Ghavami S. Autophagy in airway diseases: A new frontier in human asthma? *Allergy.* 2016;71(1):5–14.
298. Mayer ML, Blohmke CJ, Falsafi R, Fjell CD, Madera L, Turvey SE, et al. Rescue of dysfunctional autophagy attenuates hyperinflammatory responses from cystic fibrosis cells. *J. Immunol.* 2013;190(3):1227–38.
299. Zhang J, Li AM, Liu BX, Han F, Liu F, Sun SP, et al. Effect of icarisid II on diabetic rats with erectile dysfunction and its potential mechanism via assessment of AGEs, autophagy, mTOR and the NO-cGMP pathway. *Asian J. Androl.* 2013;15(1):143–8.
300. Jackson WT. Viruses and the autophagy pathway. *Virology.* 2015;479–480:450–6.
301. Lee HK, Mattei LM, Steinberg BE, Alberts P, Lee YH, Chervonsky A, et al. In vivo requirement for Atg5 in antigen presentation by dendritic cells. *Immunity.* 2010;32(2):227–39.
302. Nguyen HTT, Lapaquette P, Bringer MA, Darfeuille-Michaud A. Autophagy and Crohn's disease. *J. Innate Immun.* 2013;5(5):434–43.
303. Dhingra R, Kirshenbaum LA. Regulation of mitochondrial dynamics and cell fate. *Circ. J.* 2014;78(4):803–10.
304. Hall AR, Burke N, Dongworth RK, Hausenloy DJ. Mitochondrial fusion and fission proteins: Novel therapeutic targets for combating cardiovascular disease. *Br. J. Pharmacol.* 2014;171(8):1890–906.
305. Zhao J, Lendahl U, Nistér M. Regulation of mitochondrial dynamics: Convergences and divergences between yeast and vertebrates. *Cell. Mol. life Sci.* 2013;70(6):951–76.
306. Chen H, Chomyn A, Chan DC. Disruption of fusion results in mitochondrial heterogeneity and dysfunction. *J. Biol. Chem.* 2005;280(28):26185–92.

307. Lee H, Yoon Y. Mitochondrial fission and fusion. *Biochem. Soc. Trans.* 2016;44(6):1725–35.
308. Piquereau J, Caffin F, Novotova M, Prola A, Garnier A, Mateo P, et al. Down-regulation of OPA1 alters mouse mitochondrial morphology, PTP function, and cardiac adaptation to pressure overload. *Cardiovasc. Res.* 2012;94(3):408–17.
309. del Dotto V, Fogazza M, Lenaers G, Rugolo M, Carelli V, Zanna C. OPA1: How much do we know to approach therapy? *Pharmacol. Res.* 2018;131:199–210.
310. Ban T, Ishihara T, Kohno H, Saita S, Ichimura A, Maenaka K, et al. Molecular basis of selective mitochondrial fusion by heterotypic action between OPA1 and cardiolipin. *Nat. Cell Biol.* 2017;19(7):856–63.
311. Kameoka S, Adachi Y, Okamoto K, Iijima M, Sesaki H. Phosphatidic acid and cardiolipin coordinate mitochondrial dynamics. *Trends Cell Biol.* 2018;28(1):67–76.
312. Dabrowska A, Venero JL, Iwasawa R, Hankir MK, Rahman S, Boobis A, et al. PGC-1 α controls mitochondrial biogenesis and dynamics in lead-induced neurotoxicity. *Aging.* 2015;7(9):629–47.
313. Zhao J, Liu T, Jin S, Wang X, Qu M, Uhlén P, et al. Human MIEF1 recruits Drp1 to mitochondrial outer membranes and promotes mitochondrial fusion rather than fission. *EMBO J.* 2011;30(14):2762–78.
314. Norton M, Ng AC-H, Baird S, Dumoulin A, Shutt T, Mah N, et al. ROMO1 is an essential redox-dependent regulator of mitochondrial dynamics. *Sci. Signal.* 2014;7(310):ra10.
315. Hoppins S, Edlich F, Cleland MM, Banerjee S, McCaffery JM, Youle RJ, et al. The soluble form of Bax regulates mitochondrial fusion via MFN2 homotypic complexes. *Mol. Cell.* 2011;41(2):150–60.
316. Landes T, Emorine LJ, Courilleau D, Rojo M, Belenguer P, Arnauné-Pelloquin L. The BH3-only Bnip3 binds to the dynamin Opa1 to promote mitochondrial fragmentation and apoptosis by distinct mechanisms. *EMBO Rep.* 2010;11(6):459–65.
317. Gegg ME, Cooper JM, Chau KY, Rojo M, Schapira AHV, Taanman JW. Mitofusin 1 and mitofusin 2 are ubiquitinated in a PINK1/parkin-dependent manner upon induction of mitophagy. *Hum. Mol. Genet.* 2010;19(24):4861–70.

318. Shen Q, Yamano K, Head BP, Kawajiri S, Cheung JTM, Wang C, et al. Mutations in Fis1 disrupt orderly disposal of defective mitochondria. *Mol. Biol. Cell.* 2014;25(1):145–59.
319. Otera H, Miyata N, Kuge O, Mihara K. Drp1-dependent mitochondrial fission via MiD49/51 is essential for apoptotic cristae remodeling. *J. Cell Biol.* 2016;212(5):531–44.
320. Losón OC, Song Z, Chen H, Chan DC. Fis1, Mff, MiD49, and MiD51 mediate Drp1 recruitment in mitochondrial fission. *Mol. Biol. Cell.* 2013;24(5):659–67.
321. Elgass KD, Smith EA, LeGros MA, Larabell CA, Ryan MT. Analysis of ER-mitochondria contacts using correlative fluorescence microscopy and soft X-ray tomography of mammalian cells. *J. Cell Sci.* 2015;128(15):2795–804.
322. Friedman JR, Lackner LL, West M, DiBenedetto JR, Nunnari J, Voeltz GK. ER tubules mark sites of mitochondrial division. *Science.* 2011;334(6054):358–62.
323. Korobova F, Gauvin TJ, Higgs HN. A role for myosin II in mammalian mitochondrial fission. *Curr. Biol.* 2014;24(4):409–14.
324. Wasiak S, Zunino R, McBride HM. Bax/Bak promote sumoylation of DRP1 and its stable association with mitochondria during apoptotic cell death. *J. Cell Biol.* 2007;177(3):439–50.
325. Lee Y, Lee HY, Hanna RA, Gustafsson ÅB. Mitochondrial autophagy by Bnip3 involves Drp1-mediated mitochondrial fission and recruitment of Parkin in cardiac myocytes. *Am. J. Physiol. Heart Circ. Physiol.* 2011;301(5):H1924–31.
326. Cribbs JT, Strack S. Reversible phosphorylation of Drp1 by cyclic AMP-dependent protein kinase and calcineurin regulates mitochondrial fission and cell death. *EMBO Rep.* 2007;8(10):939–44.
327. Rambold AS, Kostecky B, Elia N, Lippincott-Schwartz J. Tubular network formation protects mitochondria from autophagosomal degradation during nutrient starvation. *Proc. Natl. Acad. Sci. USA.* 2011;108(25):10190–5.
328. Kashatus DF, Lim KH, Brady DC, Pershing NLK, Cox AD, Counter CM. RalA and RalBP1 regulate mitochondrial fission at mitosis. *Nat. Cell Biol.* 2011;13(9):1108–15.

329. Franz A, Kevei É, Hoppe T. Double-edged alliance: Mitochondrial surveillance by the UPS and autophagy. *Curr. Opin. Cell Biol.* 2015;37:18–27.
330. Chourasia AH, Boland ML, Macleod KF. Mitophagy and cancer. *Cancer Metab.* 2015;3:4.
331. Hamacher-Brady A, Brady NR. Mitophagy programs: Mechanisms and physiological implications of mitochondrial targeting by autophagy. *Cell. Mol. Life Sci.* 2016;73(4):775–95.
332. Campello S, Strappazzon F, Cecconi F. Mitochondrial dismissal in mammals, from protein degradation to mitophagy. *Biochim. Biophys. Acta.* 2014;1837(4):451–60.
333. Gomes LC, Di Benedetto G, Scorrano L. During autophagy mitochondria elongate, are spared from degradation and sustain cell viability. *Nat. Cell Biol.* 2011;13(5):589–98.
334. Jin SM, Lazarou M, Wang C, Kane LA, Narendra DP, Youle RJ. Mitochondrial membrane potential regulates PINK1 import and proteolytic destabilization by PARL. *J. Cell Biol.* 2010;191(5):933–42.
335. Meissner C, Lorenz H, Hehn B, Lemberg MK. Intramembrane protease PARL defines a negative regulator of PINK1- and PARK2/Parkin-dependent mitophagy. *Autophagy.* 2015;11(9):1484–98.
336. Fedorowicz MA, De Vries-Schneider RLA, Rüb C, Becker D, Huang Y, Zhou C, et al. Cytosolic cleaved PINK1 represses Parkin translocation to mitochondria and mitophagy. *EMBO Rep.* 2014;15(1):86–93.
337. Lazarou M, Jin SM, Kane LA, Youle RJ. Role of PINK1 binding to the TOM complex and alternate intracellular membranes in recruitment and activation of the E3 ligase Parkin. *Dev. Cell.* 2012;22(2):320–33.
338. Chen Y, Dorn II GW. PINK1-phosphorylated mitofusin 2 is a Parkin receptor for culling damaged mitochondria. *Science.* 2013;340(6131):471–5.
339. Matsuda N. Phospho-ubiquitin: Upending the PINK-Parkin-ubiquitin cascade. *J. Biochem.* 2016;159(4):379–85.

340. Wang X, Winter D, Ashrafi G, Schlehe J, Wong YL, Selkoe D, et al. PINK1 and Parkin target Miro for phosphorylation and degradation to arrest mitochondrial motility. *Cell*. 2011;147(4):893–906.
341. Poole AC, Thomas RE, Yu S, Vincow ES, Pallanck L. The mitochondrial fusion-promoting factor mitofusin is a substrate of the PINK1/parkin pathway. *PLoS One*. 2010;5(4):e10054.
342. Sarraf SA, Raman M, Guarani-Pereira V, Sowa ME, Huttlin EL, Gygi SP, et al. Landscape of the Parkin-dependent ubiquitylome in response to mitochondrial depolarization. *Nature*. 2013;496(7445):372–6.
343. Liu X, Gal J, Zhu H. Sequestosome 1/p62: A multi-domain protein with multi-faceted functions. *Front. Biol.* 2012;7(3):189–201.
344. Okatsu K, Saisho K, Shimanuki M, Nakada K, Shitara H, Sou Y-S, et al. p62/SQSTM1 cooperates with Parkin for perinuclear clustering of depolarized mitochondria. *Genes cells*. 2010;15(8):887–900.
345. Lazarou M, Sliter DA, Kane LA, Sarraf SA, Burman JL, Sideris DP, et al. The ubiquitin kinase PINK1 recruits autophagy receptors to induce mitophagy. *Nature*. 2015;524(7565):309–14.
346. Lin A, Yao J, Zhuang L, Wang D, Han J, Lam EWF, et al. FoxO-BNIP3 axis exerts a unique regulation of mTORC1 and cell survival under energy stress. *Oncogene*. 2014;33(24):3183–94.
347. Springer MZ, Macleod KF. In Brief: Mitophagy: Mechanisms and role in human disease. *J. Pathol.* 2016;240(3):253–5.
348. Gálvez AS, Brunskill EW, Marreez Y, Benner BJ, Regula KM, Kirschenbaum LA, et al. Distinct pathways regulate proapoptotic Nix and BNip3 in cardiac stress. *J. Biol. Chem.* 2006;281(3):1442–8.
349. Dayan F, Roux D, Brahim-Horn MC, Pouyssegur J, Mazure NM. The oxygen sensor factor-inhibiting hypoxia-inducible factor-1 controls expression of distinct genes through the bifunctional transcriptional character of hypoxia-inducible factor-1 α . *Cancer Res.* 2006;66(7):3688–98.

350. Tracy K, Dibling BC, Spike BT, Knabb JR, Schumacker P, Macleod KF. BNIP3 is an RB/E2F target gene required for hypoxia-induced autophagy. *Mol. Cell. Biol.* 2007;27(17):6229–42.
351. Baetz D, Regula KM, Ens K, Shaw J, Kothari S, Yurkova N, et al. Nuclear factor- κ B-mediated cell survival involves transcriptional silencing of the mitochondrial death gene BNIP3 in ventricular myocytes. *Circulation.* 2005;112(24):3777–85.
352. Burton TR, Gibson SB. The role of Bcl-2 family member BNIP3 in cell death and disease: NIPping at the heels of cell death. *Cell Death Differ.* 2009;16(4):515–23.
353. Li Y, Wang Y, Kim E, Beemiller P, Wang CY, Swanson J, et al. Bnip3 mediates the hypoxia-induced inhibition on mammalian target of rapamycin by interacting with Rheb. *J. Biol. Chem.* 2007;282(49):35803–13.
354. Liu L, Feng D, Chen G, Chen M, Zheng Q, Song P, et al. Mitochondrial outer-membrane protein FUNDC1 mediates hypoxia-induced mitophagy in mammalian cells. *Nat. Cell Biol.* 2012;14(2):177–85.
355. Drake LE, Springer MZ, Poole LP, Kim CJ, Macleod KF. Expanding perspectives on the significance of mitophagy in cancer. *Semin. Cancer Biol.* 2017;47:110–24.
356. Chen M, Chen Z, Wang Y, Tan Z, Zhu C, Li Y, et al. Mitophagy receptor FUNDC1 regulates mitochondrial dynamics and mitophagy. *Autophagy.* 2016;12(4):689–702.
357. Murakawa T, Yamaguchi O, Hashimoto A, Hikoso S, Takeda T, Oka T, et al. Bcl-2-like protein 13 is a mammalian Atg32 homologue that mediates mitophagy and mitochondrial fragmentation. *Nat. Commun.* 2015;6:7527.
358. Sentelle RD, Senkal CE, Jiang W, Ponnusamy S, Gencer S, Selvam SP, et al. Ceramide targets autophagosomes to mitochondria and induces lethal mitophagy. *Nat. Chem. Biol.* 2012;8(10):831–8.
359. Chu CT, Ji J, Dagda RK, Jiang JF, Tyurina YY, Kapralov AA, et al. Cardiolipin externalization to the outer mitochondrial membrane acts as an elimination signal for mitophagy in neuronal cells. *Nat. Cell Biol.* 2013;15(10):1197–205.
360. Wei Y, Chiang WC, Sumpter Jr. R, Mishra P, Levine B. Prohibitin 2 is an inner mitochondrial membrane mitophagy receptor. *Cell.* 2017;168(1–2):224–38.

361. Kulikov A V., Luchkina EA, Gogvadze V, Zhivotovsky B. Mitophagy: Link to cancer development and therapy. *Biochem. Biophys. Res. Commun.* 2017;482(3):432–9.
362. Deas E, Wood NW, Plun-Favreau H. Mitophagy and Parkinson's disease: The PINK1–Parkin link. *Biochim. Biophys. Acta.* 2011;1813(4):623–33.
363. Peker N, Donipadi V, Sharma M, McFarlane C, Kambadur R. Loss of Parkin impairs mitochondrial function and leads to muscle atrophy. *Am J Physiol Cell Physiol.* 2018;In press.
364. Savitskaya MA, Onishchenko GE. Mechanisms of Apoptosis. *Biochemistry.* 2015;80(11):1393–405.
365. Ouyang L, Shi Z, Zhao S, Wang FT, Zhou TT, Liu B, et al. Programmed cell death pathways in cancer: A review of apoptosis, autophagy and programmed necrosis. *Cell Prolif.* 2012;45(6):487–98.
366. Wong RSY. Apoptosis in cancer: From pathogenesis to treatment. *J. Exp. Clin. cancer Res.* 2011;30:87.
367. García de la Cadena S, Massieu L. Caspases and their role in inflammation and ischemic neuronal death. Focus on caspase-12. *Apoptosis.* 2016;21(7):763–77.
368. Voskoboinik I, Whisstock JC, Trapani JA. Perforin and granzymes: Function, dysfunction and human pathology. *Nat. Rev. Immunol.* 2015;15(6):388–400.
369. Tait SWG, Green DR. Mitochondria and cell death: Outer membrane permeabilization and beyond. *Nat. Rev. Mol. Cell Biol.* 2010;11(9):621–32.
370. Ichim G, Tait SWG. A fate worse than death: Apoptosis as an oncogenic process. *Nat. Rev. Cancer.* 2016;16(8):539–48.
371. Chipuk JE, Moldoveanu T, Llambi F, Parsons MJ, Green DR. The Bcl-2 family reunion. *Mol. Cell.* 2010;37(3):299–310.
372. Ashkenazi A. Targeting the extrinsic apoptosis pathway in cancer. *Cytokine Growth Factor Rev.* 2008;19(3–4):325–31.
373. Rubinstein AD, Kimchi A. Life in the balance—a mechanistic view of the crosstalk between autophagy and apoptosis. *J. Cell Sci.* 2012;125(22):5259–68.
374. Mukhopadhyay S, Panda PK, Sinha N, Das DN, Bhutia SK. Autophagy and apoptosis: Where do they meet? *Apoptosis.* 2014;19(4):555–66.

375. Yin X, Cao L, Kang R, Yang M, Wang Z, Peng Y, et al. UV irradiation resistance-associated gene suppresses apoptosis by interfering with BAX activation. *EMBO Rep.* Nature Publishing Group; 2011;12(7):727–34.
376. Bincoletto C, Bechara A, Pereira GJS, Santos CP, Antunes F, Peixoto da-Silva J, et al. Interplay between apoptosis and autophagy, a challenging puzzle: New perspectives on antitumor chemotherapies. *Chem. Biol. Interact.* 2013;206(2):279–88.
377. Slominski AT, Hardeland R, Zmijewski MA, Slominski RM, Reiter RJ, Paus R. Melatonin: A cutaneous perspective on its production, metabolism, and functions. *J. Invest. Dermatol.* 2018;138(3):490–9.
378. Hardeland R. Melatonin in plants—diversity of levels and multiplicity of functions. *Front. Plant Sci.* 2016;7:198.
379. Reiter RJ, Rosales-Corral S, Tan DX, Jou MJ, Galano A, Xu B. Melatonin as a mitochondria-targeted antioxidant: One of evolution’s best ideas. *Cell. Mol. Life Sci.* 2017;74(21):3863–81.
380. Villela D, Atherino VF, de Sá Lima L, Moutinho AA, do Amaral FG, Peres R, et al. Modulation of pineal melatonin synthesis by glutamate involves paracrine interactions between pinealocytes and astrocytes through NF-kappaB activation. *Biomed Res. Int.* 2013;2013:618432.
381. Tan DX, Xu B, Zhou X, Reiter RJ. Pineal calcification, melatonin production, aging, associated health consequences and rejuvenation of the pineal gland. *Molecules.* 2018;23(2):301.
382. Stehle JH, Saade A, Rawashdeh O, Ackermann K, Jilg A, Sebesteny T, et al. A survey of molecular details in the human pineal gland in the light of phylogeny, structure, function and chronobiological diseases. *J. Pineal Res.* 2011;51(1):17–43.
383. Acuña-Castroviejo D, Escames G, Venegas C, Díaz-Casado ME, Lima-Cabello E, López LC, et al. Extrapineal melatonin: Sources, regulation, and potential functions. *Cell. Mol. life Sci.* 2014;71(16):2997–3025.
384. Arendt J. Melatonin and the pineal gland: Influence on mammalian seasonal and circadian physiology. *Rev. Reprod.* 1998;3(1):13–22.

385. Tan DX, Manchester LC, Esteban-Zubero E, Zhou Z, Reiter RJ. Melatonin as a potent and inducible endogenous antioxidant: Synthesis and metabolism. *Molecules*. 2015;20(10):18886–906.
386. Tan DX, Manchester LC, Qin L, Reiter RJ. Melatonin: A mitochondrial targeting molecule involving mitochondrial protection and dynamics. *Int. J. Mol. Sci*. 2016;17(12):2124.
387. Slominski AT, Semak I, Fischer TW, Kim TK, Kleszczyński K, Hardeland R, et al. Metabolism of melatonin in the skin: Why is it important? *Exp. Dermatol*. 2017;26(7):563–8.
388. Olsen LF, Kummer U, Kindzelskii AL, Petty HR. A model of the oscillatory metabolism of activated neutrophils. *Biophys. J*. 2003;84(1):69–81.
389. Boutin JA. Quinone reductase 2 as a promising target of melatonin therapeutic actions. *Expert Opin. Ther. Targets*. 2016;20(3):303–17.
390. He B, Zhao Y, Xu L, Gao L, Su Y, Lin N, et al. The nuclear melatonin receptor ROR α is a novel endogenous defender against myocardial ischemia/reperfusion injury. *J. Pineal Res*. 2016;60(3):313–26.
391. Bonmati-Carrion MA, Arguelles-Prieto R, Martinez-Madrid MJ, Reiter R, Hardeland R, Rol MA, et al. Protecting the melatonin rhythm through circadian healthy light exposure. *Int. J. Mol. Sci*. 2014;15(12):23448–500.
392. González S, Moreno-Delgado D, Moreno E, Pérez-Capote K, Franco R, Mallol J, et al. Circadian-related heteromerization of adrenergic and dopamine D₄ receptors modulates melatonin synthesis and release in the pineal gland. *PLoS Biol*. 2012;10(6):e1001347.
393. Jung-Hynes B, Reiter RJ, Ahmad N. Sirtuins, melatonin and circadian rhythms: Building a bridge between aging and cancer. *J. Pineal Res*. 2010;48(1):9–19.
394. Haus EL, Smolensky MH. Shift work and cancer risk: Potential mechanistic roles of circadian disruption, light at night, and sleep deprivation. *Sleep Med. Rev*. 2013;17(4):273–84.
395. Srinivasan V, De Berardis D, Shillcutt SD, Brzezinski A. Role of melatonin in mood disorders and the antidepressant effects of agomelatine. *Expert Opin. Investig. Drugs*. 2012;21(10):1503–22.

396. Emet M, Ozcan H, Ozel L, Yayla M, Halici Z, Hacimuftuoglu A. A review of melatonin, its receptors and drugs. *Eurasian J. Med.* 2016;48(2):135–41.
397. Comai S, Gobbi G. Unveiling the role of melatonin MT2 receptors in sleep, anxiety and other neuropsychiatric diseases: A novel target in psychopharmacology. *J. psychiatry Neurosci.* 2014;39(1):6–21.
398. Govitrapong P, Ekthuwapranee K, Ruksee N, Boontem P. Melatonin, a neuroprotective agent: Relevance for stress-induced neuropsychiatric disorders. In: López-Muñoz F, Srinivasan V, de Berardis D, Álamo C, Kato TA, editors. *Melatonin, neuroprotective agents and antidepressant therapy.* New Delhi: Springer International Publishing; 2016. p. 101–16.
399. Banach M, Gurdziel E, Jędrych M, Borowicz KK. Melatonin in experimental seizures and epilepsy. *Pharmacol. Reports.* 2011;63(1):1–11.
400. Danilov A, Kurganova J. Melatonin in chronic pain syndromes. *Pain Ther.* 2016;5(1):1–17.
401. Carrillo-Vico A, Lardone PJ, Alvarez-Sánchez N, Rodríguez-Rodríguez A, Guerrero JM. Melatonin: Buffering the immune system. *Int. J. Mol. Sci.* 2013;14(4):8638–83.
402. Radogna F, Diederich M, Ghibelli L. Melatonin: A pleiotropic molecule regulating inflammation. *Biochem. Pharmacol.* 2010;80(12):1844–52.
403. Srinivasan V, Pandi-Perumal SR, Brzezinski A, Bhatnagar KP, Cardinali DP. Melatonin, immune function and cancer. *Recent Pat. Endocr. Metab. Immune Drug Discov.* 2011;5(2):109–23.
404. Fan LL, Sun GP, Wei W, Wang ZG, Ge L, Fu WZ, et al. Melatonin and doxorubicin synergistically induce cell apoptosis in human hepatoma cell lines. *World J. Gastroenterol.* 2010;16(12):1473–81.
405. Yamanishi M, Narazaki H, Asano T. Melatonin overcomes resistance to clofarabine in two leukemic cell lines by increased expression of deoxycytidine kinase. *Exp. Hematol.* 2015;43(3):207–14.
406. Carbajo-Pescador S, Steinmetz C, Kashyap A, Lorenz S, Mauriz JL, Heise M, et al. Melatonin induces transcriptional regulation of Bim by FoxO3a in HepG2 cells. *Br. J. Cancer.* 2013;108(2):442–9.

407. Martín-Renedo J, Mauriz JL, Jorquera F, Ruiz-Andres O, González P, González-Gallego J. Melatonin induces cell cycle arrest and apoptosis in hepatocarcinoma HepG2 cell line. *J. Pineal Res.* 2008;45(4):532–40.
408. Moreira AJ, Ordoñez R, Cerski CT, Picada JN, García-Palomo A, Marroni NP, et al. Melatonin activates endoplasmic reticulum stress and apoptosis in rats with diethylnitrosamine-induced hepatocarcinogenesis. *PLoS One.* 2015;10(12):e0144517.
409. Taheem DK, Foyt DA, Loaiza S, Ferreira SA, Ilic D, Auner HW, et al. Differential regulation of human bone marrow mesenchymal stromal cell chondrogenesis by hypoxia inducible factor-1 α hydroxylase inhibitors. *Stem Cells.* 2018;In press.
410. Denizot F, Lang R. Rapid colorimetric assay for cell growth and survival. Modifications to the tetrazolium dye procedure giving improved sensitivity and reliability. *J. Immunol. Methods.* 1986;89(2):271–7.
411. Vermes I, Haanen C, Reutelingsperger C. Flow cytometry of apoptotic cell death. *J Immunol Methods.* 2000;243(1–2):167–90.
412. Gerber HP, McMurtrey A, Kowalski J, Yan M, Keyt BA, Dixit V, et al. Vascular endothelial growth factor regulates endothelial cell survival through the phosphatidylinositol 3'-kinase/Akt signal transduction pathway. Requirement for Flk-1/KDR activation. *J. Biol. Chem.* 1998;273(46):30336–43.
413. Mahmood T, Yang PC. Western blot: Technique, theory, and trouble shooting. *N. Am. J. Med. Sci.* 2012;4(9):429–34.
414. Romkes M, Buch SC. Strategies for measurement of biotransformation enzyme gene expression. In: Keohavong P, Grant SG, editors. *Molecular Toxicology Protocols.* 2nd ed. New York: Springer Science + Business Media; 2014. p. 85–97.
415. Livak KJ, Schmittgen TD. Analysis of relative gene expression data using real-time quantitative PCR and the $2^{-\Delta\Delta CT}$ method. *Methods.* 2001;25(4):402–8.
416. Furda A, Santos JH, Meyer JN, van Houten B. Quantitative PCR-based measurement of nuclear and mitochondrial DNA damage and repair in mammalian cells. *Methods Mol. Biol.* 2014;1105:419–37.
417. Wang X, Roper MG. Measurement of DCF fluorescence as a measure of reactive oxygen species in murine islets of Langerhans. *Anal. Methods.* 2014;6(9):3019–24.

418. Perelman A, Wachtel C, Cohen M, Haupt S, Shapiro H, Tzur A. JC-1: Alternative excitation wavelengths facilitate mitochondrial membrane potential cytometry. *Cell Death Dis.* 2012;3:e430.
419. Thomé MP, Filippi-Chiela EC, Villodre ES, Migliavaca CB, Onzi GR, Felipe KB, et al. Ratiometric analysis of acridine orange staining in the study of acidic organelles and autophagy. *J. Cell Sci.* 2016;129(24):4622–32.
420. Dolman NJ, Chambers KM, Mandavilli B, Batchelor RH, Janes MS. Tools and techniques to measure mitophagy using fluorescence microscopy. *Autophagy.* 2013;9(11):1653–62.
421. Joshi BH, Pachchigar KP. SiRNA: Novel therapeutics from functional genomics. *Biotechnol. Genet. Eng. Rev.* 2014;30(1):1–30.
422. Zhao M, Yang H, Jiang X, Zhou W, Zhu B, Zeng Y, et al. Lipofectamine RNAiMAX: An efficient siRNA transfection reagent in human embryonic stem cells. *Mol. Biotechnol.* 2008;40(1):19–26.
423. Shacka JJ, Klocke BJ, Shibata M, Uchiyama Y, Datta G, Schmidt RE, et al. Bafilomycin A1 inhibits chloroquine-induced death of cerebellar granule neurons. *Mol. Pharmacol.* 2006;69(4):1125–36.
424. Song E, Tang S, Xu J, Yin B, Bao E, Hartung J. Lenti-siRNA Hsp60 promote Bax in mitochondria and induces apoptosis during heat stress. *Biochem. Biophys. Res. Commun.* 2016;481(1–2):125–31.
425. Zhang HM, Zhang Y. Melatonin: A well-documented antioxidant with conditional pro-oxidant actions. *J. Pineal Res.* 2014;57(2):131–46.
426. Lin D, Wu J. Hypoxia inducible factor in hepatocellular carcinoma: A therapeutic target. *World J. Gastroenterol.* 2015;21(42):12171–8.
427. Park JW, Hwang MS, Suh SI, Baek WK. Melatonin down-regulates HIF-1 α expression through inhibition of protein translation in prostate cancer cells. *J. Pineal Res.* 2009;46(4):415–21.
428. Dunlop RA, Cox PA, Banack SA, Rodgers KJ. The non-protein amino acid BMAA is misincorporated into human proteins in place of L-serine causing protein misfolding and aggregation. *PLoS One.* 2013;8(9):e75376.

429. El-Serag HB. Epidemiology of viral hepatitis and hepatocellular carcinoma. *Gastroenterology*. 2012;142(6):1264–73.
430. Llovet JM, Hernandez-Gea V. Hepatocellular carcinoma: Reasons for phase III failure and novel perspectives on trial design. *Clin. cancer Res*. 2014;20(8):2072–9.
431. Bolondi L, Craxi A, Trevisani F, Daniele B, Di Costanzo GG, Fagioli S, et al. Refining sorafenib therapy: Lessons from clinical practice. *Futur. Oncol*. 2015;11(3):449–65.
432. Briz O, Perez MJ, Marin JJG. Further understanding of mechanisms involved in liver cancer chemoresistance. *Hepatoma Res*. 2017;3:22–6.
433. Geier A, Macias RIR, Bettinger D, Weiss J, Bantel H, Jahn D, et al. The lack of the organic cation transporter OCT1 at the plasma membrane of tumor cells precludes a positive response to sorafenib in patients with hepatocellular carcinoma. *Oncotarget*. 2017;8(9):15846–57.
434. Herraiz E, Lozano E, Macias RIR, Vaquero J, Bujanda L, Banales JM, et al. Expression of SLC22A1 variants may affect the response of hepatocellular carcinoma and cholangiocarcinoma to sorafenib. *Hepatology*. 2013;58(3):1065–73.
435. Morisaki T, Umebayashi M, Kiyota A, Koya N, Tanaka H, Onishi H, et al. Combining celecoxib with sorafenib synergistically inhibits hepatocellular carcinoma cells *in vitro*. *Anticancer Res*. 2013;33(4):1387–95.
436. Cheng Y, Luo R, Zheng H, Wang B, Liu Y, Liu D, et al. Synergistic anti-tumor efficacy of sorafenib and fluvastatin in hepatocellular carcinoma. *Oncotarget*. 2017;8(14):23265–76.
437. Gu HR, Park SC, Choi SJ, Lee JC, Kim YC, Han CJ, et al. Combined treatment with silibinin and either sorafenib or gefitinib enhances their growth-inhibiting effects in hepatocellular carcinoma cells. *Clin. Mol. Hepatol*. 2015;21(1):49–59.
438. Cao H, Wang Y, He X, Zhang Z, Yin Q, Chen Y, et al. Codelivery of sorafenib and curcumin by directed self-assembled nanoparticles enhances therapeutic effect on hepatocellular carcinoma. *Mol. Pharm*. 2015;12(3):922–31.
439. Petrini I, Lencioni M, Ricasoli M, Iannopollo M, Orlandini C, Oliveri F, et al. Phase II trial of sorafenib in combination with 5-fluorouracil infusion in advanced hepatocellular carcinoma. *Cancer Chemother. Pharmacol*. 2012;69(3):773–80.

440. Tuñón MJ, San Miguel B, Crespo I, Jorquera F, Santamaria E, Alvarez M, et al. Melatonin attenuates apoptotic liver damage in fulminant hepatic failure induced by the rabbit hemorrhagic disease virus. *J. Pineal Res.* 2011;50(1):38–45.
441. Tuñón MJ, San-Miguel B, Crespo I, Laliena A, Vallejo D, Álvarez M, et al. Melatonin treatment reduces endoplasmic reticulum stress and modulates the unfolded protein response in rabbits with lethal fulminant hepatitis of viral origin. *J. Pineal Res.* 2013;55(3):221–8.
442. Sun H, Wang X, Chen J, Song K, Gusdon AM, Li L, et al. Melatonin improves non-alcoholic fatty liver disease via MAPK-JNK/p38 signaling in high-fat-diet-induced obese mice. *Lipids Health Dis.* 2016;15(1):202.
443. Carbajo-Pescador S, Martín-Renedo J, García-Palomo A, Tuñón MJ, Mauriz JL, González-Gallego J. Changes in the expression of melatonin receptors induced by melatonin treatment in hepatocarcinoma HepG2 cells. *J. Pineal Res.* 2009;47(4):330–8.
444. Carbajo-Pescador S, García-Palomo A, Martín-Renedo J, Piva M, González-Gallego J, Mauriz JL. Melatonin modulation of intracellular signaling pathways in hepatocarcinoma HepG2 cell line: Role of the MT1 receptor. *J. Pineal Res.* 2011;51(4):463–71.
445. Koşar PA, Nazıroğlu M, Övey İS, Çiğ B. Synergic effects of doxorubicin and melatonin on apoptosis and mitochondrial oxidative stress in MCF-7 breast cancer cells: Involvement of TRPV1 channels. *J. Membr. Biol.* 2016;249(1):129–40.
446. Gao Y, Xiao X, Zhang C, Yu W, Guo W, Zhang Z, et al. Melatonin synergizes the chemotherapeutic effect of 5-fluorouracil in colon cancer by suppressing PI3K/AKT and NF- κ B/iNOS signaling pathways. *J. Pineal Res.* 2017;62(2):e12380.
447. Hong Y, Won J, Lee Y, Lee S, Park K, Chang KT, et al. Melatonin treatment induces interplay of apoptosis, autophagy, and senescence in human colorectal cancer cells. *J. Pineal Res.* 2014;56(3):264–74.
448. Choi S-I, Kim KS, Oh J-Y, Jin J-Y, Lee G-H, Kim EK. Melatonin induces autophagy via an mTOR-dependent pathway and enhances clearance of mutant-TGFB1p. *J. Pineal Res.* 2013;54(4):361–72.

449. Liu C, Jia Z, Zhang X, Hou J, Wang L, Hao S, et al. Involvement of melatonin in autophagy-mediated mouse hepatoma H22 cell survival. *Int. Immunopharmacol.* 2012;12(2):394–401.
450. San-Miguel B, Crespo I, Vallejo D, Alvarez M, Prieto J, González-Gallego J, et al. Melatonin modulates the autophagic response in acute liver failure induced by the rabbit hemorrhagic disease virus. *J. Pineal Res.* 2014;56(3):313–21.
451. Feng YM, Jia YF, Su LY, Wang D, Lv L, Xu L, et al. Decreased mitochondrial DNA copy number in the hippocampus and peripheral blood during opiate addiction is mediated by autophagy and can be salvaged by melatonin. *Autophagy.* 2013;9(9):1395–406.
452. Zhang M, Lin J, Wang S, Cheng Z, Hu J, Wang T, et al. Melatonin protects against diabetic cardiomyopathy through Mst1/Sirt3 signaling. *J. Pineal Res.* 2017;63(2):e12418.
453. Koh PO. Melatonin prevents ischemic brain injury through activation of the mTOR/p70S6 kinase signaling pathway. *Neurosci. Lett.* 2008;444(1):74–8.
454. Li W, Fan M, Chen Y, Zhao Q, Song C, Yan Y, et al. Melatonin induces cell apoptosis in AGS cells through the activation of JNK and p38 MAPK and the suppression of nuclear factor-kappa B: A novel therapeutic implication for gastric cancer. *Cell. Physiol. Biochem.* 2015;37(6):2323–38.
455. Wang K, Liu R, Li J, Mao J, Lei Y, Wu J, et al. Quercetin induces protective autophagy in gastric cancer cells: Involvement of Akt-mTOR- and hypoxia-induced factor 1 α -mediated signaling. *Autophagy.* 2011;7(9):966–78.
456. Kim S, Kim K, Yu S, Park S, Choi H, Ji J, et al. Autophagy inhibition enhances silibinin-induced apoptosis by regulating reactive oxygen species production in human prostate cancer PC-3 cells. *Biochem. Biophys. Res. Commun.* 2015;468(1–2):151–6.
457. Shen YC, Ou DL, Hsu C, Lin KL, Chang CY, Lin CY, et al. Activating oxidative phosphorylation by a pyruvate dehydrogenase kinase inhibitor overcomes sorafenib resistance of hepatocellular carcinoma. *Br. J. Cancer.* 2013;108(1):72–81.
458. Fischer TD, Wang JH, Vlada A, Kim JS, Behrns KE. Role of autophagy in differential sensitivity of hepatocarcinoma cells to sorafenib. *World J. Hepatol.* 2014;6(10):752–8.

459. Chae S, Kim YB, Lee J-S, Cho H. Resistance to paclitaxel in hepatoma cells is related to static JNK activation and prohibition into entry of mitosis. *AJP Gastrointest. Liver Physiol.* 2012;302(9):G1016–24.
460. Lin S, Hoffmann K, Gao C, Petrulionis M, Herr I, Schemmer P. Melatonin promotes sorafenib-induced apoptosis through synergistic activation of JNK/c-jun pathway in human hepatocellular carcinoma. *J. Pineal Res.* 2017;62(3):e12398.
461. Jakubowicz-Gil J, Langner E, Badziul D, Wertel I, Rzeski W. Quercetin and sorafenib as a novel and effective couple in programmed cell death induction in human gliomas. *Neurotox. Res.* 2014;26(1):64–77.
462. Shen YQ, Guerra-Librero A, Fernandez-Gil BI, Florido J, García-López S, Martínez-Ruiz L, et al. Combination of melatonin and rapamycin for head and neck cancer therapy: Suppression of AKT/mTOR pathway activation, and activation of mitophagy and apoptosis via mitochondrial function regulation. *J. Pineal Res.* 2018;64(3):e12461.
463. Fernández A, Ordóñez R, Reiter RJ, González-Gallego J, Mauriz JL. Melatonin and endoplasmic reticulum stress: Relation to autophagy and apoptosis. *J. Pineal Res.* 2015;59(3):292–307.
464. Wang W, Lu J, Zhu F, Wei J, Jia C, Zhang Y, et al. Pro-apoptotic and anti-proliferative effects of mitofusin-2 via Bax signaling in hepatocellular carcinoma cells. *Med. Oncol.* 2012;29(1):70–6.
465. Müller-Rischart AK, Pilsl A, Beaudette P, Patra M, Hadian K, Funke M, et al. The E3 ligase Parkin maintains mitochondrial integrity by increasing linear ubiquitination of NEMO. *Mol. Cell.* 2013;49(5):908–21.
466. Pei S, Minhajuddin M, Adane B, Khan N, Stevens BM, Mack SC, et al. AMPK/FIS1-mediated mitophagy is required for self-renewal of human AML stem cells. *Cell Stem Cell.* 2018;In press.
467. Bejarano I, Espino J, Barriga C, Reiter RJ, Pariente JA, Rodríguez AB. Pro-oxidant effect of melatonin in tumour leucocytes: Relation with its cytotoxic and pro-apoptotic effects. *Basic Clin. Pharmacol. Toxicol.* 2011;108(1):14–20.
468. Osseni RA, Rat P, Bogdan A, Warnet JM, Touitou Y. Evidence of prooxidant and antioxidant action of melatonin on human liver cell line HepG2. *Life Sci.* 2000;68(4):387–99.

469. Chiou JF, Tai CJ, Wang YH, Liu TZ, Jen YM, Shiau CY. Sorafenib induces preferential apoptotic killing of a drug- and radio-resistant HepG2 cells through a mitochondria-dependent oxidative stress mechanism. *Cancer Biol. Ther.* 2009;8(20):1904–13.
470. Uguz AC, Cig B, Espino J, Bejarano I, Naziroglu M, Rodríguez AB, et al. Melatonin potentiates chemotherapy-induced cytotoxicity and apoptosis in rat pancreatic tumor cells. *J. Pineal Res.* 2012;53(1):91–8.
471. Wang F, Denison S, Lai JP, Philips LA, Montoya D, Kock N, et al. Parkin gene alterations in hepatocellular carcinoma. *Genes Chromosom. Cancer.* 2004;40(2):85–96.
472. Carr BI, Carroll S, Muszbek N, Gondek K. Economic evaluation of sorafenib in unresectable hepatocellular carcinoma. *J. Gastroenterol. Hepatol.* 2010;25(11):1739–46.
473. Sanchez-Barcelo EJ, Mediavilla MD, Alonso-Gonzalez C, Reiter RJ. Melatonin uses in oncology: breast cancer prevention and reduction of the side effects of chemotherapy and radiation. *Expert Opin. Investig. Drugs.* 2012;21(6):819–31.
474. Luo D, Wang Z, Wu J, Jiang C, Wu J. The role of hypoxia inducible factor-1 in hepatocellular carcinoma. *Biomed Res. Int.* 2014;2014:409272.
475. Xu H, Zhao L, Fang Q, Sun J, Zhang S, Zhan C, et al. MiR-338-3p inhibits hepatocarcinoma cells and sensitizes these cells to sorafenib by targeting hypoxia-induced factor 1 α . *PLoS One.* 2014;9(12):e115565.
476. Vriend J, Reiter RJ. Melatonin and the von Hippel-Lindau/HIF-1 oxygen sensing mechanism: A review. *Biochim. Biophys. Acta.* 2016;1865(2):176–83.
477. Park SY, Jang WJ, Yi EY, Jang JY, Jung Y, Jeong JW, et al. Melatonin suppresses tumor angiogenesis by inhibiting HIF-1 α stabilization under hypoxia. *J. Pineal Res.* 2010;48(2):178–84.
478. Zhang Y, Liu Q, Wang F, Ling EA, Liu S, Wang L, et al. Melatonin antagonizes hypoxia-mediated glioblastoma cell migration and invasion via inhibition of HIF-1 α . *J. Pineal Res.* 2013;55(2):121–30.
479. Fan L, Sun G, Ma T, Zhong F, Lei Y, Li X, et al. Melatonin reverses tunicamycin-induced endoplasmic reticulum stress in human hepatocellular carcinoma cells and

- improves cytotoxic response to doxorubicin by increasing CHOP and decreasing survivin. *J. Pineal Res.* 2013;55(2):184–94.
480. Pan Y, Niles LP. Epigenetic mechanisms of melatonin action in human SH-SY5Y neuroblastoma cells. *Mol. Cell. Endocrinol.* 2015;402:57–63.
481. Qian W, Wang J, Roginskaya V, McDermott LA, Edwards RP, Stolz DB, et al. Novel combination of mitochondrial division inhibitor 1 (mdivi-1) and platinum agents produces synergistic pro-apoptotic effect in drug resistant tumor cells. *Oncotarget.* 2014;5(12):4180–94.
482. Gharanei M, Hussain A, Janneh O, Maddock H. Attenuation of doxorubicin-induced cardiotoxicity by mdivi-1: A mitochondrial division/mitophagy inhibitor. *PLoS One.* 2013;8(10):e77713.
483. Zhou J, Li G, Zheng Y, Shen HM, Hu X, Ming QL, et al. A novel autophagy/mitophagy inhibitor liensinine sensitizes breast cancer cells to chemotherapy through DNMI1L-mediated mitochondrial fission. *Autophagy.* 2015;11(8):1259–79.
484. Graham RM, Thompson JW, Webster KA. Inhibition of the vacuolar ATPase induces BNIP3-dependent death of cancer cells and a reduction in tumor burden and metastasis. *Oncotarget.* 2014;5(5):1162–73.
485. Giatromanolaki A, Koukourakis MI, Gatter KC, Harris AL, Sivridis E. BNIP3 expression in endometrial cancer relates to active hypoxia inducible factor 1 α pathway and prognosis. *J. Clin. Pathol.* 2008;61(2):217–20.
486. Chen X, Gong J, Zeng H, Chen N, Huang R, Huang Y, et al. MicroRNA145 targets BNIP3 and suppresses prostate cancer progression. *Cancer Res.* 2010;70(7):2728–38.



universidad
de león

